DOCTOR OF SCIENCES

Dynamical analysis and feedback control of age-structured epidemic models

Sonveaux, Candy

Award date:
2023

Awarding institution:
University of Namur

UNIVERSITY OF NAMUR

FACULTY OF SCIENCES

NAXYS RESEARCH INSTITUTE
DEPARTMENT OF MATHEMATICS

Dynamical analysis and feedback control of age-structured epidemic models

A thesis submitted by
Candy Sonveaux
in fulfillment of the
requirements for the
degree of Doctor
in Sciences

Composition of the Jury:

Elarbi ACHHAB (Université Chouaïb Doukkali, El Jadida, Morocco)
Timoteo CARLETTI (UNamur, President of de jury)
Amaury HAYAT (Ecole des Ponts Paristech, Paris, France)
Alexandre MAUROY (UNamur)
Christophe PRIEUR (Gipsa-Lab, Grenoble, France)
Joseph WINKIN (UNamur, Advisor, Secretary of the jury)

December 2023

Cover design: ©Presses universitaires de Namur

Rue Grandgagnage 19
B-5000 Namur (Belgium)
pun@unamur.be - www.pun.be

Registration of copyright: D/2023/1881/23
ISBN: 978-2-39029-187-9
Printed in Belgium.

University of Namur
Faculty of Sciences
Rue de Bruxelles, 61
B-5000 Namur (Belgium)

Dynamical analysis and feedback control of age-structured epidemic models

by Candy Sonveaux

Abstract: The field of epidemiology concerns notably the study of the distribution of diseases (in terms of location, occurrence and characteristics) and the study of the health states of a given population. But il also relies on such analysis for the control of health problems. The first part can be dealt with mathematical modeling whereas the second part benefits from advances in the field of control theory. In this work, both subjects are tackled. Firstly, a case study concerning the covid-19 disease is performed thanks to a nonlinear SIRD model described by ordinary differential equations. The dynamical analysis of this model is developed to ensure the quality of the model (well-posedness) and to provide prediction for the future (stability). Then two vaccination strategies are proposed in order to imply disease eradication, by using two methods of control theory: observer-based output feedback design and model predictive control. Secondly, a nonlinear SIR model described by partial integro-differential equations is studied. This model is well-suited to describe the evolution of long-term diseases. Results concerning the dynamical analysis of the model in terms of existence and uniqueness of solution, nonnegativity of the state variables and stability are established. In view of the stability results, a control law is needed to obtain disease eradication. An innovative extension of the linearizing state feedback approach is given for the infinite-dimensional case to obtain a stabilizing vaccination law whose properties are proven.

Analyse dynamique et commande par rétroaction de modèles épidémiologiques structurés par âge

par Candy Sonveaux

Résumé : Le domaine de l'épidémiologie concerne notamment l'étude de la répartition de maladies (au point de vue de leurs localisations, leurs apparitions et leurs caractéristiques) et l'étude de l'état de santé d'une population donnée. Mais, il s'appuie également sur ces analyses pour le contrôle des problèmes de santé. La première partie peut être réglée grâce à la modélisation mathématique alors que la seconde partie bénéficie des avancées dans le domaine de la théorie du contrôle. Dans ce travail, les deux sujets sont traités. Premièrement, une étude de cas concernant la maladie de covid-19 est réalisée à l'aide d'un modèle SIRD structuré par âge. Ce dernier est décrit grâce à un système d'équations différentielles ordinaires non linéaires. L'analyse dynamique de ce modèle est étudiée pour assurer la qualité du modèle (problème bien posé) ainsi que pour fournir des prédictions concernant le futur (stabilité). Ensuite, deux stratégies de vaccination sont proposées afin d'obtenir l'éradication de la maladie. Cela est réalisé en utilisant deux méthodes provenant de la théorie du

contrôle : la conception d'une commande de sortie basée sur un observateur et la commande prédictive. Deuxièmement, l'étude d'un modèle SIR dépendant de l'âge est proposée. Ce dernier est décrit à l'aide d'équations aux dérivées partielles non linéaires avec termes intégrales. Ce modèle est approprié pour décrire l'évolution de maladies de longues durées. Des résultats concernant l'analyse dynamique du modèle en termes d'existence et d'unicité de la solution, de positivité des variables d'état et de stabilité, ont été démontrés. Étant donné les résultats de l'analyse de stabilité, une loi de contrôle est nécessaire afin d'obtenir l'éradication d'une maladie. Une extension innovante de l'approche de linéarisation par feedback d'état est donnée pour le cas en dimension infinie. Et cela, afin d'obtenir une loi de vaccination stabilisante dont les propriétés ont été démontrées.

Ph.D. thesis in Mathematics
Date: 19/12/23
naXys Research Institute, Department of Mathematics
Advisor: Joseph Winkin

"Mathematics may not teach us to add love or subtract hate, but it gives us hope that every problem has a solution."

ANONYMOUS

Remerciements

Cette thèse est le fruit de rencontres, d'échanges, de collaboration et de soutien. A travers ces lignes j'aimerais donc remercier toutes les personnes qui, de près ou de loin, ont permis d'une part à cette thèse d'aboutir et d'autre part, d'évoluer et de prendre confiance en moi.

Joseph Winkin (Joseph), je ne te remercierai jamais assez pour tout ce que tu m'as apporté. Merci pour ta confiance accordée dès le début lorsque tu m'as proposé cette aventure. Merci encore d'avoir accepté de m'accompagner sur ce sujet où tu n'étais pas spécialement expert. Merci également pour tes encouragements au long de ces six années lorsque j'étais tentée de baisser les bras. J'ai apprécié de trouver ta porte toujours ouverte, ton humour DEBORDANT et ta passion du métier. Nos nombreuses discussions sur la recherche (au tableau ou non), sur l'enseignement mais aussi sur tout autre sujet, tes anecdotes, tes conseils pertinents m'ont donné un élan et une motivation qui m'ont permis de me dépasser et de donner le meilleur de moi-même. Merci également pour ton implication dans cette thèse, tes commentaires avisés, tes relectures et tes annotations au bic rouge. Sans toi, cette thèse ne serait pas ce qu'elle est aujourd'hui. Finalement, je te présente toute ma gratitude pour avoir pensé à moi concernant le voyage de recherche à Grenoble. Cela a marqué un tournant dans ma thèse. D'un point de vue personnel, cela a également permis de développer ma confiance.

Cela m'amène naturellement vers la deuxième personne à qui je souhaite exprimer toute ma gratitude, Christophe Prieur. Christophe, merci d'avoir relancé le projet Tournesol auprès de Joseph. Avoir l'opportunité de collaborer avec toi durant ma thèse a été la meilleure chose qui me soit arrivée. Quel plaisir d'échanger avec toi. Tu m'as accueillie les bras grands ouverts, plein

de bienveillance et de passion. Merci pour tes conseils éclairés, tes nombreuses idées et tes remarques constructives en tant que membre de mon jury mais également en tant que collaborateur.

Merci également à toi Christophe, de m'avoir sortie de ma zone de confort en me mettant en relation avec d'autres chercheurs. Cela a engendré des collaborations fructueuses. Je pense notamment au travail réalisé avec Gildas Besançon, Mirko Fiacchini et Robin Vaudry. Pour cela, je les remercie chaleureusement.
Gildas, tu as toujours trouvé le temps de me rencontrer lors de mes passages à Grenoble. Tes commentaires ont été très pertinents.
Mirko, ta motivation à travailler sur la partie MPC de cette thèse a été un véritable bonheur. Tu t'es toujours montré compréhensif lorsque je ne parvenais pas à maintenir les délais fixés et tu as pu dégager du temps pour répondre à toutes mes questions, avec le sourire.
Robin, merci de m'avoir challengée avec un sujet que je connaissais moins. Cela a été un réel plaisir d'échanger avec toi.
Concernant les collaborations, je ne pouvais passer sous silence le travail avec Morgane Dumont. Morgane, tu es tout d'abord ma super (ex-)collègue de bureau qui me tentait avec des chocolats et avec qui j'ai partagé de nombreux fous rires (petite pensée pour nos pauvres voisins de bureau). Tu m'a permis de remettre le pied à l'étrier dans la partie calibration de paramètres, merci pour cela.

Toute ma gratitude également à Alexandre Mauroy et Elarbi Achhab pour avoir accepté de faire partie de mon comité d'accompagnement. Vous avez été à l'écoute des projets que je souhaitais mener. Votre regard critique et bienveillant m'a poussée à réaliser le meilleur de moi-même.
Merci aussi à Timoteo Carletti et Amaury Hayat pour leur participation à mon jury de thèse. Vos remarques pertinentes dans la bienveillance et votre souci du détail ont contribué à l'amélioration de cette thèse.

Merci à tous les membres du département (assistants, collaborateurs didactiques, chercheurs, professeurs, secrétaires, informaticien). Vous avez fait du département un lieu où il fait bon vivre et un endroit de travail agréable. Je tenais à remercier particulièrement Pascale et Alice, qui ont toujours été présentes pour m'épauler, m'aider et me donner les bonnes informations sur le plan organisationnel. Merci aussi à toi, Juan, pour ta disponibilité et ton talent ! C'était rassurant de savoir qu'en cas de soucis informatiques je pouvais toujours compter sur toi.
Je ne pourrais pas faire ces remerciements sans aborder le bureau du BONHEUR ! Merci à mes supers collègues de bureau. J'ai eu la chance d'être

merveilleusement bien entourée durant toutes ces années. Merci donc à vous, Ambi, Morgane, Marie P., Gaëtan et Marie D..
Au département, les collègues sont devenus des amis: Ambi, Gaëtan, FG, Nico, Charles, Alexis, Arnaud, Pauline, Manon, Julien, Eve-Aline, François S., Joanna, Martin M., Alexis, Marie P., Morgane, Riccardo,... merci pour les bons moments passés ensemble avec vous et les discussions scientifiques (ou non) qu'on a pu avoir !
Merci aussi aux collègues de la team contrôle, Judicaël, FG, Anthony, Pauline, Jérémy pour les échanges intéressants et les prises de tête avec certains concernant le drone ! C'était agréable de se sentir entourée et d'être à plusieurs dans le même bateau.
Finalement je souhaite remercier Anne-Sophie et Joseph. Avoir été votre assistante pendant toutes ces années a été un réel plaisir.

Mes remerciements vont également à tous mes étudiants. Vous avez été ma bouffée d'oxygène entre deux théorèmes. C'était un bonheur de vous enseigner les mathématiques et de voir vos regards s'illuminer lorsqu'un concept était compris.

Merci également à toutes les personnes que j'ai eu la chance de rencontrer grâce à cette recherche. Je pense notamment aux échanges à Grenoble. Nicolas, Andrea, Mohammed,... merci pour votre accueil. Mais également lors du concours MT180, merci Aline et Jacques pour vos conseils et pour cette magnifique expérience humaine.

Merci à tous mes amis et amies pour les repas du vendredi soir, samedi soir et dimanche midi permettant de faire un break dans la recherche et de se vider l'esprit en bonne compagnie. Je pense notamment à Charline et Will, Guillaume et Laura, Marie et Aude, Pitou et Clem, Bastien, Sarah, Virginie, Astrid, Alex et Alice...

Je ne peux conclure ces remerciements sans parler de ma famille. Mamy et papy, merci de m'avoir acceptée comme colloc au début de cette thèse et de m'avoir toujours si bien entourée même si vous ne compreniez pas toujours ce que je faisais. Papa et maman merci de m'avoir toujours soutenue, dans les bons comme dans les mauvais moments. Merci de m'avoir toujours laisser faire ce que je voulais, de m'avoir appris à affirmer mes choix et à ne pas baisser les bras. Mela, toi aussi tu as toujours cru en moi et tu as toujours veillé à m'encourager lors des étapes cruciales de la thèse (parfois même en avance pour ne pas oublier !)
Catherine, Patrick, Nicolas et Mélanie, vous êtes presque de la famille main-

tenant ! Merci pour votre soutien sans faille et votre oreille attentive quand je parlais de mes projets de recherche, de vulgarisation scientifique (MT180) et d'enseignement.

Le meilleur reste pour la fin, merci à toi Arnaud. En commençant cette thèse, je ne pensais pas qu'elle m'amènerait l'amour ! Et nous voilà à présent fiancé. Cette étape est également liée à ma thèse. En effet, tu m'as fait ta demande en mariage à Grenoble. Durant cette thèse, tu as su être mon collègue, mon collaborateur, mon support informatique, mon psy mais surtout mon ami, mon confident, mon amour. Merci pour tout, pour toi, pour ta présence à mes côtés, pour avoir pris soin de moi dans les moments difficiles.

Candy

Contents

Introduction **1**

Notation **7**

I Preliminaries **11**

1 Epidemic Models **13**
1.1 A brief history of the beginning of epidemiology 13
1.2 Epidemic models 15
1.2.1 Types of models 15
1.2.2 Compartmental models 17
1.2.3 Age-structured compartmental models 21
1.3 Successful control strategies in epidemiology 24

II Discretized age-dependent epidemic model **27**

2 Theoretical concepts **31**
2.1 Essential nonnegativity 31
2.2 Existence and uniqueness of solution 32
2.3 Stability for continuous-time systems 33
2.4 Stability for discrete-time systems 38
2.5 Linearizing state feedback 41
2.6 Observer-based output feedback 44
2.7 Model predictive control 46

3 Model calibration **51**
3.1 Data . . . 52
3.2 Parameter calibration . . . 56
3.2.1 Cost function . . . 57
3.2.2 Optimization method . . . 58
3.3 Results . . . 60

4 Dynamical analysis **65**
4.1 Well-posedness . . . 66
4.2 Stability . . . 68
4.3 Numerical simulations . . . 70

5 Observer-based output feedback **73**
5.1 Aim of the control . . . 73
5.2 State feedback . . . 75
5.2.1 Unconstrained linearizing state feedback design . . . 75
5.2.2 Nonnegativity of the feedback . . . 79
5.2.3 Constrained state feedback design . . . 82
5.3 Observer-based output feedback . . . 89
5.4 Numerical simulations . . . 95
5.4.1 Unsaturated state feedback . . . 96
5.4.2 Amplitude constrained control . . . 97

6 Model predictive control **103**
6.1 Problem formulation . . . 103
6.2 Dynamical analysis . . . 106
6.3 Numerical simulations . . . 112
6.3.1 Wallonia case . . . 113
6.3.2 Academic case . . . 115

III Distributed parameter age-dependent epidemic model 119

7 Theoretical concepts **123**
7.1 A state-space approach for linear infinite dimensional systems . 123
7.2 Existence and uniqueness of solution . . . 127
7.3 Method of characteristics . . . 127
7.4 Principle of linearized stability . . . 130
7.5 Spectrum theory for stability analysis . . . 132

8 Dynamical analysis **139**
8.1 Well-posedness . . . 139
8.1.1 Normalized SIR model . . . 139
8.1.2 Homogeneous normalized SIR model . . . 140
8.1.3 Existence and uniqueness . . . 141
8.1.4 Nonnegativity of the states . . . 143
8.2 Stability . . . 146
8.2.1 Existence of steady-states . . . 146
8.2.2 Stability analysis . . . 148
8.3 Numerical simulations . . . 161

9 State feedback **165**
9.1 Finite dimensional model . . . 165
9.1.1 Age-discretized normalized model . . . 166
9.1.2 Well-posedness . . . 168
9.1.3 Linearizing state feedback design . . . 169
9.1.4 Numerical simulations . . . 174
9.2 Infinite dimensional model . . . 175
9.2.1 Feedback design . . . 175
9.2.2 Stabilizing law . . . 177
9.2.3 Nonnegativity of the feedback . . . 186
9.2.4 Numerical simulations . . . 186

Conclusions and Perspectives **191**

A Lipschitz property of the saturated feedback **195**

Bibliography **201**

Introduction

Now, even more than before, we know that infectious diseases may lead to huge damage once out of control. The successful eradication of those diseases implies in particular the ability to understand their transmission dynamics. This has became a particularly hot topic with the recent covid-19 pandemic that occurred in November 2019. (Nane et al. (2023)) cited that over half a million of covid-19-related papers were published by early 2021. Among all those articles, and in epidemiology in general, different kind of models are used to study the dynamics of infectious diseases: statistic versus mechanistic, deterministic versus stochastic, discrete versus continuous... All have some advantages and disadvantages. This thesis focuses on a particular class of epidemic models: mechanistic and deterministic models, known as compartmental models. As mentioned in (Tolles and Luong (2020)), those simple models consider the average behavior of the system at a population level. In this case, the whole population is assumed to be divided into distinct groups with given characteristics. Moreover, the particularity of the models considered in this thesis is that the age-dependency of the parameters are taken into account. Hence, the models studied are best-suited for diseases with different transmission dynamics according to the age of individuals. One can cite childhood diseases or long-term diseases for instance. The main features of those models is that they are nonlinear. This nonlinearity brings complexity since solutions can often not been obtained explicitly. The key questions studied in this thesis concern the dynamical analysis and control of the models considered. The first question, about the dynamical analysis, can be divided into two sub-questions. The first one, refereed as the well-posedness, focuses on the existence and uniqueness of a solution for the model considered. This is particularly important because if the model does not admit a solution it should not be considered. Moreover, if it admits several solutions, it would not be possible to perform accurate predic-

tions. Furthermore, the physical meaning of the solution is also tackled when dealing with well-posedness. Indeed, for systems dealing with physical quantities it is often required to impose the nonnegativity of the state variables to maintain physical meaning. Those types of systems are called positive systems. The second sub-question concerns the concept of stability that allows to characterize the trajectories of the states of the system. This gives an idea of the behavior of the system's solution. If the solution has not the desired behavior, it is sometimes possible to act on it so that it reaches some wanted state. This brings us to the second question of this thesis concerning the control of a system. In epidemiology, there are different ways of controlling a disease, such as quarantine, the wearing of masks, social distancing and hygiene measures,... In this thesis, vaccination is considered as a way of controlling a disease. The field of control theory in mathematics provides a wide range of methods to control dynamical systems described with different equations according to different desired objectives. Those methods are used in different fields such as, robotics, chemical engineering, pharmacology.... In this work, two different designs are considered, namely the output-feedback control and the model predictive control, in order to obtain disease eradication.

Structure of the thesis

This thesis is intended to be self-contained. Hence, theoretical concepts are recalled in preliminary chapters of Parts II and III. The informed reader can skip those parts and go back to them when needed.

The thesis is divided in three main parts, according to the point of view adopted. The first part gives the fundamentals of epidemic models, whereas the second part focuses on finite-dimensional models and the third part is dedicated to the infinite-dimensional models.

The first part, composed of Chapter 1 only, is dedicated to preliminaries concerning epidemic models. After a brief history of epidemiology, the main types of epidemic models are introduced, with a focus on the ones of interest for this thesis, namely the age-dependent compartmental models. Then, an overview concerning some control strategies that lead to disease eradication is introduced.

The second part concerns an epidemic model where the ages are gathered by class of age. This corresponds to a nonlinear finite-dimensional model. Useful concepts needed throughout this part are recalled in Chapter 2. Then a case

study concerning covid-19 is presented. Indeed, Chapter 3 is dedicated to the calibration of the model parameters when no control is applied. Then, those parameters are used in the next chapters. At first, the dynamical analysis of the model is performed in Chapter 4. Then, since the good properties of the solution of the studied model are ensured, the design of a control law can be performed. This is detailed in Chapters 5 and 6, using two different design methods. The first one uses state feedback whereas the second one is based on an optimal control approach, namely model predictive control.

Finally, the third part is dedicated to an epidemic model where the age is considered to be continuous. This corresponds to a nonlinear infinite-dimensional model. As previously, the first chapter of this part, Chapter 7, gathers the necessary concepts used in this part. Then, Chapter 8 concerns the dynamical analysis of this model. In view of the stability result, a control law is needed. It is developed in Chapter 9, using a state feedback design.

Contributions

The contributions of this thesis have been obtained thanks to fruitful collaborations (see co-authors of the publications listed below). The contributions of this thesis concern mainly the control of epidemic models using some known approaches but also a new control design method. They are summarized in Figure 0.2.

A first main contribution concerns the design of an observer-based output feedback, introduced in Chapter 5. This has the advantage to propose an implementable output feedback law, by combining two known theories about state-feedback for finite-dimensional nonlinear systems and about the design of an observer-based feedback. This theory has been applied on real covid-19 data whose parameters have been calibrated in Chapter 3.

The second contribution that can also be highlighted concerns the design of a control law for finite-dimensional systems but this time using a model predictive control (MPC). MPC is widely used in all kinds of applications. However in this thesis, a proof of the stability of the closed-loop system is performed in Chapter 6, ensuring that it can be used safely. This law was also implemented in the context of the covid-19 disease.

Finally, a third major contribution worth mentioning concerns the design of a control law for a nonlinear infinite-dimensional system. The approach proposed in this case is an extension of the theory about stabilizing state feedback in finite dimension to the infinite-dimensional case. This is presented in Chapter 9.

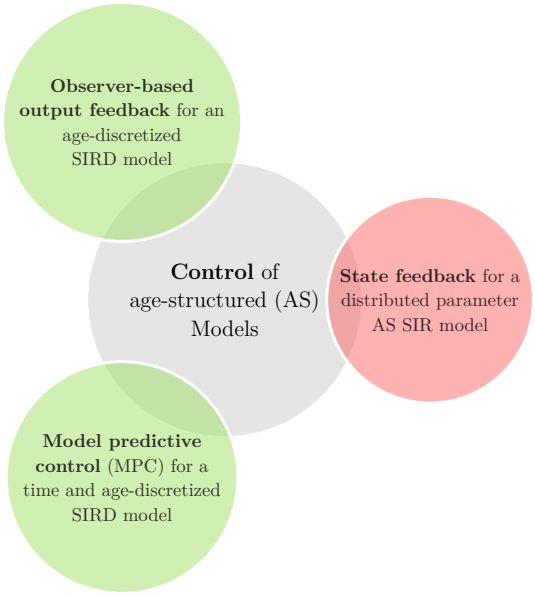

Figure 0.2 – Main contributions of the thesis concerning control theory. In green, Part II of the thesis, in red, Part III of the thesis

Note to the reader: in order to ease the reading, in the derivation of intricate formulas, some terms are colored in blue for highlighting calculation tricks.

Communication

- Sonveaux, C., and Winkin, J. J., *Design of a vaccination law for an age-dependent epidemic model using state feedback*, IFAC-PapersOnLine, pp. 65-70, vol. 55, 2022.
- Sonveaux, C., and Winkin, J. J., *State feedback control law design for an age-dependent SIR model*, Automatica, vol. 158, 2023.
- Sonveaux C., Prieur C., Besançon G. and Winkin J. J., *Observer-based output feedback for an age-structured SIRD model*, submitted to IEEE Transactions on Automatic Control, July 2023.

Moreover, chapters 3 and 6 of the thesis are based on a joint work with Morgane Dumont (HEC, ULiège, Belgium) and Mirko Fiacchini (Gipsa-Lab, Grenoble, France), respectively.

Acknowledgments

This research used resources of the "Plateforme Technologique de Calcul Intensif (PTCI)" (http://www.ptci.unamur.be) located at the University of Namur, Belgium, which is supported by the FNRS-FRFC, the Walloon Region, and the University of Namur (Conventions No. 2.5020.11, GEQ U.G006.15, 1610468, RW/GEQ2016 et U.G011.22). The PTCI is member of the "Consortium des Équipements de Calcul Intensif (CÉCI)" (http://www.ceci-hpc.be). Moreover, Chapter 3 was made possible thanks to the data provided by the AVIQ ("Agence pour une Vie de Qualité").

Notations

	Symbol	Meaning
Parameters		
	N	Number of individuals in the whole population
	N_k	Number of individuals in the population in the kth class of age
	β	Infection rate
	$\beta(\bar{\alpha})$	Infection rate after a time $\bar{\alpha}$ since the infection
	γ	"Recovery" rate (includes death and recovery rate)
	γ_R	Recovery rate
	γ_{R_k}	Recovery rate for the kth class of age
	γ_D	Death rate
	γ_{D_k}	Death rate for the kth class of age
	λ	Transmission probability
	λ_k	Transmission probability for the kth class of age
	σ	Infectiousness rate (inverse of the latent period)
	ω	Loss of immunity (inverse of the protection period)
	$\mu(a)$	Mortality rate
	$c(t, a, a')$	Contact kernel
	$c(a)$	Simplified contact kernel
	C	Contact rate matrix
	α_k	Proportion of recovered people that needed hospital care
	p_k	Probability of succesful vaccination for an individual in the kth class of age
	$p(a)$	Probability of successful vaccination for an individual of age a
	B	Birth rate

Variables

t	Time
a	Individual age
$\bar{\alpha}$	Age of infection
a_{max}	Maximum age
n_a	Number of classes of age
$\propto$	Proportionality coefficient
$S(t)$	Number of susceptible individuals at time t
$I(t)$	Number of infected individuals at time t
$R(t)$	Number of recovered individuals at time t
$D(t)$	Number of dead individuals at time t
$E(t)$	Number of exposed individuals at time t
$S_k(t)$	Number of susceptible individuals at time t with age in $[a_{k-1}, a_k)$
$I_k(t)$	Number of infected individuals at time t with age in $[a_{k-1}, a_k)$
$R_k(t)$	Number of recovered individuals at time t with age in $[a_{k-1}, a_k)$
$D_k(t)$	Number of dead individuals at time t with age in $[a_{k-1}, a_k)$
$S(t, a)$	Density of susceptible individuals of age a at time t
$I(t, a)$	Density of infected individuals of age a at time t
$R(t, a)$	Density of recovered individuals of age a at time t
$P(t, a)$	Density of the total population
$P^\star(t, a)$	Density of the total population at steady state
$I(t, \bar{\alpha})$	Density of infected individuals at time t that are infected since time $\bar{\alpha}$
$\bar{\beta}(t, a, I)$	Force of infection
$\theta_k(t)$	Vaccination rate for the kth class of age
$\theta(t, a)$	Vaccination rate for an individual for age a
$s(t, a)$	Density of the proportion of susceptible individuals of age a at time t
$i(t, a)$	Density of the proportion of infected individuals of age a at time t
$r(t, a)$	Density of the proportion of recovered individuals of age a at time t
$\hat{s}(t, a)$	Normalized density of susceptible individuals of age a at time t

Sets & Operators

$\dot{x}$	Time derivative of x (other notation, $\frac{dx}{dt}$)
∂_t	Partial derivative with respect to t
$\mathbb{R}^+$	Sets of nonnegative real numbers

$\overline{\mathbb{R}}$	Extended real number line, i.e $[-\infty, \infty]$
$\mathbb{R}_0$	Sets of non zero real numbers
$\mathbb{R}^n$	Sets of real vectors od dimension n
$\mathbb{R}^n_+$	Nonnegative orthant of $\mathbb{R}^n$
$\mathcal{B}_\delta$	Open ball of radius δ in $\mathbb{R}^n$
$\mathcal{B}$=$\mathcal{B}_1$	Open unit ball in $\mathbb{R}^n$
Id_n	Identity matrix of size $n \times n$
$0_{n\times n}$	Null matrix of size $n \times n$
$\mathcal{X}$	State space
$\mathcal{U}$	Input space
$\mathcal{Y}$	Output space
$L^k_a b$	kth order Lie derivative of b along the vector field a
$\nabla f(x)$	Gradient of $f(x)$
id_X	Identity operator on the space X
X'	Dual space of X
$\mathcal{L}(X)$	Set of linear and bounded operators on the space X
$\mathcal{L}(X, Y)$	Set of linear and bounded operators from the space X to the space Y
$\mathcal{B}(X)$	Set of bounded operators on the space X
$L^\infty(X)$	Space of essentially bounded functions defined on X
$L^1(a, b)$	Space of Lebesgue integrable functions from $[a, b]$, equipped with the L^1-norm.
$L^1_+(a, b)$	Space of nonnegative Lebesgue integrable functions from $[a, b]$, equipped with the L^1-norm.
$AC[a, b]$	Set of absolutely continuous functions on $[a, b]$
Ker A	Kernel of the operator A
Im A	Range of the operator A
$C^n(X)$	Space of n-times continuously differentiable functions defined on X
$W^{k,n}(X)$	Sobolev space of functions defined on X which are in $L^n(X)$ and whose generalized derivatives up to order k are in $L^n(X)$
∂B	Boundary of B
$\rho(A)$	resolvent set of A
$\sigma(A)$	spectrum of A
$R_\lambda(A)$	resolvent operator of A
$r(A)$	spectral radius of A
$s(A)$	spectral bound of A
$P_\sigma(A)$	Point spectrum of A

Miscellaneous

$\lvert \cdot \rvert$	Modulus
$\lVert \cdot \rVert$	Norm

	$\|\cdot\|_{l^1}$	l^1-norm in $\mathbb{R}^n$
	$\|\cdot\|_1$	Usual norm on $L^1(a,b)$
	$\|x\|_M = d(x,M)$	Distance between the point x and the set M
	$x^\star$	Equilibrium
	$X^\star$	Set of equilibria
	$Re\ \lambda$	Real part of λ
	$\langle\cdot,\cdot\rangle$	Inner product
	$[F,x]$	Pairing between an element, F, of the dual of the positive cone of X, X'_+, and an element x of the positive cone, X_+.
Abbreviations		
	BC.	Before Christ
	cst	Constant
	GAS	Global asymptotic stability
	MPC	Model Predictive Control
	not.	Notation
	ODE	Ordinary differential equation
	PDE	Partial differential equation
	PIDE	Partial integro-differential equation
	WHO	World Health Organization

Part I

Preliminaries

Chapter 1

Epidemic Models

This chapter is dedicated to the introduction of basic notions in epidemiology. First, an overview of the evolution and complexity of the epidemic models over the years is provided. Then, a discussion is proposed to emphasize the variety of epidemic models. Afterwards, the focus is on compartmental models, which are the ones of interest in this thesis. Finally, the end of this chapter is dedicated to the compartmental age-structured models which play a crucial role to capture the evolution of diseases and to be able to act on them through various policies, such as vaccination for instance.

1.1 A brief history of the beginning of epidemiology

Over the last decade, the number of major epidemics has significantly increased. One can cite the Ebola virus disease, the Sudan virus disease outbreak in Uganda or, more recently, the coronavirus disease 2019 (covid-19) pandemic, that officially occurred in Wuhan (China) in November 2019. All those diseases showed that the outbreaks can both spread rapidly through the community and undermine the health care system. Those showed notably the importance of mathematical models in order to understand the spreading of a disease and be able to act effectively on it. Especially since experts agree on saying that one can expect an upsurge of epidemics in the world. This is mainly due, as mentioned in (Institut Pasteur (2019)) to the increase of the world population, the accelerated urbanization, the development of air transport, the global warming, but also the deforestation that puts the Human in contact of new animals. Nevertheless, epidemic modeling is not recent and this is related to the

fact that there have been numerous epidemic diseases in the world, in the past. One can cite, for instance, the Plague of Athens (430-265 BC), the Black Death (1346-1353), the smallpox (XVIIIe), the HIV/AIDS (1981-nowadays),... Those diseases can either disappear after causing lots of deaths, reappear, sometimes with less severity, come back seasonally,... Epidemiology aims at understanding the process of diseases propagation in order to predict their evolution and in a second time, in order to develop control measures to stop their spreading.
The first known analysis of epidemic data was performed by John Graunt. He published in his book "Natural and Political Observations made upon the Bills of Mortality", (Graunt (1662)), an analysis of the deaths ensuing from infectious diseases. Those observations were based on weekly records about the numbers and causes of deaths occurring in the London parishes. Concerning mathematical epidemic models, the first known model is the one by Daniel Bernoulli. He developed a statistical model to study the benefits of the variolation (inoculation of the smallpox) on the life expectancy of the population (see (Bernoulli (1760)) and (Bernoulli (1766))). Some other works have been developed in order to understand epidemic diseases without knowing their transmission processes. For instance, John Snow found the source of a cholera infection, in London, by focusing on the distribution of cholera cases in time and space (see (Snow (1855))). However, those approaches are limited because they are not driven by *"an appropriate theory to explain the mechanisms by which epidemics spread"* (Daley and Gani (2007)). The twentieth century marked a turning point in epidemiology. Indeed the idea of disease transmission by contact through a germ was introduced in 1840 by Jacob Henley and was then popularized in the late nineteenth and the early twentieth centuries. In 1906, W. H. Hammer introduced the principle of mass action in epidemiology for a discrete time model (Hamer (1906)). According to this principle, the rate of transition from a category to another one is proportional to the number of individuals in those categories, and hence, proportional to the number of contacts in the population. Concerning continuous time epidemic models, one can cite the work of Ross that provides a compartmental model to study malaria (Ross (1911)). This paper is the first reference to the concept of basic reproduction number (even though it was not named), a key notion in epidemic modeling since it gives a threshold to disease propagation. However, the most common compartmental model was introduced by (Kermack and McKendrick (1927)) and is well-known as the SIR model. Until then, numerous models and techniques have been developed to tackle the complexity of the diseases propagation. Some of them, of interest for this thesis, are introduced in what follows.

1.2 Epidemic models

The previous section showed the evolution of epidemic models until 1930. However, instead of looking at the evolution of epidemic models in history, an interesting approach is also to compare the models according to the way they are built, the type of solution they give, their intrinsic properties,... This is done here to motivate the choice of models used in this thesis. After comparing the different types of models, the focus is given on compartmental models and more precisely, the age-structured ones.

1.2.1 Types of models

Different kinds of models can be identified. Two types can be distinguished and the choice of one type or another can depend on the research question or on the considered context.

Statistical versus Mechanistic

When dealing with data, two choices can be made in the development of a model. Either statistical models (such as Machine Learning, Artificial Intelligence, Deep Learning,...) can be used. In this case the model derives from the data, in order to describe them as well as possible. Or mechanistic models are used. In this case, the equations (often ordinary differential equations (ODE)) are obtained from the understanding of the natural laws (biological, physical or epidemiological laws). Both points of view have pros and cons. In the case of statistical models lots of data are needed to initialize the model and the initial assumptions about the mechanisms that drive the system need to be correct. In the mechanistic models, on the other hand, the equations are more complex but less data are needed. They even can be used without any data. Notice that data are still required to describe real epidemics. Moreover, thanks to the biological definition of the parameters, they can be studied independently of the choice of the data set. In this thesis, only mechanistic models are used because they have the advantage to allow extrapolation (prediction outside the range of data that are used) and to provide a better understanding of the considered system. Moreover, they are used preferably to evaluate the impact of control measures, which is one of the main goals of this thesis.

Deterministic versus Stochastic

For deterministic modeling, the output is entirely determined by the input. Hence, a given input will always lead to the same output. Those models are well-suited for large populations, where the mean number of infected individuals

can be approximated by a deterministic model. However, in small populations, as the spread of an infectious disease is a random process, the approximation is not valid anymore and this random phenomenon needs to be taken into account. In stochastic models, it is assumed that the transition between two states follows a probability law (Poisson law or Binomial law for instance). Since random processes are taken into account in stochastic models, a given input will lead to different outputs if the simulation is performed several times. Therefore, sensibility analysis of the model is needed when dealing with this type of model. In this thesis, only deterministic models are considered. Indeed, a trade-off is needed between complexity and usable theory. In the following, it is shown that complexity is introduced in other parts of the modeling.

Individual level versus Population level

Two different approaches can be used when simulating epidemic models. The population can be considered as a whole and the focus is on its global evolution. This approach is often linked to the use of mechanistic models. For compartmental models, where the population is divided into different classes and the transition from one group to another is described by rates or differential equations, the population level is used. Another approach is to focus on each individual as an independent unit and to consider the interactions between individuals and possibly their interactions with their environment. It is also possible to mix the two approaches by using for instance networks where each node consists of individual level models: such models are called metapopulation models (see for instance (Colizza and Vespignani (2008))). This thesis is dedicated to compartmental models, so the population level is used.

Discrete versus Continuous

Another important question that arises when choosing a model concerns the type of states and variables.
In epidemic models, the state represents (either directly or through an integration) numbers of individuals in the population. Therefore, it is a discrete variable. However, when dealing with the evolution dynamics, the states are often smoothed to use continuous variables, which are more appropriate for differential equations models.
A second important feature of the model is the type of time and age variables considered in this thesis. Both variables are continuous in reality. However, in simulation, it is not possible to implement continuous variables. Therefore, for simulation (especially for the model predictive control stability analysis of Part II), those variables are discretized. Concerning the age variable, one can group the age by class since the data are often collected that way. Therefore

a discrete number of classes of age is used. This is developed in Part II of this thesis. However, for long-time disease as HIV/AIDS for instance, the aging effect can influence the disease propagation. This is why the age is considered continuously in Part III of this thesis.

1.2.2 Compartmental models

This part is dedicated to the introduction of several basic epidemic compartmental models. Those are mechanistic models and it is chosen to present their deterministic, continuous-time version. In the case of compartmental disease transmission models, it is assumed that the whole population is divided in different compartments according to the state of illness of the individuals. Then, assumptions coming from biological laws describe the transition from one compartment to another. As introduced earlier, the key assumption for compartmental model in epidemiology is the principle of mass action which states that the number of new infections, when a contact occurs between a susceptible individual and an infected individual, is proportional to the number of individuals in both categories. For the other compartments, it is assumed that the transitions are proportional to the number of individuals in the original compartment.
The most known model in epidemiology is the SIR model of (Kermack and McKendrick (1927)). In this model, the population N is divided in three distinct classes. The group S of susceptible individuals who can catch the disease when a contact happens with infected individuals of the group I. Then infected individuals can recover (or die) to enter the group R of recovered (or removed) individuals. The propagation of the disease in the population can be viewed as the compartmental diagram in Figure 1.1. In continuous version, this corresponds to the following set of nonlinear ordinary differential equations,

$$\begin{cases} \dfrac{dS(t)}{dt} = -\dfrac{\beta}{N} S(t) I(t) \\ \dfrac{dI(t)}{dt} = \dfrac{\beta}{N} S(t) I(t) - \gamma I(t) \\ \dfrac{dR(t)}{dt} = \gamma I(t) \end{cases} \tag{1.1}$$

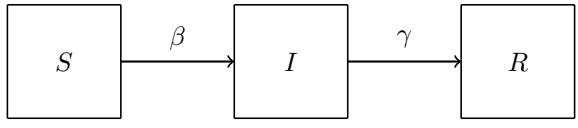

Figure 1.1 – Propagation of the disease in the SIR model

where the total population $N = S(t) + I(t) + R(t)$ is constant, due to the nature of the equations (summing all the equations leads to the fact that the time-variation of the total number of individuals equals zero). The parameter β, named "the infection rate" in the following, is the product between the mean number of contacts and the probability λ of the disease transmission when a contact occurs with an infected individual. Moreover, γ denotes the recovery rate and $\frac{1}{\gamma}$ represents the average time period of infection. One can notice that the parameters are assumed constant in time. More refined versions of this model allow the parameters to vary in time, allowing, for instance, the disease to become less virulent with time. Finally, in this model, as it is the case for the ones considered in this thesis, the considered disease is assumed to confer total immunity. Therefore, once recovered it is not possible to catch the disease again. To allow possible loss of immunity, a transition between the R and S compartment is added. Those models are named $SIRS$ model, where the last S refers to loss of immunity.

In some cases, like in control design, it can be interesting to keep track of the deceased population. In this thesis, this will be essential in order to calibrate the parameters of the model for the covid-19 disease, as detailed in Chapter 3. Indeed, the only satisfactory available data are the data about the dead individuals. Therefore, the R compartment is decomposed in two compartments, one for the (alive) recovered individuals, named R and another one for the deceased individuals, denoted by D. In this case, the propagation of the disease can be represented by the diagram in Figure 1.2 and the dynamics in continuous time is given by the following set of ordinary differential equations,

$$\begin{cases} \dfrac{dS\,(t)}{dt} = -\dfrac{\beta}{N} S(t) I(t) \\ \dfrac{dI\,(t)}{dt} = \dfrac{\beta}{N} S(t) I(t) - (\gamma_R + \gamma_D)\, I(t) \\ \dfrac{dR\,(t)}{dt} = \gamma_R I(t) \\ \dfrac{dD\,(t)}{dt} = \gamma_D I(t) \end{cases} \tag{1.2}$$

where γ_R and γ_D denote the recovery rate and the death rate, respectively.

Some other compartments can be added to tackle features of the pathogen. One can cite, for instance, the SEIRS model. Figure 1.3, adapted from (Keeling and Rohani (2008)), helps to understand the new compartment E of exposed individuals by representing the dynamic of an infection by comparing the medical point of view and the modeling point of view. Before the infection, any

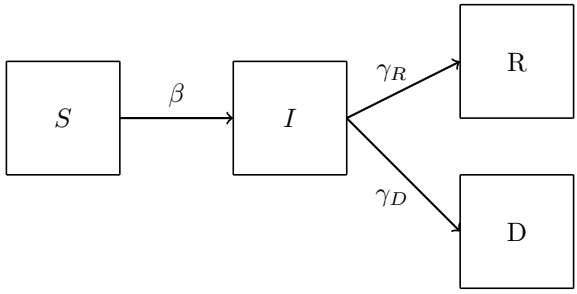

Figure 1.2 – Propagation of the disease in the SIRD model

individual is susceptible and they may have some intrinsic immunity and no pathogen is present in their organism. When the susceptible individual encounters an infected individual they becomes infected. From the medical point of view, two status are considered when a patient catches a disease: the incubation period which corresponds to the time interval between the infection and the beginning of the symptoms; and the period during which the patient is sick until they has no more symptoms. However, from the epidemiology point of view, other status are considered and their duration is not the same as for the medical status. At first, the level of pathogen is too low to enable disease transmission. The individual is considered exposed to the disease. For diseases that have a long latent period, it is important to consider this status to emphasize that there is no on-and-off switch process between susceptibility and infectiousness. After the exposed phase, when the level of pathogen is sufficiently high, the host becomes infectious. Finally, once the individual's immune system has fought the virus, the patient is no longer infectious and becomes recovered. However, with time their immunity decreases and they becomes susceptible again. Notice that it is important to adopt the epidemiological point of view since, even without symptoms, the individuals can transmit the disease. As suggested by Figure 1.3, to implement the SEIR model it suffices to add an "E" compartment to the SIR model. Therefore, the dynamics of the epidemic is given, in the continuous-time version, by a set of four nonlinear ordinary

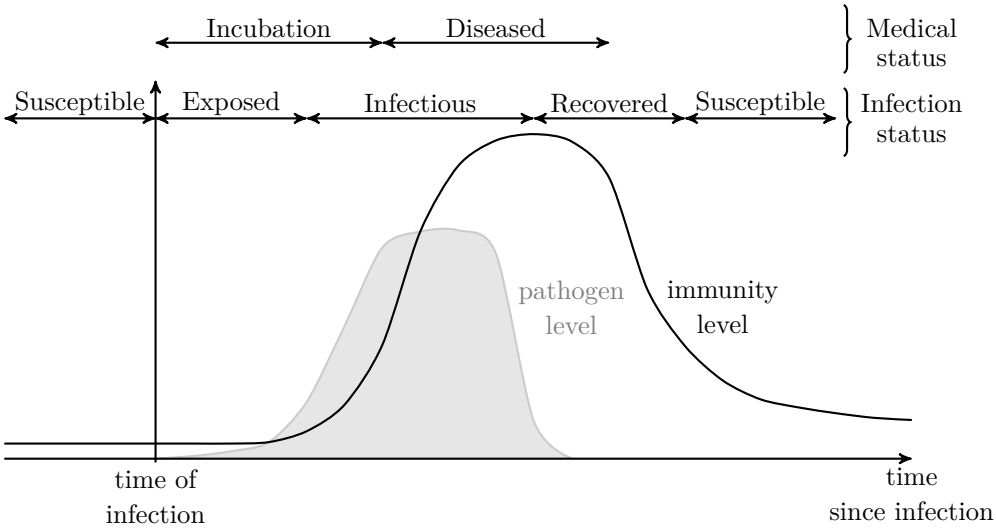

Figure 1.3 – Propagation of the infection in a SEIRS structure

differential equations given by

$$\begin{cases} \dfrac{dS(t)}{dt} = -\dfrac{\beta}{N} S(t)I(t) + \omega R(t) \\ \dfrac{dE(t)}{dt} = \dfrac{\beta}{N} S(t)I(t) - \sigma E(t) \\ \dfrac{dI(t)}{dt} = \sigma E(t) - \gamma I(t) \\ \dfrac{dR(t)}{dt} = \gamma I(t) - \omega R(t) \end{cases} \tag{1.3}$$

where the parameter σ is named "infectiousness rate" and is such that $\frac{1}{\sigma}$ is the latent period. The parameter ω represents the fact that the recovered individuals lose immunity with an average protection period of $1/\omega$.

As shown in this section, numerous modifications can be made from the classical SIR model. Those modifications can either occur by adding new compartments in order to have a better understanding of the disease propagation and/or to match available data or one can also consider other variables of interest in the disease evolution: for instance the dynamics may depend on the spatial (geographical) distribution of the population, the distribution by age of the population... The next section focuses on age-structured compartmental models, which are of interest in this thesis.

1.2.3 Age-structured compartmental models

The study of age-structured models is motivated by the fact that some diseases can be highly age-dependent and therefore, the control strategies need to take into account this age-dependency to give adapted solutions. For instance, the way the disease propagates can depend on the age of the individuals at the level of susceptibility of catching the disease, at the level of the transmission of the disease once infected but also in terms of the individuals habits (contacts are more important among young people). In this part, different types of age-structured models are presented.

Continuous age-structured model

In reality, the age variable is a continuous variable. Therefore, it is natural to consider it continuously in the models. The difference with previous compartmental models is that some of the states depend both on time and age. Therefore they do not represent numbers of individuals anymore but densities. Hence, $S(t,a), I(t,a)$ and $R(t,a)$ denote the density of susceptible, infected and recovered individuals, whose age is a, at time t respectively. Integrating these quantities between two given ages gives the total number of individuals in the given state between those two ages. In terms of host-age, the SIR model (1.1) extends to its age-dependent version as the following set of three partial integro-differential equations (PIDE),

$$\begin{cases} \dfrac{\partial S}{\partial t}(t,a) + \dfrac{\partial S}{\partial a}(t,a) = -\mu(a)S(t,a) - \bar{\beta}(t,a,I)S(t,a) \\ \dfrac{\partial I}{\partial t}(t,a) + \dfrac{\partial I}{\partial a}(t,a) = -\mu(a)I(t,a) + \bar{\beta}(t,a,I)S(t,a) - \gamma(a)I(t,a) \\ \dfrac{\partial R}{\partial t}(t,a) + \dfrac{\partial R}{\partial a}(t,a) = -\mu(a)R(t,a) + \gamma(a)I(t,a) \end{cases} \tag{1.4}$$

under some given initial and boundary conditions which model the birth process. In this case the force of infection, which is the per capita rate at which the susceptible individuals are infected, is given by

$$\bar{\beta}(t,a,I) = \int_0^{a_{max}} c(t,a,a')I(t,a')da'$$

where $c(t,a,a')$ is the contact kernel that represents the contact between an individual of age a with one of age a' at time t. In this thesis, a simplified version of the force of infection is used where $c(t,a,a') =: c(a)$. The fact that c is considered independent of the time t is crucial for the analysis. However the dependency with respect to the age a could be readily extended, although more computationally demanding, to the case where the contact function depends on

the age of the two individuals involved in the contact under the assumption of proportionate mixing, i.e $c(a, a') = c(a)c(a')$. This assumption, used in (Inaba (2017)) for instance, allows to calculate explicitly the threshold condition (in terms of the parameter R_0) for an epidemic to occur. Moreover, notice that in this equation, the natural mortality rate $\mu(a)$ is added since this model is best-fitted for long-term diseases. Then, the individual natural mortality needs to be taken into account.

In the context of disease-age-dependent models, the first model was introduced by (Kermack and McKendrick (1927)) with the study of an infection-age-dependent SIR Model. In fact, although (1.1) is the most popular model, it is just a simplification of the following hybrid ODE - PIDE model, introduced by Kermack and McKendrick in 1927,

$$\begin{cases} \dfrac{dS(t)}{dt} = -\bar{\beta}(t, I)S(t) \\ \dfrac{\partial I}{\partial t}(t, \bar{\alpha}) + \dfrac{\partial I}{\partial \bar{\alpha}}(t, \bar{\alpha}) = -\gamma(\bar{\alpha})I(t, \bar{\alpha}) \\ I(t, 0) = \bar{\beta}(t, I)S(t) \\ \dfrac{dR(t)}{dt} = \displaystyle\int_0^\infty \gamma(\bar{\alpha})I(t, \bar{\alpha})d\bar{\alpha} \end{cases} \tag{1.5}$$

where $I(t, \bar{\alpha})$ represents the density of infected individuals at time t that are infected since time $\bar{\alpha}$. Moreover, $\bar{\beta}(t, I)$, which denotes the force of infection as in the previous case, is now defined by $\bar{\beta}(t, I) = \displaystyle\int_0^\infty \beta(\bar{\alpha})I(t, \bar{\alpha})d\bar{\alpha}$, where $\beta(\bar{\alpha})$ is the infection rate after a time $\bar{\alpha}$ since the infection. It is worth mentioning that other ages can be considered to model the evolution of a disease and the equations of the model are similar to the ones presented here. However, those models are not studied in this thesis.

Discretized age-structured model

In order to use the model in practice, it can be more appropriate to use a discretized version of the previous models. In this thesis, the discretization is developed for the host-age model only. One easy way to do so is to group ages in n_a classes and to duplicate the classical SIR model (1.1) for each class of age. Therefore, the equations remain almost the same as for (1.1) but they are indexed by k. The hardest difficulty is to generalize the parameter β. It becomes a matrix that indicates who acquires infection from whom (and not a vector as for the other parameters). However, when the model parameters are calibrated, there are too many parameters to identify. Therefore, an assumption is made on the transmission of the pathogen. This is the social contact hypothesis that

states that the number of contacts by age leading to an infection is proportional to the age-specific number of social contacts. This translates as

$$\begin{pmatrix} \frac{\beta_{11}}{N_1} & \cdots & \frac{\beta_{1n_a}}{N_1} \\ \vdots & \ddots & \vdots \\ \frac{\beta_{n_a1}}{N_{n_a}} & \cdots & \frac{\beta_{n_an_a}}{N_{n_a}} \end{pmatrix} = \begin{pmatrix} \lambda_1 C_{11} & \cdots & \lambda_1 C_{1n_a} \\ \vdots & \ddots & \vdots \\ \lambda_{n_a} C_{n_a1} & \cdots & \lambda_{n_a} C_{n_an_a} \end{pmatrix}$$

where C is the contact rate matrix and represents the per capita daily contact rate between the classes of age. Therefore, C_{ij} is the probability for an individual in the ith class of age to encounter an individual in the jth class of age. Sometimes, instead of C_{ij} one can use $\frac{M_{ij}}{N_j}$. C is a known matrix in the literature and it does not have to be estimated. Moreover, λ_k is the proportionality factor that represents the probability of transmission of the disease when an individual of the kth class of age has a contact. Therefore, the dynamics of the disease propagation is given by a set of $3n_a$ ODEs,

$$\begin{cases} \frac{dS_k(t)}{dt} = -\lambda_k S_k(t) \sum_{j=1}^{n_a} C_{kj} I_j(t) \\ \frac{dI_k(t)}{dt} = \lambda_k S_k(t) \sum_{j=1}^{n_a} C_{kj} I_j(t) - \gamma_{R_k} I_k(t) \\ \frac{dR_k(t)}{dt} = \gamma_{R_k} I_k(t) \end{cases} \tag{1.6}$$

for $k = 1, ..., n_a$.

Obviously, this methodology can be extended to models with more compartments. In this thesis, an extension of the SIR model (1.6) with an additional compartment that incorporates the dynamics of the dead individuals independently to the one of recovered people is introduced. This choice of model is motivated by the fact that it is used here to simulate the covid-19 pandemic, which is a lethal disease. Moreover, the importance of taking into account the ages of the individuals for the covid-19 disease is established in several articles such as in (Davies et al. (2020)) or (Dowd et al. (2020)), for instance. This motivates the consideration of an age-structured model. The age-dependent SIRD epidemic model used in this thesis groups ages by class and is inspired by the works of (Calafiore and Fracastoro (2022)) and (Franco (2021)). However, some adaptations have been made. Indeed, as introduced in Model (1.6), the transmission probability λ_k is assumed to be different among classes of age. Therefore, the disease propagation for a fixed class of age, k, is given by a set

of $4n_a$ nonlinear ordinary differential equations,

$$\begin{cases} \dfrac{dS_k(t)}{dt} = -\lambda_k S_k(t) \displaystyle\sum_{j=1}^{n_a} C_{kj} I_j(t) \\ \dfrac{dI_k(t)}{dt} = \lambda_k S_k(t) \displaystyle\sum_{j=1}^{n_a} C_{kj} I_j(t) - (\gamma_{R_k} + \gamma_{D_k}) I_k(t) \\ \dfrac{dR_k(t)}{dt} = \gamma_{R_k} I_k(t) \\ \dfrac{dD_k}{dt}(t) = \gamma_{D_k} I_k(t), \end{cases} \tag{1.7}$$

$k = 1, ..., n_a$.

Remark that for ODE models as (1.6) and (1.7), initial conditions are needed. Those conditions are introduced later in this thesis.
Finally, notice that for long term diseases, as the ones studied in Part III, the aging effect needs to be taken into account. This is made possible by allowing transfers between classes of age.

1.3 Successful control strategies in epidemiology

As mentioned in Section 1.1, infectious diseases are expected to occur more often nowadays. Therefore, it is essential to find ways to deal with them and eventually achieve their eradication. In this section, several strategies, based on (Roser et al. (2014)) are detailed to emphasize the possible approaches used in epidemiology to control a disease. To date, only two diseases are declared eradicated by the World Health Organization (WHO). Those are the smallpox, which is a human disease, eradicated in 1980 and the rinderpest, a disease attacking the cattle, that was declared eradicated in 2011. The first disease was eradicated thanks to vaccination. According to the WHO, vaccination allows to protect an individual against harmful diseases, before entering into contact with them. The idea is to inject killed or weakened forms of the germs (viruses or bacteria) or molecules of antigen-encoding messenger RNA, so that the immune system creates antibodies and the individual becomes resistant to the disease. The second disease was eradicated thanks to vaccination and sanitary measures such as quarantine and slaughter.
Another disease, named Guinea worm disease, is almost eradicated. Unofficial

data from (The Carter Center (2023)) report six cases from January 1st 2023 to August 31st 2023. This disease is treated through hygiene measures, water decontamination and health education.
Other control strategies are also possible as preventive chemotherapy or drugs. In the case of this thesis, the focus is made on one preventive treatment that was alluded to earlier, namely vaccination. This control action is studied in Part II and Part III of this thesis.

In summary, all the basic ingredients of age-structured epidemic models have been introduced in this part and the motivation behind the importance of considering the age has been emphasized. Moreover, some particular models used in this thesis, which represent extensions of the classical ones, were described. In the next parts, questions regarding their well-posedness and stability will be studied. Then, in some cases, control laws representing the vaccination are designed. Finally, numerical simulations are implemented. Some of them are based on covid-19 data. Therefore, the model parameters need to be calibrated appropriately. This method will be developed in Part II.

Part II

Discretized age-dependent epidemic model

Introduction

The aim of this part is to study fatal diseases. Hence modeling requires to consider the deceased individuals. Moreover, it is assumed that the studied diseases are short-term diseases. Therefore, the aging effect is not considered. Examples of diseases with those features are covid-19, Hepatitis B, flu... To deal with those kinds of illness, this part focuses on the discretized age-dependent epidemic model (1.7) introduced in Part I. Once the model formulated, one may want to calibrate the model parameters. In this thesis, this is done in Chapter 3 using covid-19 data. Then, in order to assess the well-posedness of the model and to understand its evolution, a dynamical analysis of the system in open-loop is performed in Chapter 4. Finally, Chapters 5 and 6 are dedicated to the design of control laws representing the vaccination. Those laws are implemented using two different methods, one is an estimated state feedback whereas the other one is an optimal law which is obtained by using model predictive control. The aim of those laws is to find a vaccination strategy based on the age of the individuals to eradicate the disease quickly enough and to achieve other interesting goals such as the minimization of the peak of infected individuals or the minimization of the number of dead individuals.

Chapter 2

Theoretical concepts

This chapter aims at gathering all the theoretical concepts needed in this part. The informed reader can skip this chapter and come back to it when complementary details about a technical aspect are needed.

2.1 Essential nonnegativity

One key feature of the epidemic models studied in this thesis is that they are nonnegative dynamical systems. Indeed, the states of those systems need to be nonnegative since they represent quantities that would not have any meaning if they were negative. Therefore, in this case, it is important to ensure that, given nonnegative initial conditions, the state trajectories remain in the nonnegative orthant of the state space. An important concept to ensure the well-posedness of a nonnegative dynamical system is the essential nonnegativity. This is introduced in this section and it is used in Chapter 4. This section is inspired by (Haddad et al., 2010a, Chapter 2).

Consider an autonomous nonlinear system of ordinary differential equations,

$$\dot{x}(t) = f(x(t)), \quad x(0) = x_0 \tag{2.1}$$

where $x(t) \in \mathcal{D} \subseteq \mathbb{R}^n$, with $\mathcal{D}$ a relatively open set (see Definition 2.1.1), $t \in [0, \tau_{x_0})$, $0 < \tau_{x_0} \leqslant \infty$, the maximal interval of existence for the solution of (2.1), and $f : \mathcal{D} \to \mathbb{R}^n$ is continuous on $\mathcal{D}$.
Some concepts, including the essential nonnegativity, are introduced before stating the main result allowing to conclude about the well-posedness of nonnegative dynamical systems.

Definition 2.1.1 ***Relatively open set***
A set $\mathcal{D} \subseteq \mathbb{R}^n_+$ is open relative to $\mathbb{R}^n_+$ if there exists an open set $\mathcal{R} \subseteq \mathbb{R}^n$ such that $\mathcal{D} = \mathcal{R} \cap \mathbb{R}^n_+$.

Definition 2.1.2 ***Invariant set***
A subset $\mathcal{D}_c \subseteq \mathcal{D}$ is an invariant set with respect to (2.1) if $\mathcal{D}_c$ contains the future orbits of all its points, i.e

$$x_0 = x(0) \in \mathcal{D}_c \Rightarrow x(t) \in \mathcal{D}_c, \forall t \in [0, \tau_{x_0}) .$$

In the case where the solution exists in $\mathbb{R}^+$, $\mathcal{D}_c$ is said to be positively invariant if $x(0) \in \mathcal{D}_c \Rightarrow x(t) \in \mathcal{D}_c, \forall t \geqslant 0$.

Definition 2.1.3 ***Essential Nonnegativity***
Let $f = [f_1, \cdots, f_n]^T : \mathcal{D} \to \mathbb{R}^n$. Then, f is essentially nonnegative if for all $i = 1, ..., n$ and for all $x \in \mathcal{D}$ such that $x_i = 0$, where x_i denotes the ith component of x, one has that $f_i(x) \geqslant 0$, where $f_i : \mathcal{D} \to \mathbb{R}$ is the ith component of the function f.

Now, all the elements are gathered to report the main result of this section.

Proposition 2.1.1
Suppose that $\mathcal{D} = \mathbb{R}^n_+$ and that the maximal interval of existence of the solution is $\mathbb{R}^+$. Then, $\mathbb{R}^n_+$ is an invariant set with respect to (2.1), that is $\mathbb{R}^+_n$ is positively invariant, if and only if $f : \mathcal{D} \to \mathbb{R}^n$ is essentially nonnegative.

2.2 Existence and uniqueness of solution

In this section a result concerning the existence and uniqueness of the solution for nonlinear differential equations systems is developed. It consists of Corollary 2.5 in (Haddad and Chellaboina, 2008, Chapter 2). Remark that this result is similar to Theorem 3.3 introduced in (Khalil (2002)). The main feature of the result detailed in the following is that, contrary to the well-known theorem of Picard, it states the existence and uniqueness of a global solution, meaning a solution defined for all $t \geqslant 0$.

Theorem 2.2.1
Consider the nonlinear dynamical system (2.1) where $\mathcal{D}$ is an open subset of $\mathbb{R}^n$ that includes 0.
Assume that $f : \mathcal{D} \to \mathbb{R}^n$ is Lipschitz continuous on $\mathcal{D}$. Furthermore, let $\mathcal{D}_c \subset \mathcal{D}$ be compact and suppose that for $x_0 \in \mathcal{D}_c$, the solution $x : [0, \tau) \to \mathcal{D}$ lies entirely in $\mathcal{D}_c$, with $[0, \tau)$, the maximal interval of existence of (2.1).
Then, this solution can be extended uniquely on $[0, \infty)$.

This theorem follows from the fact that, if τ is finite, then the solution must leave any compact subset of $\mathcal{D}$. Since the solution always lies entirely in the compact set $\mathcal{D}_c$ then, by a contrapositive argument, $\tau = \infty$.

2.3 Stability for continuous-time systems

In this section, based on (Khalil, 2002, Chapter 4) a quick introduction to the concept of stability for continuous-time systems is given. This topic is discussed in the case of an age-dependent SIRD model in Section 4.2. The focus is given on the stability of equilibrium points. In this part, no input is considered but the definition easily extends to the case where an input is taken into account. Indeed, as mentioned in (How and Frazzoli (2010)) for instance, it suffices to find equilibria consisting in couples "state-input" that leave the system constant for the future times when it starts at those points.

Consider the autonomous nonlinear system (2.1) where $f : \mathcal{D} \to \mathbb{R}^n$ is a locally Lipschitz map from $\mathcal{D} \subset \mathbb{R}^n$ into $\mathbb{R}^n$.

Definition 2.3.1 ***Equilibrium for continuous-time systems***
The point $x^\star \in \mathcal{D}$ is an equilibrium point of the system (2.1) if $f(x^\star) = 0$. In other words an equilibrium point is a point that cancels the derivative. Hence, the system, starting at an equilibrium point remains at the same state indefinitely.

In nonlinear systems, the stability of an equilibrium cannot be checked by a single overall criteria, contrary to the linear case where it suffices to check the eigenvalues of A where $\dot{x} = Ax$. Therefore, in the case where the system has multiple distinct equilibrium points, one needs to study the stability of each of them.
As it is classically done, the following definitions and propositions are stated for a null equilibrium point. In the case where the origin is not an equilibrium, the change of variables $\tilde{x} = x - x^\star$ implies that the system in the new variables

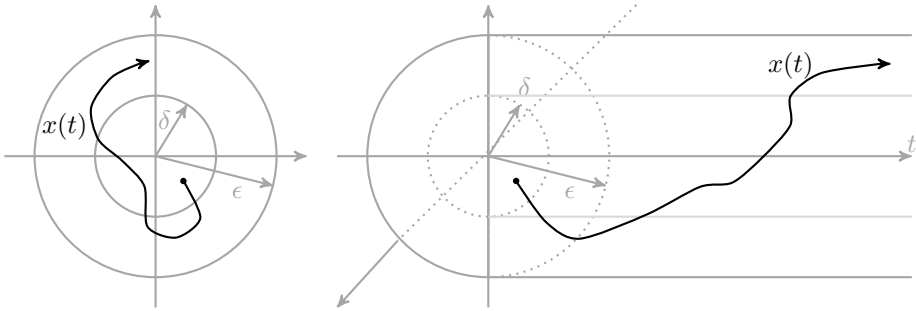

Figure 2.1 – Illustration of the definition of (Lyapunov) stability, inspired by (Kundur et al. (2004))

has an equilibrium at the origin. Hence, in the following, it is assumed that $f(0) = 0$.

Definition 2.3.2 ***Stability for continuous-time systems***
The equilibrium point $x^\star = 0$ *of system* (2.1) *is*

— *(Lyapunov) stable if, for each* $\epsilon > 0$*, there exists* $\delta = \delta_\epsilon > 0$ *such that*

$$\|x(0)\| < \delta \Rightarrow \|x(t)\| < \epsilon, \forall t \geqslant 0.$$

— *unstable if it is not stable.*
— *asymptotically stable if it is stable and* δ *can be chosen such that*

$$\|x(0)\| < \delta \Rightarrow \lim_{t\to\infty} \|x(t)\| = 0.$$

— *exponentially stable if there exist* $\delta > 0, M > 0$ *and* $\alpha > 0$ *such that*

$$\|x(0)\| < \delta \Rightarrow \|x(t)\| \leqslant Me^{-\alpha t}\|x(0)\|, \forall t \geqslant 0.$$

If the conditions are satisfied for any initial state, the system (2.1) is said to be globally (exponentially/asymptotically) stable.
Note that other forms of stability can be considered, such as uniform stability for instance. However, they are not used in this thesis.

Those definitions are illustrated in Figures 2.1 and 2.2 for a state $x(t)$ in $\mathbb{R}^2$. In the first figure, one can observe that by choosing an initial condition x_0 sufficiently close to the origin (in a sphere of radius δ around the origin), the state trajectory remains entirely in a sphere of radius ϵ around the origin. That corresponds to the definition of Lyapunov stability. Moreover, in the case of asymptotic stability, depicted in Figure 2.2, the same occurs but the origin is attractive, meaning that the state tends to the equilibrium point as time goes

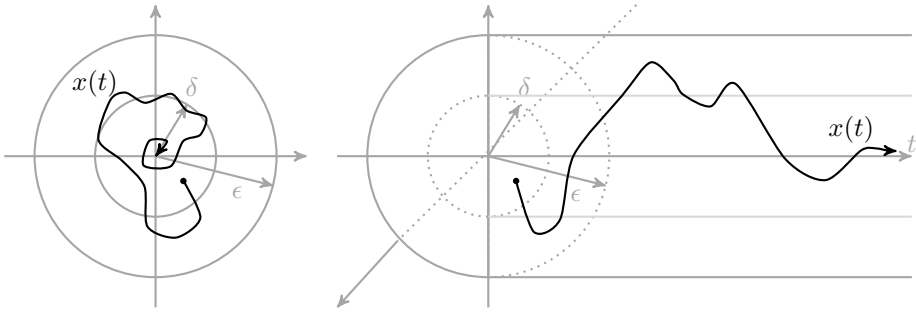

Figure 2.2 – Illustration of the definition of asymptotic stability, inspired by (Kundur et al. (2004))

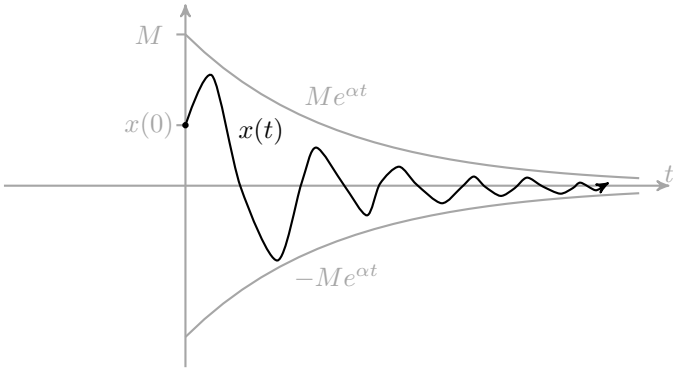

Figure 2.3 – Illustration of the definition of exponential stability, inspired by (Kundur et al. (2004))

to infinity. Furthermore, Figure 2.3 shows the behavior of an exponentially stable solution $x(t) \in \mathbb{R}$. One can observe that an exponentially stable solution decays at an exponential rate and asymptotically tends to the equilibrium point. Therefore, exponentially stable solutions can not blow up.

Now that the concepts are defined, some theorems are introduced to characterize the stability of an equilibrium point. The first one is due to the Russian mathematician Lyapunov, who contributed a lot to the field of stability of dynamical systems. The formulation of this theorem is taken from (Khalil, 2002, Theorem 4.1).

Theorem 2.3.1: Lyapunov stability
Let $x^\star = 0$ be an equilibrium point of (2.1) and let $V : \mathcal{D} \to \mathbb{R}$ be a continuously differentiable function defined in a domain (that is an open and connected subset) $\mathcal{D} \subset \mathbb{R}^n$ that contains the origin such that

$$V(0) = 0 \text{ and } V(x) > 0 \text{ in } \mathcal{D}\backslash\{0\} \tag{2.2}$$

$$\dot{V}(x) \leqslant 0 \text{ in } \mathcal{D} \tag{2.3}$$

then, $x^\star = 0$ is stable. Moreover, if

$$\dot{V}(x) < 0 \text{ in } \mathcal{D}\backslash\{0\} \tag{2.4}$$

then $x^\star = 0$ is asymptotically stable.

A continuously differentiable function V satisfying conditions (2.2) and (2.3) is called a *Lyapunov function*. The previous Lyapunov's theorem gives a local result. However, under some assumptions, one can conclude about the global asymptotic stability (GAS). This is presented in the theorem below, stated in (Khalil, 2002, Theorem 4.2).

Theorem 2.3.2: Barbashin-Krasovskii's theorem
Let $x^\star = 0$ be an equilibrium point of (2.1). Let $V : \mathbb{R}^n \to \mathbb{R}$ be a continuously differentiable function such that

$$V(0) = 0 \text{ and } V(x) > 0 \text{ in } \mathbb{R}_0 \tag{2.5}$$

$$\|x\| \to \infty \Rightarrow V(x) \to \infty \tag{2.6}$$

$$\dot{V}(x) < 0 \text{ in } \mathbb{R}_0 \tag{2.7}$$

then $x^\star = 0$ is globally asymptotically stable.

Remark that global asymptotic stability is only possible if the system has a unique equilibrium. In the case studied in this thesis, there is a continuum of equilibrium points. Therefore, a new concept of stability, introduced in (Hui et al., 2008, Definition 3.1), is needed.

Definition 2.3.3 ***Semistability***

— *An equilibrium point $x^\star \in \mathcal{D}$ of (2.1) is semistable if*

1. *$x^\star$ is a Lyapunov stable equilibrium,*
2. *there exists a set $\mathcal{U} \subseteq \mathcal{D}$ that is open relative to $\mathcal{D}$ and containing*

$x^\star$ such that, for all initial conditions in $\mathcal{U}$, the trajectory of (2.1) *converges to a Lyapunov equilibrium point, that is, $\lim_{t\to\infty} x(t, x_0) = y$, where $y \in \mathcal{D}$ is a Lyapunov stable equilibrium point of* (2.1) *and $x_0 \in \mathcal{U}$.*

- *In addition, the equilibrium point $x^\star \in \mathcal{D}$ of* (2.1) *is a globally semistable equilibrium if conditions 1 and 2 above hold with $\mathcal{U} = \mathcal{D} = \mathbb{R}^n$.*
- *The system* (2.1) *is semistable if every equilibrium point $x^\star$ of* (2.1) *is semistable.*
- *A set $X^\star$ is semistable if all its elements are semistable equilibria, i.e if $\forall x^\star \in X^\star, x^\star$ is a semistable equilibrium.*

In other words, an equilibrium is semistable if it is Lyapunov stable and if every solution starting from an appropriate set containing this equilibrium of the system converges to one of the equilibria.
The following theorem, stated in (Khalil, 2002, Theorem 4.4), is helpful to prove the second condition in the definition of semistable equilibrium point.

Theorem 2.3.3: LaSalle's theorem
Let $\mathcal{D}_c \subset \mathcal{D}$ be a compact set that is positively invariant with respect to (2.1). Let $V : \mathcal{D} \to \mathbb{R}$ be a continuously differentiable function such that $\dot{V}(x) \leqslant 0$ in $\mathcal{D}_c$. Let E be the set of all points in $\mathcal{D}_c$ where $\dot{V}(x) = 0$. Finally, let M be the largest invariant set in E. Then, every solution starting in $\mathcal{D}_c$ approaches M as time tends to ∞, i.e $\forall\ x_0 \in \mathcal{D}_c$,

$$d\left(x(t), M\right) = \inf_{m\in M} \|x(t) - m\| \underset{t\to\infty}{\longrightarrow} 0.$$

All the propositions detailed previously use the property of Lyapunov function to conclude about stability. However, in the case of linear systems, defined by

$$\dot{x}(t) = Ax(t), \quad x(0) = x_0, \tag{2.8}$$

where $A \in \mathbb{R}^{n\times n}$, it is possible to characterize stability using eigenvalues.

Theorem 2.3.4
The linear system (2.8) is exponentially stable if and only if the eigenvalues λ_i of the matrix A have a negative real part, i.e $Re\ \lambda_i < 0$, for all $i = 1, ..., n$ (counting multiplicities).

2.4 Stability for discrete-time systems

In the model predictive control approach, studied in Chapter 6 and briefly explained in Section 2.7, a discrete-time system is used. This section, based on (Rawlings et al., 2020, Appendix B) provides a brief overview of the concept of stability for those systems. Notice that the following definitions are similar to the ones introduced in previous section but for the discrete-time case.
The following notations are used in this part: x denotes the current state, x^+ is the state at the next sample time, also called the successor state and $x(n) = \phi(n; x_0)$ is the solution of $x^+ = f(x)$ at time n with x_0 the initial state at time 0.

Definition 2.4.1 ***Equilibrium for discrete-time systems***
The point $x^\star \in \mathbb{R}^n$ is an equilibrium point of the system $x^+ = f(x)$ if $x(0) = x^\star$ implies that $x(n) = \phi(n; x^\star) = x^\star$ for all $n \geqslant 0$. Therefore, $x^\star$ is an equilibrium point of $x^+ = f(x)$ if it satisfies $x^\star = f(x^\star)$.

Now it is possible to characterize the stability and attractivity of an equilibrium point corresponding to the origin, i.e for systems such that $f(0) = 0$. The following definitions can easily be extended to any non null equilibrium point thanks to an obvious change of variables (shift).

Definition 2.4.2 ***Stabilty and attractivity for discrete-time systems***
The equilibrium point $x^\star = 0$ of the system $x^+ = f(x), x(0) = x$ is

— *locally stable if, for each $\epsilon > 0$, there exists $\delta = \delta_\epsilon > 0$ such that*

$$\|x\| < \delta \Rightarrow \|\phi(n; x)\| < \epsilon, \forall n \in \mathbb{N}.$$

— *unstable, if it is not locally stable.*
— *globally attractive if*

$$\lim_{n\to\infty} \|\phi(n; x)\| = 0 \quad \forall x \in \mathbb{R}^n.$$

— *globally asymptotically stable if it is locally stable and globally attractive*
— *globally exponentially stable if there exist $M > 0$ and $\eta \in (0, 1)$ such that*

$$\|\phi(n; x)\| \leqslant M\|x\|\eta^n, \forall n \in \mathbb{N}.$$

In some cases the convergence to a set of equilibria, $X^\star$, is wanted. The previous definition extends to this case, where the equilibrium $x^\star = 0$ is replaced by a closed, positively invariant set $X^\star$. In this case, the norm $\|\cdot\|$ is replaced with $\|\cdot\|_{X^\star}$, where $\|x\|_{X^\star} = d(x, X^\star) := \inf_{z\in X^\star} \|x - z\|$ denotes the distance of the point x from the set $X^\star$.

In practice, due to some state constraints, the global asymptotic stability of the system cannot be achieved. Hence the following definitions, that extend the previous ones are introduced. Those definitions require the property of positively invariant sets, ensuring that the solution starting in a positively invariant set remains in this set, for all time. This concept is first recalled.

Definition 2.4.3 ***Positively invariant set for discrete-time systems***
A set $\mathcal{D} \subseteq \mathbb{R}^n$ is positively invariant with respect to $x^+ = f(x)$ if $x \in \mathcal{D}$ implies $f(x) \in \mathcal{D}$.

In the following, $\mathcal{B}_\delta$ denotes the open ball in $\mathbb{R}^n$ of radius δ, centered at the origin.

Definition 2.4.4 ***Stabilty and attractivity for constrained discrete-time systems***
Assume that $\mathcal{D}$ is positively invariant with respect to $x^+ = f(x)$. The equilibrium point $x^\star = 0$ of the system $x^+ = f(x)$ is

— *locally stable in $\mathcal{D}$ if, for each $\epsilon > 0$, there exists $\delta = \delta_\epsilon > 0$ such that*

$$x \in \mathcal{D} \cap \mathcal{B}_\delta \Rightarrow \|\phi(n; x)\| < \epsilon, \forall n \in \mathbb{N}.$$

— *(globally) attractive in $\mathcal{D}$ if*

$$\lim_{n \to \infty} \|\phi(n; x)\| = 0 \ \ \forall x \in \mathcal{D}.$$

— *(globally) asymptotically stable in $\mathcal{D}$ if it is locally stable in $\mathcal{D}$ and (globally) attractive in $\mathcal{D}$.*

In this case, the set $\mathcal{D}$ is called the region of attraction for the origin.

— *(globally) exponentially stable in $\mathcal{D}$ if there exist $M > 0$ and $\eta \in (0, 1)$ such that*

$$\|\phi(n; x)\| \leqslant M\|x\|\eta^n, \forall x \in \mathcal{D} \text{ and } \forall n \in \mathbb{N}.$$

Finally, the previous concepts can be characterized thanks to Lyapunov functions. However, intermediate concepts that characterize some classes of function need to be recalled. Those types of function are often used in control theory to check the stability of a system and can be used for discrete-time systems as well as to continuous-time systems.

Definition 2.4.5 ***Comparison function***

— *A function $\sigma : \mathbb{R}^+ \to \mathbb{R}^+$ belongs to class $\mathcal{K}$ if it is continuous, with $\sigma(0) = 0$ and strictly increasing.*

— *A function $\sigma : \mathbb{R}^+ \to \mathbb{R}^+$ is of class $\mathcal{K}_\infty$ if it is of class $\mathcal{K}$ and unbounded.*

— *A function $\beta : \mathbb{R}^+ \times \mathbb{N} \to \mathbb{R}^+$ is of class $\mathcal{KL}$ if for each $n \in \mathbb{N}$, $\beta(\cdot, n)$ is a function of class $\mathcal{K}$, and for each $s \in \mathbb{R}^+$, $\beta(s, \cdot)$ is nonincreasing and satisfies $\lim_{n \to \infty} \beta(s, n) = 0$.*

— *A function* $\eta : \mathbb{R} \to \mathbb{R}^+$ *belongs to class* $\mathcal{PD}$ *if* $\eta(0) = 0$ *and is positive everywhere else. Such a function is called positive definite.*

With those definitions, the global asymptotic stability of the origin for the system $x^+ = f(x)$ can be defined equivalently by

$$\forall x \in \mathbb{R}^n, \|\phi(n; x)\| \leqslant \beta(\|x\|, n) \text{ for all } n \in \mathbb{N}, \text{ for some } \beta(\cdot) \in \mathcal{KL}.$$

Notice that in the case of a set of equilibria $X^\star$, the definitions of global asymptotic stability of $X^\star$ for the system $x^+ = f(x)$ are equivalent if $X^\star$ is compact and positively invariant and $f(\cdot)$ is continuous.

Now all the elements are gathered to characterize the stability. The following result is the analogous of Theorem 2.3.2 for discrete-time systems and when a set of equilibria, $X^\star$, is considered.

Theorem 2.4.1: Lyapunov function for GAS
Suppose that $\mathcal{D}$ is positively invariant and that the set $X^\star \subseteq \mathcal{D}$ is closed and positively invariant with respect to $x^+ = f(x)$, and $f(\cdot)$ is locally bounded.

Let $V : \mathbb{R}^n \to \mathbb{R}^+$ such that there exist functions $\alpha_1, \alpha_2 \in \mathcal{K}_\infty$ and a continuous function $\alpha_3 \in \mathcal{PD}$ satisfying for any $x \in \mathbb{R}^n$,

$$\alpha_1(\|x\|_{X^\star}) \leqslant V(x) \leqslant \alpha_2(\|x\|_{X^\star}), \tag{2.9}$$
$$V(f(x)) - V(x) \leqslant -\alpha_3(\|x\|_{X^\star}). \tag{2.10}$$

Then $X^\star$ is globally asymptotically stable.

A function V satisfying conditions of Theorem 2.4.1 is called a *Lyapunov function for the system* $x^+ = f(x)$ *and the set* $X^\star$.
In the constrained case, the previous theorem is stated as follows.

Theorem 2.4.2: Lyapunov function for GAS (constrained case)
Suppose that $\mathcal{D}$ is positively invariant and that the set $X^\star \subseteq \mathcal{D}$ is closed and positively invariant with respect to $x^+ = f(x)$, and $f(\cdot)$ is locally bounded.
Let $V : \mathcal{D} \to \mathbb{R}^+$ such that there exist functions $\alpha_1, \alpha_2 \in \mathcal{K}_\infty$ and a continuous function $\alpha_3 \in \mathcal{PD}$ satisfying for any $x \in \mathcal{D}$,

$$\alpha_1 (\|x\|_{X^\star}) \leqslant V(x) \leqslant \alpha_2 (\|x\|_{X^\star}) \tag{2.11}$$
$$V(f(x)) - V(x) \leqslant -\alpha_3 (\|x\|_{X^\star}) \tag{2.12}$$

then $X^\star$ is globally asymptotically stable in $\mathcal{D}$ for $x^+ = f(x)$.

A function V satisfying conditions of Theorem 2.4.2 is called a *Lyapunov function in $\mathcal{D}$ for the system $x^+ = f(x)$ and set $X^\star$*.
Finally, a characterization of exponential stability is also possible using Lyapunov function, as presented in the next theorem.

Theorem 2.4.3: Lyapunov function for exponential stability
Suppose that $\mathcal{D}$ is positively invariant and that the set $X^\star \subseteq \mathcal{D}$ is closed and positively invariant with respect to $x^+ = f(x)$, and $f(\cdot)$ is locally bounded.
Let $V : \mathcal{D} \to \mathbb{R}^+$ satisfying for any $x \in \mathcal{D}$,

$$a_1 \|x\|^\sigma_{X^\star} \leqslant V(x) \leqslant a_2 \|x\|^\sigma_{X^\star} \tag{2.13}$$
$$V(f(x)) - V(x) \leqslant -a_3 \|x\|_{X^\star} \tag{2.14}$$

in which a_1, a_2, a_3 and $\sigma > 0$.
Then $X^\star$ is exponentially stable in $\mathcal{D}$ for $x^+ = f(x)$.

2.5 Linearizing state feedback

In this section, based on (Isidori, 1995, Chapter 5), a summary of the theory of linearizing state feedback design for multi-input multi-output systems is given. This method is used in Chapters 5 and 9.

Consider a system in state space form given by

$$\dot{x} = f(x) + \sum_{k=1}^{m} g_k(x)u_k$$
$$y_k = h_k(x) \text{ for } k = 1, ..., m,$$

which can be rewritten in a more compact way as

$$\begin{aligned} \dot{x} &= f(x) + g(x)u \\ y &= h(x), \end{aligned} \tag{2.15}$$

where $f(x)$ and $g_k(x)$, $k = 1, ..., m$, are smooth vector fields and $h_k(x)$, $k = 1, ..., m$ are smooth functions, defined on an open set of $\mathbb{R}^n$. Moreover, $u = col(u_1, ..., u_m), y = col(y_1, ..., y_m), h(x) = col(h_1, ..., h_m)$ are vectors in $\mathbb{R}^m$ and $g(x) = (g_1(x), ..., g_m(x))$ is an $n \times m$ matrix.

The goal of the control is defined below.

Problem 2.5.1 ***State space exact linearization Problem***
Given a set of vector fields $f(x)$ and $g_k(x)$, $k = 1, ..., m$ and an initial state x_0, find a neighborhood $\mathcal{D}$ of x_0, a feedback $u = \alpha(x) + \beta(x)v$ and a coordinates transformation (diffeomorphism) $z = \Phi(x)$ such that (2.15) is linear (given by $\dot{z} = \bar{A}z + \bar{B}v$).

A key concept in the design of a linearizing state feedback is the notion of relative degree. This concept, which is explained in the following, requires the computation of a Lie derivative. The kth order Lie derivative of b along the vector field a is denoted by $L_a^k b(x) = L_a L_a^{k-1} b(x) = \langle \nabla L_a^{k-1} b(x), a(x) \rangle$.

Definition 2.5.1 ***Relative degree***
A multivariable nonlinear system of the form (2.15) has a relative degree $\{r_1, ..., r_m\}$ at a point x_0 if

1. *$L_{g_j} L_f^k h_i(x) = 0$ for all $1 \leqslant j \leqslant m$, $k < r_i - 1$, $1 \leqslant i \leqslant m$ and for all x in a neighborhood of x_0.*
2. *the $m \times m$ matrix*

$$A(x) = \begin{pmatrix} L_{g_1} L_f^{r_1 - 1} h_1(x) & \cdots & L_{g_m} L_f^{r_1 - 1} h_1(x) \\ \vdots & \ddots & \vdots \\ L_{g_1} L_f^{r_m - 1} h_m(x) & \cdots & L_{g_m} L_f^{r_m - 1} h_m(x) \end{pmatrix} \tag{2.16}$$

is nonsingular at $x = x_0$.

The next result ensures that the design of a linearizing state feedback is feasible.

Lemma 2.5.1
Suppose the matrix $g(x_0)$ has rank m. Then, the state space exact linearization problem, defined in Problem 2.5.1 is solvable if and only if there exists a neighborhood $\mathcal{D}$ of x_0 and m real-valued functions $h_k(x)$, $k = 1, ..., m$ defined on $\mathcal{D}$, such that the system (2.15) has some relative degree $\{r_1, ..., r_m\}$ at x_0 and $r_1 + ... + r_m = n$.

Finally, one can state under what coordinates change and control law it is possible to have a linearizing state feedback.

Proposition 2.5.1
Let the functions

$$\phi_i^k(x) = z_{ik} = L_f^{i-1} h_k(x) \tag{2.17}$$

for $1 \leqslant i \leqslant r_k, 1 \leqslant k \leqslant m$ define some coordinates change.
Moreover, define

$$u = A^{-1}(x)\left(v(x) - b(x)\right) \tag{2.18}$$

where A is given by (2.16) and $b(x) = \left(L_f^{r_1} h_1(x), ..., L_f^{r_m} h_m(x)\right)^T$. Then, the system in the new coordinates is given by

$$\dot{z} = \bar{A}z + \bar{B}v \tag{2.19}$$

where $A = \begin{pmatrix} 0 & 1 & 0 & \cdots & 0 \\ 0 & 0 & 1 & \cdots & 0 \\ \vdots & \vdots & \ddots & \vdots & \\ 0 & 0 & 0 & \cdots & 1 \\ 0 & 0 & 0 & \cdots & 0 \end{pmatrix}$ and $B = \begin{pmatrix} 0 \\ \vdots \\ 0 \\ 1 \end{pmatrix}$, which is a linear and controllable system.

Notice that this result is obtained by plugging the input (2.18) in system (2.15), expressed in the variables z thanks to the change of coordinates (2.17). To control the linear system (2.19), it suffices to choose v appropriately so that the system in closed-loop is stable. According to Theorem 2.3.4, v needs to be chosen such that the real parts of the eigenvalues of the system in closed-loop are negative. A useful proposition taken from (Fortmann and Hitz, 1977, Chapter 5) is helpful to establish the stability of linear systems.

Definition 2.5.2 ***Polynomial stability***
Consider the polynomial of degree n given by $p(s) = s^n + p_{n-1}s^{n-1} + ... + p_1 s + p_0$.
Denote the roots of $p(s)$ *as* $\lambda_1, ..., \lambda_n$.
Then, $p(s)$ *is a stable polynomial if* $Re(\lambda_i) < 0$ *for all* $i = 1, ..., n$.

Now, a corollary of Liénard-Chipart Theorem can be stated, in the case of a second-order polynomial.

Proposition 2.5.2: Corollary of Liénard-Chipart theorem
The second-order polynomial $p(s) = s^2 + p_1 s + p_0$ is stable if and only if the coefficients p_1 and p_0 are both positive.

2.6 Observer-based output feedback

In this section, a theorem from (Atassi and Khalil (1999)) is recalled. Notice that the matrix sizes can be more general but have been already adapted to the framework of Section 5.3, where this theorem is used. The aim of this result is to design an observer-based output feedback, which is implementable in practice. In other words, this theorem gives conditions ensuring that the state trajectories of a system under an observer-based output feedback, $\gamma(\hat{z}(t))$ (where $\hat{z}(t)$ denotes the estimated state), converges to the one under exact state feedback, $\gamma(z(t))$. This is paramount since, in order to be implementable, the vaccination law needs to be based only on the measurements and not on the whole state of the system (which is not available).

Theorem 2.6.1: (Atassi and Khalil, 1999, Theorem 3 and Theorem 4)
Consider a multivariable nonlinear system given by

$$\begin{cases} \dot{z}(t) = Az(t) + B\phi(z(t), u(t)) \\ y(t) = Cz(t) \end{cases} \tag{2.20}$$

with $z(0) = z_0$, where $z \in \mathcal{Z} \subseteq \mathbb{R}^{3n}$ is the state vector,

$$u = \gamma(z(t)), \tag{2.21}$$

such that $u \in \mathcal{U} \subseteq \mathbb{R}^n$, is the control input (i.e. the exact state feedback) and $y \in \mathcal{Y} \subseteq \mathbb{R}^n$ is the measured output.

The matrices A, B and C are given by $A = \text{blockdiag}[\tilde{A}, ..., \tilde{A}]_{3n\times 3n}$, $B = \text{blockdiag}[\tilde{B}, ..., \tilde{B}]_{3n\times n}$ and $C = \text{blockdiag}[\tilde{C}, ..., \tilde{C}]_{n\times 3n}$, where

$$\tilde{A} = \begin{pmatrix} 0 & 1 & 0 \\ 0 & 0 & 1 \\ 0 & 0 & 0 \end{pmatrix}, \tilde{B} = \begin{pmatrix} 0 & 0 & 1 \end{pmatrix}^T, \tilde{C} = \begin{pmatrix} 1 & 0 & 0 \end{pmatrix}.$$

Assume that

1. the function $\phi : \mathcal{Z} \times \mathcal{U} \to \mathbb{R}^n$ is locally Lipschitz in its arguments on its domain, with $\phi(0, 0) = 0$.
2. the function ϕ is globally bounded in z.
3. the function γ is a locally Lipschitz function in its arguments on its domain and $\gamma(0) = 0$.
4. the function γ is a globally bounded function of z.
5. the origin ($z = 0$) is an asymptotically stable equilibrium point of the closed-loop system.

Consider the high-gain observer given by

$$\dot{\hat{z}}(t) = A\hat{z}(t) + B\phi(\hat{z}(t), \gamma(\hat{z}(t))) + H(y(t) - C\hat{z}(t)), \tag{2.22}$$

with $\hat{z}(0) = \hat{z}_0$, where H denotes the observer gain, defined by $H = \text{blockdiag}[H_1, ..., H_n]_{3n\times n}$ where

$$H_i = \begin{pmatrix} \frac{\beta_1^i}{\epsilon} & \frac{\beta_2^i}{\epsilon^2} & \frac{\beta_3^i}{\epsilon^3} \end{pmatrix}^T$$

with the parameters β_i^j, $j = 1, 2, 3$ chosen such that the roots of $s^3 + \beta_1^i s^2 + \beta_2^i s + \beta_3^i$ are in the open left-half plane, for $i = 1, ..., n$. Then, the solution $\tilde{z}(t, \epsilon)$ of the system (2.20) under the observer-based output feedback

$$u = \gamma(\hat{z}(t)), \tag{2.23}$$

converges to the solution $z(t)$ of the system (2.20) under the exact state feedback (2.21) uniformly in t, i.e. for all $\zeta > 0$, there exists $\epsilon^\star > 0$ such that for every $0 < \epsilon \leqslant \epsilon^\star$, for all $t \geqslant 0$

$$\|\tilde{z}(t, \epsilon) - z(t)\| \leqslant \zeta,$$

where $\|\cdot\|$ denotes any norm on $\mathbb{R}^{3n}$.
Moreover, there exists $\tilde{\epsilon}^\star$ such that, for every $0 < \epsilon \leqslant \tilde{\epsilon}^\star$, the origin of system (2.20) under observer-based feedback is asymptotically stable.

2.7 Model predictive control

This section is based on the book by (Rawlings et al. (2020)) that provides fundamentals of the theory and design of model predictive control (MPC). Model predictive control can be used to tackle regulation problems as well as estimation problems. In the context of this thesis, only the regulation problem is studied. The idea of model predictive control for regulation is, as mentioned in (Rawlings et al. (2020)), to "use a dynamical model to forecast system behavior and optimize the forecast to produce the best decision, hence the best control move, at current time". Indeed, MPC is a particular form of control where the control action is obtained by online calculation, at each sampling time, "by solving a finite horizon optimal control problem in which the initial state is the current state of the plant." The solution of the finite horizon optimal control problem is a finite sequence of controls and only the first control action in the sequence is applied to the plant at the current sample time. The methodology used in MPC can be illustrated for a single-input, single-output system as in Figure 2.4. As explained previously and developed in (Seborg et al., 2004, Chapter 20), the goal of MPC is to provide the optimal sequence of control moves, $\mathbf{u^o}$, based on current measurements, y, and predictions of the

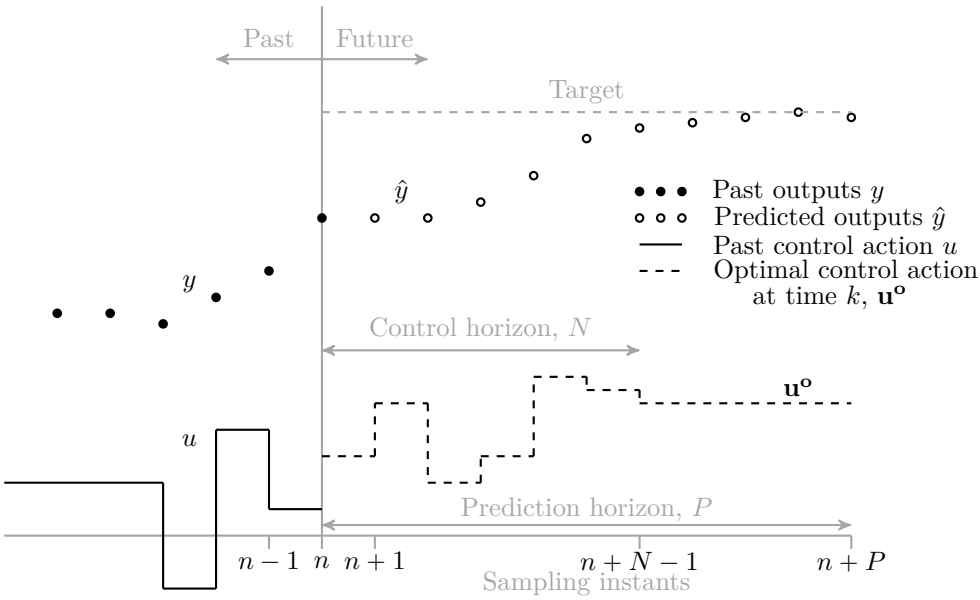

Figure 2.4 – Illustration of the MPC calculation, inspired by (Seborg et al., 2004, Chapter 20)

future values of the outputs, $\hat{y}$, obtained by the dynamical model to reach some desired target. Therefore, as explained in (Seborg et al. (2004)), "at the current sampling instant, n, the MPC strategy calculates a sequence of N values of the input, consisting of the current input $u(n)$ and the $N-1$ future inputs. Then, the input is held constant after the N control moves." Those inputs are obtained to ensure that the set of P predicted outputs reaches the target in an optimal way, based on the optimization of an objective function (see Problem 2.7.1). MPC is called a receding horizon approach since only the first move of the optimal control sequence $\mathbf{u^o}$ is implemented at the current sampling time n. At the next sampling instant, a new optimal sequence is calculated, using the new available measurements and only the first move is implemented. In the following, it is assumed that the whole state is known, therefore, $y = x$. In this case, the system can precisely predict future trajectories and the MPC solution at a given state is given by a receding horizon control law obtained by dynamic programming, and evaluated at this state.

One of the main advantages of the MPC approach is that it needs to solve an open-loop optimal control problem which is often solved rapidly enough. Hence MPC can be used to deal with nonlinear systems with constraints on both states and inputs, which is the case in this thesis.

In the following, the attention is focused on MPC for the control of constrained nonlinear discrete time-invariant systems of the form

$$x^+ = f(x, u), \tag{2.24}$$

$x(0) = x_0$, where $x \in \mathcal{X} \subseteq \mathbb{R}^n$ is the current state, $u \in \mathcal{U} \subseteq \mathbb{R}^m$ is the current control action and $x^+ \in \mathcal{X} \subseteq \mathbb{R}^n$ is the state at the next sample time, also called the successor state. The sets $\mathcal{X}$ and $\mathcal{U}$ are assumed to be closed and denote the set of state constraints and input constraints respectively. The system (2.24) can also be subject to hard constraints. Hence one can introduce the set $\mathcal{Z} \subseteq \mathcal{X} \times \mathcal{U}$, which is the set of all constraints in the problem. The function $f : \mathcal{X} \times \mathcal{U} \to \mathcal{X}$ is assumed to be continuous and to vanish at the origin, such that $(0, 0)$ is the desired equilibrium pair. Thanks to an appropriate coordinate change, the subsequent theory easily extends to non trivial equilibria. In the following, (finite or infinite) sequences are denoted by bold letters. Moreover, the solution of (2.24) at time n with x the initial state at time 0 and the control sequence $\mathbf{u}$ is denoted by $x(n) = \phi(n; x; \mathbf{u})$.
Now that the system is defined, it remains to express the optimization problem to be solved at each time step. The goal is to minimize a given cost function. To ensure practical (fast) resolution of the problem, this cost needs to be defined over a finite horizon N. The goal of MPC presented here is to steer the state to the target state, which is the origin in the remainder of this section. This is

refereed to the regulation problem to the origin. To solve this, it is necessary to find the solution of the following optimal control problem over the control horizon N.

Problem 2.7.1 ***Optimal control problem***

$$\mathbb{P}_N(x): \quad \min_{\boldsymbol{x},\boldsymbol{u}} \sum_{n=0}^{N-1} l\left(x(n), u(n)\right) + V_f\left(x(N)\right)$$

subject to $\boldsymbol{x}$ *and* $\boldsymbol{u}$ *satisfy* (2.24)*, with* $x(0) = x$,

$\boldsymbol{x}$ *and* $\boldsymbol{u}$ *satisfy the state and input constraints.*

Using a priori the fact that the state sequence $\mathbf{x}$ is the solution of $x^+ = f(x,u)$, problem 2.7.1 can be expressed equivalently, for analysis purpose, as an optimization with respect to the variable of decision $\mathbf{u}$ only. Hence the cost to minimize is given by

$$V_N(x,\mathbf{u}) = \sum_{n=0}^{N-1} l\left(x(n), u(n)\right) + V_f\left(x(N)\right), \text{ where } x(n) = \phi(n; x, \mathbf{u}) \quad (2.25)$$

which depends only on the initial state x and the control sequence $\mathbf{u}$.
An additional terminal constraint,

$$x(N) \in \mathcal{X}_f \subseteq \mathcal{X}$$

can sometimes be imposed in order to obtain some desired properties. Taking this into account, considering the new equivalent cost function (2.25), and introducing the set $\mathcal{U}_N(x)$ of (feasible) control sequences satisfying all the (input, state and terminal) constraints, namely the control constraint set, yields to the following equivalent optimal control problem formulation:

$$\mathbb{P}_N(x): \quad \min_{\mathbf{u}\in\mathcal{U}_N(x)} V_N(x,\mathbf{u}) =: V_N^{\mathbf{o}}(x).$$

One can also define the set

$$\mathcal{X}_N := \{x \in \mathcal{X} : \mathcal{U}_N(x) \neq \varnothing\}$$

which corresponds, as seen in the sequel, to the set of states in $\mathcal{X}$ for which $\mathbb{P}_N(x)$ has a solution. So that the previous problem is well-posed, it needs to admit a solution. The following proposition ensures that this holds under some mild assumptions. The first assumption concerns the continuity of the system functions and cost function.

Assumption 2.7.1 *The functions* $f : \mathcal{Z} \to \mathcal{X}$, $l : \mathcal{Z} \to \mathbb{R}^+$ *and* $V_f : \mathcal{X}_f \to \mathbb{R}_+$ *are continuous and such that* $f(0,0) = l(0,0) = V_f(0) = 0$.

The second assumption imposes some properties about the constraint sets.

Assumption 2.7.2 *The set $\mathcal{Z}$ is closed, the set $\mathcal{X}_f \subseteq \mathcal{X}$ is compact and each set contains the origin. Furthermore, if $\mathcal{U}$ is bounded, then the set $\mathcal{U}(x) := \{u \in \mathcal{U} : (x,u) \in \mathcal{Z}\}$ is compact for all $x \in \mathcal{X}$. If $\mathcal{U}$ is unbounded, the function $\boldsymbol{u} \to V_N(x,\boldsymbol{u})$ is coercive, hence $V_N(x,\boldsymbol{u}) \to \infty$ as $|\boldsymbol{u}| \to \infty$ for all $x \in \mathcal{X}$.*

Proposition 2.7.1

Suppose that Assumptions 2.7.1 and 2.7.2 hold. Then,

1. The function $V_N(\cdot)$ is continuous in $\mathcal{Z}_N$, the set of $(x,\mathbf{u})$ for which the constraints of the optimal control problem $\mathbb{P}_N(x)$ are satisfied. Those $(x,\mathbf{u})$ are called admissible.
2. For each $x \in \mathcal{X}_N$, the control constraint set $\mathcal{U}_N(x)$ is compact.
3. For each $x \in \mathcal{X}_N$, a solution to $\mathbb{P}_N(x)$ exists.

Therefore, under Assumptions 2.7.1 and 2.7.2, $\mathbb{P}_N(x)$ admits a solution for all $x \in \mathcal{X}_N$. For this solution, the optimal control sequence is denoted by $\mathbf{u}^{\mathbf{o}}(x) = (u^{\mathbf{o}}(0,x),...,u^{\mathbf{o}}(N-1,x)) = \arg\min_{\mathbf{u}\in\mathcal{U}_N(x)} V_N(x,\mathbf{u})$. In the MPC approach, the control applied to the system is the first element $u^{\mathbf{o}}(0;x)$ of the solution of the optimal control problem and is denoted $\kappa_N(x)$.

Another important question concerns the stability of the controlled system. This stability will ensure that small perturbations of the initial state do not cause large variations in the subsequent behavior of the system and that the state trajectories converge to the desired state or set of states. Since MPC requires to solve a finite horizon optimal problem, (Kalman (1960)) pointed out that optimality does not ensure stability unlike the infinite horizon case. In order to ensure the design of a stabilizing MPC scheme, the function $V_f(\cdot), l(\cdot)$ and the set $\mathcal{X}_f$ need to be chosen in an appropriate way. The idea is to show that under some assumptions, presented below, the value function $V_N^{\mathbf{o}}$ is a valid choice of Lyapunov function for the closed-loop system $x^+ = f(x,\kappa_N(x))$. Hence by Theorem 2.4.2, one can conclude about the global asymptotic stability of the origin of the closed-loop system. Details of the proof, available in (Rawlings et al., 2020, Chapter 2), are not presented here. However, some elements are used in the proof of Theorem 6.2.1 in the context of an age-dependent SIRD model.

Assumption 2.7.3 ***Basic stability assumption***

The functions $V_f(\cdot)$ and $l(\cdot)$, and the set $\mathcal{X}_f$ have the following properties:

1. *For all $x \in \mathcal{X}_f$, there exists a u (such that $(x,u) \in \mathcal{Z}$) satisfying*

(a) $f(x,u) \in \mathcal{X}_f$

(b) $V_f\left(f(x,u)\right) - V_f(x) \leqslant -l(x,u)$

2. *There exist* $\mathcal{K}_\infty$ *functions* $\alpha_1(\cdot)$ *and* $\alpha_f(\cdot)$ *satisfying*

(a) $l(x,u) \geqslant \alpha_1\left(\|x\|\right)\ \forall x \in \mathcal{X}_N$, $\forall u$ *such that* $(x,u) \in \mathcal{Z}$

(b) $V_f(x) \leqslant \alpha_f\left(\|x\|\right)\ \forall x \in \mathcal{X}_f$

Assumption 2.7.4 ***Weak controllability***
There exists a $\mathcal{K}_\infty$ *function* $\alpha(\cdot)$ *such that*

$$V_N^o(x) \leqslant \alpha\left(\|x\|\right) \forall x \in \mathcal{X}_N.$$

This assumption is called weak controllability since it restricts the attention to the states that can be steered to $\mathcal{X}_f$ in N steps and requires to do so with an non excessive cost.

Theorem 2.7.1
Suppose that Assumptions 2.7.1 to 2.7.4 hold. Then

1. there exist $\mathcal{K}_\infty$ functions $\alpha_1(\cdot)$ and $\alpha_2(\cdot)$ such that for all $x \in \mathcal{X}_N$

(a) $\alpha_1\left(\|x\|\right) \leqslant V_N^{\mathbf{o}}(x) \leqslant \alpha_2\left(\|x\|\right)$

(b) $V_N^{\mathbf{o}}\left(f(x,\kappa_N(x))\right) - V_N^{\mathbf{o}}(x) \leqslant -\alpha_1\left(\|x\|\right)$

2. the origin is asymptotically stable in $\mathcal{X}_N$ for $x^+ = f(x,\kappa_N(x))$.

Note that in this theorem, Assumptions 2.7.1 and 2.7.2 are needed. Hence this theorem allows to conclude the existence of a solution for the optimization problem (see Proposition 2.7.1), as well as the stability of the closed-loop system. Therefore, the two questions can be answered all at once.

Chapter 3

Model calibration

The aim of this chapter is to calibrate the parameters of the age-dependent SIRD model (1.7), recalled here:

$$\begin{cases} \dfrac{dS_k(t)}{dt} = -\lambda_k S_k(t) \displaystyle\sum_{j=1}^{n_a} C_{kj} I_j(t) \\ \dfrac{dI_k(t)}{dt} = \lambda_k S_k(t) \displaystyle\sum_{j=1}^{n_a} C_{kj} I_j(t) - (\gamma_{R_k} + \gamma_{D_k}) I_k(t) \\ \dfrac{dR_k(t)}{dt} = \gamma_{R_k} I_k(t) \\ \dfrac{dD_k}{dt}(t) = \gamma_{D_k} I_k(t), \end{cases}$$

$k = 1, ..., n_a$, by using covid-19 data in Wallonia (Belgium). Only one method of parameter identification is used since this chapter is a support to the other ones of this thesis. Indeed, its goal is to provide parameters based on a real disease (instead of academic examples), useful in the simulations of the following chapters in order to illustrate theoretical results. Hence, those parameters are used first to simulate the covid-19 disease in Wallonia (under some assumptions developed below). This is developed in the numerical simulations of Section 4.3. Secondly, the parameters are used to see the effects of feasible vaccination laws on the eradication of the covid-19 in Wallonia. This is developed in the numerical simulations of Chapters 5 and 6.
Notice that the parameter calibration is not an "observable" problem: different sets of parameters can lead to similar results in terms of quality of the estimation. Hence, this chapter is an attempt to derive a possible set of parameters that could explain the covid-19 data in Wallonia. Then, this set of parameters

is used to illustrate the theoretical arguments developed in the thesis.

3.1 Data

In order to calibrate the model parameters several available data from Wallonia (Belgium) are used. Some of them are directly linked to the covid-19 pandemic whereas the others concern the population and its behavior.
Remark that, unfortunately, the available data are not the optimal data that could ease the fitting. Indeed, data about the infected individuals are available only after the beginning of the testing. Moreover, tests were not systematic for the complete population and testing policies were not constant over the time (e.g. for one period, all contacts of positive cases were tested, then, at some points, to be tested an individual needed to be in contact with an infected individual and to have symptoms, etc.). Hence, this made the consideration of the cases data very hazardous for research purposes. Knowing the weaknesses of cases data, only data from the hospital and data about the dead individuals in the population are considered. Indeed, in the hospitals, the decision to test was more constant since during a long period, everyone entering the hospital was tested. However, since individuals coming to the hospital are maybe infected since several days or even weeks, data concerning recovered from hospital instead of infected from hospital are taken into account. Therefore, the total number of recovered individuals in the population is estimated assuming that a proportion of the recovered individuals are passing through the hospital and this proportion, denoted α_k, is supposed to be age-dependent. Indeed, it is obvious that the proportion of young infected individuals going to the hospital is different from the proportion of older people. Furthermore, data concerning the dead individuals are assumed to be reliable and are used to calibrate the model. However, as mentioned in (Sciensano et al. (2023)), one has to keep in mind that Belgium has adopted a "broad inclusion strategy" for the surveillance of deaths from covid-19, by also reporting deaths in cases confirmed by radiology and possible cases based on clinical symptoms. So it is possible that the number of dead individuals in Wallonia has been overestimated.

Thanks to the AVIQ ("Agence pour une Vie de Qualité"), data coming from the RHM ("Résumé Hospitalier Minimum") has been available for this research. The extracted data base contains for every day from mid March to December 2020, the number of patients in Wallonia, positive to covid, deceased at the hospital and leaving the hospital alive, per age.

Thanks to Sciensano, the Belgian institute for health, some open data sets

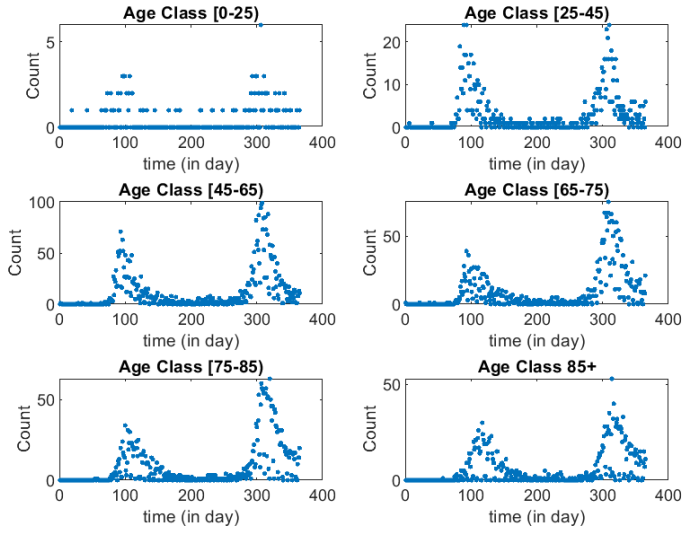

Figure 3.1 – Recovered from hospital, initial data from RHM

about covid-19 in Belgium are available in (Sciensano (2023)). The dataset "Mortality by date, age, sex, and region of death" gathers data about individuals who died from covid-19 from 7$^{\text{th}}$ March 2020 until now since it is updated weekly. The different classes of age considered in those data are the following,

$$[0-25)\,,[25-45)\,,[45-65)\,,[65-75)\,,[75-85) \text{ and } 85+\,.$$

This choice of classes of age seems relevant for this study since the covid-19 is particularly virulent for old population, this is why the discretization by age is more important for old ages than for young ages. Hence this distribution is used in the sequel.

Figures 3.1 and 3.2 show the number of recovered individuals from the hospitals and the number of deceased individuals in the population, respectively, per class of age. Those data are not well distributed on a smooth curve contrary to what the model will produce. This is probably due to the fact that the data are provided by healthcare actors: the way of collecting data during the week and the week-end can cause differences. Hence, a moving average is calibrated on the week around each data (3 days before and after). The new curves which are smoother than the previous ones thanks to the moving average are illustrated on Figures 3.3 and 3.4.

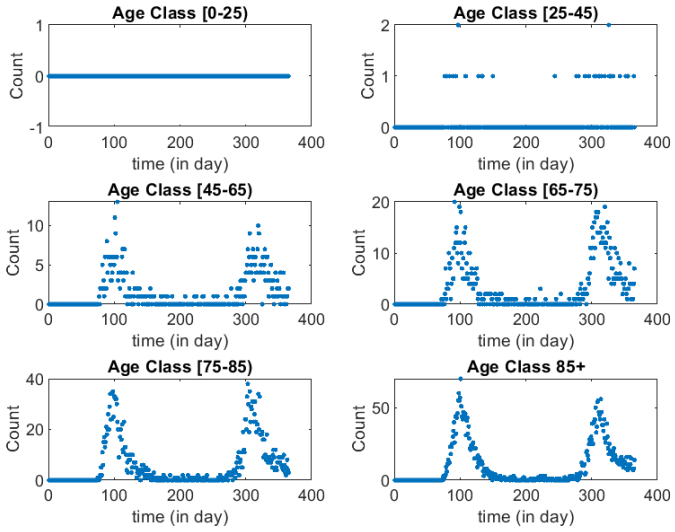

Figure 3.2 – Dead individuals, initial data from (Sciensano (2023))

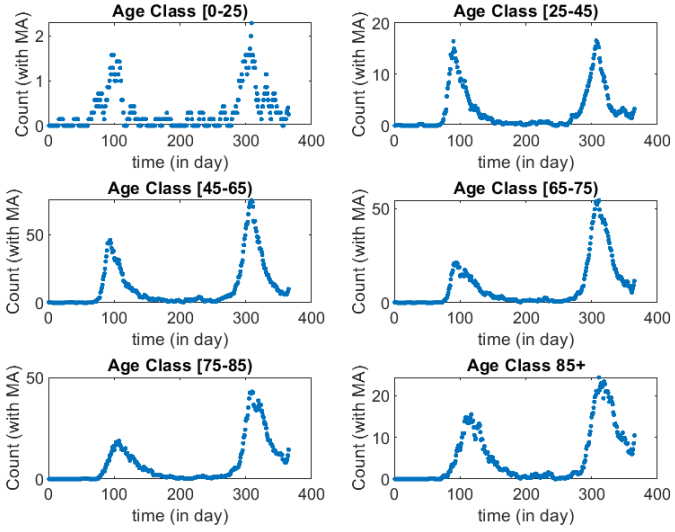

Figure 3.3 – Recovered from hospital, RHM data with weekly moving average

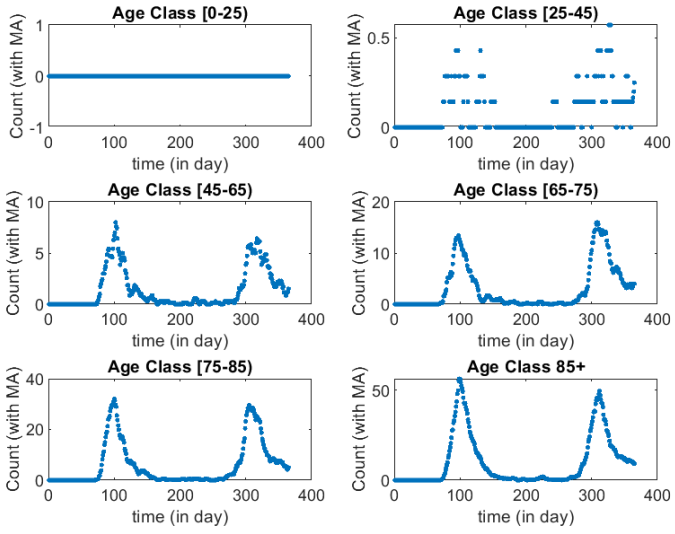

Figure 3.4 – Dead individuals, data from (Sciensano (2023)) with weekly moving average (MA)

In Section 3.2, the model parameters are calibrated using real data introduced earlier. However, since the considered model is age-dependent, the number of parameters increases with the considered number of classes of age. In order to limit the number of parameters to be calibrated, the contact matrix is chosen using the online tool Socrates (Social contact rates) from (SIMID group and Funk (2020)); (Willem et al. (2020)). The data are obtained thanks to different surveys collecting the contact habits of the participants. For this thesis, data collected for Belgium in 2010 are used under the assumption that the social behavior of individuals has not change much the past ten years. However, in the age-dependent SIRD model (1.7), the contact rate matrix per capita, C, is needed. Therefore, the elements of the social contact matrix M obtained in (SIMID group and Funk (2020)) need to be divided by the total number of individuals in the appropriate class of age. Hence, data about the distribution of the Walloon population by class of age are needed. Those data are available in the website of the Belgian office of statistics, (Statbel (2023)) and more precisely the file about the "Population, place of residence, nationality (Belgian/non-Belgian), marital status, age and sex" in 2020 is considered.

3.2 Parameter calibration

This section is dedicated to the calibration of the parameters of an age-dependent SIRD model using covid-19 data introduced in the previous section.

The data available from the RHM and considered in this thesis are from March 2020 to December 2020. This corresponds to a period where no vaccine was available, which is coherent with the aim of this thesis of designing a vaccination law. Therefore this law needs to apply to a situation where no vaccine has been applied before.

To start the simulation with the theoretical model it is mandatory to begin with non-zero initial conditions that correspond to a given starting date for the epidemic. Hence those quantities (initial conditions and starting date) need to be chosen. Since both quantities are too correlated, it has been decided to choose a given starting date and to calibrate the initial conditions. However, the starting date has been chosen to be before the first deceased individual (so, $D_k(0) = 0, k = 1, ..., n_a$) and early enough to have no recovered individuals at time 0 ($R_k(0) = 0, k = 1, ..., n_a$). Since the first death attributed to covid-19 in Belgium is on March 11^{th} 2020 and since the first known apparition of covid-19 in Belgium occurs on the 1^{st} February with people coming back from China but those people went in quarantine for 14 days, then the chosen starting date is February 10^{th} 2020. This corresponds to the 41^{st} day after the 1^{st} January. Hence, at this date it is assumed that there were no recovered individuals from covid-19 in Belgium. Of course, another choice could have been made and it would be interesting to study the impact of this choice on the parameters calibration. Moreover, the initial number of infected individuals for each class of age is a parameter and needs to be calibrated. Note that for this part, the fact that the simulation considers real numbers is an advantage, since this can model the fact that the chosen starting date is not the precise moment of a new case, but between two moments.

Ideally, in order to calibrate the parameters in a more appropriate way, data should be collected for several weeks with a population living normally. Of course, this is not the case in practice. Indeed, in Belgium some restrictive measures have been adopted for short periods of time and then reevaluated. For instance, one can cite the fact that on 10^{th} March 2020, the visits to retirement home have been forbidden, or also on 16^{th} March 2020 the schools have been closed, and so on. Those measures impact the contact matrix used in the theoretical model. However, in this thesis, this has not been taken into account. A way to improve this is to use several contact matrices that capture the effect of the measures taken by the government, instead of a fixed one. However, as discussed below, this choice of constant matrix can be relevant in

the context of this thesis. Indeed this thesis intends to study the control of the epidemic via the vaccination only. Therefore, it seems meaningful to remove the effect of other control measures, such as distancing, by ignoring variations in the contact matrix.
Finally, a last choice concerns the number of days considered to perform the calibration. This choice has been motivated by the shape of Figures 3.3 and 3.4. Indeed it is well known that the model considered in this thesis can only capture one "peak" of the epidemic. Hence, since the initial time t_0 has been chosen to be the day 41, the calibration is performed on the first peak. Moreover, since the aim of the thesis is to design a control law, the calibration is performed only on the increasing part of the epidemic, this is why the final time considered for the calibration is the day 100 (9^{th} April 2020). Indeed, the fact that the epidemic reaches its maximum and then is almost eradicated in a short period of time is due to the sanitary control measures imposed by the governments. However, the interest in this thesis is to demonstrate the performance of the vaccination in order to imply disease eradication in the absence of other measures. Hence, calibrating only on the increasing part of the epidemic will lead to simulations where the number of infected individuals will increase after some time (recall that the contact matrix does not capture the sanitary control measures). Hence, the application of the vaccination to eradicate the epidemic reveals itself relevant.

3.2.1 Cost function

In order to be able to calibrate the parameters of Model (1.7), it is important to use tools quantifying the quality of the estimation. The cost function allows to quantify the error between predicted values, $\hat{y}_i$ and real data, y_i. Hence it gives a measure of the quality of the estimation. The cost function produces a real number to characterize the quality of the calibration. Indeed, the parameters that minimize the cost function are the ones whose predicted values fit the data best. So, before introducing the optimization method, it is important to design this cost function appropriately.
The choice of the cost function is highly dependent on the considered problem and the type of available data. As mentioned in (Towers (2014)), when dealing with count data, particularly with small numbers of counts, the Poisson likelihood statistic is often used to assess the performance of a model to describe the data. In the framework of epidemic models, the available data are count data, so the use of Poisson likelihood statistic makes sense. In this approach, it is assumed that the daily data follow a Poisson distribution. It follows that, for a fixed day, the probability of observing y counts in the data when the model

predicted $\hat{y}$ counts is given by $\mathbb{P}(y|\hat{y}) = \dfrac{\hat{y}^y e^{-\hat{y}}}{y!}$. Hence, for a set of N data points $y_i, i = 1, ..., N$ the probability (or likelihood) that those observed data correspond to model's predictions, $\hat{y}_i$, for each point, is

$$\mathcal{L} = \prod_{i=1}^{N} \frac{\hat{y}_i^{y_i} e^{-\hat{y}_i}}{y_i!}. \tag{3.1}$$

Therefore, the optimal parameters are the ones which maximize this likelihood. However, in practice it is computationally more convenient to use sums instead of products. So, it is best to maximize the logarithm of (3.1). Moreover, most optimization methods deal with minimization problems. Thus it is standard to work with negative log likelihood, which for the Poisson distribution is

$$-\log \mathcal{L} = \sum_{i=1}^{N} \log(y_i!) - \log(\hat{y}_i) y_i + \hat{y}_i.$$

Since the term $\log(y_i!)$ is constant with respect to the model, then it can be ignored in the minimization. Therefore, the log-likelihood function to minimize is given by

$$-\log \mathcal{L} = \sum_{i=1}^{N} -\log(\hat{y}_i) y_i + \hat{y}_i. \tag{3.2}$$

This quantity corresponds to the cost function that is used to estimate the adequacy between the model prediction and the real data.

3.2.2 Optimization method

In order to minimize the cost function (3.2), an optimization algorithm is needed. In this thesis a genetic algorithm is used in order to solve the optimization problem. Those types of algorithms consist of heuristic search and optimization techniques that mimic the Darwinian evolution process. Even if those algorithms can be sensitive to the choice of the parameters of the algorithm such as the size of the population or the rate of mutation for instance, their main advantage is that they can explore vast spaces of solution and so they are less likely to get stuck in local extrema than other methods. In the simulations, the "ga" function from R is used. However, in the following a brief explanation, based on (Obitko (1998)), of the method is given. As mentioned earlier, the genetic algorithms are inspired by Darwin's theory of evolution. The algorithm starts with a random initial population consisting of possible solutions (called chromosomes). Each chromosome is characterized by a set of parameters called genes. In the context of parameters calibration, one possible solution corresponds to a set of admissible parameters for the model. Then, the

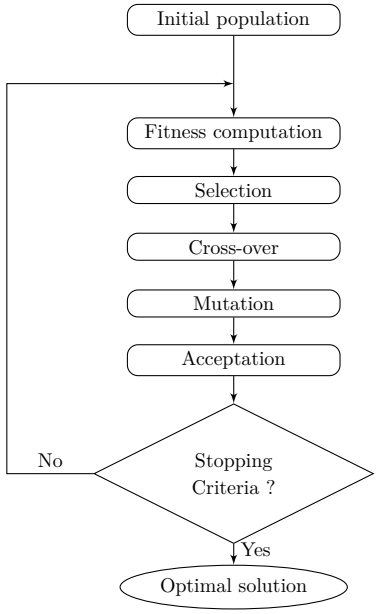

Figure 3.5 – Flowchart for the Genetic Algorithm

quality of those solutions is evaluated thanks to a given cost function. Then, a new population is obtained by applying a sequence of operations to some chosen solutions. Those operations are

1. Selection: Two chromosomes (parents) are selected from the population to transmit their genes to the next generation according to their fitness (value of the cost function). Indeed, the individuals with the highest fitness score have more chance to be selected.
2. Cross-over: With some cross-over probability, the parents genes are crossed to form a new offspring (child). If no crossover is performed, the offspring is the exact copy of the parents.
3. Mutation: According to some mutation probability the offspring genes are mutated in a new offspring.
4. Accepting: The new offspring is placed in the new population.

Then the process can be reiterated until some given condition is fulfilled. A schematic representation of the algorithm is presented in Figure 3.5.

3.3 Results

As mentioned previously, 6 classes of age are considered in this study. Hence, $6 \times 5 = 30$ variables need to be calibrated. This corresponds to the model parameters namely, the transmission probability, λ_k, the recovery rate, γ_{R_k}, and the death rate, γ_{D_k} for each class of age. But it is also required, as developed earlier, to estimate the number of infected individuals at the chosen start of the simulation (day 41), I_{0_k}, for each class. Finally, since the recovered data concern only the recovered individuals from the hospital, it also requires to estimate the proportion of recovered individuals that needs hospitalization, α_k, in order to perform the data calibration.

Simulations were performed using the Hercules cluster from the "Plateforme Technologique de Calcul Intensif" (PTCI) and the code was run 20 times, where the genetic algorithm was set to use a population of 150 chromosomes and to stop after 200000 iterations. Figure 3.6 gathers information about the distribution of the parameters obtained during the 20 runs of simulation. Notice that α_k is not presented since it is a parameter useful for the calibration but not in simulations for prediction purpose. In this figure, one can observe that the

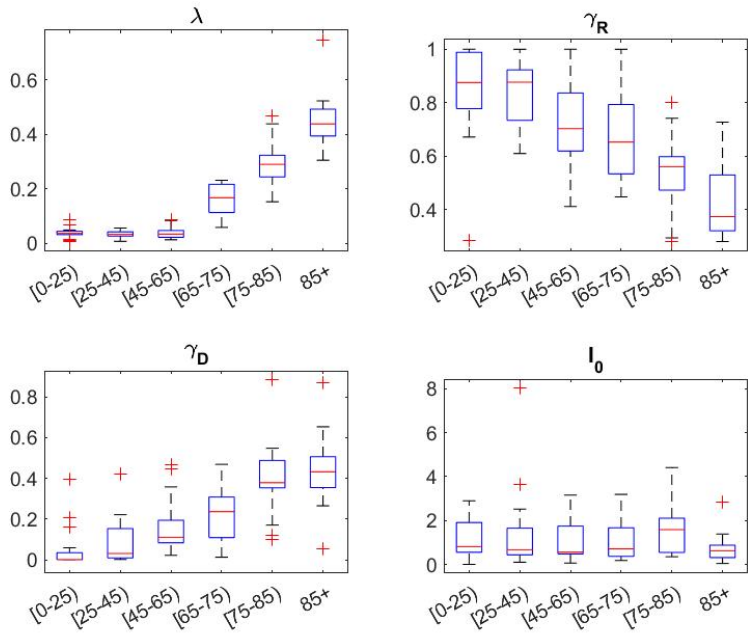

Figure 3.6 – Boxplot of estimated parameters

parameters obtained for the different runs are relatively spread. This is not surprising since, as mentioned earlier, the problem is not "observable". Therefore, different sets of parameters give estimation with the same quality level. Moreover to achieve the best quality of the calibration it is important to consider the combination of parameters and not to look at them separately. Hence it is impossible to draw a conclusion by taking the median parameters for instance. Therefore, in the following, it is chosen to pursue the analysis using the set of parameters associated with the smallest log-likelihood value, given in Table 3.1. Those parameters suggest, without surprise, that the young individuals recover best from the covid-19. A more surprising result is that the mortality occurs principally for the individuals older than 65 years old but with a higher rate in the class $[65, 75)$ instead of the class 85+, as expected. Moreover, in view of the parameter λ_k the older individuals are more susceptible to catch the disease. Those results can be compared to the ones obtained in (Cartocci et al. (2021)). In this article, parameter calibration has been performed on covid-19 data in Italy. Although this article deals with Italian data instead of Belgian data, it has the advantage to use the same SIRD continuous-time model than in this thesis. In this paper, the authors use time-varying parameters. Hence the idea is to perform the comparaison on the parameters obtained at the beginning of the epidemic. As in this thesis, the parameter λ_k (b_k in (Cartocci et al. (2021))) is higher for the oldest individuals. And the order of magnitude is the same, around 0.3, for the older individuals and less than 0.02 for the younger ones. In terms of recovery rate, the results are much more different. Indeed, the recovery rate obtained in April 2020 (which is the final month of calibration in this thesis) in Italy is lower than 0.03 in all classes of age whereas the parameters obtained for Belgium are all above 0.28. This can be partly explained by the fact that there was a saturation of the hospitals in Italy during that period, which was not the case in Belgium. Notice that, even if the order of magnitude is not the same, the idea that the younger individuals recover best remains. Finally, in terms of mortality rate, in Italy, this is decreasing with the age of individuals, which is not the case in the parameters obtained for the Belgian case, since the individuals with age between 65 and 75 years old have the higher mortality rate. In view of this, it could be interesting, for a future work, to deepen this research or to take parameters from the literature. However, to the best of our knowledge, there is no work on calibration of a simple age-dependent SIRD model for Belgian data. This is why, in the following, those parameters are used in the numerical simulations.

Figures 3.7 and 3.8 represent the number of recovered individuals from the hospital and the number of dead individuals, respectively. The blue lines are obtained thanks to a simulation that uses the parameters of Table 3.1 (as well as the proportion parameter, $\alpha_k = (0.07616054, 0.2533263, 0.2259822, 0.3252174,$

Class of age	k	λ_k	γ_{R_k}	γ_{D_k}	I_{0_k}
$[0, 25)$	1	0.01041746	0.9874599	0	2.369302
$[25, 45)$	2	0.01641594	0.7657494	0.005532648	2.519808
$[45, 65)$	3	0.04816858	0.7972883	0.0221575	0.6859303
$[65, 75)$	4	0.05924954	0.6839887	0.1412507	0.8195691
$[75, 85)$	5	0.2210087	0.5968281	0.09957165	1.511804
85+	6	0.3217112	0.2811098	0.05519273	2.842605

Table 3.1 – Parameters with the best fitness function

$0.07708276, 0.02689599$), which is used to deduce the number of recovered individuals from the hospital). Moreover, the red dots correspond to the real data from RHM and sciensano, respectively. Notice that the time considered in those Figures range from 41 to 100 since it is the initial and end time chosen to calibrate the data. In Figure 3.7, one can observe that the simulation obtained is relatively close from the real data, but the match is clearly not perfect. It seems that the calibration performs well to get the initial and final data but not the intermediate ones. The same conclusion holds for Figure 3.8. Notice that the simulation seems far away from the real data for the deceased individuals in the first class of age but this is due to the fact that the scale for the y axis is not constant for all the graphs. One can try to improve those results by using another optimization method or different assumptions than the ones made before. However, as mentioned previously, since the goal of this thesis is not the calibration of data in itself, the set of parameters of Table 3.1 will be considered acceptable for the rest of this thesis.

Thanks to those parameters, it is now possible to perform predictions concerning the behavior of the covid-19 disease (if no sanitary measures are applied). This is done in Section 4.3. Then, vaccination laws can be designed to obtain the eradication of covid-19 according to desired objectives. This is developed in Section 5.4 and Section 6.3.

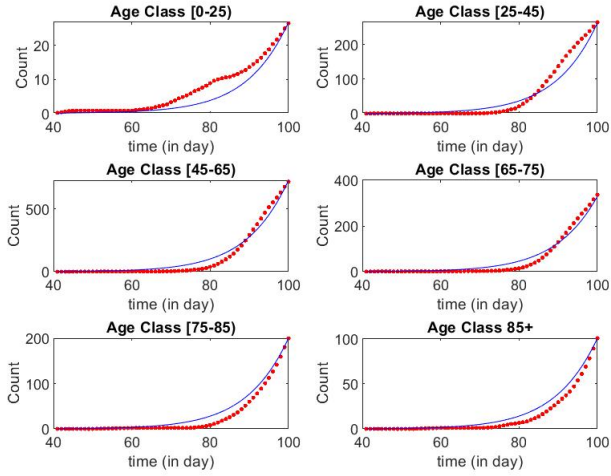

Figure 3.7 – Recovered from hospital, obtained from simulation (blue lines) and from RHM data (red dots)

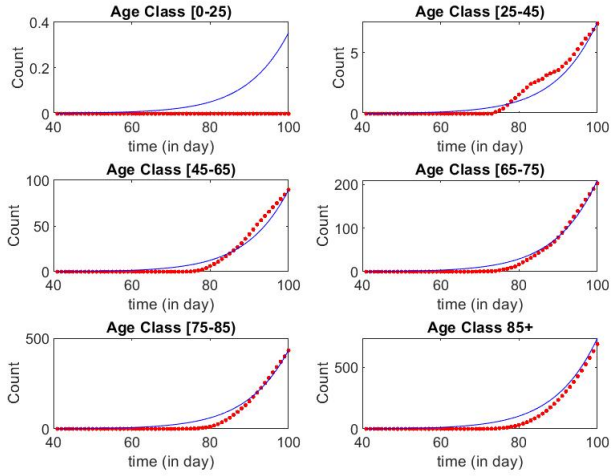

Figure 3.8 – Dead individuals, obtained from simulation (blue lines) and from Sciensano data (red dots)

Chapter 4

Dynamical analysis

This chapter is dedicated to the dynamical analysis of the discretized age-dependent epidemic model (1.7) where a vaccination law is added in open-loop. Then, in view of this analysis, control laws will be designed in Chapter 5 and 6 in order to improve the performance of the system, i.e to enable quicker eradication of the disease. Therefore, model (1.7) becomes

$$\begin{cases} \dfrac{dS_k(t)}{dt} = -\lambda_k S_k(t) \displaystyle\sum_{j=1}^{n_a} C_{kj} I_j(t) - p_k \theta_k(t) S_k(t) \\ \dfrac{dI_k(t)}{dt} = \lambda_k S_k(t) \displaystyle\sum_{j=1}^{n_a} C_{kj} I_j(t) - \left(\gamma_{R_k} + \gamma_{D_k}\right) I_k(t) \\ \dfrac{dR_k(t)}{dt} = \gamma_{R_k} I_k(t) + p_k \theta_k(t) S_k(t) \\ \dfrac{dD_k}{dt}(t) = \gamma_{D_k} I_k(t), \end{cases} \tag{4.1}$$

$k = 1, ..., n_a$, where $\theta_k(t)$ represents the vaccination rate for the kth class of age. The parameter $p_k \in (0, 1]$ represents the probability of efficiency of the vaccination for the kth class of age. Remark that vaccination works as a preventive treatment since it is applied on the susceptible individuals. Moreover, it is assumed to give permanent immunity when the vaccination is a success. In the case of covid-19, this is a strong assumption since in practice there is a loss of vaccine immunity. A possible way to take this into account is, for instance, to consider an SIRDS model that allows recovered individuals to become infected again. The methodology presented in this thesis could be adapted to this new model and some adaptations would be needed. Table 4.1 gathers the interpretation and units of the variables and parameters involved in Model

(4.1).

Variables	Interpretation	Range	Unit
t	Time	$\mathbb{R}^+$	day
a_{max}	Maximum age	$\mathbb{R}^+$	year
n_a	number of class of age	$\mathbb{N}$	
$S_k(t)$ $I_k(t)$ $R_k(t)$ $D_k(t)$	Number of susceptible, infected recovered and dead individuals at age in $[a_{k-1}, a_k)$	$\mathbb{R}^+$	Human
$\theta_k(t)$	Rate of vaccinated individuals at age in $[a_{k-1}, a_k)$	$\mathbb{R}^+$	$\frac{1}{\text{day}}$
Parameters			
N_k	Total number of individuals at age in $[a_{k-1}, a_k)$	$\mathbb{R}^+$	Human
λ_k	Probability of transmission of the disease for ages in $[a_{k-1}, a_k)$	$[0,1]$	no unit
C_{kj}	Probability for an individual in the kth class of age to encounter an individual in the jth class of age	$[0,1]$	$\frac{1}{\text{Human.day}}$
γ_{R_k}	Recovery rate at age in $[a_{k-1}, a_k)$	$\mathbb{R}^+$	$\frac{1}{\text{day}}$
γ_{D_k}	Disease mortality rate at age in $[a_{k-1}, a_k)$	$\mathbb{R}^+$	$\frac{1}{\text{day}}$
p_k	Probability of successful vaccination for individuals at age in $[a_{k-1}, a_k)$	$(0,1]$	no unit

Table 4.1 – Parameters and variables for the NODE

4.1 Well-posedness

When dealing with a model, one important question that can arise concern its physical coherence. In the case of epidemic models with discrete age, the states are (continuous) numbers of individuals. Therefore, those quantities can not become smaller than zero. Moreover, they represent individuals, with a given state of health, in a population. Hence, the states need to be upper bounded by the number of individuals in each class of age, N_k. Thus, the states should stay in the feasible set

$$\mathcal{X} = \{x = (S_1, ..., S_{n_a}, I_1, ..., I_{n_a}, R_1, ..., R_{n_a}, D_1, ..., D_{n_a})^T \in \mathbb{R}^{4n_a} : \\ 0 \leqslant S_k, I_k, R_k, D_k \text{ such that } S_k + I_k + R_k + D_k = N_k \text{ for } k = 1, ..., n_a\}. \tag{4.2}$$

Moreover, it is important to be confident that the set of equations admits a solution and that this solution is unique to ensure that the predictions made by

the model are reliable and that the results can be interpreted. Those important properties of the model are developed in the following results.

Proposition 4.1.1

Assume that Model (4.1) admits a solution on $\mathbb{R}^+$ and that $\theta_k(t) \geqslant 0$ for $k = 1, ..., n_a$ and for all $t \geqslant 0$.
Then the compact set $\mathcal{X}$, given by (4.2), is positively invariant with respect to Model (4.1).

Proof. This proof is based on the concept of essential nonnegativity of the vector field (see Definition 2.1.3). Define $f = [f_1, ..., f_{4n_a}]^T : \mathbb{R}_+^{4n_a} \to \mathbb{R}^{4n_a}$ such that, for $x = (S_1, ..., S_{n_a}, I_1, ..., I_{n_a}, R_1, ..., R_{n_a}, D_1, ..., D_{n_a})^T$,

$$\begin{aligned} f_k(x) &= -\lambda_k S_k \sum_{j=1}^{n_a} C_{kj} I_j - p_k \theta_k S_k \\ f_{n_a+k}(x) &= \lambda_k S_k \sum_{j=1}^{n_a} C_{kj} I_j - (\gamma_{R_k} + \gamma_{D_k}) I_k \\ f_{2n_a+k}(x) &= \gamma_{R_k} I_k + p_k \theta_k S_k \\ f_{3n_a+k}(x) &= \gamma_{D_k} I_k \end{aligned} \tag{4.3}$$

for $k = 1, ..., n_a$. The function f is essentially nonnegative since $f_k(x) = 0$ when $S_k = 0$, $f_{n_a+k}(x) = \lambda_k S_k \sum_{j=1, j\neq k}^{n_a} C_{kj} I_j \geqslant 0$ when $I_k = 0$, $f_{2n_a+k}(x) = \gamma_{R_k} I_k + \theta_k S_k \geqslant 0$ when $R_k = 0$ since θ_k is assumed to be nonnegative and $f_{3n_a+k}(x) = \gamma_{D_k} I_k \geqslant 0$ when $D_k = 0$. Therefore, thanks to Proposition 2.1.1, the set $\mathbb{R}_+^{4n_a}$ is invariant.
Moreover the fact that the states variables are bounded by N_k is a direct consequence of the fact that $N_k = S_k + I_k + R_k + D_k$ and the nonnegativity of the states. □

Now, the existence of a unique global solution can be established thanks to theorem 2.2.1.

Proposition 4.1.2

Let $x = (S_1, ..., S_{n_a}, I_1, ..., I_{n_a}, R_1, ..., R_{n_a}, D_1, ..., D_{n_a})^T$, and $x_0 \in \mathcal{X}$, given by (4.2). Assume that θ_k is bounded for $k = 1, ..., n_a$, i.e there exists $\bar{\theta}_k > 0$ such that $|\theta_k(t)| \leqslant \bar{\theta}_k$ for all $t \geqslant 0$ and $k = 1, ..., n_a$.
Then, there exists a unique solution $x(t)$ to the system (4.1) for all $t \geqslant 0$.

Proof. Define the open set $\mathcal{D} = [0, N+1[^{4n_a}$.
The function $f : [0, N+1[^{4n_a} \to \mathbb{R}^{4n_a}$ whose components are defined by (4.3) is Lipschitz continuous on $\mathcal{D}$. Indeed, let $x, \tilde{x} \in \mathcal{D}$,

$$\begin{aligned}\|f(x) - f(\tilde{x})\|_{l^1} &= \sum_{i=1}^{4n_a} |f_i(x) - f_i(\tilde{x})| \\ &\leqslant \sum_{i=1}^{4n_a} L_i \|x - \tilde{x}\|_{l^1} \\ &=: L\|x - \tilde{x}\|_{l^1}.\end{aligned}$$

The second inequality follows from the definition of the functions f_i, the choice of $\mathcal{D}$ and the boundness of θ_k. The following development gives a proof of this relation for $k = 1, ..., n_a$. Similar calculations can be obtained for the other values of k. Let $k = 1, ..., n_a$,

$$\begin{aligned}|f_k(x) - f_k(\tilde{x})| &= \left|\lambda_k \left\{\tilde{S}_k \sum_{j=1}^{n_a} C_{kj}\tilde{I}_j - S_k \sum_{j=1}^{n_a} C_{kj} I_j\right\} + p_k\theta_k\left(\tilde{S}_k - S_k\right)\right| \\ &\leqslant \lambda_k \left\{\left|\tilde{S}_k \left(\sum_{j=1}^{n_a} C_{kj}\tilde{I}_j - \sum_{j=1}^{n_a} C_{kj} I_j\right)\right| + \left|\sum_{j=1}^{n_a} C_{kj} I_j \left(\tilde{S}_k - S_k\right)\right|\right\} \\ &\quad + |\theta_k| \left|\tilde{S}_k - S_k\right| \\ &\leqslant \lambda_k \left\{\left|\tilde{S}_k\right| \sum_{j=1}^{n_a} C_{kj} \left|\tilde{I}_j - I_j\right| + \left|\sum_{j=1}^{n_a} C_{kj} I_j\right| \left|\tilde{S}_k - S_k\right|\right\} + \bar{\theta}_k \left|\tilde{S}_k - S_k\right| \\ &\leqslant L_k \|x - \tilde{x}\|_{l^1},\end{aligned}$$

where $L_k = \max\left\{\lambda_k (N+1) \sum_{j=1}^{n_a} C_{kj}, \bar{\theta}_k\right\} > 0$.

Moreover, the compact set $\mathcal{X}$ is positively invariant with respect to Model (4.1) by Proposition 4.1.1. So the solution lies entirely in $\mathcal{X}$. Theorem 2.2.1 completes the proof. □

4.2 Stability

In the previous section, the well-posedness of the system in terms of existence and uniqueness of a solution and in term of coherent physical interpretation was established. Another important question to answer when one wants to a design control law concerns the stability of the system. The study of the system stability helps to predict its behavior over time. Moreover, it gives a hint on how one can act on the system to, for instance, prevent some

undesired behavior or to increase the performance of the system. The concept of stability is an important area in mathematics. In this section, a proposition concerning the semistability (see Definition 2.3.3) of the equilibria in open-loop is developed. For interested readers, Section 2.3 provides a brief overview of the concept of stability and gathers the key elements for the following proof.

Proposition 4.2.1

Let $\theta_k(\cdot) \geqslant 0$ for all $k = 1, ..., n_a$. The set of disease-free equilibria of the system (4.1),

$$X^\star = \{x \in \mathcal{X} : I_k = 0, k = 1, ..., n_a\}$$

is semistable. Hence, any trajectory starting in $\mathcal{X}$ converges to a given equilibrium point in this set, i.e. for all initial conditions $x_0 = (S_1(0), ..., S_{n_a}(0), I_1(0), ..., I_{n_a}(0), R_1(0), ..., R_{n_a}(0), D_1(0), ..., D_{n_a}(0))^T \in \mathcal{X}$, there exists a unique equilibrium $x^\star \in X^\star$ such that $x(t) \to x^\star$, as t tends to infinity, where $x(t)$ is the solution of System (4.1) with initial condition x_0.

Proof. An equation admits equilibrium points if the derivative of the variables with respect to time is zero. It is equivalent to cancel the right hand-side of Model (4.1). Therefore, it follows from the last ODE of (4.1) that $I_k^\star$ equals 0 for $k = 1, ..., n_a$. Moreover, the first and third equations imply to solve the relation $\theta_k^\star S_k^\star = 0$. Three cases can be considered, either $S_k^\star \neq 0$ then $\theta_k^\star = 0$ or $S_k^\star = 0$ and $\theta_k^\star \neq 0$ or $S_k^\star = \theta_k^\star = 0$. Furthermore, since there is no condition on the other variables, it follows that there is an infinity of possible equilibrium points $(S_k^\star, R_k^\star, D_k^\star)$ corresponding to the disease-free case $(I_k^\star = 0)$.
LaSalle's theorem 2.3.3 leads to the conclusion about the stability for the infected individuals. Indeed, consider $x = (S_1, ..., S_{n_a}, I_1, ..., I_{n_a}, R_1, ..., R_{n_a}, D_1, ..., D_{n_a})^T \in \mathcal{X} \subset \mathbb{R}_+^{4n_a}$ where $\mathcal{X}$ is a compact set which is positively invariant with respect to Model (4.1), by Proposition 4.1.1. Define the Lyapunov functional $V(x) = \sum_{k=1}^{n_a} S_k + I_k + R_k + \frac{1}{2} D_k \geqslant 0$. The time derivative of V along the trajectories of the System (4.1) is given by

$$\begin{aligned}
\dot{V}(x) &= \sum_{k=1}^{n_a} \frac{\delta V}{\delta S_k}\frac{dS_k}{dt} + \frac{\delta V}{\delta I_k}\frac{dI_k}{dt} + \frac{\delta V}{\delta R_k}\frac{dR_k}{dt} + \frac{\delta V}{\delta D_k}\frac{dD_k}{dt} \\
&= \sum_{k=1}^{n_a} -\gamma_{D_k} I_k(t) + \frac{1}{2}\gamma_{D_k} I_k(t)
\end{aligned}$$

$$= \sum_{k=1}^{n_a} \frac{-1}{2} \gamma_{D_k} I_k(t)$$
$$\leqslant 0$$

in $\mathcal{X}$. Therefore, by LaSalle's theorem 2.3.3, any solution starting in $\mathcal{X}$ converges to the set $X^\star$ as time goes to infinity. Moreover, since $\frac{dS_k(t)}{dt} \leqslant 0$ and $S_k(t) \geqslant 0$ for all $t \geqslant 0$, it follows that $S_k(t)$ converges to an equilibrium point $S_k^\star$. The same applies for $R_k(t)$ and $D_k(t)$ that are increasing and upper bounded by N_k for all $t \geqslant 0$. Therefore they converge to an equilibrium point $R_k^\star$ and $D_k^\star$. Finally, the semistability is obtained by combining LaSalle's theorem and convergence of bounded monotone functions. □

Notice that when computing the equilibria, the case $S_k^\star = 0$ and $\theta_k^\star \neq 0$ has no physical sense because it means that we need to pursue the vaccination whereas there is no more susceptible individual to vaccinate. Hence, in practice, null input at the equilibrium is imposed.

4.3 Numerical simulations

In this section, numerical simulations are performed, using parameters obtained in Chapter 3, recalled in Table 3.1. Notice that the time 0 in this simulation correspond to the day 41, which is the chosen start of the epidemic. Simulations are stopped when there remains less than one individuals in the simulation. The code is performed using an explicit Runge-Kutta (4,5) formula, thanks to the ODE45 function in MATLAB.

The dynamics of the proportion of infected population in open-loop, without vaccination, is illustrated in Figure 4.1. Without surprise, the disease eradication is observed, even if no vaccination is applied. This is due to the choice of the model, which is stable in open-loop, as mentioned in Proposition 4.2.1. Intuitively, this result is not surprising since there is a finite number of susceptible individuals and those individuals can only leave their compartment. After some time, the disease dies out since there is not enough susceptible individuals to infect anymore. Moreover, one can notice that the disease eradication occurs after 192 days. Therefore, one may aim to design a control law to reduce this time. Furthermore, the maximal total proportion of infected individuals is equal to 0.0432. This number can also be reduced thanks to the control law in order to not exceed the hospital beds capacity.
In addition, Figure 4.1 shows that the system is well-posed since all the quantities are greater than 0 and smaller that one in each class of age. This means that the number of individuals is smaller than the total number of individuals in each

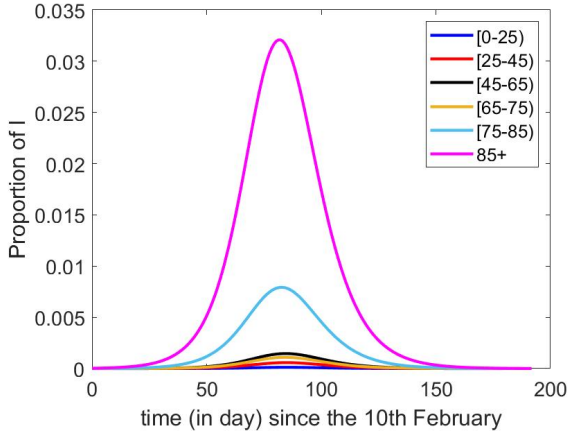

Figure 4.1 – Dynamics of the proportion of infected individuals without vaccination

class of age, given according to (Statbel (2023)) by $(1058304, 915796, 983789, 384803, 203035, 99516)$. The same applies for the susceptible, recovered and deceased individuals.
It can be surprising that, in Figure 4.1 the class of age with the most infected individuals is the class 85+. Indeed, for the covid-19 in Belgium, it seems (one needs to be careful about cases data) that there were more young individuals that were infected than the older ones. However, looking at the parameters obtained in Table 3.1 this result is not surprising since the transmission probability is much higher for the older classes of age.

Now that the dynamical analysis is performed, the considered system is better understood. Therefore, it can be interesting to act on it to improve some features of the system, such as the convergence time for instance. This is discussed in the following chapters.

Chapter 5

Observer-based output feedback

In this chapter a first control law is implemented. This vaccination law consists in an observer-based output feedback. It is built in two steps. First, a state feedback is developed in Section 5.2. Its feature is to linearize the system in closed-loop. Then, some control parameters are adjusted to ensure disease eradication exponentially fast. The characteristics of this feedback, in term of well-posedness, are studied. However, since this control law requires the knowledge of all the state, which is not available in practice, in a second step an observer-based output feedback is designed in Section 5.3. Finally, numerical simulations that corroborate the theoretical results are performed in Section 5.4.

5.1 Aim of the control

The control developed in the following is designed to decrease the largest number of infected individuals in the population, $\sum_{k=1}^{n_a} I_k(t)$. This is motivated by the fact that there are limited numbers of beds in hospitals. So the maximum number of infected individuals, all ages considered, at a given time should not be too large. This condition will indirectly decrease the number of deceased individuals. The next proposition emphasizes that vaccinating individuals helps to decrease the peak of infected individuals in the population.

Proposition 5.1.1

Consider two trajectories $x(t)$ and $\bar{x}(t)$ of Model (4.1) where only one class of age is considered, with the same initial conditions, $x(0) = \bar{x}(0) \in \mathcal{X}$, defined in (4.2). The first trajectory $x(\cdot)$ is obtained without vaccination whereas the second one $\bar{x}(\cdot)$ is obtained with

$$\theta(t) \geqslant 0 \quad \forall t \geqslant 0.$$

Then, the maximum number of infected individuals, all ages considered subject to the input $\theta(t)$ is smaller than the one without input, i.e

$$\max_{t \geqslant 0} \bar{I}(t) \leqslant \max_{t \geqslant 0} I(t).$$

Proof. When only one class of age is considered, the dynamics of the infected individuals are given by $\dot{I}(t) = \lambda_1 C_{11} S(t) I(t) - (\gamma_R + \gamma_D) I(t) =: \alpha S(t) I(t) - \gamma I(t)$ and the dynamics for the susceptible are given by $\dot{S}(t) = -\alpha S(t) I(t) - p_1 \theta(t) S(t)$.
Moreover, $\max_{t \geqslant 0} I(t) =: I_{\max}$ and $\max_{t \geqslant 0} \bar{I}(t) =: \bar{I}_{\max}$ are reached at times t_m and $\bar{t}_m$ such that $\dot{I}(t_m) = 0$ and $\dot{\bar{I}}(\bar{t}_m) = 0$ and $0 < I(t_m), \bar{I}(\bar{t}_m) \leqslant N_1$ since the C^1 functions $I(t)$ and $\bar{I}(t)$ tend to 0 as time tends to infinity, by Proposition 4.2.1. This implies that $S(t_m) = \bar{S}(\bar{t}_m) := \hat{S} = \dfrac{\gamma}{\alpha}$.
Now, considering $\dfrac{dS}{dI} = \dfrac{-\alpha S I - p_1 \theta S}{\alpha S I - \gamma I}$, defining $\tilde{\theta}(I) := \theta(t(I))$, for $t \in [0, t_m]$, and integrating, one gets

$$\int_{S_0}^{\hat{S}} \frac{\alpha S - \gamma}{S} dS = -\int_{I_0}^{\bar{I}_{\max}} \frac{\alpha I + p_1 \tilde{\theta}}{I} dI$$

$$\alpha \left(\hat{S} - S_0 \right) - \gamma \ln \left(\frac{\hat{S}}{S_0} \right) = -\alpha \left(\bar{I}_{\max} - I_0 \right) - p_1 \int_{I_0}^{\bar{I}_{\max}} \frac{\tilde{\theta}(I)}{I} dI,$$

where $x(0) = \bar{x}(0)$ is used. It follows that

$$\bar{I}_{\max} = -\frac{\gamma}{\alpha} + S_0 + \frac{\gamma}{\alpha} \ln \left(\frac{\gamma}{\alpha S_0} \right) + I_0 - \frac{p_1}{\alpha} \int_{I_0}^{\bar{I}_{\max}} \frac{\tilde{\theta}(I)}{I} dI, \tag{5.1}$$

In the case where no input is considered, (5.1) still holds with $\tilde{\theta}$ replaced by 0. Hence,

$$I_{max} = \bar{I}_{\max} + \frac{p_1}{\alpha} \int_{I_0}^{\bar{I}_{\max}} \frac{\tilde{\theta}(I)}{I} dI \geqslant \bar{I}_{\max}$$

because $\bar{I}_{max} \geqslant I_0$, $\tilde{\theta}(I) \geqslant 0$ for all I and $0 < I_0 < I < \bar{I}_{\max}$. □
Remark that this proposition implies that in order to decrease the maximum number of infected individuals in the whole population, it is better to vaccinate than doing nothing. This proposition still holds thanks to similar arguments, in the case of a state feedback law, $\theta(t) = \theta(S(t), I(t))$, since S is decreasing. Notice that attempts to demonstrate this proposition by comparing two vaccination laws have been made. However, the structure of the equations make this analysis complicated. Hence, this is still an open question.

5.2 State feedback

In this part, the model is put into normal form to implement a control law that implies that the infected individuals for each class of age are bounded by a decreasing exponential function, improving the result of asymptotic stability obtained in Proposition 4.2.1. However, this first law is not bounded. Hence, a second law, reducing the total number of infected individuals thanks to Proposition 5.1.1 is proposed. Then, conditions ensuring its physical feasibility are obtained. Those conditions concern the nonnegativity of the feedback and the fact that it is bounded.

5.2.1 Unconstrained linearizing state feedback design

In view of Model (4.1) and the control objectives, only the $2n_a$ first equations are needed in the feedback design. Indeed, for $k = 1, ..., n_a$, the control of $I_k(t)$ (and therefore $D_k(t)$) implies to take the dynamics of S_k and I_k into consideration. Therefore, the $2n_a$ first equations of Model (4.1) are a nonlinear control affine system, written in state space form as

$$\begin{cases} \dot{x}(t) &= f(x(t)) + g(x(t))\,\theta(t) \\ y(t) &= h(x(t)) \end{cases} \tag{5.2a}$$

where $x(t) = (I_1(t), ..., I_{n_a}(t), S_1(t), ..., S_{n_a}(t))^T \in \mathbb{R}^{2n_a}$, for all $t \geqslant 0$ is the state space vector, $h(x(t)) = (I_1(t), ..., I_{n_a}(t))^T \in \mathbb{R}^{n_a}, \forall t \geqslant 0$ is the measurable output function chosen equal to the infectious population and $\theta(t) = (\theta_1(t), ..., \theta_{n_a}(t))^T \in \mathbb{R}^{n_a}, \forall t \geqslant 0$ is the input function. Moreover,

$$g(x(t)) = \begin{pmatrix} 0_{n_a \times n_a} \\ -p_k diag(S_k(t))_{k=1,...,n_a} \end{pmatrix} \tag{5.2b}$$

and

$$f(x(t)) := (f_1(x(t)), ..., f_{2n_a}(x(t)))^T \tag{5.2c}$$

where

$$f_k(x(t)) = \lambda_k S_k(t) \sum_{k=1}^{n_a} C_{kj} I_j(t) - (\gamma_{R_k} + \gamma_{D_k}) I_k(t)$$
$$f_{n_a+k}(x(t)) = -\lambda_k S_k(t) \sum_{k=1}^{n_a} C_{kj} I_j(t)$$

for $k = 1, ..., n_a$.
In this case, the relative degree of the system, whose definition is recalled in Definition 2.5.1, equals the dimension of the state space for any $x \in \mathcal{D} \subset \mathbb{R}^{2n_a}$ where

$$\mathcal{D} = \left\{ x \in \mathbb{R}^{2n_a} \text{ s.t } S_k \neq 0 \text{ and } \sum_{j=1}^{n_a} C_{kj} I_j \neq 0, k = 1, ..., n_a \right\}. \tag{5.3}$$

Therefore, by Lemma 2.5.1 the "state space exact linearization problem", mentioned in Problem 2.5.1 is feasible. Hence, one can introduce a nonlinear invertible (for $x \in \mathcal{D}$) coordinate change

$$\begin{aligned} z_{1k}(t) &= h_k(x(t)) = I_k(t), \\ z_{2k}(t) &= L_f h_k(x(t)) = f_k(x(t)) \end{aligned} \tag{5.4}$$

for $k = 1, ..., n_a$. Notice that this change of variable is only invertible for $x \in \mathcal{D}$. However, the aim of the control is to bring the number of infected to zero, which does not belong to $\mathcal{D}$. Hence, in Subsection 5.2.3, a constrained feedback law is implemented to take this fact into account.
Thanks to this change of variable, the model dynamics in normal form, in the neighborhood of any $x \in \mathcal{D}$ is given by

$$\begin{cases} \dfrac{dz_{1k}(t)}{dt} = z_{2k}(t), \\ \dfrac{dz_{2k}(t)}{dt} = L_f^2 h_k(x(t)) + L_{g_k} L_f h_k(x(t)) \theta_k(t) \end{cases} \tag{5.5}$$

for $k = 1, ..., n_a$, where

$$\begin{aligned} L_f^2 h_k(x(t)) = \lambda_k S_k(t) \sum_{j=1}^{n_a} C_{kj} f_j(x(t)) \\ - (\gamma_{R_k} + \gamma_{D_k}) f_k(x(t)) + f_{n_a+k}(x(t)) \sum_{j=1}^{n_a} C_{kj} I_j(t). \end{aligned}$$

Let $A(x(t)) = diag\left(-p_k \lambda_k S_k(t) \sum_{j=1}^{n_a} C_{kj} I_j(t) \right)$, $k = 1, ..., n_a$. One can notice that this matrix is not invertible for all $x \in \mathcal{D}$. This will be taken care of in

Subsection 5.2.3 by using a constrained feedback, defined for all x such that $A(x)$ is invertible.
Moreover, define the vector $v\left(x\left(t\right)\right) = \begin{pmatrix} v_1\left(x\left(t\right)\right) & \cdots & v_{n_a}\left(x\left(t\right)\right) \end{pmatrix}^T$ such that $v_k\left(x\left(t\right)\right) = -\alpha_2^k f_k\left(x\left(t\right)\right) - \alpha_1^k I_k\left(t\right)$, where α_1^k and α_2^k are some free parameters that will be tuned in order to get stability.
Furthermore, $b\left(x\left(t\right)\right) = \begin{pmatrix} b_1\left(x\left(t\right)\right) & \cdots & b_{n_a}\left(x\left(t\right)\right) \end{pmatrix}^T$,
where $b_k\left(x\left(t\right)\right) = L_f^2 h_k\left(x\left(t\right)\right)$. This allows to design a stabilising and linearising state feedback.

Lemma 5.2.1
The state feedback control law defined by

$$\theta\left(t\right) = A^{-1}\left(x\left(t\right)\right)\left(v\left(x\left(t\right)\right) - b\left(x\left(t\right)\right)\right), \tag{5.6}$$

for all $x(t) \in \mathcal{D}$, where A, b and v are defined above, applied on system (5.2), induces the linear closed-loop output dynamics given by

$$\ddot{y}\left(t\right) + \tilde{A}_2 \dot{y}\left(t\right) + \tilde{A}_1 y\left(t\right) = 0. \tag{5.7}$$

where $\tilde{A}_i = diag(\alpha_i^k)$ for $i = 1, 2$ and $k = 1, ..., n_a$.

Proof. The control law (5.6) is obtained, inspired by Proposition 2.5.1. It can be rewritten as

$$\begin{aligned}
\theta\left(t\right) &= A^{-1}\left(x\left(t\right)\right)\left(v\left(x\left(t\right)\right) - b\left(x\left(t\right)\right)\right) \\
&= \begin{pmatrix} \dfrac{v_1(x(t)) - b_1\left(x\left(t\right)\right)}{p_1 \lambda_1 S_1(t) \displaystyle\sum_{j=1}^{n_a} C_{kj} I_j(t)} & \cdots & \dfrac{v_{n_a}(x(t)) - b_{n_a}\left(x\left(t\right)\right)}{p_{n_a} \lambda_{n_a} S_{n_a}(t) \displaystyle\sum_{j=1}^{n_a} C_{kj} I_j(t)} \end{pmatrix}^T. \\
&= \begin{pmatrix} \dfrac{v_1(x(t)) - L_f^2 h_1\left(x\left(t\right)\right)}{L_{g_1} L_f h_1\left(x\left(t\right)\right)} & \cdots & \dfrac{v_{n_a}(x(t)) - L_f^2 h_{n_a}\left(x\left(t\right)\right)}{L_{g_{n_a}} L_f h_{n_a}\left(x\left(t\right)\right)} \end{pmatrix}^T.
\end{aligned}$$

The closed-loop equations of Model (5.5) are linear and given by, for $k = 1, ..., n_a$,

$$\begin{cases} \dfrac{dz_{1k}\left(t\right)}{dt} = z_{2k}\left(t\right) \\ \dfrac{dz_{2k}\left(t\right)}{dt} = -\alpha_2^k z_{2k}\left(t\right) - \alpha_1^k z_{1k}\left(t\right) \end{cases}$$

which can be written as

$$\dot{z}\left(t\right) = \begin{pmatrix} 0_{n_a \times n_a} & Id_{n_a} \\ -\tilde{A}_1 & -\tilde{A}_2 \end{pmatrix} z\left(t\right),$$

$$:= \bar{A} z(t)$$

where $z(t) = \left(z_{1_1}(t) \cdots z_{1_n}(t)\, z_{2_1}(t) \cdots z_{2_{n_a}}(t)\right)^T$. The solution of this ODE yields the following expression of the output $y(t) = Cz(t) = \left(z_{1_1}(t) \cdots z_{1_{n_a}}(t)\right)^T$. $\dot{y}(t) = \left(z_{2_1}(t) \cdots z_{2_n}(t)\right)^T$ and

$$\ddot{y}(t) = \tilde{A}_1 y(t) + \tilde{A}_2 \dot{y}(t).$$

□

Moreover, the infected individuals converge exponentially to zero for the closed-loop system under some appropriate conditions.

Theorem 5.2.1
Pick an initial condition $x_0 \in \mathcal{D}$, where $\mathcal{D}$ is given by (5.3). Assume that the control tuning parameters satisfy $\alpha_j^k > 0$ for $j = 1, 2$ and $k = 1, ..., n_a$. Then, as long as the closed-loop states with the state feedback (5.6) remain in $\mathcal{D}$, the infected populations $I_k(t)$, for $k = 1, ..., n_a$, of Model (4.1), are bounded by a decreasing exponential function, i.e there exists $\mu > 0$ and $C > 0$ such that $x(t) \in \mathcal{D}$ and

$$I_k(t) \leqslant C \|I_k(0)\| e^{-\mu t}, \forall t \geqslant 0 \text{ and } k = 1, ..., n_a.$$

Moreover the susceptible, recovered and deceased populations converge asymptotically to some constants $S_k^\star, R_k^\star$ and $D_k^\star$ respectively, for $k = 1, ..., n_a$.

Proof. Since the closed-loop dynamics (5.7) is a system of decoupled ODEs it can be written as

$$\begin{cases} \dot{z}_{new}(t) = \hat{A} z_{new}(t), \\ y(t) = C z_{new}(t) \end{cases} \tag{5.8}$$

with $z_{new} = \begin{pmatrix} z_{1_1} & z_{2_1} & \cdots & z_{1_{n_a}} & z_{2_{n_a}} \end{pmatrix}^T$, $\hat{A} = blockdiag(\bar{A}_k)$, where $\bar{A}_k = \begin{pmatrix} 0 & 1 \\ -\alpha_1^k & -\alpha_2^k \end{pmatrix}$ and $C = \begin{pmatrix} 1 & 0 & 1 & \cdots & 1 & 0 \end{pmatrix}$.
Therefore, $\hat{A}$ is stable if all its eigenvalues are in the open left half-plane. However, the eigenvalues of $\hat{A}$ are those of the $\bar{A}_k$'s matrices. Moreover, those eigenvalues are the roots of the characteristic polynomial $P(s) = det(\bar{A}_k - sI) = s^2 + s\alpha_2^i + \alpha_1^i$. By the corollary of Lienard-Chipart, Theorem 2.5.2, since α_1^k and α_2^k are positive, the real parts of the eigenvalues of $\hat{A}$, are negative. Then the control law (5.6) exponentially stabilizes the model in normal form (5.5). Therefore, $z_{new}(t)$ exponentially converges asymptotically to zero. It follows

that $z_{1k}(t) = I_k(t)$ converges to zero as time goes to infinity for $k = 1, ..., n_a$. Moreover, by the convergence of bounded monotone functions, it follows that, for $k = 1, ..., n_a$, $S_k(t) \to S_k^\star$, $R_k(t) \to R_k^\star$ and $D_k(t) \to D_k^\star$ as times goes to infinity. □

Remark that the trajectory leaves $\mathcal{D}$ if there exists k such that $S_k = 0$ or $I_k = 0$ $\forall k = 1, ..., n_a$, which asymptotically happens. In those cases, the state feedback is not well defined. Therefore, an adapted feedback law, based on (5.6), will be introduced in Subsection 5.2.3.

5.2.2 Nonnegativity of the feedback

Obviously a vaccination law should be described by a nonnegative function. This in turn will ensure both a physical meaning and the nonnegativity of the state, as stated in Proposition 4.1.1. The following theorem provides sufficient conditions for the nonnegativity of the control law.

Theorem 5.2.2
Define

$$\Gamma = \max_{k=1,...,n_a} (\gamma_{R_k} + \gamma_{D_k})$$

For all $k = 1, ..., n_a$, select α_1^k and α_2^k such that

$$\alpha_1^k > (\gamma_{R_k} + \gamma_{D_k}) \left(\Gamma + \sum_{j=1}^{n_a} M_{kj} \right) \tag{5.9}$$

and

$$\alpha_2^k = \gamma_{R_k} + \gamma_{D_k} + \Gamma + \sum_{j=1}^{n_a} M_{kj}. \tag{5.10}$$

Then the state trajectories of Model (4.1) starting in $\mathcal{X}$ remain in $\mathcal{X}$, the input generated by the control law (5.6) is nonnegative and the conclusions of Theorem 5.2.1 hold.

Proof. First, one can notice that $S_k(t), I_k(t)$ and $D_k(t)$ are nonnegative for all $t \geqslant 0$ and $k = 1, ..., n_a$. This follows a same reasoning as in the proof of Proposition 4.1.1 (since the essential nonnegativity of the functions f_k is independent of the choice of θ_k for those variables).
The nonnegativity of $R_k(t)$, which is needed to conclude about the nonnegativity of $\theta_k(t)$, for all $t \geqslant 0$ and $k = 1, ..., n_a$ is not straightforward and

additional details are needed. First, since x_0 is in $\mathcal{X}$, it follows that $0 \leqslant S_k(0), I_k(0), R_k(0), D_k(0) \leqslant N_k$. Moreover, using (4.1),

$$\begin{aligned}
\dot{R}_k(0) &= \gamma_{R_k} I_k(0) + p_k \theta_k(0) S_k(0) \\
&\geqslant p_k \theta_k(0) S_k(0) \\
&= \frac{1}{\lambda_k \sum_{j=1}^{n_a} C_{kj} I_j(0)} \left[\alpha_1^k I_k(0) + f_k(x(0)) \left(\alpha_2^k - (\gamma_{R_k} + \gamma_{D_k})\right)\right. \\
&+ \lambda_k S_k(0) \sum_{j=1}^{n_a} C_{kj} \left\{ \lambda_j S_j(0) \sum_{l=1}^{n_a} C_{jl} I_l(0) \right. \\
&\left.\left. - \left(\gamma_{R_j} + \gamma_{D_j}\right) I_j(0) \right\} - \lambda_k S_k(0) \left(\sum_{j=1}^{n_a} C_{kj} I_j(0) \right)^2 \right]
\end{aligned}$$

by the vaccination law in (5.6) and the nonnegativity of I_k. Furthemore, by using the inequalities $I_j(0) \leqslant N_j$, $\gamma_{R_k} + \gamma_{D_k} \leqslant \Gamma$ and the nonnegativity of the states at time 0,

$$\begin{aligned}
\dot{R}_k(0) \geqslant & \frac{1}{\lambda_k \sum_{j=1}^{n_a} C_{kj} I_j(0)} \left[\alpha_1^k I_k(0) + f_k(x(0)) \left(- (\gamma_{R_k} + \gamma_{D_k}) + \alpha_2^k \right) \right. \\
& \left. - \lambda_k S_k(0) \Gamma \sum_{j=1}^{n_a} C_{kj} I_j(0) - \lambda_k S_k(0) \left(\sum_{j=1}^{n_a} C_{kj} I_j(0) \right) \left(\sum_{j=1}^{n_a} M_{kj} \right) \right] \\
\geqslant & \frac{1}{\lambda_k \sum_{j=1}^{n_a} C_{kj} I_j(0)} \times \left[I_k(0) \left\{ \alpha_1^k - (\gamma_{R_k} + \gamma_{D_k}) \left(\Gamma + \sum_{j=1}^{n_a} M_{kj} \right) \right\} \right. \\
& \left. + f_k(x(0)) \left\{ \alpha_2^k - \gamma_{R_k} - \gamma_{D_k} - \Gamma - \sum_{j=1}^{n_a} M_{kj} \right\} \right],
\end{aligned}$$

where the fact that

$$\lambda_k S_k(t) \sum_{j=1}^{n_a} C_{kj} I_j(t) = f_k(x(t)) + (\gamma_{R_k} + \gamma_{D_k}) I_k(t) \tag{5.11}$$

was used as long as the relation $C_{kj} = \dfrac{M_{kj}}{N_j}$. Hence, using conditions (5.9) and (5.10), $\dot{R}_k(0) > 0$. Using continuity of $\dot{R}_k$, there exists a time $t_1 > 0$ such

that $\dot{R}_k(t) > 0$ for all $t \in [0, t_1)$. Moreover, since R_k is strictly increasing on $[0, t_1)$ and $R_k(0) = 0$, there exists $t_2 > t_1$ such that $R_k(t) > 0 \ \forall \ t \in [0, t_2)$. The aim of this part is to prove that $R_k(t) > 0$ for all $t \geqslant 0$ because this assumption will lead to the nonnegativity of the state feedback. Thus, by an absurd reasoning, assume there exists a time $t_3 > t_1$ such that $R_k(t_3) = 0$ for the first time and $R_k(t) \leqslant 0$ for $t \in (t_3, t_4]$. This is only possible if $\dot{R}_k(t) \leqslant 0$ for all t in $I \subseteq [t_1, t_3]$. However, let $t \in [t_1, t_3]$,

$$\begin{aligned} \dot{R}_k(t) \leqslant 0 &\Leftrightarrow -\left(\dot{S}_k + \dot{I}_k + \dot{D}_k\right)(t) \leqslant 0 \\ &\Leftrightarrow -p_k\theta_k(t)S_k(t) - \gamma_{R_k} I_k(t) \geqslant 0, \end{aligned} \tag{5.12}$$

by equations (4.1). Moreover, for $t \in [0, t_3]$,

$$\begin{aligned} p_k\theta_k(t)\, S_k(t) =& \frac{1}{\lambda_k \sum_{j=1}^{n_a} C_{kj} I_j(t)} \left[\alpha_1^k I_k(t) + f_k(x(t))\left(\alpha_2^k - (\gamma_{R_k} + \gamma_{D_k})\right)\right] \\ &+ \lambda_k S_k(t) \sum_{j=1}^{n_a} C_{kj} \left\{ \lambda_j S_j(t) \sum_{l=1}^{n_a} C_{kl} I_l(t) \right. \\ &\left. - \left(\gamma_{R_j} + \gamma_{D_j}\right) I_j(t) \right\} - \lambda_k S_k(t) \left(\sum_{j=1}^{n_a} C_{kj} I_j(t) \right)^2 \Bigg] \\ \geqslant& \frac{1}{\lambda_k \sum_{j=1}^{n_a} C_{kj} I_j(t)} \left[\alpha_1^k I_k(t) + f_k(x(t))\left(\alpha_2^k - (\gamma_{R_k} + \gamma_{D_k})\right)\right] \\ &- \lambda_k S_k(t) \sum_{j=1}^{n_a} C_{kj} \left(\gamma_{R_j} + \gamma_{D_j}\right) I_j(t) \\ &- \lambda_k S_k(t) \left(\sum_{j=1}^{n_a} C_{kj} I_j(t) \right)^2 \Bigg] \end{aligned}$$

By using $I_k(t) \leqslant N_k$, since $S_k(t) + I_k(t) + R_k(t) + D_k(t) = N_k$ and all the quantities are nonnegative for $t \in [0, t_3]$, by definition of t_3 and using $\gamma_{R_k} + \gamma_{D_k} \leqslant \Gamma$ for $k = 1, ..., n_a$, it follows that

$$\begin{aligned} p_k\theta_k(t)S_k(t) \geqslant& \frac{1}{\lambda_k \sum_{j=1}^{n_a} C_{kj} I_j(t)} \left[\alpha_1^k I_k(t) + f_k(x(t))\left(\alpha_2^k - (\gamma_{R_k} + \gamma_{D_k})\right)\right] \\ &- \lambda_k S_k(t)\, \Gamma \sum_{j=1}^{n_a} C_{kj} I_j(t) \end{aligned}$$

$$
\begin{aligned}
&-\lambda_k S_k(t)\left(\sum_{j=1}^{n_a} C_{kj} I_j(t)\right)\left(\sum_{j=1}^{n_a} M_{kj}\right)\Bigg] \\
\geqslant &\frac{1}{\lambda_k \sum_{j=1}^{n_a} C_{kj} I_j(t)} \times \Bigg[I_k(t)\left\{\alpha_1^k - (\gamma_{R_k}+\gamma_{D_k})\left(\Gamma + \sum_{j=1}^{n_a} M_{kj}\right)\right\} \\
&+ f_k(x(t))\left\{\alpha_2^k - \gamma_{R_k} - \gamma_{D_k} - \Gamma - \sum_{j=1}^{n_a} M_{kj}\right\}\Bigg],
\end{aligned}
$$

by using equality (5.11). Then, $p_k\theta_k(t)S_k(t) > 0\ \forall t \in [0, t_3]$, thanks to the choice of conditions (5.9) and (5.10). Hence, $-p_k\theta_k(t)S_k(t) - \gamma_{R_k} I_k(t) < 0$ and a contradiction occurs with (5.12). Therefore, $R_k(t) > 0$ for all $t \geqslant 0$. Then, the previous reasoning for θ_k can be performed for all $t \geqslant 0$, where the assumption $I_k(t) \leqslant N_k$ holds for all $t \geqslant 0$ since it has just be proven that the states are nonnegative, and it is known that their sum equals N_k, yielding the nonnegativity of the vaccination law thanks to the choice of conditions (5.9) and (5.10).
Moreover, since the feedback design parameters are positive, Theorem 5.2.1 concludes the proof. □

5.2.3 Constrained state feedback design

Previously, a stabilizing state feedback law has been defined by

$$
\theta(t) = \left(\frac{v_1 - L_f^2 h_1(x(t))}{L_{g_1} L_f h_1(x(t))} \quad \cdots \quad \frac{v_{n_a} - L_f^2 h_{n_a}(x(t))}{L_{g_{n_a}} L_f h_{n_a}(x(t))}\right)^T,
$$

where $L_{g_k} L_f h_k(x(t)) = -p_k \lambda_k S_k(t) \sum_{j=1}^{n_a} C_{kj} I_j(t)$, by definition of the Lie derivative and of the functions g_k, f and h_k. As predicted in Theorem 5.2.1, $\sum_{j=1}^{n_a} C_{kj} I_j(t)$ tends to 0 and the feedback blows up. To avoid this and to take into account an amplitude constraint on the vaccination, denoted by θ_{sup}, a new control law is defined, inspired by the previous one but with saturation and insurance that x is in $\mathcal{D}$ when the law (5.6) is used. This law will solve the second problem that consists, as mentioned before, of designing an amplitude limited control that improves performance with respect to the open-loop system regarding the peak of total infected individuals (thanks to Proposition 5.1.1), while maintaining asymptotic convergence.

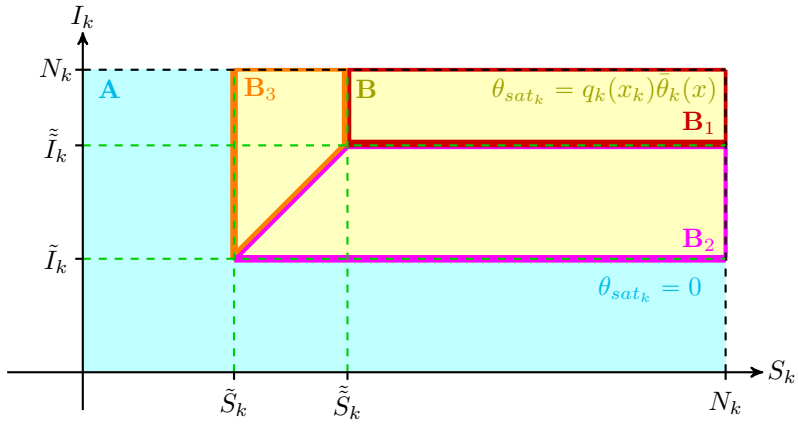

Figure 5.1 – Representation of the construction of the constrained feedback law, $\theta_{sat_k}(x)$

Let us define a new state feedback law by

$$\theta_{sat_k} : [0, N_k]^{n_a+1} \to \mathbb{R}$$

where, with $x = (S_k, I_1, ..., I_{n_a})$,

$$\theta_{sat_k}(x) = \begin{cases} (q_k\bar{\theta}_k)(x) & \text{if } S_k \geqslant \tilde{S}_k \text{ and } I_k \geqslant \tilde{I}_k \ (B \text{ region}) \\ 0 & \text{otherwise} \ \ (A \text{ region}) \end{cases} \tag{5.13}$$

where $(q_k\bar{\theta}_k)(x)$ denotes $q_k(x)\bar{\theta}_k(x)$ and the regions refer to the visual representation, available in Figure 5.1.

The functions $\bar{\theta}_k$ and q_k are defined on $\left[\tilde{S}_k, N_k\right] \times [0, N_k] \times \cdots \times [0, N_k] \times \left[\tilde{I}_k, N_k\right] \times [0, N_k] \times \cdots \times [0, N_k]$ and allow the new state feedback law (5.13) to have desired properties, such as bounded and Lipschitz properties. They are given by

$$\bar{\theta}_k(x) = \begin{cases} \theta_k(x) & \text{if } \theta_k(x) \leqslant \theta_{sup} \\ \theta_{sup} & \text{otherwise.} \end{cases} \tag{5.14}$$

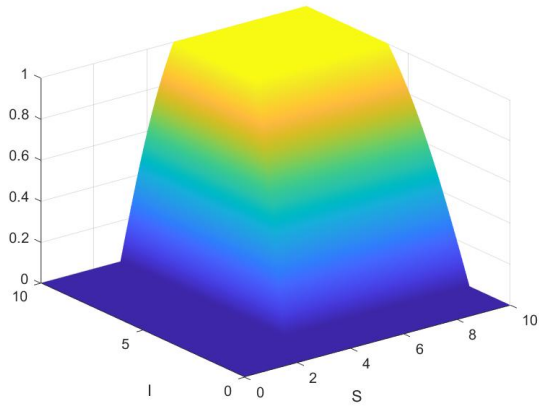

Figure 5.2 – Representation of the vaccination law $\theta_{sat_k}(t)$

and

$$q_k(x) = \begin{cases} 1 & \text{if } S_k \geqslant \tilde{\tilde{S}}_k \text{ and } I_k \geqslant \tilde{\tilde{I}}_k (B_1 \text{ region}) \\ \dfrac{4}{\pi} \arctan\left(\dfrac{I_k - \tilde{I}_k}{\tilde{\tilde{I}}_k - \tilde{I}_k}\right) & \text{if } I_k \leqslant \dfrac{\tilde{\tilde{I}}_k - \tilde{I}_k}{\tilde{\tilde{S}}_k - \tilde{S}_k}\left(S_k - \tilde{S}_k\right) + \tilde{I}_k \\ & \text{and } I_k < \tilde{\tilde{I}}_k \ (B_2 \text{ region}) \\ \dfrac{4}{\pi} \arctan\left(\dfrac{S_k - \tilde{S}_k}{\tilde{\tilde{S}}_k - \tilde{S}_k}\right) & \text{otherwise } (B_3 \text{ region}), \end{cases} \tag{5.15}$$

where the constants $\tilde{\tilde{S}}_k$ and $\tilde{\tilde{I}}_k$ are chosen larger than $\tilde{S}_k$ and $\tilde{I}_k$, respectively. Moreover, $\tilde{S}_k$ and $\tilde{I}_k$ have to be selected appropriately as shown in the following. The intuition for the choice of the function $q(x)$ can be understood thanks to Figure 5.1, where the idea is to obtain the value 1 at the common boundary of regions B_2 and B_3 with B_1 and to obtain 0 at the common boundary of those two regions with A. The computational details in Appendix A help to understand the relevance of this choice.
This new vaccination law is represented in Figure 5.2 for $\tilde{S} = 3, \tilde{\tilde{S}} = 5, \tilde{I} = 2, \tilde{\tilde{I}} = 6$. With this definition, θ_{sat_k} is globally bounded and Lipschitz as function of I_k and S_k. Those properties will be useful in the design of the observer-based output feedback, developed in Section 5.3. Some performance properties of this law are shown in the sequel.

The first result states the asymptotic stability of the trajectories for the closed-loop model under saturated feedback.

Proposition 5.2.1
Assume that the control tuning parameters satisfy assumptions of Theorem 5.2.2. Then, the saturated state feedback (5.13) implies the semistability of the disease-free equilibria of Model (4.1). Moreover the susceptible, recovered and deceased populations converge asymptotically to some constants $S_k^\star, R_k^\star$ and $D_k^\star$, respectively, for $k = 1, ..., n_a$.

Proof. This proposition is a direct consequence of Proposition 4.2.1 since the saturated state feedback (5.13) is, by construction, nonnegative. □

The following lemma introduces an invariant set helpful to prove that the constrained feedback law (5.13) has a finite number of jumps.

Lemma 5.2.2
Let $\tilde{I}_k > 0$ and $\tilde{S}_k \leqslant \dfrac{(\gamma_{R_k} + \gamma_{D_k})\,\tilde{I}_k}{\lambda_k \displaystyle\sum_{j=1}^{n_a} M_{kj}}$. Then, the set $\left[0, \tilde{S}_k\right] \times \left[0, \tilde{I}_k\right]$ is invariant with respect to Model (4.1), for any nonnegative input.

Proof. First, observe that the nonnegativity follows from Proposition 4.1.1 since θ_{sat_k} is nonnegative. Moreover, let $(S_k(t), I_k(t)) \in \left[0, \tilde{S}_k\right] \times \left[0, \tilde{I}_k\right]$, for some $t \geqslant 0$ arbitrarily fixed.
For, S_k, two cases can happen. Either there exists t_1 such that $S_k(t_1) = 0$, in that case, $\dot{S}_k(t_1) = 0$. It follows that $S_k(t) = 0$ for all $t \geqslant t_1$ and remains in $\left[0, \tilde{S}_k\right]$. Either $S_k(t) \neq 0$ for all $t \geqslant 0$. It follows that $\dfrac{dS_k(t)}{dt} < 0$ since the input is nonnegative. Therefore, at the border, when $S_k(t) = \tilde{S}_k$, the solution remains in the set $\left[0, \tilde{S}_k\right] \times \left[0, \tilde{I}_k\right]$. Furthemore, focus on what happens at the other border, when $I_k(t) = \tilde{I}_k$ and $S_k(t) \leqslant \tilde{S}_k(t)$. Then,

$$
\begin{aligned}
S_k(t) \leqslant \tilde{S}_k \leqslant \frac{(\gamma_{R_k} + \gamma_{D_k})\,\tilde{I}_k}{\lambda_k \displaystyle\sum_{j=1}^{n_a} M_{kj}} &\leqslant \frac{(\gamma_{R_k} + \gamma_{D_k})\,\tilde{I}_k}{\lambda_k \displaystyle\sum_{j=1}^{n_a} C_{kj} I_j} \\
\Rightarrow \lambda_k S_k(t) \sum_{j=1}^{n_a} C_{kj} I_j - (\gamma_{R_k} + \gamma_{D_k})\,\tilde{I}_k &\leqslant 0 \\
\Leftrightarrow \frac{dI_k(t)}{dt} &\leqslant 0.
\end{aligned}
$$

Therefore, it holds that the set $\left[0, \tilde{S}_k\right] \times \left[0, \tilde{I}_k\right]$ is invariant. □

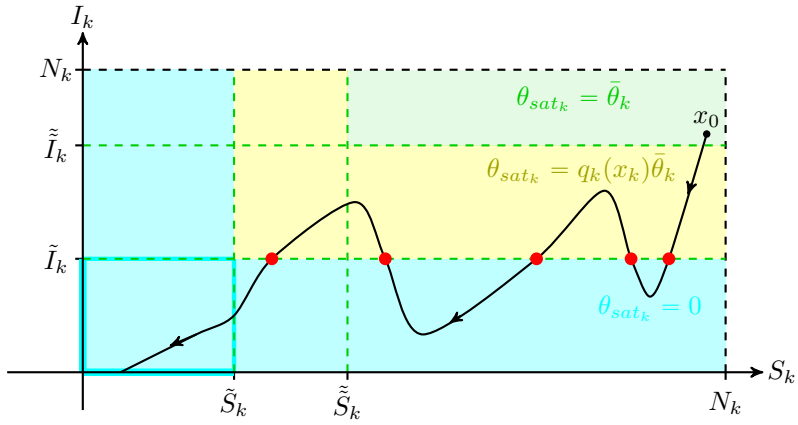

Figure 5.3 – Illustration of the finite number of jumps for the saturated vaccination law, $\theta_{sat_k}(t)$

The next property ensures that the solution will end up in a situation where the vaccination law (5.13) can not switch anymore, in finite time.

Property 5.2.1

Let $\tilde{I}_k$ and $\tilde{S}_k$ be chosen as in Lemma 5.2.2 and let $x_0 \in \mathcal{X}$. Then, there exists $n_{x_0} \in \mathbb{N}$ such that $I_k(t_{n_{x_0}}) = \tilde{I}_k$. Therefore, there is a finite number of jumps $m \leqslant n_{x_0}$ for the function θ_{sat_k} defined in (5.13).

Proof. Let $k = 1, ..., n_a$, and consider three cases. First, assume that there exists $T > 0$ such that $S_k(T) = 0$. In that case, $S_k(t) = 0$ for all $t \geqslant T$ since $\dot{S}_k(T) = 0$, implying that $S_k(t) = 0 < \tilde{S}_k$ for all $t \geqslant T$. Then, no more jump is possible thanks to the definition (5.13) of θ_{sat_k}.

Second, assume that there exists $T > 0$ such that $\lambda_k \sum_{j=1}^{n_a} C_{kj} I_j(T) + p_k \theta_{sat_k}(T) = 0$. Thanks to the nonnegativity of the elements in the equation, this case is only possible if $I_k(T) = 0$ for all $k = 1, ..., n_a$ and if $\theta_{sat_k}(T) = 0$. Therefore, $\dot{I}_k(T) = 0$ implying that $I_k(t) = 0 < \tilde{I}_k$ for all $t \geqslant T$. Then, no more jump is possible thanks to the definition (5.13) of θ_{sat_k}.

Finally, in the case where $S_k(t) \neq 0$ and $\lambda_k \sum_{j=1}^{n_a} C_{kj} I_j(t) + p_k \theta_{sat_k}(t) \neq 0$, $k = 1, ..., n_a$, $t \geqslant 0$ then $S_k(t)$ is strictly decreasing, since the feedback $\theta_{sat_k}(t)$

is nonnegative. Moreover, S_k has zero as a lower bound therefore it converges to some equilibrium $S_k^\star$. Since $I_k(t)$ tends to zero, thanks to Proposition 5.2.1, so the couple $(S_k(t), I_k(t))$ tends to $(S_k^\star, 0)$ when t goes to infinity. By contradiction, assume that there exists an infinite number of switches. In this case, there always exist time instants t such that $I_k(t) \geqslant \tilde{I}_k$, for the switches to occur. This contradicts the fact that the infected individuals tend to zero. Remark that, in the case where the equilibrium is such that $S_k^\star < \tilde{S}_k$, illustrated in Figure 5.3, the strictly decreasing property of S_k can be invoked to show that there exists a finite time instant T where $S_k(T) = \tilde{S}_k$. Afterwards, the control law will remain switch off and the trajectory will enter the invariant region $\left[0, \tilde{S}_k\right] \times \left[0, \tilde{I}_k\right]$ since the infected individuals tend to 0. □

Finally, it can be shown that the constrained feedback law, as defined in (5.13), is Lipschitz. This property is a crucial assumption for the design of an observer-based output feedback, presented in the next section.

Property 5.2.2
The function θ_{sat_k} is Lipschitz on its domain.

Proof. This proof is quite computational. Therefore, only some key elements are presented here. Some additional information is available in Appendix A. Moreover, the reader can refer to Figure 5.1 to better understand the regions considered in each case.
Let $z_k = (x_k, y_1, \cdots, y_k, \cdots, y_{n_a})^T$ and $z'_k = (x'_k, y'_1, \cdots, y'_k, \cdots, y'_{n_a})^T \in [0, N_k]^{n_a+1}$. Three main cases can be identified.

1. Assume that z_k and z'_k are such that $x_k, x'_k < \tilde{S}_k$ or $y_k, y'_k < \tilde{I}_k$ (z_k and $z'_k \in A$). Hence, $|\theta_{sat_k}(z_k) - \theta_{sat_k}(z'_k)| = 0 \leqslant L_0 \|z_k - z'_k\|_{l^1}$ for all $L_0 > 0$.

2. Assume that z_k and z'_k are such that (x_k, y_k) and $(x'_k, y'_k) \in \left[\tilde{S}_k, N_k\right] \times \left[\tilde{I}_k, N_k\right]$ (z_k and $z'_k \in B$). Therefore,

$$\begin{aligned} |\theta_{sat_k}(z_k) - \theta_{sat_k}(z'_k)| &= |(q_k\bar{\theta}_k)(z_k) - (q_k\bar{\theta}_k)(z'_k)| \\ &\leqslant L\|z_k - z'_k\|_{l^1}, \end{aligned}$$

   with $L > 0$, the Lipschitz constant of $q_k\bar{\theta}_k$ (see details in Appendix A).

3. Assume that z_k and z'_k are such that $(x_k, y_k) \in \left[\tilde{S}_k, N_k\right] \times \left[\tilde{I}_k, N_k\right]$ and $x'_k < \tilde{S}_k$ or $y'_k < \tilde{I}_k$ ($z_k \in B$ and $z'_k \in A$). Then,

$$\begin{aligned} |\theta_{sat_k}(z_k) - \theta_{sat_k}(z'_k)| &= |(q_k\bar{\theta}_k)(z_k)| \\ &= (q_k\bar{\theta}_k)(z_k). \end{aligned}$$

Three subcases can again be identified.

(a) z_k such that $(x_k, y_k) \in \left[\tilde{S}_k, N_k\right] \times \left[\tilde{I}_k, N_k\right]$ with $x_k \geqslant \tilde{\tilde{S}}_k$ and $y_k \geqslant \tilde{\tilde{I}}_k$ ($z_k \in B_1$). Hence,

$$\begin{aligned} |\theta_{sat_k}(z_k) - \theta_{sat_k}(z'_k)| &= \bar{\theta}_k(z_k) \\ &\leqslant \theta_{sup} \\ &\leqslant L_1 \|z_k - z'_k\|_{l^1} \end{aligned}$$

where $L_1 = \dfrac{\theta_{sup}}{d(A, B_1)}$ with

$$d(A, B_1) = \inf_{a \in A, b \in B_1} \|a - b\|_{l^1},$$

since by definition, $d(A, B_1) \leqslant \|z_k - z'_k\|_{l^1}$.

(b) z_k such that $(x_k, y_k) \in \left[\tilde{S}_k, N_k\right] \times \left[\tilde{I}_k, N_k\right]$ with $y_k \leqslant \dfrac{\tilde{\tilde{I}}_k - \tilde{I}_k}{\tilde{\tilde{S}}_k - \tilde{S}_k}\left(x_k - \tilde{S}_k\right) + \tilde{I}_k$ and $y_k < \tilde{\tilde{I}}_k$ ($z_k \in B_2$). Therefore,

$$\begin{aligned} |\theta_{sat_k}(z_k) - \theta_{sat_k}(z'_k)| &= q_k(z_k)\bar{\theta}_k(z_k) \\ &\leqslant \frac{4}{\pi} \arctan\left(\frac{y_k - \tilde{I}_k}{\tilde{\tilde{I}}_k - \tilde{I}_k}\right) \theta_{sup} \\ &\leqslant \frac{4\theta_{sup}}{\pi(\tilde{\tilde{I}}_k - \tilde{I}_k)}(y_k - \tilde{I}_k) \\ &=: L_2(y_k - \tilde{I}_k) \end{aligned}$$

since arctan is a Lipschitz function with constant 1. Now, if $y'_k \leqslant \tilde{I}_k$, then

$$\begin{aligned} |\theta_{sat_k}(z_k) - \theta_{sat_k}(z'_k)| &\leqslant L_2\left[(y_k - y'_k) + (y'_k - \tilde{I}_k)\right] \\ &\leqslant L_2(y_k - y'_k) \\ &\leqslant L_2 \|z_k - z'_k\|_{l^1}. \end{aligned}$$

On the other hand, if $y'_k > \tilde{I}_k$, that means that $x'_k \leqslant \tilde{S}_k$ and we have that

$$\begin{aligned} |\theta_{sat_k}(z_k) - \theta_{sat_k}(z'_k)| &\leqslant L_2 \frac{\tilde{\tilde{I}}_k - \tilde{I}_k}{\tilde{\tilde{S}}_k - \tilde{S}_k}(x_k - \tilde{S}_k) \\ &=: L_3\left[(x_k - x'_k) + (x'_k - \tilde{S}_k)\right] \\ &\leqslant L_3(x_k - x'_k) \\ &\leqslant L_3 \|z_k - z'_k\|_{l^1}. \end{aligned}$$

(c) z_k such that $(x_k, y_k) \in \left[\tilde{S}_k, N_k\right] \times \left[\tilde{I}_k, N_k\right]$ with $y_k > \dfrac{\tilde{\tilde{I}}_k - \tilde{I}_k}{\tilde{\tilde{S}}_k - \tilde{S}_k}\left(x_k - \tilde{S}_k\right) + \tilde{I}_k$ and $x_k < \tilde{\tilde{S}}_k$ ($z_k \in B_3$). By using similar reasoning as (b), it follows that

$$|\theta_{sat_k}(z_k) - \theta_{sat_k}(z'_k)| \leqslant L_4 \|z_k - z'_k\|_{l^1}.$$

Therefore, there exists $K = \max\{L_0, L, L_1, L_2, L_3, L_4\} > 0$ such that, for all z_k and $z'_k \in [0, N_k]^{n_a+1}$,

$$|\theta_{sat_k}(z_k) - \theta_{sat_k}(z'_k)| \leqslant K \|z_k - z'_k\|_{l^1}.$$

□

5.3 Observer-based output feedback

The feedback law introduced in the previous section is a state feedback law. This means that the knowledge of the full state at each time is assumed in order to compute the feedback. However, it is not often the case in practice. Usually, only a part of the state is known, corresponding to some measurements. In the case of epidemic, one usually measures the number of dead individuals in each class of age. Therefore, the goal of this section is to design and analyze an observer-based output feedback law which is based only on such measurements. The technique used in this work is based on the separation principle introduced in (Atassi and Khalil (1999)) and recalled in Theorem 2.6.1 for multi-input multi-output systems.

Moreover since in the case of epidemic, data on the dead individuals can be collected, Model (4.1) is used where only the equations of S_k, I_k and D_k are kept due to the constant population assumption, with outputs given by $y_k(t) = D_k(t)$, $k = 1, ..., n_a$.

In order to fit the framework of Theorem 2.6.1, a change of variable is performed:

$$\begin{aligned} z_{1k}(t) &= D_k^\star - D_k(t), \\ z_{2k}(t) &= -\dot{D}_k(t) = -\gamma_{D_k} I_k(t) \\ z_{3k}(t) &= -\gamma_{D_k} \dot{I}_k(t) \\ &= -\gamma_{D_k} \left\{ \lambda_k S_k(t) \sum_{j=1}^{n_a} C_{kj} I_j(t) - (\gamma_{R_k} + \gamma_{D_k}) I_k(t) \right\} \end{aligned} \tag{5.16}$$

for $k = 1, ..., n_a$, where $D_k^\star$ is assumed to be known and stands for the equilibrium for the dead individuals, obtained for the closed-loop system under exact state feedback (5.13). Remark that this change of variable corresponds to the

change of variable (5.4) introduced previously, for z_{2k} and z_{3k}, $k = 1, ..., n_a$, up to multiplication by the factor $-\gamma_{D_k}$. Therefore, it is also invertible if $\sum_{j=1}^{n_a} C_{kj} I_j \neq 0$. Indeed, the nominal coordinates can be obtained by

$$\begin{aligned} D_k(t) &= D_k^\star - z_{1k}(t), \\ I_k(t) &= \frac{-z_{2k}(t)}{\gamma_{D_k}} \\ S_k(t) &= \begin{cases} S_k^\star & \text{if } z_{2j} = 0 \ \ \forall j \\ \dfrac{\dfrac{z_{3k}(t)}{\gamma_{D_k}} + (\gamma_{R_k} + \gamma_{D_k}) \dfrac{z_{2k}(t)}{\gamma_{D_k}}}{\lambda_k \sum_{j=1}^{n_a} \tilde{C}_{kj} z_{2j}(t)} & \text{otherwise} \end{cases} \end{aligned} \tag{5.17}$$

where $\tilde{C}_{kj} = \dfrac{C_{kj}}{\gamma_{D_j}} = \dfrac{M_{kj}}{\gamma_{D_j} N_j}$ and $S_k^\star$ is the equilibrium for the susceptible individuals in the kth class of age. Remark that this value does not need to be computed since it is known that the state feedback is 0 in this case. In simulation, one does not need to compute the output feedback in this case, it can just be set to 0.

One can notice that $z_{2j} = 0$ for all $j = 1, ..., n_a$ is equivalent to the fact that $I_j = 0$ for all $j = 1, ..., n_a$. Therefore, it implies that $z_{3j} = 0$ for all $j = 1, ..., n_a$ in view of the change of variable (5.16).

Therefore, in the new variables, Model (4.1) becomes

$$\begin{cases} \dot{z}_{1_k}(t) = z_{2k}(t) \\ \dot{z}_{2_k}(t) = z_{3k}(t) \\ \dot{z}_{3_k}(t) = \begin{cases} 0 & \text{if } z_{2j}, z_{3j} = 0 \ \ \forall j \\ h_k(z(t)) & \text{otherwise} \end{cases} \end{cases} \tag{5.18a}$$

where

$$\begin{aligned} h_k(z(t)) &= (z_{3k}(t) + (\gamma_{R_k} + \gamma_{D_k}) z_{2k}(t)) \\ &\times \left[\lambda_k \sum_{j=1}^{n_a} \tilde{C}_{kj} z_{2j}(t) - p_k \theta_{sat_k}(t) + \frac{\sum_{j=1}^{n_a} \tilde{C}_{kj} z_{3j}(t)}{\sum_{j=1}^{n_a} \tilde{C}_{kj} z_{2j}(t)} - (\gamma_{R_k} + \gamma_{D_k}) \right] \\ &+ (\gamma_{R_k} + \gamma_{D_k})^2 z_{2k}(t) \end{aligned} \tag{5.18b}$$

Letting $z = \begin{pmatrix} z_{11} & z_{21} & z_{31} & z_{12} & z_{22} & z_{32} & ... & z_{3n_a} \end{pmatrix}^T$ and A, B and C as in Theorem 2.6.1, i.e. $A = \text{blockdiag}[\tilde{A}, ..., \tilde{A}]_{3n_a \times 3n_a}$, $B = \text{blockdiag}[\tilde{B}, ..., \tilde{B}]_{3n_a \times n_a}$ and $C = \text{blockdiag}[\tilde{C}, ..., \tilde{C}]_{n_a \times 3n_a}$, where

$$\tilde{A} = \begin{pmatrix} 0 & 1 & 0 \\ 0 & 0 & 1 \\ 0 & 0 & 0 \end{pmatrix}, \tilde{B} = \begin{pmatrix} 0 & 0 & 1 \end{pmatrix}^T, \tilde{C} = \begin{pmatrix} 1 & 0 & 0 \end{pmatrix},$$

(5.18) is rewritten under the form (2.20), i.e.

$$\begin{cases} \dot{z}(t) = Az(t) + B\phi(z(t), u(t)) \\ y(t) = Cz(t) \end{cases}$$

with $z(0) = z_0$, where $z \in \mathcal{Z} \subseteq \mathbb{R}^{3n_a}$, $u = \theta_{sat}(z(t)) = \begin{pmatrix} \theta_{sat_1}(z(t)) & ... & \theta_{sat_{n_a}} \end{pmatrix}^T$ such that $u \in \mathcal{U} = \{\theta \in \mathbb{R}^{n_a} : 0 \leqslant \theta_k \leqslant \theta_{sup}\} \subseteq \mathbb{R}^{n_a}$, $y \in \mathcal{Y} \subseteq \mathbb{R}^{n_a}$ and $\phi(z, u) = \begin{pmatrix} \phi_1(z, u) & ... & \phi_{n_a}(z, u) \end{pmatrix}^T$ where $\phi_k(z, u) = \begin{cases} 0 & \text{if } z_{2j}, z_{3j} = 0 \ \forall j \\ h_k(z(t)) & \text{otherwise,} \end{cases}$

for $k = 1, ..., n_a$.

It remains to prove that the assumptions of Theorem 2.6.1 are satisfied. Then, the desired observer-based output feedback will be obtained using the high-gain observer (2.22). For this proof the uniform norm on $\mathbb{R}^{3n_a}$ is used.

Lemma 5.3.1

The function $\phi : \mathcal{Z} \times \mathcal{U} \to \mathbb{R}^{n_a}$ is locally Lipschitz in its arguments on its domain. In addition, $\phi(0, 0) = 0$.

Proof.

— First, observe that $\forall k = 1, ..., n_a$ and $\forall z$ such that $z_{2j} \neq 0$ and $z_{3j} \neq 0$ for some $j \in \{1, ..., n_a\}$, $\phi_k(x, u)$ is locally Lipschitz in z and in u on the set $\mathcal{Z}$,

$$\mathcal{Z} = \Bigg\{ z \in \mathbb{R}^{3n_a} : D_k^\star - N_k \leqslant z_{1k} \leqslant D_k^\star, \frac{-N_k}{\gamma_{D_k}} \leqslant z_{2k} \leqslant 0,$$
$$N_k \gamma_{D_k} \lambda_k \sum_{j=1}^{n_a} \tilde{C}_{kj} z_{2j} - (\gamma_{R_k} + \gamma_{D_k}) z_{2k} \leqslant z_{3k} \leqslant -(\gamma_{R_k} + \gamma_{D_k}) z_{2k} \ \forall k = 1, ..., n_a \Bigg\}$$

which corresponds to the set $\mathcal{X}$ for the original variables, and $\mathcal{U} = \{\theta \in \mathbb{R}^{n_a} : 0 \leqslant \theta_k \leqslant \theta_{sup}\}$ since ϕ_k is of class C^1 on $\{z \in \mathcal{Z} : z_{2j} \neq 0 \text{ or } z_{3j} \neq 0 \text{ for some } j \in \{1, ..., n_a\}\}$ and on $\mathcal{U}$.

— Moreover, for all $z_0 = \begin{pmatrix} z_{0_{11}} & \cdots & z_{0_{1n_a}} & 0 & \cdots & 0 \end{pmatrix}^T$, $\phi_k(z_0, u)$ is locally Lipschitz in $\mathcal{Z}$.

This means that for any $\delta > 0$ such that $\forall z \in \mathcal{Z},\ \|z - z_0\| \leqslant \delta$, there exists $M > 0$ such that $|\phi_k(z,u) - \phi_k(z_0,u)| \leqslant M\|z - z_0\|$. Indeed, for $z \in \mathcal{Z}$ such that z equal to z_0, the result is trivial.
In addition, considering $z \neq z_0$, it follows from the definition of ϕ_k that

$$
\begin{aligned}
&|\phi_k(z,u) - \phi_k(z_0,u)| = |\phi_k(z,u)|, \qquad (5.19)\\
&\leqslant |\left(z_{3k} + \left(\gamma_{R_k} + \gamma_{D_k}\right) z_{2k}\right)| \left[\lambda_k \sum_{j=1}^{n_a} \tilde{C}_{kj} |z_{2j}| + |p_k \theta_{sat_k}| + \left| \frac{\sum_{j=1}^{n_a} \tilde{C}_{kj} z_{3j}}{\sum_{j=1}^{n_a} \tilde{C}_{kj} z_{2j}} \right| + \left(\gamma_{R_k} + \gamma_{D_k}\right) \right]\\
&\quad + \left(\gamma_{R_k} + \gamma_{D_k}\right)^2 |z_{2k}|,\\
&\leqslant \left(1 + \left(\gamma_{R_k} + \gamma_{D_k}\right)\right) \|z - z_0\| \left[\lambda_k \sum_{j=1}^{n_a} \tilde{C}_{kj} |z_{2j}| + |\theta_{sat_k}| \ + \left| \frac{\sum_{j=1}^{n_a} \tilde{C}_{kj} z_{3j}}{\sum_{j=1}^{n_a} \tilde{C}_{kj} z_{2j}} \right| + \left(\gamma_{R_k} + \gamma_{D_k}\right) \right]\\
&\quad + \left(\gamma_{R_k} + \gamma_{D_k}\right)^2 \|z - z_0\|,
\end{aligned}
$$

by using the definition of z_0 in this case which implies $\phi_k(z0,u) = 0$. It follows that for all $z \in \mathcal{Z}$ such that $\|z - z_0\| < \delta$,

$$
\begin{aligned}
&|\phi_k(z,u) - \phi_k(z_0,u)| \leqslant \left(1 + \left(\gamma_{R_k} + \gamma_{D_k}\right)\right) \|z - z_0\|\\
&\times \left[\lambda_k \sum_{j=1}^{n_a} \tilde{C}_{kj} \delta + \theta_{sup} + \left| \frac{\sum_{j=1}^{n_a} \tilde{C}_{kj} z_{3j}}{\sum_{j=1}^{n_a} \tilde{C}_{kj} z_{2j}} \right| + \left(\gamma_{R_k} + \gamma_{D_k}\right) \right] + \left(\gamma_{R_k} + \gamma_{D_k}\right)^2 \|z - z_0\|. \qquad (5.20)
\end{aligned}
$$

The fraction term is smaller than a constant. Indeed,

$$
\begin{aligned}
\left| \frac{\sum_{j=1}^{n_a} \tilde{C}_{kj} z_{3j}}{\sum_{j=1}^{n_a} \tilde{C}_{kj} z_{2j}} \right| &\leqslant \frac{\sum_{j=1}^{n_a} \tilde{C}_{kj} |z_{3j}|}{\left| \sum_{j=1}^{n_a} \tilde{C}_{kj} z_{2j} \right|}\\
&= \frac{\sum_{j=1}^{n_a} \tilde{C}_{kj} \left| \left\{ \gamma_{D_j} \lambda_j S_j \sum_{l=1}^{n_a} C_{jl} z_{2_l} - \left(\gamma_{R_j} + \gamma_{D_j}\right) z_{2j}(t) \right\} \right|}{-\sum_{j=1}^{n_a} \tilde{C}_{kj} z_{2j}}
\end{aligned}
$$

$$\leqslant \frac{\sum_{j=1}^{n_a} \lambda_j \tilde{C}_{kj} \gamma_{D_j} N_j \sum_{l=1}^{n_a} C_{jl} |z_{2_l}|}{-\sum_{j=1}^{n_a} \tilde{C}_{kj} z_{2j}} + \frac{\Gamma \sum_{j=1}^{n_a} \tilde{C}_{kj} |z_{2j}|}{-\sum_{j=1}^{n_a} \tilde{C}_{kj} z_{2j}}$$

using the fact that $\gamma_{R_j} + \gamma_{D_j} \leqslant \Gamma$ for all j, where Γ is given as in Theorem 5.2.1, and the fact that $0 \leqslant S_j \leqslant N_j$ for all j over the domain of interest. Then,

$$\left| \frac{\sum_{j=1}^{n_a} \tilde{C}_{kj} z_{3j}}{\sum_{j=1}^{n_a} \tilde{C}_{kj} z_{2j}} \right| \leqslant \frac{\sum_{j=1}^{n_a} \lambda_j \tilde{C}_{kj} \gamma_{D_j} N_j \sum_{\substack{l=1 \\ z_{2l} \neq 0}}^{n_a} C_{jl} z_{2_l}}{\sum_{j=1}^{n_a} \tilde{C}_{kj} z_{2j}} + \Gamma$$

$$= \sum_{j=1}^{n_a} \lambda_j \tilde{C}_{kj} \gamma_{D_j} N_j \left\{ \sum_{\substack{l=1 \\ z_{2l} \neq 0}}^{n_a} \frac{C_{jl}}{\sum_{j=1}^{n_a} \tilde{C}_{kj} \frac{z_{2j}}{z_{2l}}} \right\} + \Gamma$$

$$= \sum_{j=1}^{n_a} \lambda_j \tilde{C}_{kj} \gamma_{D_j} N_j \left\{ \sum_{\substack{l=1 \\ z_{2l} \neq 0}}^{n_a} \frac{C_{jl}}{\tilde{C}_{kl} \left(1 + \sum_{\substack{j=1 \\ j \neq l}}^{n_a} \frac{\tilde{C}_{kj}}{\tilde{C}_{kl}} \frac{z_{2j}}{z_{2l}} \right)} \right\} + \Gamma$$

$$\leqslant K$$

where $K = \sum_{j=1}^{n_a} \lambda_j \tilde{C}_{kj} \gamma_{D_j} N_j \sum_{l=1}^{n_a} \frac{C_{jl}}{\tilde{C}_{kl}} + \Gamma$. Therefore, inequality (5.20) becomes

$$|\phi_k(z, u) - \phi_k(z_0, u)| \leqslant M \|z - z_0\|$$

where $M = (1 + \Gamma) \left[\sum_{j=1}^{n_a} \lambda_j \tilde{C}_{kj} \delta + \theta_{sup} + K + \Gamma \right] + \Gamma^2 > 0$.
Finally, observe that $\phi_k(0, 0) = 0$. Therefore, Assumption 1 of Theorem 2.6.1 is satisfied. □

Lemma 5.3.2
The function ϕ is globally bounded in $z \in \mathcal{Z}$.

Proof. This proof is based on a similar reasoning as for Lemma 5.3.1. An additional argument, stating that z_{3k} is bounded, is useful for the following developments. This follows from the fact that, since z is in $\mathcal{Z}$, there holds

$$N_k\lambda_k\gamma_{D_k}\sum_{j=1}^{n_a}\frac{M_{kj}}{N_j\gamma_{D_j}}z_{2j}-\left(\gamma_{R_k}+\gamma_{D_k}\right)z_{2k}\leqslant z_{3k}\leqslant-\left(\gamma_{R_k}+\gamma_{D_k}\right)z_{2k}.$$

It follows that

$$-N_k\lambda_k\gamma_{D_k}\sum_{j=1}^{n_a}\tilde{C}_{kj}\frac{N_j}{\gamma_{D_j}}\leqslant z_{3k}\leqslant\frac{N_k}{\gamma_{D_k}}\left(\gamma_{R_k}+\gamma_{D_k}\right),$$

hence, since z_{2k} is bounded,

$$|z_{3k}|\leqslant\tilde{K}$$

where

$$\tilde{K}=\max\left\{\frac{N_k}{\gamma_{D_k}}\left(\gamma_{R_k}+\gamma_{D_k}\right),N_k\lambda_k\gamma_{D_k}\sum_{j=1}^{n_a}\tilde{C}_{kj}\frac{N_j}{\gamma_{D_j}}\right\}>0.$$

It follows that

$$\begin{aligned}|\phi_k(z)|&\leqslant|\left(z_{3k}+\left(\gamma_{R_k}+\gamma_{D_k}\right)z_{2k}\right)|\left[\lambda_k\sum_{j=1}^{n_a}\tilde{C}_{kj}|z_{2j}|+|p_k\theta_{sat_k}|+\left|\frac{\sum_{j=1}^{n_a}\tilde{C}_{kj}z_{3j}}{\sum_{j=1}^{n_a}\tilde{C}_{kj}z_{2j}}\right|\right.\\&\quad\left.+\left(\gamma_{R_k}+\gamma_{D_k}\right)\right]\\&\leqslant\left(\tilde{K}+\left(\gamma_{R_k}+\gamma_{D_k}\right)\frac{N_k}{\gamma_{D_k}}\right)\left[\lambda_k\sum_{j=1}^{n_a}\tilde{C}_{kj}\frac{N_k}{\gamma_{D_k}}+\theta_{sup}+K+\left(\gamma_{R_k}+\gamma_{D_k}\right)\right]\\&\quad+\left(\gamma_{R_k}+\gamma_{D_k}\right)^2\frac{N_k}{\gamma_{D_k}}\\&=:\tilde{M}.\end{aligned}$$

□

Lemma 5.3.3
The function $\gamma=\theta_{sat_k}$ defined in (5.13) is a locally Lipschitz function, bounded and such that $\gamma(0)=0$.

Proof. By Property 5.2.2, the function θ_{sat_k} has been defined to be Lipschitz. Moreover, $\gamma(0)$ corresponds to the case where $S_k = I_k = 0$. In this case, $\theta_{sat_k} = 0$ by definition. Finally, the boundness follows the definition of θ_{sat_k}, where saturation is imposed. □

Lemma 5.3.4
The origin ($z = 0$) is an asymptotically stable equilibrium point of the closed-loop system.

Proof. This assumption is a direct consequence of Theorem 5.2.1 combined with the change of variables (5.16). □

The following theorem states the main result of this section.

Theorem 5.3.1
The observer-based output feedback, based on the high-gain observer (2.22) implies the semistability of the disease-free equilibria of Model (4.1).

Proof. Lemmas 5.3.1 to 5.3.4 show that the assumptions of Theorem 2.6.1 are satisfied. Therefore, an observer-based output feedback can be obtained for Model (5.18), based on the design of a high-gain observer defined by (2.22). Moreover, there exists $\tilde{\epsilon}^\star > 0$ such that for every $0 < \epsilon \leqslant \tilde{\epsilon}^\star$, the origin $z = 0$ of Model (5.18a) is asymptotically stable. Using the change of variables (5.17), this implies that $(S_1^\star, ..., S_{n_a}^\star, 0, ..., 0, R_1^\star, ..., R_{n_a}^\star, D_1^\star, ..., D_{n_a}^\star)$ is asymptotically stable. □

5.4 Numerical simulations

In this section, numerical simulations, which illustrate Theorems 5.2.1, 5.2.2 and 5.3.1, are presented. Those simulations are performed with the parameters used in Section 4.3 and calibrated in Chapter 3 on covid-19 data. However, to mimic the fact that a vaccine is not available at the beginning of the epidemic, it has been chosen to apply the vaccine one month after the assumed start of the epidemic, that is on the 10^{th} of March. Therefore, in the following simulations, time 0 corresponds to the 10^{th} March. Furthermore, since the aim of this chapter is to design a vaccination law implementable in practice, vaccination data are needed. Indeed, as mentioned previously, there is a maximum number of vaccine doses that can be administrated each day. To be aware of this number

the dataset, named "Administered vaccines by date, region, age, sex, brand and dose" and available in (Sciensano (2023)), is used. Hence, the maximum number of vaccines that have been administrated in Wallonia in one day is 55191 and happened on the 16^{th} June 2021. Therefore, in the following, it will be assumed that it is not possible to vaccinate more than 55191 individuals (1.5141% of the population) per day. This number will be helpful to define the upper bound on the control law allowing to design an implementable vaccination strategy. Moreover, it is assumed that the vaccine efficacy corresponds to 80% for the individuals less than 65 years old and to 60% for the ones older. This estimation is inspired from the results obtained in (Braeye et al. (2022)), for the variant Delta in the case of a primary vaccination. As for the previous simulations, the code is stopped when some convergence criteria is satisfied. In this case, it corresponds to the time when there remains less than one infected individuals in the whole population. Moreover, ODE45 function from MATLAB is used to solve the ODEs.

5.4.1 Unsaturated state feedback

In view of Figure 4.1, one can wish to obtain disease eradication faster and with less infected individuals in the population. This can be done with the state feedback law (5.6) that implies exponential convergence to zero of the infected individuals. This law was implemented numerically satisfying parameter conditions mentioned in Theorem 5.2.2, with

$$\alpha_1^k = (\gamma_{R_k} + \gamma_{D_k}) \left(\max(\gamma_{D_k} + \gamma_{R_k}) + \sum_{j=1}^{n_a} M_{kj} \right) + 0.1$$

and

$$\alpha_2^k = \gamma_{R_k} + \gamma_{D_k} + \max(\gamma_{D_k} + \gamma_{R_k}) + \sum_{j=1}^{n_a} M_{kj}.$$

Figure 5.4 shows that the convergence of individuals to zero is much faster than without control. This occurs in $30 + 13 = 43$ days compared to 192 days in absence of control. Notice that 30 corresponds to the assumed time needed to develop a vaccine. Moreover, the peak of infected individuals is much lower. The total proportion of infected individuals is at most 0.0011 in the closed-loop case, which is smaller than 0.0432 in Figure 4.1 for the open-loop case. Notice that this phenomenon of reduction is also seen for the dead individuals, as it can be expected. Indeed, in simulations, a percentage of 11.82% of the population is deceased in the open-loop case but only 0.0788% of the population die when the control law is applied. However, the dynamics of the control law, not represented here, tends quickly to infinity as expected and will not be applicable in practice.

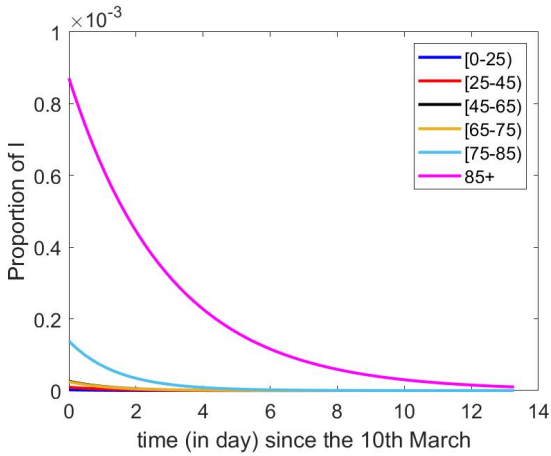

Figure 5.4 – Dynamics of the proportion of infected individuals with unconstrained state feedback

5.4.2 Amplitude constrained control

To ensure a feasible vaccination law, the state feedback is saturated and is given by (5.13). The upper bound is fixed to 0.05 to ensure a physical meaning, as shown in Figure 5.10. Indeed, Figure 5.10 shows the percentage of vaccines needed to be administrated per day, all age groups being combined. By the reasonable assumption mentioned previously, it is not possible to vaccinate more than 1.5141% of the population each day, one can see that the proposed vaccination law can be applied in practice. Notice that the upper bound 0.05 was obtained by trial and error in order to ensure applicability of the vaccination law.

Moreover, the switch in the vaccination law $\theta_{sat_k}(t)$ is chosen to satisfy Lemma 5.2.2 where $\tilde{I}_k$ is arbitrarily set to 20 for all k and we take the equality to choose $\tilde{S}_k$. Under this feedback, the convergence of the infected individuals to 0 is no longer exponential. However, disease eradication occurs with a smaller peak of infected individuals than in the open-loop case, a proportion of 0.0016 infected individuals instead of 0.0432. The dynamics of the proportion of infected individuals for each class of age is represented in Figure 5.5. The same holds for the dead individuals (not represented here), a proportion of 0.0026 is observed with the state feedback instead of 0.1182 in open-loop. Moreover, it is interesting to see that the law is highly age-dependent, as emphasized in Figure 5.6. It recommends to focus effort on the older class of age 75+ but also to the group $[45, 65)$. Moreover, it is also time dependent. Finally, the

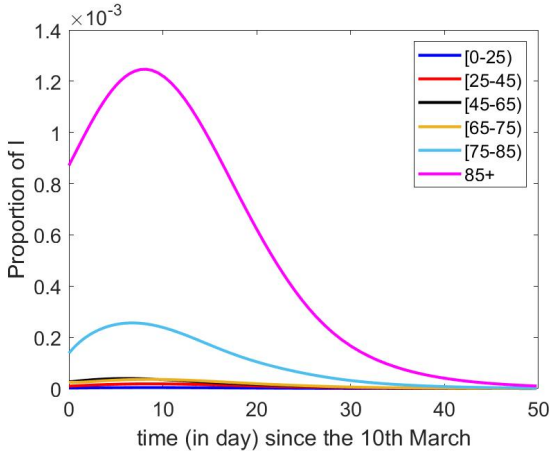

Figure 5.5 – Dynamics of the proportion of infected individuals with constrained state feedback

disease eradication is reached after $30 + 50 = 80$ days instead of 192 days if no vaccination is applied.

Furthermore, thanks to the input θ_{sat_k}, it is possible to design an observer-based output feedback, which can be used in practice. As viewed in Figure 5.7, the estimated closed-loop trajectory converges to the trajectory obtained with the system under state feedback. Moreover, as one can see by comparing Figures 5.8 and 5.9, taking ϵ smaller implies more precision in the approximation. Indeed, for the last class of age, the maximal absolute error is 5.6332×10^{-6} and 1.4349×10^{-7} for ϵ equals to 0.5 and 0.1 respectively. The same holds for the other classes of age.

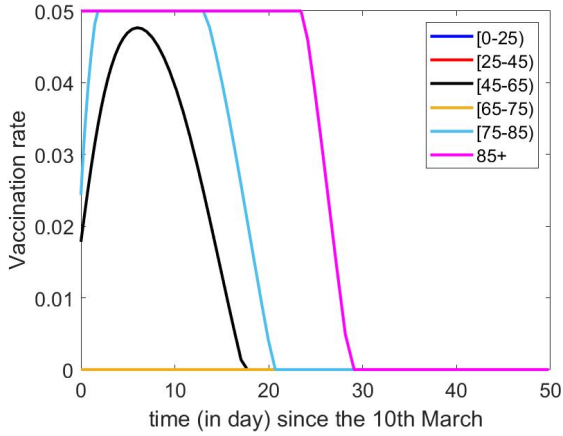

Figure 5.6 – Dynamics of the constrained vaccination law

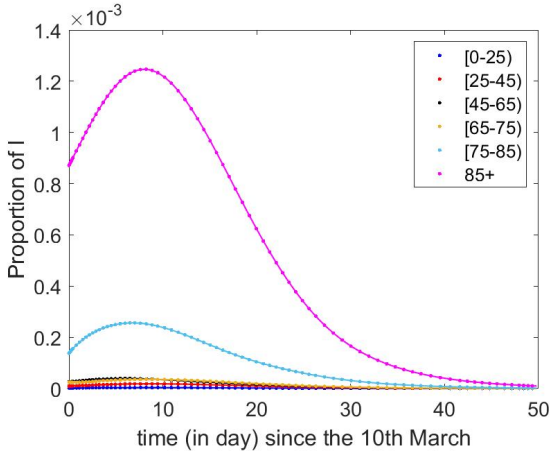

Figure 5.7 – Dynamics of the proportion of infected individuals with constrained state feedback in plain line and observer-based output feedback in dots, for $\epsilon = 0.1$

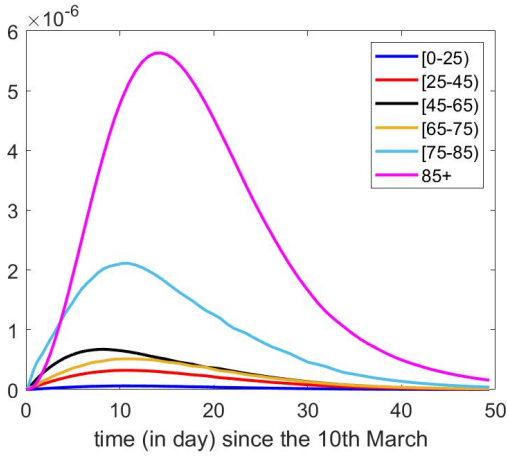

Figure 5.8 – Absolute error between the proportion of infected individuals with constrained state feedback and observer-based output feedback, for $\epsilon = 0.5$

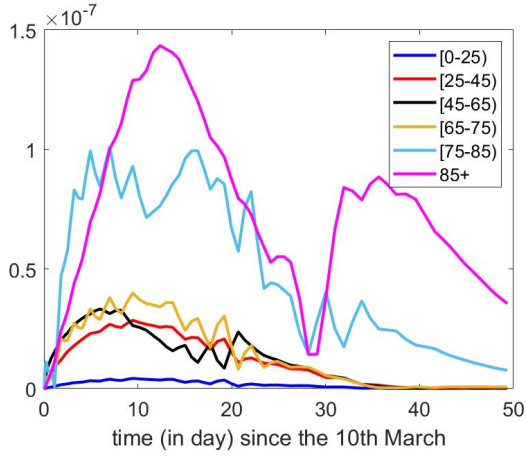

Figure 5.9 – Absolute error between the number of infected individuals with constrained state feedback and observer-based output feedback, for $\epsilon = 0.1$

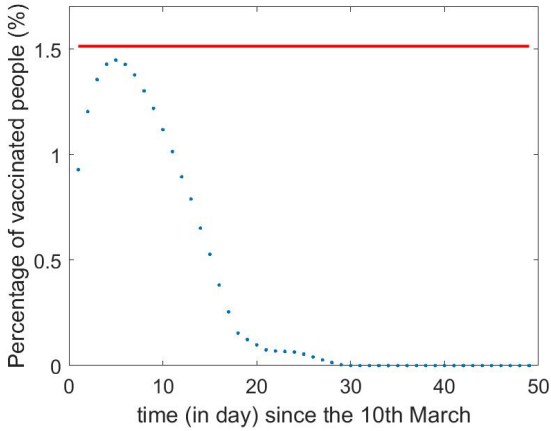

Figure 5.10 – Percentage of vaccinated people per day

In view of the results obtained in this Chapter, a natural question that arises is how to choose the feedback gains in the best way possible. For instance, by finding the parameters that minimize the number of dead individuals. In view of the equations, this will minimize the number of infected individuals. This remains an open question in this thesis. However, in the following chapter, the model predictive control strategy is used to implement a control law, with the property of minimizing the number of dead individuals and ensuring disease eradication.

Chapter 6

Model predictive control

This chapter, based on a joint work with Mirko Fiacchini [1], concerns the design of a vaccination control law based on the model predictive control (MPC) approach. Therefore, contrary to the previous chapter, the age-dependent vaccination strategy is chosen in an optimal way, according to criteria presented later. A brief reminder of MPC is presented in Chapter 2, Section 2.7.
The first section of this chapter presents the formulation of the problem of interest. Then, Section 6.2 is dedicated to the proof of the feasibility and stability of the closed-loop system obtained with model predictive control. Finally, numerical simulations are given in Section 6.3.

6.1 Problem formulation

This chapter is dedicated to the design of an age-dependent vaccination law in order to achieve one main objective, the disease eradication. However, in view of the model equations, this is obtained even in open-loop. Hence, some additional desirable objectives are added such as the minimization of the number of dead individuals in the population (which has for consequence to ensure that the total number of infected individuals is not too high). Moreover, in order to obtain a vaccination law that is implementable in practice, additional constraints on the control are added: the nonnegativity of the vaccination law as well as the limitation in the number of available vaccines per day. Hence, an optimization problem of a nonlinear system with constraints needs to be solved. To achieve this, model predictive control theory is used. In order to numerically

1. Mirko Fiacchini performed the numerical simulations with model predictive control, whereas the stability analysis was a joint work.

implement the algorithm, a discrete version of Model (4.1) is introduced. This choice allows to perform the simulation directly on the studied model, contrary to the previous chapter, where the model is discretized after the analyis. Both approaches can be justified and the theory proposed here could be developed in the case of a continuous-time model, of course with suitable modifications. The discretized model is obtained by using Euler discretization of the previous model with a time step of one day. In the case of another choice of discretization step Δt the model equations should be rescaled accordingly. The discrete-time age-structured SIRD epidemic model is given by

$$\begin{cases} S_k(n+1) &= S_k(n) - \lambda_k S_k(n) \sum_{j=1}^{n_a} C_{kj} I_j(n) - p_k u_k(n) \\ I_k(n+1) &= I_k(n) + \lambda_k S_k(n) \sum_{j=1}^{n_a} C_{kj} I_j(n) - (\gamma_{R_k} + \gamma_{D_k}) I_k(n) \\ R_k(n+1) &= R_k(n) + \gamma_{R_k} I_k(n) + p_k u_k(n) \\ D_k(n+1) &= D_k(n) + \gamma_{D_k} I_k(n), \end{cases} \tag{6.1}$$

where $k = 1, ..., n_a$. Notice that the control law $u_k(n) = \theta_k(n) S_k(n)$ has been introduced. It corresponds to the number of vaccines administrated at time n. Model (6.1) can be equivalently rewritten as

$$x^+ = f(x, u)$$

where $x = (S_1, ..., S_{n_a}, I_1, ..., I_{n_a}, R_1, ..., R_{n_a}, D_1, ...D_{n_a})^T \in \mathcal{X} := \left\{x \in \mathbb{R}^{4n_a} : 0 \leqslant S_k, I_k, R_k, D_k \leqslant N_k, k = 1, ..., n_a\right\}$, x^+ denotes the successor state, $u = (u_1, ..., u_{n_a})^T \in \mathcal{U} := [0, b_{sup}]^{n_a}$ and $f : \mathcal{X} \times \mathcal{U} \to \mathcal{X}$ is bounded.

As mentioned previously, the goal of this research is to find the best age-dependent vaccination law u with desired properties (disease eradication while minimizing the total number of deceased individuals at each day, therefore reduction of the number of infected individuals) and under some constraints (vaccination law that fulfills the physical constraints). This law can be obtained, thanks to model predictive control theory, by solving the following optimal control problem, over the finite time horizon N,

Problem 6.1.1

$$\min_{\boldsymbol{u}(\cdot)} \; V_N(x, \boldsymbol{u}) := \sum_{n=0}^{N-1} \sum_{k=1}^{n_a} D_k(n+1) - D_k(n) + V_f(x(N))$$

with respect to $(\boldsymbol{x}, \boldsymbol{u}) = (x(0), ..., x(N), u(0), ..., u(N-1))$

subject to the fact that (6.1) *is satisfied with initial condition* $x(0) = x$, *and*

$$(x(n), u(n)) \in \mathcal{Z} =: \mathcal{X} \times \left\{ u \in \mathcal{U} : \sum_{k=1}^{n_a} u_k \leqslant b_{sup} \right\} \subset \mathcal{X} \times \mathcal{U} \ \ \forall n \in \mathbb{N}$$

where V_f is a terminal constraint defined in order to ensure that the MPC algorithm steers the state to the positively invariant equilibrium set defined by $X^\star = \{x \in \mathcal{X} : I_k = 0, k = 1, ..., n_a\}$. This terminal constraint is discussed in Subsection 8.2.2 since it is a key element to ensure the stability of the closed-loop system.

For analysis purpose, it is best to reformulate the optimal control Problem 6.1.1 by using the fact that $x(n) = \phi(n; x; \mathbf{u})$, the solution of (6.1) at time n with the initial state x at time 0 and the control sequence $\mathbf{u}$. Adding an additional terminal constraint,

$$x(N) \in \mathcal{X}_f \subseteq \mathcal{X}$$

where $\mathcal{X}_f$ will be defined later, as well as the function V_f, in order to ensure the stabilizing property of the MPC, the optimal control problem to be solved is given by

$$\begin{aligned} &\min_{\mathbf{u}(\cdot)} \sum_{n=0}^{N-1} \sum_{k=1}^{n_a} \gamma_{D_k} I_k(n) + V_f(x(N)) \text{ where } x(n) = \phi(n; x; \mathbf{u}) \ \ \forall n \in \{0 ..., N\} \\ &\text{with respect to } \mathbf{u} = (u(0), ..., u(N-1)) \\ &\text{subject to } \ (x(n), u(n)) \in \mathcal{Z} \\ &\qquad x(N) \in \mathcal{X}_f \subseteq \mathcal{X}. \end{aligned} \tag{6.2}$$

Observe that the term $\sum_{k=1}^{n_a} \gamma_{D_k} I_k(n)$ represents the number of dead individuals at day n: see the last equation of Model (6.1). Furthermore, as mentioned previously, V_f and $\mathcal{X}_f$ are specified in the next section and the following analysis will show that this choice is appropriate for the pursued goals. Moreover, for the following analysis, let us define

$$l(x, u) = \sum_{k=1}^{n_a} \gamma_{D_k} I_k,$$

$$V_N(x, \mathbf{u}) = \sum_{n=0}^{N-1} l\left(x(n), u(n)\right) + V_f\left(x(N)\right), \text{ where } x(n) = \phi(n; x, \mathbf{u})$$

and $\mathcal{U}_N(x)$, the set of (feasible) control sequences satisfying all the (input, state and terminal) constraints, namely the control constraint set. Then, the optimal control problem rewrites shortly as

$$\mathbb{P}_N(x) : \quad \min_{\mathbf{u} \in \mathcal{U}_N(x)} V_N(x, \mathbf{u}) := V_N^{\mathbf{o}}(x)$$

Notice that, thanks to equation (6.1), the control of I_k implies the control of R_k and D_k. Therefore, in the following, the attention is focused on the $2n_a$ first equations concerning the susceptible and infected individuals. Hence, in what follows, $x = (S_1, ..., S_{n_a}, I_1, ..., I_{n_a})^T \in \mathcal{X} := \{x \in \mathbb{R}^{2n_a} : 0 \leqslant S_k, I_k \leqslant N_k, k = 1, ..., n_a\}$.
Finally, the optimal control sequence obtained by solving problem (6.2) is denoted

$$\mathbf{u^o}(x) = (u^{\mathbf{o}}(0, x), ..., u^{\mathbf{o}}(N-1, x)) = \arg\min_{\mathbf{u}(\cdot)} V_N(x, \mathbf{u}).$$

In the MPC approach, the control applied to the system is the first element $u^{\mathbf{o}}(0; x)$ of the solution of the optimal control problem and is denoted $\kappa_N(x)$.

6.2 Dynamical analysis

In order to perform the model predictive control approach, it is important to ensure the feasibility of the problem, i.e the existence of a solution of the MPC problem, as well as the stability guarantee. Indeed, when applying MPC, there is no guarantee that the trajectories converge. In the following, those two points are studied to show that the MPC problem introduced in Section 6.1 is well-posed in terms of existence of a solution and stability. This ensures that the solution obtained thanks to the model predictive control calculations converges to the desired disease-free equilibrium.

A useful notation is introduced in this part. Let $x = (x_1 \ \dots \ x_n)^T$. The notation $x > 0$ ($x \geqslant 0$) means that each component x_i of x is positive (non-negative).

Now, all the elements are gathered to define the terminal cost $V_f(x(N))$ and the terminal constraint $\mathcal{X}_f$ that will help to obtain stability.

Definition 6.2.1 *Let $\epsilon \in (0, 1]$, $\gamma_D = \left(\gamma_{D_1}, ..., \gamma_{D_{n_a}}\right)^T$, $I = (I_1, ..., I_{n_a})^T$ and $S = (S_1, ..., S_{n_a})^T$. Define*

$$V_f(x(N)) = \frac{1}{\epsilon} \sum_{k=1}^{n_a} \gamma_{D_k} I_k(N) = \frac{1}{\epsilon} \gamma_D^T I(N)$$

and

$$\mathcal{X}_f = \left\{x \in \mathcal{X} : C^T diag(\gamma_D \lambda) S \leqslant \Gamma\right\}$$

with $C = \begin{pmatrix} C_{11} & \cdots & C_{1n_a} \\ \vdots & \ddots & \vdots \\ C_{n_a 1} & \cdots & C_{n_a n_a} \end{pmatrix}$, $diag(\gamma_D \lambda) = \begin{pmatrix} \gamma_{D_1}\lambda_1 & & \\ & \ddots & \\ & & \gamma_{D_{n_a}}\lambda_{n_a} \end{pmatrix}$ *and*

$$\Gamma = \begin{pmatrix} \gamma_{D_1}\left(\gamma_{R_1} + \gamma_{D_1} - \epsilon\right) \\ \dots \\ \gamma_{D_{n_a}}\left(\gamma_{R_{n_a}} + \gamma_{D_{n_a}} - \epsilon\right) \end{pmatrix}.$$

Notice that $\mathcal{X}_f$ is chosen such that the number of total deceased individuals per sampling interval is decreasing. Indeed, the choice of this region implies that, for $I \in \mathcal{X}_f$,

$$\gamma_D^T I(n+1) - \gamma_D^T I(n) \leqslant -\epsilon \gamma_D^T I(n) \tag{6.3}$$

with $\epsilon \in (0, 1]$. To prove this result, one can use the discrete-time dynamics (6.1) to notice that condition (6.3) is equivalent to

$$\begin{aligned} &\sum_{k=1}^{n_a} \gamma_{D_k} \lambda_k S_k \sum_{j=1}^{n_a} C_{kj} I_j - \sum_{j=1}^{n_a} \gamma_{D_j}(\gamma_{R_j} + \gamma_{D_j} - \epsilon) I_j \leqslant 0 \\ &\sum_{j=1}^{n_a} \Big(\sum_{k=1}^{n_a} \gamma_{D_k} \lambda_k S_k C_{kj} - \gamma_{D_j}(\gamma_{R_j} + \gamma_{D_j} - \epsilon) \Big) I_j \leqslant 0, \end{aligned} \tag{6.4}$$

where the time dependence has been dropped for ease of notation. From the nonnegativity of I, a sufficient condition for (6.4) to hold is

$$\sum_{k=1}^{n_a} \gamma_{D_k} \lambda_k S_k C_{kj} \leqslant \gamma_{D_j}(\gamma_{R_j} + \gamma_{D_j} - \epsilon), \qquad \forall j = 1, \dots, n_a$$

which is equivalent, in matrix form, to

$$C^T \begin{pmatrix} \gamma_{D_1}\lambda_1 & 0 & \dots & 0 \\ 0 & \gamma_{D_2}\lambda_2 & \dots & \dots \\ \dots & \dots & \dots & \dots \\ 0 & 0 & \dots & \gamma_{Dn_a}\lambda_{n_a} \end{pmatrix} S \leqslant \begin{pmatrix} \gamma_{D_1}(\gamma_{R_1} + \gamma_{D_1} - \epsilon) \\ \gamma_{D_2}(\gamma_{R_2} + \gamma_{D_2} - \epsilon) \\ \dots \\ \gamma_{Dn_a}(\gamma_{Rn_a} + \gamma_{Dn_a} - \epsilon) \end{pmatrix}.$$

Some lemmas are introduced to demonstrate the main assumptions needed to conclude about the stability of the set of disease-free equilibria $X^\star$ and the solvability of problem (6.2). Those are the same as the "basic stability assumption", recalled in Assumption 2.7.3 but adapted to the concept of convergence to a set.

In the following, the set $\mathcal{X}_N$ denotes the set of states x in $\mathcal{X}$ for which there exist (feasible) control sequences $\mathbf{u} \in \mathcal{U}_N(x)$.

Lemma 6.2.1
Let V_f and $\mathcal{X}_f$ be given as in Definition 6.2.1, for some $\epsilon \in (0, 1]$. Then

1. $\forall x \in \mathcal{X}_f$, there exists u (such that $(x, u) \in \mathcal{Z}$) satisfying
   (a) $f(x, u) \in \mathcal{X}_f$,
   (b) $V_f(f(x, u)) - V_f(x) \leqslant -l(x, u)$.
2. There exist $\mathcal{K}_\infty$ functions $\alpha_1(\cdot)$ and $\alpha_f(\cdot)$ satisfying
   (a) $l(x, u) \geqslant \alpha_1(\|x\|_{X^\star})$ $\forall x \in \mathcal{X}_N$, $\forall u$ such that $(x, u) \in \mathcal{Z}$,
   (b) $V_f(x) \leqslant \alpha_f(\|x\|_{X^\star})$ $\forall x \in \mathcal{X}_f$

   where $\|x\|_{X^\star} =: \underset{\tilde{x} \in X^\star}{inf} \|x - \tilde{x}\|_{l^1}$.

Proof.

1. Assume that $x \in \mathcal{X}_f$.
   (a) Since $x \in \mathcal{X}_f$, the following inequalities hold:

$$\sum_{k=1}^{n_a} \gamma_{D_k} \lambda_k S_k C_{kj} \leqslant \gamma_{D_j}(\gamma_{R_j} + \gamma_{D_j} - \epsilon), \qquad \forall j = 1, \ldots, n_a.$$

   Moreover, it follows from the fact that $(x, u) \in \mathcal{Z}$ that $u \geqslant 0$ and $x \geqslant 0$. Hence, since by (6.1), $S_k(n)$ is non-increasing for every $n \in \mathbb{N}$ and $k = 1, ..., n_a$, it follows that $\sum_{k=1}^{n_a} \gamma_{D_k} \lambda_k C_{kj} S_k \geqslant \sum_{k=1}^{n_a} \gamma_{D_k} \lambda_k C_{kj} S_k^+$, for $j = 1, ..., n_a$. Thus, the set $\mathcal{X}_f$ is an invariant set for System (6.1).
   (b) For $u = 0$, $V_f(f(x, 0)) - V_f(x) \leqslant -l(x, 0)$. Indeed,

$$\begin{aligned} V_f(x^+) - V_f(x) &= \frac{1}{\epsilon} \gamma_D^T \left(I^+ - I\right) \\ &\leqslant -\gamma_D^T I = -l(x, 0) \end{aligned} \tag{6.5}$$

   by (6.3), since $x \in \mathcal{X}_f$.

2. The following relations holds for the l^1 norm, $\|(a_1, ..., a_n)\|_{l^1} = \sum_{k=1}^{n} |a_k|$.
   (a) Let $x \in \mathcal{X}_N$ and u such that $(x, u) \in \mathcal{Z}$. By defining $\underline{\gamma_D} = \underset{k=1...n_a}{min} \{\gamma_{D_k}\}$ it follows that

$$l(x, u) = \gamma_D^T I \geqslant \underline{\gamma_D} \sum_{k=1}^{n_a} I_k = \underline{\gamma_D} \|I\|_{l^1} = \underline{\gamma_D} \|x\|_{X^\star}.$$

Indeed, $\|x\|_{X^\star} = \underset{\tilde{x}\in X^\star}{inf} \|x-\tilde{x}\|_{l^1} = \underset{\tilde{x}\in X^\star}{inf} \sum_{k=1}^{n_a} |S_k - \tilde{S}_k + I_k| = \sum_{k=1}^{n_a} |I_k| = \|I\|_{l^1}$.

The function $\alpha_1(\|x\|_{X^\star}) = \underline{\gamma_D}\|I\|_{l^1}$ is of class $\mathcal{K}_\infty$ (i.e. continuous, strictly increasing, unbounded function that cancels in 0).

(b) By the same reasoning, the proof is completed with $\alpha_f(\|x\|_{X^\star}) = \frac{1}{\epsilon}\bar{\gamma}_D\|I\|_{l^1}$ which is of class $\mathcal{K}_\infty$, where $\bar{\gamma}_D = \underset{k=1\ldots n_a}{max}\{\gamma_{D_k}\}$.

□

The main result of this section is presented below.

Theorem 6.2.1

Let V_f and $\mathcal{X}_f$ be given as in Definition 6.2.1, for some $\epsilon \in (0,1]$. Then

1. for each $x \in \mathcal{X}_N$, a solution to problem (6.2), denoted $\mathbf{u^o}(x)$, exists;
2. the set $X^\star$ is asymptotically stable in $\mathcal{X}_N$ for $x^+ = f(x, \kappa_N(x))$, with $\kappa_N(x) = u^{\mathbf{o}}(0,x)$.

Proof. This proof is based on the stabilizing conditions developed in (Rawlings et al., 2020, Chapter 2) and recalled in Section 2.7 but adapted to the concept of convergence to a set.

1. This immediately follows from Proposition 2.7.1. Indeed, the functions $f : \mathcal{Z} \to \mathcal{X}$; $l : \mathcal{Z} \to \mathbb{R}_+$ and $V_f : \mathcal{X}_f \to \mathbb{R}_+$ are continuous and satisfy $f(x^\star, 0) = l(x^\star, 0) = V_f(x^\star) = 0$, with $x^\star \in X^\star$. Hence, Assumption 2.7.1 holds. Moreover, the set $\mathcal{Z}$ is closed and $\mathcal{X}_f \subseteq \mathcal{X}$ is compact. Furthermore, each set contains the set of equilibria and since $\mathcal{U} = \mathcal{U}(x)$ is closed and bounded, $\mathcal{U}(x)$ is compact for all $x \in \mathcal{X}$. Thus Assumption 2.7.2 holds and Proposition 2.7.1 can be used to conclude the first item.
2. The proof of asymptotic stability for the set $X^\star$ is based on Theorem 2.4.2 which characterizes the global asymptotic stability of a set, when there are state constraints, using a Lyapunov function. Hence, some assumptions about the sets must be fulfilled.
   (a) Firstly, $\mathcal{X}$ needs to be positively invariant with respect to $x^+ = f(x, \kappa_N(x))$. In view of Model (6.1), this is the case if and only if $p_k u_k(n)/S_k(n) \leqslant 1 - \lambda_k \sum_{k=1}^{n_a} M_{kj}$ and if $\gamma_{R_k} + \gamma_{D_k} \leqslant 1$ for $k = 1, ..., n_a$. Remark that the implementation of the control law in the numerical simulations ensures that the first condition is satisfied, whereas the second condition holds for the covid-19 parameters calibrated in Chapter 3.

(b) Moreover, it is obvious that the set $X^\star \subseteq \mathcal{X}$ is closed and positively invariant with respect to $x^+ = f(x, \kappa_N(x))$.

(c) Furthermore, f is bounded thanks to the invariance property of $\mathcal{X}$.

(d) Finally, it remains to show that there exists a Lyapunov function in $\mathcal{X}$ for $x^+ = f(x, \kappa_N(x))$ and the set $X^\star$. The optimal objective value function $V_N^{\mathbf{o}}(x)$ is a good candidate. Indeed, thanks to Lemma 6.2.1, it can be established, by using similar arguments as in (Rawlings et al., 2020, Section 2.4), that

i. there exists a $\mathcal{K}_\infty$ function α_1 such that the value function $V_N^{\mathbf{o}}(x)$ satisfies $\alpha_1(\|x\|_{X^\star}) \leqslant V_N^{\mathbf{o}}(x)$.
Indeed,

$$\begin{aligned} V_N^{\mathbf{o}}(x) &= V_N(x, \mathbf{u}^{\mathbf{o}}(x)) \\ &= l(x, \kappa_N(x)) + \sum_{j=1}^{N-1} l\left(x^{\mathbf{o}}\left(j; x\right), u^{\mathbf{o}}\left(j; x\right)\right) + V_f\left(x^{\mathbf{o}}(N; x)\right) \qquad (6.6) \\ &\geqslant l(x, \kappa_N(x)) \\ &\geqslant \alpha_1(\|x\|_{X^\star}) \end{aligned}$$

by Lemma 6.2.1, condition 2(b).

ii. $V_N^{\mathbf{o}}\left(f\left(x, \kappa_N\left(x\right)\right)\right) - V_N^0(x) \leqslant -\alpha_1\left(\|x\|_{X^\star}\right)$ for all $x \in \mathcal{X}_N$, with $\alpha_1\left(\|x\|_{X^\star}\right)$ a $\mathcal{PD}$ function (i.e. function that cancels in 0 and is positive evrywhere else).
Indeed, recall that

$$\begin{aligned} \mathbf{u}^{\mathbf{o}}(x) &= (u^{\mathbf{o}}(0; x), ..., u^{\mathbf{o}}(N-1; x)) \\ &= (\kappa_N(x), u^{\mathbf{o}}(1; x), ..., u^{\mathbf{o}}(N-1; x)) \end{aligned}$$

and the resulting optimal state sequence is given by

$$\mathbf{x}^{\mathbf{o}}(x) = (x^{\mathbf{o}}(0; x), ..., x^{\mathbf{o}}(N; x)),$$

where $(x^{\mathbf{o}}(0; x) = x$ and $x^{\mathbf{o}}(1; x) = f(x, \kappa_N(x)) = x^+$.
Second, notice that

$$\begin{aligned} V_N^{\mathbf{o}}\left(f\left(x, \kappa_N\left(x\right)\right)\right) := V_N^{\mathbf{o}}\left(x^+\right) &= V_N\left(x^+, \mathbf{u}^{\mathbf{o}}\left(x^+\right)\right) \\ &\leqslant V_N(x^+, \tilde{\mathbf{u}}), \qquad (6.7) \end{aligned}$$

for any $\tilde{\mathbf{u}} \in \mathcal{U}_N(x)$. In particular, it holds for

$$\tilde{\mathbf{u}}(x) = (u^{\mathbf{o}}(1; x), ..., u^{\mathbf{o}}(N-1; x), u)$$

in which $u \in \mathcal{U}$ can be chosen. Hence, the state sequence due to $\tilde{\mathbf{u}}$ is given by

$$\tilde{\mathbf{x}} = \left(x^{\mathbf{o}}(1;x), ..., x^{\mathbf{o}}(N;x), f\left(x^{\mathbf{o}}(N;x), u\right)\right).$$

Therefore,

$$\begin{aligned} V_N(x^+, \tilde{u}) = \sum_{j=1}^{N-1} l\left(x^{\mathbf{o}}\left(j;x\right), u^{\mathbf{o}}\left(j;x\right)\right) + l\left(x^{\mathbf{o}}\left(j;x\right), u\right) \\ + V_f\left(f(x^{\mathbf{o}}(N;x), u)\right) \end{aligned} \tag{6.8}$$

From (6.6), the equality

$$\sum_{j=1}^{N-1} l\left(x^{\mathbf{o}}\left(j;x\right), u^{\mathbf{o}}\left(j;x\right)\right) = V_N^{\mathbf{o}}(x) - l(x, \kappa_N(x)) - V_f\left(x^{\mathbf{o}}(N;x)\right)$$

follows. Replacing it in (6.8) implies that

$$\begin{aligned} V_N(x^+, \tilde{u}) &= V_N^{\mathbf{o}}(x) - l(x, \kappa_N(x)) - V_f\left(x^{\mathbf{o}}(N;x)\right) \\ &\qquad + l\left(x^{\mathbf{o}}\left(j;x\right), u\right) + V_f\left(f(x^{\mathbf{o}}(N;x), u)\right) \\ &\leqslant V_N^{\mathbf{o}}(x) - l(x, \kappa_N(x)) \end{aligned}$$

by choosing u such that Lemma 6.2.1, condition 1(b) holds. Finally, using (6.7), it follows that $V_N^{\mathbf{o}}(x^+) \leqslant V_N^{\mathbf{o}}(x) - l(x, \kappa_N(x))$ and Lemma 6.2.1, condition 2(b) concludes this part.

iii. there exists a $\mathcal{K}_\infty$ function α_f such that $V_N^{\mathbf{o}}(x) \leqslant \alpha_f(\|x\|_{X^\star})$. Indeed, let $x(i) = (S(i), I(i))^T$, where $x \in \mathcal{X}$,

$$S_d = \begin{pmatrix} S_1 & & \\ & \ddots & \\ & & S_{n_a} \end{pmatrix}, diag(\gamma_{RD}) = \begin{pmatrix} \gamma_{R_1} + \gamma_{D_1} & & \\ & \ddots & \\ & & \gamma_{R_{n_a}} + \gamma_{D_{n_a}} \end{pmatrix},$$

$$\Lambda = \begin{pmatrix} \lambda_1 & & \\ & \ddots & \\ & & \lambda_{n_a} \end{pmatrix} \text{ and } diag(N_{pop}) = \begin{pmatrix} N_1 & & \\ & \ddots & \\ & & N_{n_a} \end{pmatrix}.$$

One has that

$$\begin{aligned} \gamma_D^T I(i+1) &= \gamma_D^T \left(Id_{n_a} + S_d(i)\Lambda C - diag(\gamma_{RD})\right) I(i) \\ &\leqslant \gamma_D^T \left(Id_{n_a} + diag(N_{pop})\Lambda C - diag(\gamma_{RD})\right) I(i) \\ &\leqslant \alpha \gamma_D^T I(i), \end{aligned} \tag{6.9}$$

where $\alpha > 0$ such that $\left(Id_{n_a} + diag(N_{pop})\Lambda C - diag(\gamma_{RD})\right)^T \gamma_D \leqslant \alpha\gamma_D$. From (6.9) it follows that

$$\gamma_D^T I(i+n) \leqslant \alpha^n \gamma_D^T I(i), \quad \forall n \in \mathbb{N}, i \in \mathbb{N}.$$

Moreover, by the definition of V_f,

$$V_f\left(x(i+N)\right) = \frac{1}{\epsilon}\gamma_D^T I(i+N) \leqslant \frac{1}{\epsilon}\alpha^N \gamma_D^T I(i).$$

Hence, the bound

$$\begin{aligned} V_N(I(i)) &= \sum_{n=0}^{N-1} \gamma_D^T I(i+n) + V_f(x(i+N)) \\ &\leqslant \left(\sum_{n=0}^{N-1} \alpha^n + \frac{1}{\epsilon\alpha^N}\right) \gamma_D^T I(i) \\ &\leqslant \left(\sum_{n=0}^{N-1} \alpha^n + \frac{1}{\epsilon}\alpha^N\right) \bar{\gamma}_D \|I\|_{l^1} := \alpha_f(\|I\|_{l^1}) \end{aligned} \tag{6.10}$$

holds.
Finally, $V_N^{\mathbf{o}}(x(i)) \leqslant V_N(x(i), 0) \leqslant \alpha_f(\|I\|_{l^1})$ by (6.10).

Therefore, the optimal value function is a Lyapunov function for the closed-loop system, which implies the global asymptotic stability of the set $X^\star$.

□

6.3 Numerical simulations

Numerical simulations are performed to illustrate the performance obtained by using model predictive control. Two examples are presented. One of them is based on the parameters obtained in Chapter 3 on covid-19 data whereas the second one is an academic example consisting in a small adaptation of the previous parameters. The latter can be viewed as a new disease, similar to the one illustrating covid-19 in Belgium, but with a transmission probability that is independent of the classes of age. In both cases, simulations are performed using the Ipopt solver for nonlinear optimization problems of Python. It consists of the implementation of an interior point line search filter method to find local solutions of nonlinear optimization problems. Moreover, the MPC strategies are built using a control horizon equal to 40 days and a prediction horizon of 60 days.

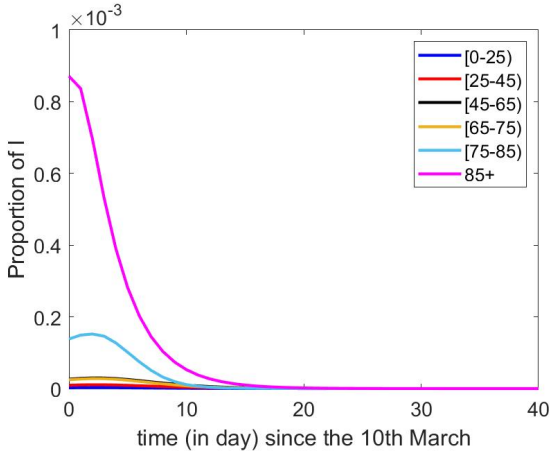

Figure 6.1 – (Discrete-time) dynamics of the proportion of infected individuals with MPC

6.3.1 Wallonia case

The idea of this part is to compare the model predictive control strategy applied on the model of the covid-19 disease to a vaccination strategy that mimics the one that was performed in Belgium. The latter consisted in vaccinating individuals in decreasing order of age. Notice that the simultaneous vaccination of vulnerable individuals and elder people is not considered here. The vaccination data used in this section are the same as in Section 5.4, namely a maximum of 55191 individuals vaccinated each day and a vaccine efficacy of 80% below 65 years old and an efficacy of 60% for people older than 65 years old.

Figure 6.1 represents the proportion of infected individuals obtained using the MPC approach. Since the goal of the MPC is not to reduce the time before disease eradication, all the figures are represented until the 19^{th} April (40 days after the 10^{th} March). Concerning the total proportion of infected individuals, it is at most 0.0011 compared to 0.0016 with the observer-based output feedback. The total proportion of dead individuals is also improved using MPC compared to the observer-based output feedback. Indeed, there is only 0.097% of the population who died with the MPC vaccination law instead of 0.26% with the output feedback law. The number of vaccines needed to be administrated each day, by class of age, to obtain those improvements is represented in Figure 6.2.

This result can also be compared with a more realistic vaccination strategy, following the idea of the vaccination implemented in Belgium to tackle the

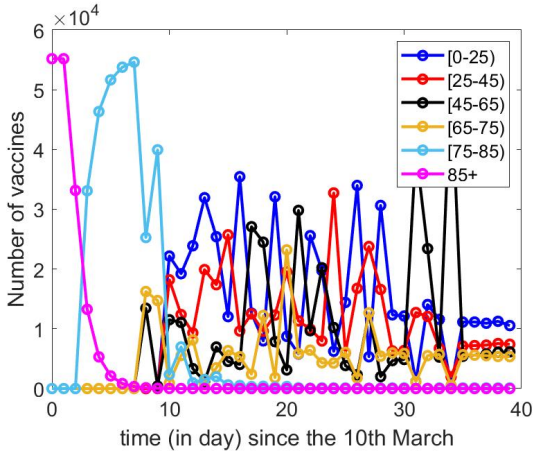

Figure 6.2 – Distribution of the number of administrated vaccines per day, by using MPC strategy

covid-19 disease, namely to vaccinate old people first. This is represented in Figure 6.3. In this case, the dynamics of the proportion of infected individuals is given in Figure 6.4. The total maximum proportion of infected individuals is the same as for the MPC case. Concerning the dead individuals (whose graph is not presented here), it is a little bit better than in the MPC case, since 0.096% of the population dies. This result can be surprising but it is explained by the fact that MPC is a suboptimal method: it gives a solution near the optimal solution. In the case considered here, the Belgian strategy appears to be adequate and sufficiently efficient to obtain disease eradication since, as one can see in Table 3.1, the transmission probability and the death rate are mostly increasing with the age (except for the 4^{th} class of age). Furthermore, remark that the vaccination strategies suggested in both cases (see Figures 6.2 and 6.3) are similar for the first days of the epidemic.
Furthermore, observing Figure 6.3, one can wonder why there is, for several days (day 2 to 6), people of more than 85 years old being vaccinated in the same time as people of age between 75 and 85 years old, knowing that the Belgian strategy is to vaccinate individuals in the decreasing order. This is due to the vaccine efficacy parameter p_k. Indeed, if the strategy is vaccinating all people from 85 years old and if there are still vaccines available then individuals from the class of age under 85+ are vaccinated. However, some of the elder people are vaccinated with an inefficient vaccine and then can get vaccinated again. Therefore, taking into account vaccine efficacy in the simulation allows for an individual to get vaccinated several times (until leaving the class of susceptible

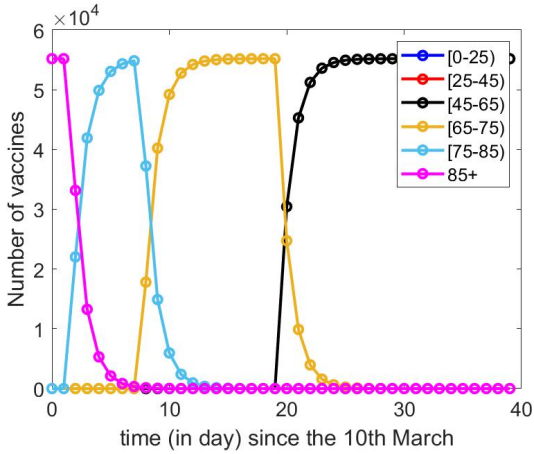

Figure 6.3 – Distribution of the number of administrated vaccines per day, following the Belgian strategy

individuals). This occurs also for the MPC strategy. With a totally efficient vaccine, the last class of age can be entirely vaccinate in two days. This is a drawback of the SIRD model considered here. In order to improve this, it is necessary to keep track of the number of individuals that have received a vaccine, for each class of age. Hence it is necessary to consider what we may call an SIRDV model, where V stands for vaccinated individuals.

6.3.2 Academic case

This academic example is presented to show that, in some cases, the MPC approach is very useful to estimate the ideal vaccination law to obtain disease eradication with less dead and infected individuals. The parameters used for this part are identical as the previous section, except that the transmission probability, λ_k, is assumed to be the same for each class of age and is taken equal to 0.05. The results presented below are compared to the ones obtained by using the vaccination strategy implemented in Belgium to tackle the covid-19 disease, illustrated in Figure 6.3. The dynamics of the proportion of the infected individuals obtained with the MPC approach is given in Figure 6.5 whereas the one obtained with the Belgian strategy is represented in Figure 6.6. Although the maximum proportion of infected individuals is the same for both classes, it is obvious to see that the MPC strategy is the best, since it achieves disease eradication in 40 days and with less infected individuals than in the other case. The MPC strategy is also much better in terms of deceased individuals, after 40 days, 0.11% of the population die with the Belgian strategy

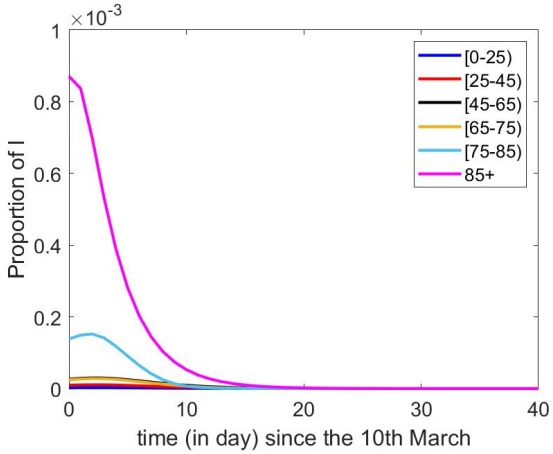

Figure 6.4 – (Discrete-time) dynamics of the proportion of infected individuals, following the Belgian strategy

and only 0.0952% with the MPC approach.
Figure 6.7 illustrates the scheme of vaccination to apply in order to minimize the number of deceased individuals. The proposed method is completely different from the one inspired by the Belgian strategy. It suggests to focus first on the young adults, $[25, 45)$, and then a mix between essentially the young people, $[0, 25)$, and the adults of ages between 45 and 65. This example shows that, minor changes in the parameters of a disease can lead to major changes in the optimal vaccination strategy in terms of number of dead individuals. Indeed, one has to find a trade-off between protecting elder people and vaccinating younger individuals who transmit the disease the most. Hence, theoretical studies are required because small changes in the disease propagation lead to totally different strategies. Therefore, this chapter provides an implementable law which is essential to guide decision policies concerning the strategy to obtain disease eradication under some desired objectives (minimizing the number of dead people) and constraints (vaccines availability and physical constraints). Other control theory approaches than model predictive control can be applied to deal with control of epidemics: one can cite for instance the Danish case reported in (Stoustrup (2023)) where the authorities and control experts worked together to mitigate the effect of covid-19.

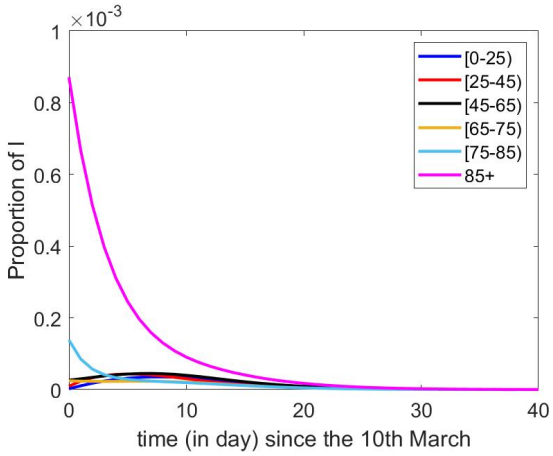

Figure 6.5 – (Discrete-time) dynamics of the proportion of infected individuals with MPC (academic case)

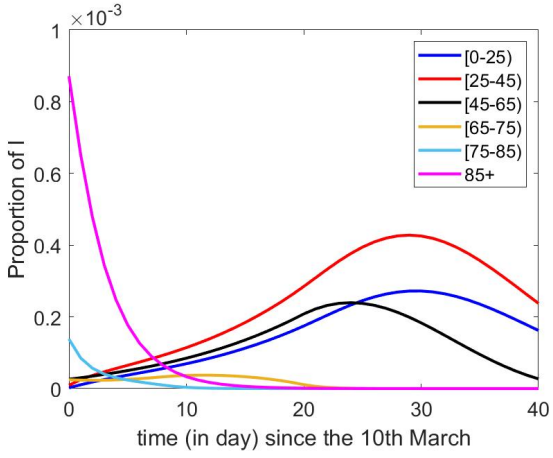

Figure 6.6 – Dynamics of the proportion of infected individuals, following the Belgian strategy (academic case)

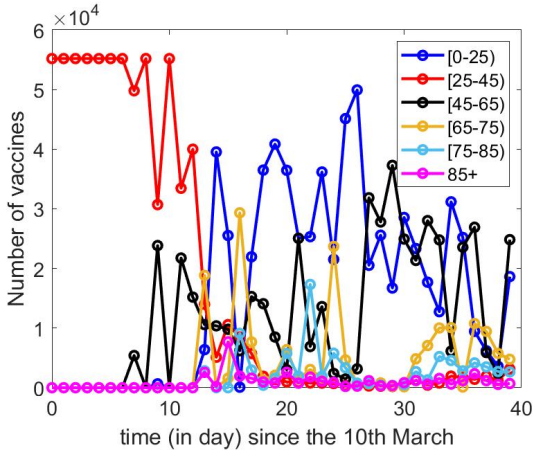

Figure 6.7 – Distribution of the number of administrated vaccines per day, by using MPC strategy (academic case)

Part III

Distributed parameter age-dependent epidemic model

Introduction

This part applies to non-lethal long-term diseases. Hence the dynamics of the deceased individuals do not need to be considered. However it is important to consider the aging of the population. Examples of illnesses with those features are Human Papillomavirus (HPV), chronic obstructive pulmonary disease (COPD), pertussis... To deal with those kinds of disease, a simplified version of the PIDE model (1.4), described in (Bastin and Coron (2016)) is studied. An input, denoted $\theta(t,a)$, representing the vaccination is added. It represents the rate at which the susceptible individuals are vaccinated at time t and age a. Those individuals leave the class of susceptible to become recovered. The parameter $p(a)$, representing the probability of successful vaccination for an individual of age a, is added to consider the fact that the vaccination does not always work perfectly. Therefore, the evolution of the different groups, in terms of densities, is described by a system of nonlinear partial integro-differential equations, called PIDE model, given by

$$\begin{cases} (\partial_t + \kappa\partial_a)\, S\,(t,a) = -\left(\mu(a) + p(a)\theta(t,a)\right) S(t,a) - c(a)S(t,a)\displaystyle\int_0^{a_{max}} I(t,b)db \\ (\partial_t + \kappa\partial_a)\, I\,(t,a) = -\left(\mu(a) + \gamma(a)\right) I(t,a) + c(a)S(t,a)\displaystyle\int_0^{a_{max}} I(t,b)db \\ (\partial_t + \kappa\partial_a)\, R\,(t,a) = -\mu(a)R(t,a) + \gamma(a)I(t,a) + p(a)\theta(t,a)S(t,a), \end{cases} \tag{6.11}$$

where the coefficient κ is introduced to balance the possible change of units for time and age. For instance, it is set to $1/365$ when time is in day and age in year, which is the case here. The initial conditions are given by $S(0,a) = S_0(a), I(0,a) = I_0(a), R(0,a) = R_0(a)$. Moreover, it is assumed that there is no vertical transmission of the disease, i.e a mother cannot transmit the disease to her child. Therefore, all new born are susceptible. This translates in terms of boundary conditions by

$$\begin{cases} S(t,0) = B \\ I(t,0) = 0 \\ R(t,0) = 0, \end{cases}$$

where B, denoting the birth rate, is assumed constant in time. In the following, it is assumed that $c(.)$ and $\gamma(.)$ are in $L^\infty\left([0,a_{max}]\right)$, the space of essentially bounded functions defined on $[0,a_{max}]$. The interpretations and units of the variables and parameters involved in the PIDE Model and in the following models, are described in Table 6.1.

Notice that, since an SIR model is used, instead of an SIRD for instance, this model is best-suited for non-lethal disease. Moreover, the age is considered continuously, which is important for long-term diseases. Hence, the study

Variables	Interpretation	Range	Unit
t	Time	$\mathbb{R}^+$	day
a_{max}	Maximum age	$\mathbb{R}^+$	year
a	Age	$[0, a_{max}]$	year
α	balancing coefficient	$\mathbb{R}^+$	$\frac{\text{year}}{\text{day}}$
$P(t,a)$	Age density of the total population	$\mathbb{R}^+$	$\frac{\text{Human}}{\text{day}}$
$S(t,a)$ $I(t,a)$ $R(t,a)$	Density of susceptible, infected and recovered individuals at time t and age a	$\mathbb{R}^+$	$\frac{\text{Human}}{\text{day}}$
$s(t,a)$ $i(t,a)$ $r(t,a)$	Normalized density of susceptible, infected and recovered individuals at time t and age a	$[0,1]$	no unit
$\hat{s}(t,a)$	Normalized density of susceptible individuals at time t and age a	$[-1,0]$	no unit
$\theta(t,a)$	Rate of vaccinated individuals	$\mathbb{R}^+$	$\frac{1}{\text{day}}$
Parameters			
B	birth rate	$\mathbb{R}_0^+$	$\frac{\text{Human}}{\text{day}}$
$\mu(a)$	Per capita natural death rate	$\mathbb{R}^+$	$\frac{1}{\text{day}}$
$c(a)$	Mean contact between all infected and a susceptible individuals of age a	$\mathbb{R}^+$	$\frac{1}{\text{Human.day}}$
$\gamma(a)$	Recovery rate	$\mathbb{R}^+$	$\frac{1}{\text{day}}$
$p(a)$	Probability of successful vaccination	$(0,1]$	no unit

Table 6.1 – Parameters and variables for PIDE models

developed in this part could be very interesting for instance for the Human papillomavirus (HPV) for which a vaccine exists.

Chapter 7 gathers the concepts needed in this Part. Then, the dynamical analysis of Model (6.11) is performed in Chapter 8 to investigate the question of existence and uniqueness of a solution but also the question of the stability of the equilibria. In view of the results obtained in previous chapter, Chapter 9 is dedicated to the design of a state feedback law for Model (6.11) in order to stabilize the disease-free equilibrium. This law is implemented in two steps. First, a linearizing state feedback law is designed on the discretization by age of Model (6.11), using classical theory for finite dimensional systems (see (Isidori (1995))). In a second time, a linearizing feedback law for the infinite dimensional system is deduced from the previous one.

Chapter 7

Theoretical concepts

In the same spirit as Chapter 2, this chapter is dedicated to the introduction of some necessary concepts to the understanding of the following chapters. The reader may skip this chapter and come back to it if needed. This part mainly develops tools that are useful for the study of infinite dimensional systems. Firstly, the background for linear systems is recalled. Then, some results concerning nonlinear systems are described.

7.1 A state-space approach for linear infinite dimensional systems

This first part, inspired by (Klaus-Jochen and Rainer (2006)) and (Curtain and Zwart (2020)), is dedicated to the development of a theory to deal with linear infinite dimensional systems.
In the case of partial differential equations (PDEs), one natural approach consists to use semigroups, defined in Definition 7.1.1, to represent the system of PDEs via an "abstract Cauchy problem" (also called an abstract differential equation),

$$\begin{cases} \dot{x}(t) = Ax(t), t > 0 \\ x(0) = x_0 \end{cases} \tag{7.1}$$

where A is a linear operator on a dense subspace $D(A)$ of a Banach space X. $D(A)$ is called the domain of the operator. If for each initial condition $x_0 \in X$, a unique solution $x(., x_0)$ exists then, $T(t)x_0 := x(t, x_0), t \geqslant 0$ defines an operator semigroup.

Definition 7.1.1 ***Operator semigroup***
Consider the linear operator-valued function $T(t)$ on X, for any $t \geqslant 0$. It is an operator semigroup if it satisfies

1. $T(0) = id_X$
2. $T(t+s) = T(t)T(s)$ *for all* $t, s \geqslant 0$.

Remark that the abstract differential equation extends the finite dimensional case, where A is given by a matrix. In this case, the solution is given by the matrix exponential $x(t) = e^{tA}x_0$. This can be generalized for any operator A in the set of linear and bounded operators on X, denoted $\mathcal{L}(X)$, by the operator valued function

$$T(t) = e^{tA} := \sum_{n=0}^{\infty} \frac{t^n A^n}{n!}.$$

In most of the cases, the operator semigroup needs to be strongly continuous to ensure that (7.1) admits a unique solution (see Section 7.2 for more details). This important property is defined in the next definition.

Definition 7.1.2 ***Strongly continuous semigroup***
A family $(T(t))_{t\geqslant 0}$ of bounded linear operators on a Banach space X is called a strongly continuous (C_0-semigroup) if it is an operator semigroup and it satisfies

$$\|T(t)x_0 - x_0\| \to 0 \text{ as } t \to 0^+ \text{ for all } x_0 \in X.$$

The following proposition will be helpful to define a particular bound of the semigroup, the growth bound, that plays an important role in the stability analysis.

Proposition 7.1.1
For every strongly continuous semigroup $(T(t))_{t\geqslant 0}$, there exist constants $\omega \in \mathbb{R}$ and $M \geqslant 1$ such that

$$\|T(t)\| \leqslant Me^{\omega t}, \forall t \geqslant 0.$$

Remark that, when $M = 1$ and $\omega = 0$, the semigroup is called a contraction semigroup. Now, the infimum of all the exponents ω can be introduced.

Definition 7.1.3 ***Growth bound***
The growth bound of a strongly continuous semigroup $(T(t))_{t\geqslant 0}$ is given by

$$\omega_0 := \omega_0(T) := \inf\left\{\omega \in \mathbb{R} : \text{there exists } M_\omega \geqslant 1 \text{ such that } \|T(t)\| \leqslant M_\omega e^{\omega t}, \forall t \geqslant 0\right\}.$$

Moreover, one can express A as a function of $T(t)$. In this case, A is called the generator of the semigroup.

Definition 7.1.4 ***Infinitesimal generator***
The infinitesimal generator A of a C_0-semigroup $(T(t))_{t\geqslant 0}$ is the operator

$$Ax_0 = \lim_{t\to 0^+} \frac{T(t)x_0 - x_0}{t}, \tag{7.2}$$

defined for every $x_0 \in D(A) = \{x_0 \in X : (7.2) \text{ exists}\}$.

As previously mentioned, $T(t)$ is crucial to express the solution of (7.1). However, solutions of (7.1) can be characterized in two types, according to their regularity with respect to the initial condition.

Definition 7.1.5 ***Classical solution***
A differentiable function $x : \mathbb{R}^+ \to X$ is a classical solution of (7.1) if for all $t \geqslant 0$, $x(t) \in D(A)$ and equation (7.1) is satisfied.

Definition 7.1.6 ***Mild solution***
A continuous function $x : \mathbb{R}^+ \to X$ is a mild solution of (7.1) if

$$\int_0^t x(s)ds \in D(A), \quad x(0) = x_0 \quad \text{and} \quad x(t) - x_0 = A\int_0^t x(s)ds,$$

for all $t \geqslant 0$.

In some particular cases, one needs to deal with so-called perturbation systems of the form

$$\begin{cases} \dot{x}(t) = (A + D)\, x(t), t > 0 \\ x(0) = x_0 \end{cases} \tag{7.3}$$

where $D \in \mathcal{L}(X)$. In this case, the following result, taken from (Curtain and Zwart, 2020, Chapter 3, Section 5) and generalized to Banach spaces, turns out to be very interesting. Notice that this result is also introduced in (Klaus-Jochen and Rainer, 2006, Chapter 3, Section 1) as the bounded perturbation theorem.

Theorem 7.1.1: Bounded perturbation Theorem
Suppose that A is the infinitesimal generator of a C_0-semigroup $T(t)$ on a Banach space X and that $D \in \mathcal{L}(X)$.
Then, $A + D$ is the infinitesimal generator of a C_0-semigroup $T_D(t)$.
Moreover, if $\|T(t)\| \leqslant Me^{\omega t}$, then $\|T_D(t)\| \leqslant Me^{(\omega+M\|D\|)t}$.
Furthermore, this C_0-semigroup satisfies the following equations for every $x_0 \in X$,

$$T_D(t)x_0 = T(t)x_0 + \int_0^t T(t-s)DT_D(s)x_0 ds$$

and

$$T_D(t)x_0 = T(t)x_0 + \int_0^t T_D(t-s)DT(s)x_0 ds.$$

Finally other ways for generating new C_0-semigroups are given below.

Proposition 7.1.2
Let $T_1(t)$ and $T_2(t)$ be C_0-semigroups on their respective Banach spaces X_1 and X_2, with infinitesimal generators A_1 and A_2, respectively.
Suppose that $\|T_i(t)\| \leqslant M_i e^{\omega_i t}, i = 1, 2$ and $D \in \mathcal{L}(X_1, X_2)$.
Then, the operator $A = \begin{pmatrix} A_1 & 0 \\ D & A_2 \end{pmatrix}$ with $\mathcal{D}(A) = \mathcal{D}(A_1) \times \mathcal{D}(A_2)$ is the infinitesimal generator of the C_0-semigroup $T(t)$ on $X = X_1 \times X_2$ given by

$$T(t) = \begin{pmatrix} T_1(t) & 0 \\ S(t) & T_2(t) \end{pmatrix}, S(t)x = \int_0^t T_2(t-s)DT_1(s)x ds.$$

Furthermore, there exists a positive constant M such that

$$\|T(t)\| \leqslant Me^{\omega t},$$

where $\omega = \max\{\omega_1, \omega_2\}$ if $\omega_1 \neq \omega_2$ and $\omega > \omega_1$ if $\omega_1 = \omega_2$.

A second way to generate new C_0-semigroups is developed in (Schumacher, 1981, Lemma 4.5) and uses a similarity transformation, defined below.

Definition 7.1.7 *Similarity transformation*
A linear mapping between two Banach spaces is a similarity transformation if the mapping is bounded and has a bounded inverse.

Hence, a semigroup can be modified thanks to such transformation, according to the following result.

Proposition 7.1.3
Suppose that $J : X_1 \to X_2$ is a similarity transformation between the Banach spaces X_1 and X_2. Let $T(t)$ be a semigroup on X_1 with infinitesimal generator A and growth bound ω_0.
Then, the function $\tilde{T}(t) = JT(t)J^{-1}$ is a semigroup on X_2.
Moreover, the infinitesimal generator of $\tilde{T}(t)$ is the operator $\tilde{A} := JAJ^{-1}$ with domain $\mathcal{D}(\tilde{A}) = \left\{x \in X_2 : J^{-1}x \in \mathcal{D}(A)\right\} = J\left[\mathcal{D}(A)\right]$, and the growth constant of $\tilde{T}(t)$ is ω_0.

Now that the foundations are established, the following section is dedicated to results about the existence and uniqueness of solution, for the semilinear case.

7.2 Existence and uniqueness of solution

This section presents an important result concerning the existence and uniqueness of the solution for semilinear partial differential equations given by

$$\begin{cases} \dot{x}(t) = Ax(t) + \mathcal{N}\left(x(t)\right), t > 0 \\ x(0) = x_0. \end{cases} \tag{7.4}$$

The result, partially presented in (Pazy, 1983, Chapter 6, Section 1) for Banach spaces, extends the proposition in (Curtain and Zwart, 2020, Chapter 11, Section 1) stated for Hilbert spaces.

Theorem 7.2.1
Let A be the infinitesimal generator of the C_0-semigroup $(T(t))$ on the Banach space X.
If $\mathcal{N} : X \to X$ is uniformly Lipschitz continuous, then (7.4) admits a unique mild solution on $[0, \infty)$, given by

$$x(t) = T\left(t\right)x_0 + \int_0^t T\left(t-s\right)\mathcal{N}x\left(s\right)ds.$$

7.3 Method of characteristics

This section gives a brief insight on the method of characteristics, designed to solve first order PDEs. This method is used several times in this thesis: in

Sections 8.1, 8.2 and 9.2. The idea of the method is to reduce a PDE into a family of ODEs along some curves, called the characteristics. This part is inspired by (Salih (2016)) but many references exist on this subject. Only the case of a first-order linear equation of the form

$$\begin{cases} \dfrac{\partial x}{\partial t}(t,a) + c\dfrac{\partial x}{\partial a}(t,a) = 0 \\ x(0,a) = f(a) \end{cases} \tag{7.5}$$

where c is a constant, is studied to introduce the methodology. The goal is to reduce this problem along some curve $a(t)$ in the (a,t)-plane. Hence, the objective is to find a curve $a(t)$ such that the PDE equation (7.5) is satisfied along this curve. Therefore, one needs that

$$\begin{aligned} &\frac{dx(t,a(t))}{dt} = \frac{\partial x}{\partial t}(t,a) + c\frac{\partial x}{\partial a}(t,a) = 0 \\ \Leftrightarrow &\frac{dx(t,a(t))}{dt} = \frac{\partial x}{\partial t}\frac{dt}{dt} + \frac{\partial x}{\partial a}\frac{da}{dt} = \frac{\partial x}{\partial t} + \frac{\partial x}{\partial a}\frac{da}{dt} \end{aligned}$$

by the chain rule of differentiation. It follows that it is satisfied if $\dfrac{da}{dt}$ equals c. Therefore, the PDE (7.5) can be viewed as the ordinary differential equation

$$\frac{dx}{dt} = 0, \tag{7.6}$$

along any curves $a(t)$ that is solution of the equation

$$\frac{da}{dt} = c. \tag{7.7}$$

By integrating equation (7.7), it follows that the characteristic curves are given by $a(t) = ct + \xi$. Moreover, from equation (7.6), one can observe that the value of x remains constant along any characteristic curve $a(t)$. Hence, this value can be determined thanks to the initial condition,

$$x(t,a) = x(0,\xi) = f(\xi).$$

Finally, since $\xi = a - ct$, then the solution of the PDE (7.5) is given by

$$x(t,a) = f(a - ct).$$

Thus, the solution of the PDE (7.5) is the transportation of the initial profile $f(a)$ along the characteristics, with a speed of $\dfrac{da}{dt} = c$, as illustrated in Figure 7.1. Indeed, $x(t_1,a) = f(a - ct_1) = x(a - ct_1, 0)$. The presented case is very simple, but the methodology can be applied to other kinds of linear PDEs.

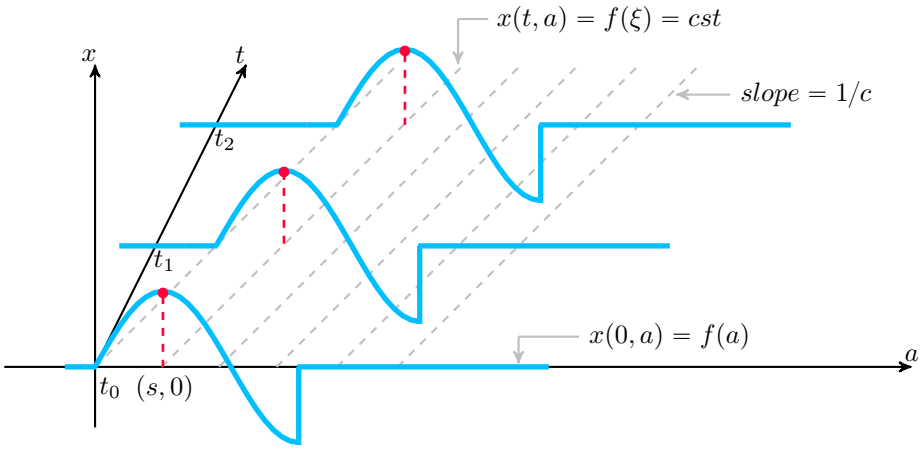

Figure 7.1 – Characteristics (in dashed) and solutions (in blue) of the PDE (7.5) at various time, inspired by (Salih (2016))

However, one helpful tool when dealing with more complex PDEs is to write the previous method of characteristic using its parametric form.

Hence, we introduce a new parameter η such that $a = a(\eta) =: a_\eta, t = t(\eta) =: t_\eta$ and $x(t,a) = x(t(\eta), a(\eta)) =: x_\eta$. Therefore, one wants that

$$\begin{aligned} &\frac{dx(t(\eta),a(\eta))}{d\eta} = \frac{\partial x}{\partial t} + c\frac{\partial x}{\partial a} = 0 \\ \Leftrightarrow &\frac{dx(t(\eta),a(\eta))}{ds} = \frac{\partial x}{\partial t}\frac{dt}{d\eta} + \frac{\partial x}{\partial a}\frac{da}{d\eta}. \end{aligned}$$

This is satisfied if

$$\frac{dt_\eta}{d\eta} = 1; \frac{da_\eta}{d\eta} = c \text{ and } \frac{dx_\eta}{d\eta} = 0.$$

Solving those equations implies

$$t_\eta = \eta + t_0; a_\eta = c\eta + a_0 \text{ and } x_\eta = cst.$$

So, as previously, the solution x_η is constant along the characteristics. Letting $t_0 = 0, a_0 = a_0$ implies that $x_0 = x(t(0), a(0)) = x(0, a_0) = f(a_0)$. Therefore, $x_\eta = x_0 = f(a_0) = f(a_\eta - c\eta)$. Hence, $x(t,a) = f(a - ct)$. Notice that, in some more complicated cases, as in Section 8.1 for instance, the domain of the variable needs to be taken into account when solving the ODEs.

7.4 Principle of linearized stability

Dealing with nonlinear PDEs systems is often difficult. However, some tools have been developed to establish conclusions about the stability of equilibria of nonlinear systems by studying their linearization. To linearize some equations, one needs to compute the derivative of a nonlinear operator. The following concepts introduce two notions of differentiability for operators that are useful for the next theorem.

Definition 7.4.1 ***Gâteaux differentiability***
Let $\mathcal{N} : \mathcal{D}(\mathcal{N}) \subseteq X \to X$ be a nonlinear operator on a Banach space X. The operator $\mathcal{N}$ is Gâteaux differentiable at $x_0 \in \mathcal{D}(\mathcal{N})$ if there exists a linear operator $d\mathcal{N}(x_0) : X \to X$ such that

$$\lim_{\epsilon \to 0} \frac{\mathcal{N}(x_0 + \epsilon z) - \mathcal{N}(x_0)}{\epsilon} = d\mathcal{N}(x_0)z,$$

for every $z \in \mathcal{D}(\mathcal{N})$ such that $x_0 + \epsilon z \in \mathcal{D}(\mathcal{N})$ for all ϵ sufficiently small. The operator $d\mathcal{N}(x_0)$ is called the Gâteaux derivative of the operator $\mathcal{N}$ at x_0.

Definition 7.4.2 ***Fréchet differentiability***
The nonlinear operator $\mathcal{N} : \mathcal{D}(\mathcal{N}) \subseteq X \to X$ is said to be Fréchet differentiable at $x_0 \in \mathcal{D}(\mathcal{N})$ if there exists a bounded linear operator $d\mathcal{N}(x_0) : X \to X$ such that

$$\lim_{h \to 0} \frac{\|\mathcal{N}(x_0 + h) - \mathcal{N}(x_0) - d\mathcal{N}(x_0)\|_X}{\|h\|_X} = 0,$$

where h is such that $x_0 + h \in \mathcal{D}(\mathcal{N})$.

Moreover, in the next theorem, the concept of exponential stability is defined for an abstract differential equation. This extends Definition 2.3.2 to infinite-dimensional systems. As for the finite case, exponential stability expresses the fact that the trajectories of (7.8), i.e the C_0-semigroup $(S(t))_{t \geqslant 0}$, decay exponentially. Formally, as introduced in (Curtain and Zwart, 2020, Section 4) (but stated here for Banach spaces), this means that the C_0-semigroup $(S(t))_{t \geqslant 0}$ satisfies the definition below.

Definition 7.4.3 ***Exponential stability***
A strongly continuous semigroup $(S(t))_{t \geqslant 0}$ of bounded linear operators on a Banach space X, is (globally) exponentially stable if there exist positive constants M and α such that

$$\|S(t)\| \leqslant Me^{-\alpha t}, \forall t \geqslant 0.$$

Finally, the following theorem needs the assumption that an operator is dissipative. The next definition, from (Engel and Nagel, 2000, Definition 3.13), recalls this concept.

Definition 7.4.4 ***Dissipative operator***
A linear operator $(A, D(A))$ on a Banach space X is called dissipative if

$$\| (\lambda Id - A) x\| \geqslant \lambda \|x\|$$

for all $\lambda > 0$ and $x \in D(A)$.

The process of studying the stability of the linearized system is called the principle of linearized stability and it shows that, under some hypothesis, the stability of the linearized system implies the local stability of the considered equilibrium for the nonlinear system. This is introduced in the following theorem, stated a particular case (with space X=Y) of a result developed in (Hastir et al., 2020, Theorem 9), that extends results of (Jamal and Morris (2018)), on Banach spaces.

Theorem 7.4.1
Consider a semilinear system of the form

$$\begin{cases} \dot{x} = Ax + \mathcal{N}(x) \\ x(0) = x_0 \end{cases} \tag{7.8}$$

where A is a linear operator on its domain $\mathcal{D}(A)$, which is a linear subspace of a Banach space X, and $\mathcal{N}$ is a nonlinear operator such that $\mathcal{N} : \mathcal{D}(A) \cap \mathcal{D}(\mathcal{N}) \subset X \to X$.
Assume that (7.8) admits an equilibrium profile x_e, i.e there exists $x_e \in \mathcal{D}(A) \cap \mathcal{D}(N)$ such that $Ax_e + \mathcal{N}(x_e) = 0$.
Assume that the following conditions hold:

1. A is quasidissipative, i.e. there exists $l_A > 0$ such that the operator $A - l_{\mathcal{A}} I$ is dissipative (see Definition 7.4.4) on $\mathcal{D}(A) \cap \mathcal{D}(\mathcal{N})$;
2. the nonlinear operator $\mathcal{N}$ is Lipschitz continuous on $\mathcal{D}(A) \cap \mathcal{D}(\mathcal{N})$ with respect to the X norm;
3. the operator $A + \mathcal{N}$ is the infinitesimal generator of a nonlinear C_0-semigroup $(S(t))_{t \geqslant 0}$ on X;
4. the Gâteaux derivative $d\mathcal{N}(x_e)$ of $\mathcal{N}$ at x_e is a bounded linear operator on X;
5. the Gâteaux linearized dynamics of (7.8) is given by

$$\begin{cases} \dot{\bar{x}} = (A + d\mathcal{N}(x_e))\, \bar{x} \\ \bar{x}(0) = x_0 - x_e = \bar{x}_0 \end{cases} \tag{7.9}$$

6. the nonlinear semigroup $(S(t))_{t\geqslant 0}$ is Fréchet differentiable with Fréchet derivative $(T_{x_e}(t))_{t\geqslant 0}$ corresponding to the linear semigroup generated by the Gâteaux derivative of $A+\mathcal{N}$ at x_e.

Then, if the linearized system (7.9) is exponentially stable, then x_e is a locally exponentially stable equilibrium of (7.8). Moreover, if x_e is an unstable equilibrium of (7.9), it is locally unstable for the nonlinear system (7.8).

In view of Proposition 7.1.1 and the Definition 7.1.3 of the growth bound, the following result is obvious.

Proposition 7.4.1
The C_0-semigroup $(S(t))_{t\geqslant 0}$ is exponentially stable if and only if $\omega_0 < 0$.

7.5 Spectrum theory for stability analysis

In this section, the main concepts and results that are needed for the stability analysis developed in Subsection 8.2.2 are gathered. The definition and results of this section are taken from (Klaus-Jochen and Rainer (2006)).
First, some concepts (linking numbers to linear operators) needed to investigate stability of a system, are defined below.
Let

$$A : \mathcal{D}(A) \subset X \to X$$

be a closed linear operator on a Banach space X.

Definition 7.5.1 ***Resolvent set, spectrum, resolvent operator***

- *The set $\rho(A) = \{\lambda \in \mathbb{C} : \lambda Id - A : \mathcal{D}(A) \to X$ is bijective$\}$ is the resolvent set of A.*
- *The complement of the resolvent set, denoted $\sigma(A) := \mathbb{C}\backslash\rho(A)$, is the spectrum of A.*
- *For $\lambda \in \rho(A)$, the operator $R_\lambda(A) := (\lambda Id - A)^{-1}$ is a bounded operator on X and is called the resolvent of A at the point λ.*

The spectrum of A can be characterized thanks to two quantities defined below.

Definition 7.5.2 ***Spectral radius and spectral bound***

- *The spectral radius, $r(A)$, of A is the supremum of the modulus of the elements of its spectrum, i.e $r(A) = \sup\{|\lambda| : \lambda \in \sigma(A)\}$.*

— *The spectral bound of A, $s(A)$, is the supremum of the real parts of the elements of its spectrum, i.e $s(A) = \sup\{Re\ \lambda : \lambda \in \sigma(A)\}$.*

Notice that $s(A)$ can be any real number or $-\infty$ (if $\sigma(A) = \varnothing$). Moreover, the spectral bound $s(A)$ is always dominated by the growth bound ω_0 (see Definition (7.1.3)). Hence, $-\infty \leqslant s(A) \leqslant \omega_0$.

The following definition concerns one subset of the spectrum of A.

Definition 7.5.3 ***Point spectrum***
The set $\{\lambda \in \mathbb{C} : \lambda Id - A$ is not injective$\}$ is the point spectrum of A, denoted by $P_\sigma(A)$.
Moreover, each $\lambda \in P_\sigma(A)$ is called an eigenvalue of A and each $x \in \mathcal{D}(A)$ such that $x \neq 0$, satisfying $(\lambda Id - A)\, x = 0$ is an eigenvector of A (corresponding to λ.)

As mentioned in (Webb (1985)), for a closed linear operator, the eigenvalues of A are the poles of the resolvent.

Proposition 7.5.1
Let A be a closed linear operator in the complex Banach space X and let λ_0 be an isolated point of $\sigma(A)$. If λ_0 is a pole of $(\lambda Id - A)^{-1}$ of order m, then λ_0 is an eigenvalue of A with multiplicity m.

Finally, the next definition characterizes a property of operators, leading to interesting results in the case of spectrum theory.

Definition 7.5.4 ***Compact operator***
An operator $T \in \mathcal{L}(X, Y)$ is said to be compact if the image $T(B)$ is relatively compact in Y, with B the closed unit ball in X.

All the necessary concepts are introduced to be able to state the following result, telling that, as in finite dimension, the spectrum and the point spectrum of an operator with compact resolvent coincide. This is a corollary of the "Spectral mapping theorem for the resolvent" (see (Klaus-Jochen and Rainer, 2006, Chapter V, Corollary 1.15))

Proposition 7.5.2
If the operator A has compact resolvent, then $\sigma(A) = P_\sigma(A)$.

Moreover the following theorem from (Heijmans (1986)) states that, under some assumptions, the spectral radius of a positive and compact operator A,

$r(A)$, is an eigenvalue of A. This theorem can thus be seen as an extension of the Perron-Frobenius theorem to the infinite-dimensional case. But first let us define some necessary concepts.

Definition 7.5.5 ***Cones and Positive operators***

- *A non-empty closed subset X_+ of a Banach space X is called a cone if the following holds:*
  1. $X_+ + X_+ \subset X_+$,
  2. $\lambda X_+ \subset X_+$ *for* $\lambda \geqslant 0$,
  3. $X_+ \cap (-X_+) = \{0\}$.
- *The cone X_+ is called total if the set $\{x - y : x, y \in X_+\}$ is dense in X.*
- *A bounded linear operator $A : X \to X$ is positive (with respect to the cone X_+) if $Ax \in X_+$ for all $x \in X_+$.*

Theorem 7.5.1
Let $A : X \to X$ be compact and positive with respect to the total cone $X_+ \subseteq X$ (a Banach space) and let $r(A)$ be the spectral radius of A. Then, there exists a $\psi \in X_+$, $\psi \neq 0$ such that $A\psi = r(A)\psi$.

In this thesis, a particular class of operators, named Volterra operators will be encountered. The following proposition, coming from (Brunner, 2017, Chapter 8, Section 1), states results about the compactness of those operators, that are linked to the property of their kernel, K.

Proposition 7.5.3: Compact Volterra operator
Let $\mathcal{V}$ be the Volterra integral operator defined by

$$(\mathcal{V}f)(t) = \int_0^t K(t,s) f(s)\, ds.$$

Then

1. if K is continuous on its domain, D, $\mathcal{V}$ is a compact (and hence bounded) operator from $L^p(0,T)$ to $L^p(0,T)$ for any $p \in [1,\infty)$.
2. if $K \in L^2(D)$, $\mathcal{V}$ is a compact (and hence bounded) operator from $L^2(0,T)$ to $L^2(0,T)$, with norm

$$\|\mathcal{V}\|_2 = \left(\int_0^T \left(\int_0^T |K(t,s)|^2 ds \right)^2 \right)^{1/2}.$$

However, if one wants to establish that an operator, which is not a Volterra operator, is compact, the next result will prove helpful. It requires the notion of operator with finite rank, defined for instance in (Brezis (2011)).

Definition 7.5.6 ***Finite-rank Operators***
Let X and Y denote two Banach spaces.
An operator $A \in \mathcal{L}(X,Y)$ is said to be finite rank it the range of A, $ImA := \{Ax : x \in D(A)\} \subset Y$, is finite-dimensional.

Proposition 7.5.4
Any finite-rank operator is compact.

Moreover, the following proposition, find in (Yosida, 1980, Chapter X, Section 2), states some interesting properties about compact operators.

Proposition 7.5.5

1. A linear combination of compact operators is compact.
2. The composition of a compact operator with a bounded linear operator is compact.
3. Let a sequence (T_n) of compact operators $\subset \mathcal{L}(X,Y)$ converge to an operator T in the sense of the uniform operator topology, i.e, $\lim_{n\to\infty} \|T - T_n\| = 0$. Then, T is also compact.

Another interesting property about operators leads to some helpful spectrum theory results, in terms of eigenvalues. This applies to analytic families of compact operators. First, let us recall what is an analytic family of operators using (Steinberg (1968)).

Definition 7.5.7 ***Analytic family of operators***
Let $T : \Omega \subset \mathbb{C} \to \mathcal{B}(X)$, where $\mathcal{B}(X)$ is the set of bounded operators on X, which is a Banach space. Then $T(x)$ is said to be analytic in Ω if, for each $x_0 \in \Omega$,

$$T(x) = \sum_{n=0}^{\infty} T_n (x - x_0)^n ,$$

where $T_n \in \mathcal{B}(X)$ and where the serie converges in the uniform operator topology in some neighbourhood of x_0.

In the case of analytic families of compact operators $T(x)$, a proposition from (Steinberg (1968)) shows that if $(I - T(x))$ is invertible for at least one x, hence each of its singular points are poles.

Proposition 7.5.6
If $T(x)$ is an analytic family of compact operators for $x \in \Omega \subset \mathbb{C}$, then $(I - T(x))$ is nowhere invertible in Ω or else $(I - T(x))^{-1}$ is meromorphic [a] in Ω.

a. A meromorphic function is an holomorphic function in a domain $\Omega \backslash \{a_1, a_2, ...\}$ which has at every singular point a_p a pole.

Concerning the spectral radius, one can state two useful results, in the case of compact non-supporting operators. But first, let us define those operators, using a definition from (Heijmans (1986)).

Definition 7.5.8 ***Non-supporting operator***
Let X be a Banach space and X' its dual (the space of all linear functionals on X).
A bounded, positive operator $A : X \to X$ is called non-supporting with respect to the cone X_+ if and only if for every pair $\psi \in X_+ \backslash \{0\}, F \in X'_+ \backslash \{0\}$, there exists a positive integer p such that for all $n \geqslant p$, the value of F at $A^n\psi$, denoted by $[F, A^n\psi]$, is positive, i.e $[F, A^n\psi] > 0$.

Now, two propositions concerning the spectral radius of non-supporting operators can be applied. They are taken from (Inaba (1990)) and derived from (Marek (1970)).

Proposition 7.5.7: Comparison Proposition
Let X be a Banach lattice [a] and let $A, B \in \mathcal{B}(X)$ be positive operators.

1. If $A \leqslant B$ then, $r(A) \leqslant r(B)$.
2. If A and B are compact (see Definition 7.5.4) and non-supporting operators such that $r(B) \neq 0$ and $A \leqslant B$ then, $r(A) < r(B)$.

a. A Banach lattice is Banach space with a lattice order, i.e such that $\forall\ x, y \in X, |x| \leqslant |y| \Rightarrow \|x\| \leqslant \|y\|$ where $|x|$ is the supremum of x and $-x$.

Proposition 7.5.8
Let X be a Banach lattice and let $A \in \mathcal{B}(X)$ be compact and non-supporting. Then, the following holds :

1. $r(A) \in P_\sigma(A) \setminus \{0\}$ and $r(A)$ is a simple pole of the resolvent, that is, $r(A)$ is an algebraically simple eigenvalue of A.
2. The eigenspace corresponding to $r(A)$, with corresponding eigenvector $\psi \in X_+$, is one-dimensional and the relation $A\phi = \mu\phi$ with $\phi \in X_+$ implies that $\phi = c\psi$ for some non-zero constant c.
3. The eigenspace of $A^\star$ corresponding to $r(A)$ is also one-dimensional subspace of $X^\star$ spanned by a strictly positive function $f \in X_+$.

Finally, a class of semigroups of interest in this thesis, with particular properties is introduced, as well as some spectrum theory results applying to those semigroups.

Definition 7.5.9 ***Eventually norm-continuous***
A strongly continuous semigroup $(T(t))_{t\geqslant 0}$ is called eventually norm-continuous if there exists $t_0 \geqslant 0$ such that the function $t \to T(t) \in (\mathcal{L}(X), \|\cdot\|)$ is continuous from (t_0, ∞) into $\mathcal{L}(X)$. It is called norm-continuous if $t_0 = 0$.

Remark that nilpotent semigroups, $(T(t))_{t\geqslant 0}$ such that there exists $r > 0$: $T(t) = 0, t > r$, are examples of eventually-continuous semigroups.

The following result, from (Arendt et al., 1983, A-II, Section 1, Theorem 1.30) is useful to characterize semigroups obtained via an addititive perturbation

Theorem 7.5.2
Let $(T(t))_{t\geqslant 0}$ be a C_0-semigroup with generator A and $B \in \mathcal{L}(X)$.
If $(T(t))_{t\geqslant 0}$ is holomorphic or norm-continuous or compact, then so is the semigroup $(S(t))_{t\geqslant 0}$ generated by $A + B$.
Moreover, if $(T(t))_{t\geqslant 0}$ is eventually-norm continuous and if B is compact, then $(S(t))_{t\geqslant 0}$ is also eventually norm-continuous.

Now, a corollary of the "Spectral mapping theorem for the eventually norm-continuous semigroups" (see (Klaus-Jochen and Rainer, 2006, Chapter V, Corollary 2.9)) can be stated. It establishes the equality between the growth bound and the spectral bound of an operator.

Proposition 7.5.9

For an eventually norm-continuous semigroup $(T(t))_{t\geqslant 0}$ with generator $(A, \mathcal{D}(A))$ on a Banach space X, it holds that $s(A) = \omega_0$.

Chapter 8

Dynamical analysis

In this chapter, questions about the well-posedness of the considered system in terms of existence and uniqueness of a solution are investigated. Moreover, a study of the stability of the equilibria is performed in order to have a better knowledge concerning the behavior of the trajectories of the system. This analysis is done by considering the system under a state feedback, contrary to what has been done in (Inaba (2017)). Moreover, in this thesis, a proof of the principle of linearized stability is given.

8.1 Well-posedness

This section is inspired by (Inaba (1990)) and (Inaba, 2017, Chapter 6). First, the existence of a unique solution is established. Then, its well-posedness in terms of physical meaning is studied. Those results are obtained using semigroup theory results, recalled in Section 7.2 and the method of characteristics, briefly introduced in Section 7.3.

8.1.1 Normalized SIR model

For the following analysis, it is easier to work with a normalized model in order to consider only two equations instead of three. This is done by taking into account the age density of the total population, $P(t,a) = S(t,a) + I(t,a) + R(t,a)$, whose dynamics is given by

$$\partial_t P(t,a) + \kappa \partial_a P(t,a) = -\mu(a) P(t,a),$$

with initial condition $P(0,a) = P_0(a)$ and boundary condition $P(t,0) = B$. The solution of this system can be determined by using the method of charac-

teristics, as mentioned in (Hethcote (2008)),

$$P(t,a) = \begin{cases} B \exp\left(-\frac{1}{\kappa}\int_0^a \mu(\eta)\, d\eta\right) \text{ for } t \geqslant \frac{a}{\kappa}, \\ P_0(a-\kappa t) \exp\left(-\int_{a-\kappa t}^a \frac{1}{\kappa}\mu(\eta)\, d\eta\right) \text{otherwise.} \end{cases}$$

One can notice that $\lim_{t\to\infty} P(t,a) = B \exp\left(-\int_0^a \frac{1}{\kappa}\mu(\eta)\, d\eta\right) =: P^\star(a)$. Hence, in the following analysis, it is assumed that the population has reached its demographic steady-state, meaning that the age density of the host population is given by $P(t,a) = P^\star(a)$.

In order to get a dimensionless model of System (6.11), new variables, s, i and r defined by $S(t,a) = P^\star(a)s(t,a)$; $I(t,a) = P^\star(a)i(t,a)$; $R(t,a) = P^\star(a)r(t,a)$ are introduced. Therefore, the PIDE model (6.11) can be rewritten as a nonlinear system of normalized partial integro-differential equations, denoted by NPIDE,

$$\begin{cases} (\partial_t + \kappa\partial_a)\, s(t,a) = -p(a)\theta(t,a)\, s(t,a) - c(a)\, s(t,a) \int_0^{a_{max}} i(t,b)P^\star(b)db, \\ (\partial_t + \kappa\partial_a)\, i(t,a) = -\gamma(a)\, i(t,a) + c(a)\, s(t,a) \int_0^{a_{max}} i(t,b)P^\star(b)db, \\ (\partial_t + \kappa\partial_a)\, r(t,a) = p(a)\theta(t,a)\, s(t,a) + \gamma(a)\, i(t,a) \end{cases} \tag{8.1}$$

under initial conditions $s(0,a) = s_0(a)$, $i(0,a) = i_0(a)$, $r(0,a) = r_0(a)$ and boundary conditions $s(t,0) = 1$, $i(t,0) = 0$, $r(t,0) = 0$. Using those variables leads to the invariance relation $s(t,a) + i(t,a) + r(t,a) = 1$. Therefore, only two equations are needed in order to characterize the dynamics of the disease propagation.

8.1.2 Homogeneous normalized SIR model

Before entering the core of this chapter, one last change is performed to the NPIDE model (8.1) in order to work with homogeneous boundary conditions. Indeed, to perform dynamical analysis and stability analysis, it is easier to deal with a system with homogeneous boundary conditions. Hence, the new variable $\hat{s}(t,a) = s(t,a) - 1$ yields an equivalent model with homogeneous boundary conditions, which is denoted as HNPIDE,

$$\begin{cases} (\partial_t + \kappa\partial_a)\, \hat{s}(t,a) = -p(a)\theta(t,a)\,(1+\hat{s}(t,a)) \\ \qquad\qquad + c(a)\,(1+\hat{s}(t,a)) \int_0^{a_{max}} i(t,b)P^\star(b)\, db, \\ (\partial_t + \kappa\partial_a)\, i(t,a) = -\gamma(a)\, i(t,a) + c(a)\,(1+\hat{s}(t,a)) \int_0^{a_{max}} i(t,b)P^\star(b)\, db, \end{cases} \tag{8.2}$$

under initial conditions $\hat{s}(0,a) = \hat{s}_0(a) = s_0(a) - 1$, $i(0,a) = i_0(a)$ and boundary conditions $\hat{s}(t,0) = 0$, $i(t,0) = 0$. With this new variables, the nonnegativity of the system is lost. However, the boundary conditions become homogeneous.

In the analysis, the state space of the model is the Banach space $X = L^1(0, a_{max}) \times L^1(0, a_{max})$ and its norm is defined for all $x = (x_1, x_2)^T \in X$ by $\|x\|_X := \|x\| = \|x_1\|_1 + \|x_2\|_1$ where $\|x\|_1$ is the usual norm on $L^1(0, a_{max})$. Moreover, the physical space is

$$\Omega = \left\{ (\hat{s}, i)^T \in L^1(0, a_{max}) \times L^1(0, a_{max}) : -1 \leqslant \hat{s} + i \leqslant 0 \right\}. \tag{8.3}$$

This choice of space has the advantage to allow the (nonnegative) state variables to be interpreted as numbers of individuals. Moreover, in the dynamical analysis developed in Chapter 9, this choice turns out to be fully appropriate. Remark that in the following, the same units in age and time are considered for the analysis, therefore κ equals 1. The results easily extend to the case where κ is not equal to 1.

8.1.3 Existence and uniqueness

A key question before starting the design of a control law is to make sure that the equations admit a unique solution. If this is not the case, no prediction could be made on the basis of the model. The following theorem shows that the HNPIDE (8.2) under state feedback has a unique solution. Therefore, it is also the case for models PIDE (6.11) and NPIDE (8.1) since they are equivalent. The choice of a state feedback has been made since this is the control method that is applied in the following. In the next part of the thesis, this analysis will be particularized since the obtained feedback will be linearizing.

Theorem 8.1.1
Assume that $\theta(t,a)$ is given by a bounded Lipschitz continuous state feedback law $\theta(t,a) = \hat{\Theta}(x(t,a))$.
Then, for every $x_0 \in L^1(0, a_{max}) \times L^1(0, a_{max})$, the system HNPIDE (8.2) has a unique mild solution on $[0, \infty)$.

Proof. In order to use Theorem 7.2.1, a semigroup formulation of the HNPIDE model (8.2) is used. Hence, HNPIDE model (8.2) rewrites

$$\frac{d\hat{x}(t)}{dt} = A\hat{x}(t) + \hat{\mathcal{N}}(\hat{x}(t)), \hat{x}(0) = \hat{x}_0 \tag{8.4}$$

where $\hat{x} = (\hat{s}, i)^T$ is the state vector. Moreover, A is defined by

$$A\hat{x} = \begin{pmatrix} -\dfrac{d\hat{s}}{da} & 0 \\ 0 & -\dfrac{di}{da} \end{pmatrix}$$

with $\mathcal{D}(A) = \left\{(\hat{s}, i)^T \in X : \hat{s}, i \in AC[0, a_{max}],\ \text{and } \hat{s}(0) = i(0) = 0\right\}$ and $\hat{\mathcal{N}}$ is defined by

$$\hat{\mathcal{N}}(\hat{x})(a) = \begin{pmatrix} -p(a)\hat{\Theta}(\hat{x})(a)(1+\hat{s}(a)) + c(a)(1+\hat{s}(a))\displaystyle\int_0^{a_{max}} i(b)P^\star(b)\,db \\ -\gamma(a)\,i(a) + c(a)(1+\hat{s}(a))\displaystyle\int_0^{a_{max}} i(b)P^\star(b)\,db \end{pmatrix}.$$

Firstly, one can notice that A is the infinitesimal generator of a C_0-semigroup of the form

$$\begin{pmatrix} T_1(t) & 0 \\ 0 & T_1(t) \end{pmatrix}$$

where

$$(T_1(t)\,x)(a) = \begin{cases} 0 & \text{if } a < t, \\ x(a-t) & \text{if } a \geqslant t. \end{cases}$$

Secondly, the operator $\hat{\mathcal{N}}$ is Lipschitz continuous on X. Indeed, when computing $\|\hat{\mathcal{N}}(\hat{x}) - \hat{\mathcal{N}}(\hat{x}')\|_X$, the Lipschitz property of the linear terms is trivial. However, for the nonlinear terms, some further calculations are needed. Two of those terms are developed here. The other ones can be handled by the same reasoning. For one of the nonlinear terms one has that

$$\begin{aligned}
&\int_0^{a_{max}} \left|-p(a)\hat{\Theta}(\hat{x})(a)\,\hat{s}(a) + p(a)\hat{\Theta}(\hat{x}')(a)\,\hat{s}'(a)\right| da \\
&= \int_0^{a_{max}} \left|p(a)\left(-\hat{\Theta}(\hat{x})(a)\,\hat{s}(a) + \hat{\Theta}(\hat{x}')(a)\,\hat{s}'(a) + \hat{\Theta}(\hat{x})(a)\,\hat{s}'(a) - \hat{\Theta}(\hat{x})(a)\,\hat{s}'(a)\right)\right| da \\
&\leqslant \int_0^{a_{max}} p(a)\hat{\Theta}(\hat{x})(a)\,|\hat{s}(a) - \hat{s}'(a)|da + \int_0^{a_{max}} p(a)|\hat{s}'(a)||\hat{\Theta}(\hat{x})(a) - \hat{\Theta}(\hat{x}')(a)|da \\
&\leqslant \bar{\hat{\Theta}}\|\hat{s} - \hat{s}'\|_1 + L_{\hat{\Theta}}\|\hat{x} - \hat{x}'\|_X \int_0^{a_{max}} |\hat{s}'(a)|da, \\
&\leqslant \bar{\hat{\Theta}}\|\hat{s} - \hat{s}'\|_1 + L_{\hat{\Theta}} M\|\hat{x} - \hat{x}'\|_X,
\end{aligned}$$

using the fact $\hat{\Theta}$ is Lipschitz with positive constant $L_{\hat{\Theta}}$, $p(a)$ is smaller than 1 for all a since it is a probability, $\hat{\Theta}(\hat{x}) \leqslant \bar{\hat{\Theta}}$ since $\hat{\Theta}$ is bounded and $\hat{s}$ is in $L^1(0, a_{max})$. Another nonlinear term satisfies

$$\int_0^{a_{max}} \left|-c(a)\hat{s}(a)\int_0^{a_{max}} i(b)P^\star(b)\,db + c(a)\hat{s}'(a)\int_0^{a_{max}} i'(b)P^\star(b)\,db\right| da$$

$$
\begin{aligned}
&= \int_0^{a_{max}} \left| c(a) \left(-\hat{s}(a) \int_0^{a_{max}} i(b) P^\star(b)\, db + \hat{s}'(a) \int_0^{a_{max}} i'(b) P^\star(b)\, db \right.\right. \\
&\quad \left.\left. + \hat{s}'(a) \int_0^{a_{max}} i(b) P^\star(b)\, db - \hat{s}'(a) \int_0^{a_{max}} i(b) P^\star(b)\, db \right) \right| da \\
&\leqslant \int_0^{a_{max}} c(a) \int_0^{a_{max}} |i(b)| P^\star(b)\, db |\hat{s}(a) - \hat{s}'(a)| da \\
&\quad + \int_0^{a_{max}} c(a) |\hat{s}'(a)| \left| \int_0^{a_{max}} (i(b) - i'(b)) P^\star(b)\, db \right| \\
&\leqslant \bar{c}\bar{P} \int_0^{a_{max}} |i(b)| db \|\hat{s} - \hat{s}'\|_1 + \bar{c}\bar{P} \|i - i'\|_1, \\
&\leqslant \bar{c}\bar{P} M' \|\hat{s} - \hat{s}'\|_1 + \bar{c}\bar{P} \|i - i'\|_1,
\end{aligned}
$$

since $c(a) \leqslant \bar{c}$ for all a and $P^\star(a) \leqslant \bar{P}$, for all $a \geqslant 0$. By similar arguments applied to the other nonlinear terms, it follows that $\|\hat{\mathcal{N}}(\hat{x}) - \hat{\mathcal{N}}(\hat{x}')\| \leqslant C\|\hat{x} - \hat{x}'\|_X$ for some positive constant C. Hence, applying Theorem 7.2.1 to the semilinear problem (8.4) implies that there exists a unique mild solution of (8.2) □

Since $\hat{x}$ is a mild solution, then $\hat{x}(t)$ equals to $T(t)\hat{x}_0 + \int_0^t T(t-s)\hat{\mathcal{N}}(\hat{x})(s)\, ds$.

8.1.4 Nonnegativity of the states

It can be shown that the model is realistic in the sense that the quantities s and i are in $[0, 1]$, since they are proportions, if a meaningful initial condition is chosen. The following stronger result, inspired by (Inaba (1990)) and extended to the case of an SIR model with input, states this fact.

Proposition 8.1.1
Let

$$\tilde{\Omega} := \left\{ (\hat{s}, i) \in L^1(0, L) \times L^1(0, L) : \hat{s} \geqslant -1, i \geqslant 0 \right\}$$

and let

$$\tilde{\Omega}_0 := \left\{ (\hat{s}, i) \in L^1(0, L) \times L^1(0, L) : -1 \leqslant \hat{s} \leqslant 0, 0 \leqslant i \leqslant 1 \right\}$$

Then the mild solution $x(t; x_0)$, with $x_0 \in \tilde{\Omega}$ enters into $\tilde{\Omega}_0$ after a finite time. Moreover, the set $\tilde{\Omega}_0$ is positively invariant with respect to (8.2).

Proof.

— Step 1: Show that $\hat{s}$ is bigger than -1. To do so, let us solve the first equation of (8.1) by using the method of characteristics (see Section 7.3 for a brief summary of this method). For ease of calculation, the

notation $\bar{\beta}(t,a) = c(a)\int_0^{a_{max}} i(t,b)P^{\star}(b)db$ is introduced, so the first equation of (8.1) is given by

$$(\partial_t + \partial_a)\, s\,(t,a) = -\left(p(a)\theta\,(t,a) + \bar{\beta}(t,a)\right) s\,(t,a)\,, \tag{8.5}$$

with the initial and boundary conditions equal to $s(0,a) = s_0(a)$ and $s(t,0) = 1$, respectively. A new variable η is introduced to parameterize the equation. Hence, $a = a_\eta, t = t_\eta$ and $s(t,a) = s(t_\eta, a_\eta) = s_\eta$. The method of characteristics implies to solve

$$\frac{dt_\eta}{d_\eta} = 1; \frac{da_\eta}{d_\eta} = 1$$

and

$$\frac{ds_\eta}{d_\eta} = -\left(p(a_\eta)\theta\,(t_\eta, a_\eta) + \bar{\beta}(t_\eta, a_\eta)\right) s\,(t_\eta, a_\eta)\,. \tag{8.6}$$

The first two ODEs give $t_\eta = \eta + t_0$ and $a_\eta = \eta + a_0$. Let $a_0 = 0$. Two cases can be identified.

Either $a < t$, then integrating (8.6) from 0 to η implies that

$$\begin{aligned}
&s_\eta = s(t_0, a_0)\exp\left(-\int_0^\eta p(a_{\eta'})\theta\,(t_{\eta'}, a_{\eta'}) + \bar{\beta}(t_{\eta'}, a_{\eta'})d\eta'\right)\\
\Leftrightarrow &s(t,a) = \exp\left(-\int_0^a p(\eta')\theta\left(\eta' + t_0, \eta'\right) + \bar{\beta}(\eta' + t_0, \eta')d\eta'\right)\\
\Leftrightarrow &s(t,a) = \exp\left(-\int_0^a p(\eta')\theta\left(\eta' + t - a, \eta'\right) + \bar{\beta}(\eta' + t - a, \eta')d\eta'\right).
\end{aligned}$$

Either $a \geqslant t$, then integrating (8.6) from $-t_0$ to η implies that

$$\begin{aligned}
&s_\eta = s(t_{-t_0}, a_{-t_0})\exp\left(-\int_{-t_0}^\eta p(a_{\eta'})\theta\,(t_{\eta'}, a_{\eta'}) + \bar{\beta}(t_{\eta'}, a_{\eta'})d\eta'\right)\\
\Leftrightarrow &s(t_\eta, a_\eta) = s(0, -t_0)\exp\left(-\int_{-t_0}^{a_\eta} p(\eta')\theta\left(\eta' + t_0, \eta'\right) + \bar{\beta}(\eta' + t_0, \eta')d\eta'\right)\\
\Leftrightarrow &s(t,a) = s_0(a-t)\exp\left(-\int_{a-t}^a p(\eta')\theta\left(\eta' + t - a, \eta'\right) + \bar{\beta}(\eta' + t - a, \eta')d\eta'\right)\\
\Leftrightarrow &s(t,a) = s_0(a-t)\exp\left(-\int_0^t p(\xi + a - t)\theta\,(\xi, \xi + a - t) + \bar{\beta}(\xi, \xi + a - t)d\xi\right),
\end{aligned}$$

by a change of integration variables. To summarize, the solution s is obtained as

$$s\,(t,a) = \begin{cases}
\exp\left(-\int_0^a p(\eta')\theta\left(\eta' + t - a, \eta'\right) + \bar{\beta}\left(\eta' + t - a, \eta'\right)d\eta'\right) & \text{if } t > a,\\
s_0\,(a-t)\,\times & \\
\exp\left(-\int_0^t p(\xi + a - t)\theta\,(\xi, \xi + a - t) + \bar{\beta}\,(\xi, \xi + a - t)\,d\xi\right) & \text{if } t \leqslant a.
\end{cases}$$

It follows that $s \geqslant 0$ when $s_0(a) \geqslant 0$. Since $x_0 \in \tilde{\Omega}$, then $\hat{s} \geqslant -1$.

— Step 2: Show that i is nonnegative. The abstract Cauchy problem for the variable $(\hat{s}, i)$ is considered, so the second equation of (8.2) is given by

$$\begin{cases} \dfrac{di(t)}{dt} = Ei(t) + (Qi(t))(1 + \hat{s}(t)), \\ \\ i(0) = i_0 \end{cases}$$

where $E = -\dfrac{d}{da} - \gamma$ on the domain

$$\mathcal{D}(E) = \left\{ i \in L^1(0, a_{max}), i \in AC[0, a_{max}], i(0) = 0 \right\}$$

and $(Qi(t)) = \displaystyle\int_0^{a_{max}} c(a)\, i(t,b)\, P^{\star}(b)\, db$. Notice that E is a closed operator on $\mathcal{D}(E)$ and it is the infinitesimal generator of the C_0-semigroup $\left(\tilde{T}(t)\right)_{t \geqslant 0}$ such that

$$\tilde{T}(t)\, i_0 = \begin{cases} i_0(a - t)\exp(-\gamma t) & \text{if } a \geqslant t, \\ \\ 0 \quad \text{otherwise.} \end{cases}$$

As seen previously, the solution of such an abstract Cauchy Problem is given by

$$i(t) = \tilde{T}(t)\, i_0 + \int_0^t \tilde{T}(t - x)\, (Qi(x))\, (1 + \hat{s}(x))\, dx.$$

Since $\tilde{T}(t)$ is nonnegative for all $t \geqslant 0$ (its expression can be easily obtained using the method of characteristics), $i_0 \geqslant 0$ because $x_0 \in \tilde{\Omega}$ and $\hat{s}$ is bigger than -1 by Step 1, then $i(t)$, which can be obtained by monotone iteration,

$$i_0(t) = i_0$$

$$i_{n+1}(t) = \tilde{T}(t)\, i_0 + \int_0^t \tilde{T}(t - x) \left(Q\tilde{T}(x)\, i_n(x)\right) (1 + \hat{s}(x))\, dx \text{ for } n = 1, 2, ...$$

is nonnegative.

— Step 3: Show that $\hat{s} \leqslant 0$ and $i \leqslant 1$. In order to do this, consider $w(t) = \hat{s}(t) + i(t)$. The abstract Cauchy problem of w is given by

$$\frac{dw}{dt} = Fw(t) - \gamma i(t)$$

where $F = -\dfrac{d}{da}$ with domain

$$\mathcal{D}(F) = \left\{ w \in L^1(0, a_{max}), w \in AC[0, a_{max}], w(0) = 0 \right\}.$$

Therefore, the solution w of this problem is given by

$$w(t) = T_1(t) w_0 - \int_0^t T_1(t-s) \gamma i(s) ds. \tag{8.7}$$

$T_1(t)$ is a positive nilpotent semigroup generated by the operator F. Therefore, it follows from (8.7) that

$$w(t) \leqslant T_1(t) w_0 = \begin{cases} w(a-t) & \text{if } a \geqslant t, \\ 0 & \text{otherwise.} \end{cases}$$

Therefore, if $t > a_{max} \geqslant a$, then $w(t) \leqslant 0$ and since $i(t) \geqslant 0$ and $\hat{s}(t) \geqslant -1$ by steps 1 and 2, it follows that $\hat{s} \leqslant 0$ and $i \leqslant 1$. Thus, the mild solution $x(t; x_0)$ with $x_0 \in \tilde{\Omega}$ enters into $\tilde{\Omega}_0$ for $t \geqslant a_{max}$. Furthermore, if $x_0 \in \tilde{\Omega}_0$, then $x(t; x_0) \in \tilde{\Omega}_0$ for all $t \geqslant 0$.

□

8.2 Stability

The previous section showed that there exists a unique solution for the PIDE model and that this solution has a physical meaning. The goal of this section is to study the stability of the distributed parameter age-dependent epidemic system to understand its long-term behavior. This analysis will justify the importance of the design of a control law in order to get disease eradication. This section is divided in several parts. First, the characterization of the equilibria of the system is performed. Then, the stability of the equilibria is analyzed, based on the principle of linearized stability, semigroup theory and property of operators.

8.2.1 Existence of steady-states

This part, dedicated to the characterization of the equilibria of system NPIDE (8.1), is inspired by (Bastin and Coron (2016)), but in this thesis an additional input, $\theta(t, a)$, is considered.

A partial differential equation admits an equilibria if the partial derivative of the variable with respect to time is zero. In the case of the PIDE model

(6.11), that means that the variables S, I and R do not depend on t. It follows, by the definition of the new variables s, i and r, that they are independent of the time. Moreover, at the equilibrium, the input $\theta(t,a)$ does not depend on time and is denoted by $\theta^\star(a)$. Therefore, from the Model (8.1), where only the two first equations are needed, a steady-state $(s^\star, i^\star)^T$ is the solution of

$$\begin{cases} \dfrac{ds^\star}{da} = -c\left(a\right) s^\star\left(a\right) \psi^\star - p(a)\theta^\star\left(a\right) s^\star\left(a\right), \\ \dfrac{di^\star}{da} = c\left(a\right) s^\star\left(a\right) \psi^\star - \gamma\left(a\right) i^\star\left(a\right) \end{cases}$$

with

$$s^\star\left(0\right) = 1, i^\star\left(0\right) = 0$$

where $\psi^\star = \displaystyle\int_0^{a_{max}} i^\star\left(b\right) P^\star\left(b\right) db.$

The solution of the first ODE is immediate as this ODE is separable. The second ODE is linear thus, by solving the homogeneous equation in first step and then by varying the constant, the solution is obtained. Therefore, the steady-state is

$$s^\star\left(a\right) = \exp\left(-\int_0^a \left(c\left(\sigma\right)\psi^\star + p(\sigma)\theta^\star\left(\sigma\right)\right) d\sigma\right), \tag{8.8}$$

$$i^\star\left(a\right) = \Gamma\left(a\right)\psi^\star \int_0^a \frac{c\left(\sigma\right) s^\star\left(\sigma\right)}{\Gamma\left(\sigma\right)} d\sigma \tag{8.9}$$

where $\Gamma\left(a\right) = \exp\left(-\displaystyle\int_0^a \gamma\left(\sigma\right) d\sigma\right)$.

In view of equation (8.9) and the definition of $\psi^\star$, there exists a steady-state if $\psi^\star$ satisfies

$$\psi^\star = \int_0^{a_{max}} P^\star\left(b\right)\Gamma\left(b\right)\psi^\star \int_0^b \frac{c\left(\sigma\right) s^\star\left(\sigma\right)}{\Gamma\left(\sigma\right)} d\sigma db. \tag{8.10}$$

A trivial solution is obtained if $\psi^\star$ equals zero. Then, the equilibrium is $\left(\exp\left(-\displaystyle\int_0^a p(\sigma)\theta^\star\left(\sigma\right) d\sigma\right), 0\right)$ which corresponds to the disease-free steady-state.

Now, let check the existence of other steady-states if $\psi^\star$ is not zero. Therefore, the equation (8.10) can be divided by $\psi^\star$ and become

$$\underbrace{\int_0^{a_{max}} P^\star\left(b\right)\Gamma\left(b\right) \int_0^b \frac{c\left(\sigma\right)}{\Gamma\left(\sigma\right)} \exp\left(-\int_0^\sigma \left(c\left(\eta\right)\psi^\star + p(\eta)\theta^\star\left(\eta\right)\right) d\eta\right) d\sigma db}_{\overset{not.}{=} R(\psi^\star)} = 1.$$

Note that $R(\psi^\star)$ is a positive decreasing function with $\lim_{\psi^\star \to \infty} R(\psi^\star) = 0$ and $\lim_{\psi^\star \to -\infty} R(\psi^\star) = \infty$. Therefore, the equation $R(\psi^\star)$ equals 1 is satisfied if and only if $R(0) > 1$ since $\psi^\star > 0$. Therefore, there is an endemic state if $R(0) > 1$.

Summary
Let

$$R(0) = \int_0^{a_{max}} P^\star(b)\,\Gamma(b) \int_0^b \frac{c(\sigma)}{\Gamma(\sigma)} \exp\left(-\int_0^\sigma p(\eta)\theta^\star(\eta)\,d\eta\right) d\sigma db, \tag{8.11}$$

where $\Gamma(\sigma) = \exp\left(-\int_0^\sigma \gamma(\eta)\,d\eta\right)$.
If $R(0) \leqslant 1$, the NPIDE model (8.1) admits only one epidemic steady-state, the disease-free equilibrium, corresponding to $\psi^\star = 0$.
If $R(0) > 1$, there are two endemic steady-states for the NPIDE model (8.1), one corresponding to the disease-free equilibrium and the other one corresponding to $\psi^\star \neq 0$.

$R(0)$, defined rigorously in (Diekmann et al. (1990)) and used in most of epidemiology papers because it expresses if a new epidemic will die out or can spread, is known as the basic reproduction number of the infection. Notice that one gets the parameter $R_0 = \dfrac{CN}{\gamma}$ of a standard SIR model without vaccination when the parameters of equation (8.11) are considered independent of the age and by taking $a_{\max} = \infty$. This last choice allows to consider all the individuals as being in the same class of age, which is the case in the standard SIR model.

8.2.2 Stability analysis

It remains to establish the stability of the equilibria, according to the value of $R(0)$.

Principle of linearized stability

The study of the stability analysis is performed using the principle of linearized stability. Proposition 8.2.1 shows that this principle holds, based on Theorem 7.4.1.

Proposition 8.2.1
If the linearization (around $x^\star$) of the nonlinear HNPIDE Model (8.2) where $\theta(t,a)$ is given by a bounded Lipschitz continuous state feedback law $\theta(t,a) = \hat{\Theta}(\hat{x}(t,a))$ is (globally) exponentially stable, then $x^\star$ is a locally exponentially stable equilibrium of Model (8.2) with $\theta(t,a) = \hat{\Theta}(\hat{x}(t,a))$. Moreover, if the linearization (around $x^\star$) of Model (8.2) with $\theta(t,a) = \hat{\Theta}(\hat{x}(t,a))$ is unstable, $x^\star$ is locally unstable (i.e. not asymptotically stable) for Model (8.2) with $\theta(t,a) = \hat{\Theta}(\hat{x}(t,a))$.

Proof.
Step 1: Equations (8.2) of the HNPIDE model can be rewritten as the abstract differential equation (8.4), where

$$\mathcal{D}(\hat{\mathcal{N}}) = \{\hat{x} \in X : -1 \leqslant \hat{s} \leqslant 0, 0 \leqslant i \leqslant 1 \text{ a.e. on } [0, a_{max}]\}.$$

This corresponds to the system introduced in Theorem 7.4.1.

Step 2: *The operator A is quasidissipative.* Indeed, let $\lambda > 0$ and $\hat{x} = (\hat{s}, i)^T \in \mathcal{D}(A) \cap \mathcal{D}(\hat{\mathcal{N}})$ be arbitrarily fixed, knowing that $-1 \leqslant \hat{s} < 0$ and $0 \leqslant i \leqslant 1$, we get the following inequalities for any $l_A > 0$:

$$\begin{aligned}
\|(\lambda Id - A + l_A Id)\hat{x}\|_X &= \int_0^{a_{max}} \left|(\lambda + l_A)\hat{s}(a) + \frac{d\hat{s}(a)}{da}\right| da \\
&\quad + \int_0^{a_{max}} \left|(\lambda + l_A) i(a) + \frac{di(a)}{da}\right| da \\
&\geqslant \left|\int_0^{a_{max}} (\lambda + l_A)\hat{s}(a)\, da\right| + \left|\int_0^{a_{max}} (\lambda + l_A) i(a)\, da\right| \\
&\geqslant \lambda \|\hat{x}\|_X.
\end{aligned}$$

Step 3: *The operator $\hat{\mathcal{N}}$ is Lipschitz continuous on $\mathcal{D}(A) \cap \mathcal{D}(\hat{\mathcal{N}})$.* The proof here is similar to the one presented in Theorem 8.1.1, except that in the previous theorem, the Lipschitz property was on X. When computing $\|\hat{\mathcal{N}}(\hat{x}) - \hat{\mathcal{N}}(\hat{x}')\|_X$, for $\hat{x}, \hat{x}' \in \mathcal{D}(A) \cap \mathcal{D}(\hat{\mathcal{N}})$, the Lipschitz property of the linear terms is trivial. However, for the nonlinear terms, some further calculation is needed. One of those terms is developed here. The other ones can be handled by the same reasoning. The nonlinear term considered satisfies

$$\begin{aligned}
&\int_0^{a_{max}} \left|-p(a)\hat{\Theta}(\hat{x})(a)\,\hat{s}(a) + p(a)\hat{\Theta}(\hat{x}')(a)\,\hat{s}'(a)\right| da \\
&\leqslant \int_0^{a_{max}} p(a)\hat{\Theta}(\hat{x})(a)\,|\hat{s}(a) - \hat{s}'(a)| da + \int_0^{a_{max}} p(a)|\hat{s}'(a)||\hat{\Theta}(\hat{x})(a) - \hat{\Theta}(\hat{x}')(a)| da
\end{aligned}$$

$\leqslant \bar{\hat{\Theta}}\|\hat{s}-\hat{s}'\|_1+\eta\|\hat{x}-\hat{x}'\|,$

using the fact $\hat{\Theta}$ is Lipschitz with positive constant η, $p(a)$ is smaller than 1 for all a since it is a probability, $\hat{\Theta}(\hat{x}) \leqslant \bar{\hat{\Theta}}$ since $\hat{\Theta}$ is bounded and $|\hat{s}| \leqslant 1$. By similar arguments applied to the other nonlinear terms, it follows that $\|\hat{\mathcal{N}}(\hat{x})-\hat{\mathcal{N}}(\hat{x}')\|_X \leqslant C|\hat{x}-\hat{x}'\|_X$ for some positive constant C.

Step 4: Theorem 8.1.1 concludes the existence of a mild solution $\hat{x}(t)=S(t)\hat{x}_0$ of (8.2) for all $t \geqslant 0$.

Step 5: *The Gâteaux derivative of $\hat{\mathcal{N}}$ satisfies assumptions of Theorem 7.4.1.* Indeed, by Definition 7.4.1, the Gâteaux derivative of $\hat{\mathcal{N}}$ at $\hat{x}^\star=(\hat{s}^\star(a), i^\star(a))^T=(s^\star(a)-1, i^\star(a))^T$ is given by

$$\begin{aligned} d\hat{\mathcal{N}}(\hat{x}^\star)z &= \lim_{\epsilon\to 0}\frac{\hat{\mathcal{N}}(\hat{x}^\star+\epsilon z)-\hat{\mathcal{N}}(\hat{x}^\star)}{\epsilon} \\ &= \begin{pmatrix} -c(\cdot)(1+\hat{s}^\star(\cdot))\Psi(y)-x(\cdot)\left(p(\cdot)\hat{\Theta}(\hat{x}^\star)(\cdot)+c(\cdot)\psi^\star\right) \\ -\gamma(\cdot)+c(\cdot)(1+\hat{s}^\star(\cdot))\Psi(y)+x(\cdot)c(\cdot)\psi^\star \end{pmatrix} \end{aligned}$$

for all $z=(x,y)^T \in X$, where $\Psi(v)=\int_0^{a_{max}} v(b)P^\star(b)\,db$ and $\psi^\star=\Psi(i^\star)$. Using the fact that $\gamma(\cdot)$ and $c(\cdot)$ are bounded and $1+\hat{s}^\star(a)\leqslant 1$ one can show that $d\hat{\mathcal{N}}(\hat{x}_e)$ is bounded. Moreover it is a linear operator.

Step 6: *The nonlinear semigroup generated by the operator $A+\hat{\mathcal{N}}$ is Fréchet differentiable.* This is the case if the nonlinear operator $\hat{\mathcal{N}}$ is Fréchet differentiable at $\hat{x}_e$ and that $(S(t))_{t\geqslant 0}$ depends continuously on the initial conditions. First, one can notice, using Definition 7.4.2, that $\hat{\mathcal{N}}$ is Fréchet differentiable at $\hat{x}^\star$ if there exists a bounded linear operator $D\hat{\mathcal{N}}(\hat{x}^\star): X\to X$ such that, for all $h=(h_1,h_2)^T\in X$, $\lim_{h\to 0}\frac{\|\hat{\mathcal{N}}(\hat{x}^\star+h)-\hat{\mathcal{N}}(\hat{x}^\star)-D\hat{\mathcal{N}}(\hat{x}^\star)h\|}{\|h\|}=0$. It can be shown that $d\hat{\mathcal{N}}(\hat{x}^\star)$ is convenient. Indeed, $\|\hat{\mathcal{N}}(\hat{x}^\star+h)-\hat{\mathcal{N}}(\hat{x}^\star)-d\hat{\mathcal{N}}(\hat{x}^\star)h\|$ $=2\int_0^{a_{max}}|c(a)h_1(a)\Psi(h_2)|da$. When this is divided by $\|h\|$, it can be shown that it is smaller than $K\|h_1\|_1$ which tends to 0. Therefore, $\hat{\mathcal{N}}$ is Fréchet differentiable.
Moreover, considering the change of variables $\tilde{x}=\hat{x}-\hat{x}^\star$, the following abstract differential equation is obtained,

$$\begin{cases} \dot{\tilde{x}} = A\tilde{x}+\tilde{\mathcal{N}}(\tilde{x}) \\ \tilde{x}(0)=\tilde{x}_0 \end{cases}$$

where $\tilde{\mathcal{N}}: X\to X$ is given by $\tilde{\mathcal{N}}(\tilde{x})=\hat{\mathcal{N}}(\tilde{x}+\hat{x}^\star)-\hat{\mathcal{N}}(\hat{x}^\star)$ and A is the

infinitesimal generator of a semigroup of contraction $(T(t))_{t\geqslant 0}$. Therefore, with $\tilde{x}(t) = S(t)\tilde{x}_0$,

$$\begin{aligned}\|\tilde{x}(t)\| &\leqslant \|T(t)\tilde{x}_0\| + \int_0^t \|T(t-s)\|\|\tilde{\mathcal{N}}(s,\tilde{x}(s))\|ds \\ &\leqslant \|\tilde{x}_0\| + \int_0^t \|\hat{\mathcal{N}}(\tilde{x}+\hat{x}^\star) - \hat{\mathcal{N}}(\hat{x}^\star)\|ds \\ &\leqslant \|\tilde{x}_0\| + K\int_0^t \|\tilde{x}(s)\|ds.\end{aligned}$$

Hence, $\|\tilde{x}(t)\| \leqslant \|\tilde{x}_0\|e^{Kt}$ by Grönwall's inequality.

Step 7: The conclusion follows from the previous steps by using Theorem 7.4.1.

□

Linearisation

The following analysis is inspired by the articles (Inaba (1990)) and (Inaba (2006)) but where an additional input is considered. The analysis is performed on Model (8.1) where $\theta(t,a)$ is assumed given by a bounded Lipschitz continuous state feedback law $\theta(t,a) = \Theta(x(t,a))$.

The NPIDE model (8.1) can be rewritten via an abstract Cauchy problem

$$\begin{cases} \dot{x} = Ax + \mathcal{N}(x) \\ x(0) = x_0 \end{cases} \tag{8.12}$$

where $x = (s,i)^T$ and

$$A = \begin{pmatrix} -\dfrac{d\cdot}{da} & 0 \\ 0 & -\dfrac{d\cdot}{da} \end{pmatrix} \tag{8.13}$$

on the domain $\mathcal{D}(A) = \{x \in X \text{ such that } s,i \in AC[0,a_{max}] \text{ and } s(0) = 1, i(0) = 0\}$. Moreover $\mathcal{N} : \mathcal{D}(\mathcal{N}) \to X$ is defined for all $x \in X$ by

$$\mathcal{N}(x) = \begin{pmatrix} -\left(p(\cdot)\Theta(x)(\cdot) + c(\cdot)\displaystyle\int_0^{a_{max}} i(b)P^\star(b)\,db\right)s(\cdot) \\ -\gamma(\cdot)i(\cdot) + c(\cdot)s(\cdot)\displaystyle\int_0^{a_{max}} i(b)P^\star(b)\,db \end{pmatrix}$$

where $\mathcal{D}(\mathcal{N}) = \{x \in X : 0 \leqslant s,i \leqslant 1 \text{ a.e. on } [0,a_{max}]\}$.
As mentioned in Theorem 7.4.1, the Gâteaux linearized dynamics of (8.12) is given by

$$\begin{cases} \dot{u} = (A+E)u \\ u(0) = x_0 - x^\star = u_0 \end{cases} \tag{8.14}$$

where $u = (u_1, u_2)^T = (s - s^\star, i - i^\star)^T$, A is given by (8.13) on the domain $\mathcal{D}(A) = \left\{ u \in L^1(0, a_{max}) \times L^1(0, a_{max}) : u_i \in AC[0, a_{max}], u(0) = (0,0)^T \right\}$. Furthermore, $E = d\mathcal{N}(x^\star)$, the Gâteaux derivative of $\mathcal{N}$ at $x^\star = (s^\star, i^\star)^T$ and is given by

$$Eu = \begin{pmatrix} -\left(p(\cdot)\Theta_u(u^\star)(\cdot) + \bar{\beta}^\star(\cdot)\right) u_1(\cdot) - (Fu_2)(\cdot)\, s^\star(\cdot) \\ \bar{\beta}^\star(\cdot)\, u_1(\cdot) - \gamma(\cdot)\, u_2(\cdot) + (Fu_2)(\cdot)\, s^\star(\cdot) \end{pmatrix}$$

where $\Theta_u(u) = \Theta(u + (s^\star, i^\star))$, $\bar{\beta}^\star(a) = c(a)\,\psi^\star$ and F is a bounded linear operator on $L^1(0, a_{max})$ given by

$$(Fu)(a) = \int_0^{a_{max}} c(a)\, P^\star(b)\, u(b)\, db = c(a)\, \Psi(u).$$

Stability analysis

In view of Proposition 8.2.1, the stability analysis can be performed for the linearised system (8.14). Hence, thanks to Proposition 7.4.1 it suffices to find the growth bound of the semigroup generated by $A + E$, $\omega_0(A + E)$ and if it is negative then the equilibrium u equals 0 is globally exponentially asymptotically stable. Therefore, this holds locally for the NPIDE model (8.1).

Several results introduced in Chapter 7 will be helpful to find this growth bound. For the sake of clarity, the main steps of the methodology are highlighted.

Step 1: Link the growth bound $\omega_0(A + E)$ to the point spectrum $P_\sigma(A + E)$.

First, let us introduce the following lemma which shows that the operator F is compact. This property will be useful in the sequel. The proof is based on Proposition 7.5.4.

Lemma 8.2.1
Let $c(\cdot) \in L^\infty(0, a_{max})$. Then, the operator F is compact.

Proof.
Let $v \in L^1(0, a_{max})$.
By definition of ImF, $v \in ImF \Leftrightarrow$ there exists $u \in L^1(0, a_{max})$ such that $v = Fu$. By using the definition of F, this means that there exists $u \in L^1(0, a_{max})$ such that $v(\cdot) = c(\cdot)\Psi(u)$, where $\Psi(u) \in \mathbb{R}$ and $c(\cdot) \in L^\infty(0, a_{max})$. Hence, $ImF = span\{c\}$, which is finite-dimensional. Therefore, F is a finite-rank

operator, so by Proposition 7.5.4 it is compact. □

The following result, using Proposition 7.5.9, shows that the growth bound $\omega_0(A+E)$ of the linear operator $A+E$ can be obtained by finding the spectral bound $s(A+E)$ of this operator.

Proposition 8.2.2

$$\omega_0(A+E) = s(A+E) =: \sup\{Re\ \lambda : \lambda \in \sigma(A+E)\}$$

Proof. The semigroup $(T(t))_{t\geqslant 0}$ generated by $A+E$ is an eventually norm-continuous semigroup. Indeed, $A+E$ can be rewritten as $(A+E_1)+E_2$ to be able to apply Theorem 7.5.2, with

$$E_1 u = \begin{pmatrix} -\left(p(\cdot)\,\Theta_u(u^\star)(\cdot) + \bar{\beta}^\star(\cdot)\right) u_1(\cdot) \\ \bar{\beta}^\star(\cdot)\,u_1(\cdot) - \gamma(\cdot)\,u_2(\cdot) \end{pmatrix} \text{ and } E_2 u = \begin{pmatrix} -(Fu_2)(\cdot)\,s^\star(\cdot) \\ (Fu_2)(\cdot)\,s^\star(\cdot) \end{pmatrix}.$$

This rewriting is needed because E is not compact. Indeed, identity operators in infinite dimensional spaces are not compact.

By using the method of characteristics, the C_0-semigroup generated by $A+E_1$ is given, accordingly to Proposition 7.1.2, by $(S(t))_{t\geqslant 0} = \begin{pmatrix} S_{11}(t) & 0 \\ S_{21}(t) & S_{22}(t) \end{pmatrix}$ where

$$(S_{11}(t)\,u_1)(a) = \begin{cases} 0 & \text{if } t > a, \\ u_{10}(a-t)\exp\left(-\displaystyle\int_{a-t}^{a} p(\eta)\Theta_u(u^\star)(\eta) + \bar{\beta}^\star(\eta)\,d\eta\right) & \text{if } t \leqslant a, \end{cases}$$

$$(S_{22}(t)\,u_2)(a) = \begin{cases} 0 & \text{if } t > a, \\ u_{20}(a-t)\exp\left(-\displaystyle\int_{a-t}^{a} \gamma(\eta)\,d\eta\right) & \text{if } t \leqslant a, \end{cases}$$

$$(S_{21}(t)\,u_1)(a) = \begin{cases} 0 & \text{if } t > a, \\ \displaystyle\int_0^t S_{22}(t-s)\,\bar{\beta}^\star(a)\,S_{11}(s)\,u_1(a)\,ds & \text{if } t \leqslant a \end{cases}$$

Therefore $A+E_1$ is the generator of a nilpotent translation semigroup and, as mentioned in Section 7.5, it is an eventually norm-continuous semigroup. Since E_2 is defined by the operator F which is a compact operator, as shown in Lemma 8.2.1, the semigroup generated by $A+E$ is an eventually norm-continuous semigroup by Theorem 7.5.2. Then applying Proposition 7.5.9, the equality between the growth bound of $A+E$ and its spectral bound follows. □

Since the study of the spectral bound of $A+E$ requires the knowledge of the spectrum of $A+E$, $\sigma(A+E)$, the next step is to link the spectrum of $A+E$ to the point spectrum of $A+E$, $P_\sigma(A+E)$ which is easier to find.

Proposition 8.2.3

$$\sigma(A+E) = P_\sigma(A+E)$$

Proof. To apply Proposition 7.5.2, one needs to show that the resolvent of $A+E$, $R_\lambda(A+E)$ is compact. Hence, its expression is needed. It is found by solving the resolvent equation

$$(\lambda Id - (A+E))\,\phi = \psi,$$

where $\phi = (\phi_1, \phi_2)^T \in \mathcal{D}(A), \psi = (\psi_1, \psi_2)^T \in L^1(0, a_{max}) \times L^1(0, a_{max}), \lambda \in \mathbb{C}$. Both ODEs are linear so by the variation of constant formula, the solution is given by, using expression (8.8) of $s^\star$,

$$\begin{cases} \phi_1(a) = e^{-\lambda a} s^\star(a) \displaystyle\int_0^a e^{\lambda\sigma} \left(\frac{\psi_1(\sigma)}{s^\star(\sigma)} - (F\phi_2)(\sigma) \right) d\sigma, & \text{(8.15a)} \\ \phi_2(a) = e^{-\lambda a} \Gamma(a) \displaystyle\int_0^a \frac{e^{\lambda\sigma}}{\Gamma(\sigma)} \left(\psi_2(\sigma) + (F\phi_2)(\sigma)\, s^\star(\sigma) \right. \\ \qquad\qquad \left. + \bar{\beta}^\star(\sigma)\, \phi_1(\sigma) \right) d\sigma & \text{(8.15b)} \end{cases}$$

This solution is unique and determined by the initial conditions of the problem. However, ϕ_2 is implicit so more calculations are needed. Multiplying both sides of the equation (8.15b), evaluated in b, by $s^\star(a)\, c(a)\, P^\star(b)$ and then integrating with respect to b from 0 to a_{max} and using equation (8.15a), gives

$$\begin{aligned} s^\star(a)(F\phi_2)(a) = s^\star(a) \int_0^{a_{max}} c(a) P^\star(b) \int_0^b e^{-\lambda(b-\sigma)} \frac{\Gamma(b)}{\Gamma(\sigma)} s^\star(\sigma)(F\phi_2)(\sigma) \\ \times \underbrace{\left(1 - \int_\sigma^b \frac{\Gamma(\sigma)\, s^\star(\eta)}{\Gamma(\eta)\, s^\star(\sigma)} \bar{\beta}^\star(\eta)\, d\eta \right)}_{\overset{not.}{=:} \Pi(b,\sigma)} d\sigma db + \chi(\lambda, a) \end{aligned}$$

where

$$\begin{aligned} \chi(\lambda, a) = & s^\star(a) \int_0^{a_{max}} c(a) P^\star(b) \int_0^b e^{-\lambda(b-\sigma)} \frac{\Gamma(b)}{\Gamma(\sigma)} \\ & \times \left(\psi_2(\sigma) + \bar{\beta}^\star(\sigma)\, s^\star(\sigma) \int_0^\sigma e^{-\lambda(\sigma-\eta)} \frac{\psi_1(\eta)}{s^\star(\eta)} d\eta \right) d\sigma db. \end{aligned}$$

This equation can be rewritten in terms of operators as

$$(Id - B(\lambda))(\omega(a)) = \chi(\lambda, a)$$

with $\omega(a) = s^\star(a)(F\phi_2)(a)$
and $(B(\lambda)\omega)(a) = s^\star(a)\int_0^{a_{max}} c(a)P^\star(b)\int_0^b e^{-\lambda(b-\sigma)}\frac{\Gamma(b)}{\Gamma(\sigma)}\Pi(b,\sigma)\omega(\sigma)\,d\sigma db.$
Remark that the resolvent equation is solvable if $Id - B(\lambda)$ is invertible in $\mathcal{L}\left(L^1(0, a_{max})\right)$. Then, the resolvent of $A + E$ is

$$\begin{cases} \phi_1(a) = e^{-\lambda a}s^\star(a)\int_0^a e^{\lambda\sigma}\left(\frac{\psi_1(\sigma)}{s^\star(\sigma)} - \frac{(I - B(\lambda))^{-1}\chi(\lambda,\sigma)}{s^\star(\sigma)}\right)d\sigma, \\ \phi_2(a) = e^{-\lambda a}\Gamma(a)\int_0^a \frac{e^{\lambda\sigma}}{\Gamma(\sigma)}\left(\psi_2(\sigma) + (I - B(\lambda))^{-1}\chi(\lambda,\sigma) + \bar{\beta}^\star(\sigma)\phi_1(\sigma)\right)d\sigma. \end{cases}$$

It is easily shown that the family of linear operators $B(\lambda)$ on $L^1(0, a_{max})$ is a family of compact operators. Indeed, let $\lambda \in \mathbb{C}$ and define

$$(U_\lambda z)(a) = \int_0^a e^{-\lambda(a-\sigma)}\frac{\Gamma(a)}{\Gamma(\sigma)}\Pi(a,\sigma)z(\sigma)\,d\sigma.$$

U_λ is a compact operator by Proposition 7.5.3 as it is a Volterra operator on $L^1(0, a_{max})$. Then, $B(\lambda)$ can be rewritten as

$$\begin{aligned}(B_\lambda\omega)(a) &= \int_0^{a_{max}} s^\star(a)c(a)P^\star(b)(U_\lambda\omega)(b)\,db, \\ &= H(U_\lambda\omega)(a)\end{aligned} \tag{8.16}$$

where $(Hz)(a) = \int_0^{a_{max}} s^\star(a)c(a)P^\star(b)z(b)\,db$ is compact hence bounded because it has finite-rank, by using similar arguments to those in Lemma 8.2.1. Therefore, $B(\lambda)$ is a compact operator by Proposition 7.5.5. By similar arguments (notice that $(I - B(\lambda))^{-1}$ is bounded), the resolvent of $A+E$ is compact. Thus, Proposition 7.5.2 concludes that $\sigma(A + E) = P_\sigma(A + E)$. □

To sum up, conclusions about stability could be made if the growth bound $\omega_0(A + E)$ is known. By the corollary of the Spectral Mapping theorem it was shown that $\omega_0(A + E) = s(A + E) = \sup\{Re\ \lambda : \lambda \in \sigma(A + E)\}$. Since $\sigma(A + E) = P_\sigma(A + E)$ then, $\omega_0(A + E) = sup\{Re\ \lambda : \lambda \in P_\sigma(A + E)\}$.

Step 2: Characterize $P_\sigma(A + E)$ by computing the resolvant $\rho(A + E)$.

Now, the point spectrum of $A + E$ is characterized to be able to study it.

Proposition 8.2.4
Let $B(\lambda)$ defined in (8.16). Then,

$$\begin{aligned} P_\sigma(A+E) &= \{\lambda \in \mathbb{C} : Id - B(\lambda) \text{ is not invertible}\} \\ &= \left\{\lambda \in \mathbb{C} : \lambda \text{ is pole of } (Id - B(\lambda))^{-1}\right\} := \Sigma \end{aligned}$$

Proof. First, one can notice that if $Id - B(\lambda)$ is invertible, then the resolvent equation is solvable.
Furthermore, $\rho(A+E) = \left\{\lambda \in \mathbb{C} : (\lambda Id - (A+E))^{-1} \text{ exists in } \mathcal{L}\left(L^1(0, a_{max})\right)\right\}$.
Moreover, by the previous proof, it can be observed that

$$\begin{aligned} (\lambda Id - (A+E))^{-1} \text{ exists } &\Leftrightarrow (Id - B(\lambda))^{-1} \text{ exists} \\ &\quad \text{and } (Id - B(\lambda))^{-1} \in \mathcal{L}\left(L^1(0, a_{max})\right) \\ &\Rightarrow (\lambda Id - (A+E))^{-1} \in \mathcal{L}\left(L^1(0, a_{max})\right) \end{aligned}$$

Thus, this means that

$$\begin{aligned} &\left\{\lambda \in \mathbb{C} : Id - B(\lambda) \text{ is invertible in } \mathcal{L}\left(L^1(0, a_{max})\right)\right\} \subset \rho(A+E) \\ \Leftrightarrow &\left(\left\{\lambda \in \mathbb{C} : Id - B(\lambda) \text{ is invertible in } \mathcal{L}\left(L^1(0, a_{max})\right)\right\}\right)^C \supset (\rho(A+E))^C \\ \Leftrightarrow &\{\lambda \in \mathbb{C} : Id - B(\lambda) \text{ is not invertible }\} \supset \sigma(A+E) = P_\sigma(A+E), \end{aligned}$$

by previous reasoning.
It remains to show that $\{\lambda \in \mathbb{C} : Id - B(\lambda) \text{ is not invertible}\} \subset P_\sigma(A+E)$.
Let $\lambda \in \mathbb{C}$ such that $Id - B(\lambda)$ is not invertible and show that λ is an eigenvalue of $A+E$. Since $B(\lambda)$ is an analytic family of compact operators and $Id - B(\lambda)$ is invertible for λ with sufficiently large real part. Indeed, $B(\lambda)$ is compact, hence bounded and $\|B(\lambda)\| < 1$ because $B(\lambda) \to 0$ for $Re\ \lambda$ large enough. Therefore, by Proposition 7.5.6, $(Id - B(\lambda))^{-1}$ is meromorphic with respect to λ. However, by assumption, $Id - B(\lambda)$ is not invertible for some λ. Thus, λ is a pole of the meromorphic family $(Id - B(\lambda))^{-1}$ and so, by the definition of $(\lambda Id - (A+E))^{-1}$, λ is a pole of the resolvent of $A+E$. Proposition 7.5.1 implies that λ is an eigenvalue of $A+E$.
The second part of the proposition, immediately follows from the fact that $(Id - B(\lambda))^{-1}$ is meromorphic. Indeed, since $(Id - B(\lambda))^{-1}$ is meromorphic,

$$\begin{aligned} P_\sigma(A+E) &= \{\lambda \in \mathbb{C} : Id - B(\lambda) \text{ is not invertible}\} \\ &= \left\{\lambda \in \mathbb{C} : \lambda \text{ is pole of } (Id - B(\lambda))^{-1}\right\} := \Sigma \end{aligned}$$

□

Step 3: Show that $\omega_0(A+E)$ is such that $r(B(\omega_0))$ is equal to 1, and conclude.

First, one can show that there exists one and only one $\lambda_0 \in \mathbb{R} \cap \Sigma$ such that $r\left(B\left(\lambda_0\right)\right) = 1$. Later, it will be proved that λ_0 corresponds to $\omega_0\left(A+E\right)$. Therefore, in the following part, λ will be assumed to be real.

A preliminary result, stating that the operator $B\left(\lambda\right)$ is non-supporting, is introduced.

Lemma 8.2.2
Assume that there exists a number $\epsilon > 0$ such that $c\left(a\right) \geqslant \epsilon$ for almost all $a \in [0, a_{max}]$ and assume that $\bar{\beta}^{\star}$ is sufficiently small such that the following inequality holds,

$$\underbrace{1 - \exp\left(-\int_0^{a_{max}} p(\sigma)\Theta_u\left(\sigma\right) - \gamma\left(\sigma\right) d\sigma\right)\left(1 - \exp\left(-\int_\sigma^b \bar{\beta}^{\star}\left(\sigma\right) d\sigma\right)\right)}_{=:\kappa} > 0.$$

Then, the operator $B\left(\lambda\right)$, defined in (8.16), is non-supporting.

Proof. Let $\lambda \in \mathbb{R}$. In view of the definition of $B\left(\lambda\right)$, the operator is positive, if $\Pi(b,\sigma)$ is positive. Since $\Pi\left(b,\sigma\right) > \kappa$, which is positive by assumption, hence $B\left(\lambda\right)$ is a positive. Moreover, it is a compact operator. Furthermore, $B\left(\lambda\right)$ is also non-supporting. Indeed,

$$\left(B\left(\lambda\right)x\right)\left(a\right) > \kappa\left(T\left(\lambda\right)x\right)\left(a\right)$$

where $\left(T\left(\lambda\right)x\right)\left(a\right) = s^{\star}\left(a\right)\int_0^{a_{max}} c\left(a\right)P^{\star}\left(b\right)\int_0^b e^{-\lambda(b-\sigma)}\dfrac{\Gamma\left(b\right)}{\Gamma\left(\sigma\right)}x\left(\sigma\right)d\sigma db$. So it suffices to show that $T\left(\lambda\right)$ is non-supporting. To conclude, a recursive proof is used. Let $\Psi \in X_+ \backslash \{0\}$ and $F \in X_+' \backslash \{0\}$, where X_+ is the positive cone of $L^1(0,a_{max}) \times L^1(0,a_{max})$.
For $n = 1$,

$$\begin{aligned}\left(T\left(\lambda\right)\psi\right)\left(a\right) &\geqslant s^{\star}\left(a\right)\epsilon\int_0^b e^{-\lambda(b-\sigma)}\frac{\Gamma\left(b\right)}{\Gamma\left(\sigma\right)}\psi\left(\sigma\right)d\sigma db,\\ &= \left[f_\lambda,\psi\right]g\left(a\right) \qquad \text{where } g\left(a\right) = 1.\end{aligned}$$

Now, consider the case $n+1$ and assume that $\left(T^n\left(\lambda\right)\psi\right)\left(a\right) \geqslant \left[f_\lambda,\psi\right]\left[f_\lambda,g\right]^{n-1}g\left(a\right)$. It follows that

$$\left(T^{n+1}\left(\lambda\right)\psi\right)\left(a\right) = \left(T\left(\lambda\right)T^n\left(\lambda\right)\psi\right)\left(a\right),$$

$$\geqslant [f_\lambda, \psi] [f_\lambda, e]^{n-1} s^\star(a) \int_0^{a_{max}} c(a) P^\star(b) \int_0^b e^{-\lambda(b-\sigma)} \frac{\Gamma(b)}{\Gamma(\sigma)} g(\sigma) d\sigma db,$$
$$\geqslant [f_\lambda, \psi] [f_\lambda, g]^{n-1} [f_\lambda, g] g(a),$$
$$= [f_\lambda, \psi] [f_\lambda, g]^n g(a).$$

Since f_λ is a positive linear functional, for arbitrary $F \in X_+^\star \setminus \{0\}$, $\psi \in X_+ \setminus \{0\}$ and $n \geqslant 1$, $[F, T^n(\lambda)\psi] \geqslant [f_\lambda, \psi] [f_\lambda, g]^{n-1} [F, g] > 0$. □

Proposition 8.2.5

Assume that there exists a number $\epsilon > 0$ such that $c(a) \geqslant \epsilon$ for almost all $a \in [0, a_{max}]$ and assume that $\bar{\beta}^\star$ is sufficiently small such that the following inequality holds,

$$\underbrace{1 - \exp\left(-\int_0^{a_{max}} p(\sigma)\Theta_u(\sigma) - \gamma(\sigma) d\sigma\right)\left(1 - \exp\left(-\int_\sigma^b \bar{\beta}^\star(\sigma) d\sigma\right)\right)}_{=:\kappa} > 0$$

and let $B(\lambda)$ be defined in (8.16). Then, there exists a unique $\lambda_0 \in \mathbb{R} \cap \Sigma$ such that $r(B(\lambda_0)) = 1$.

Proof. Let F_λ be a positive eigenfunctional corresponding to the eigenvalue $r(B(\lambda))$ of $B(\lambda)$ (which exists by Theorem 7.5.1) and let $g \in X_+$. Then,

$$[F_\lambda, B(\lambda) g] = r(B(\lambda)) [F_\lambda, g]$$

By previous developments, it was established that

$$(B(\lambda) x)(a) > \kappa (T(\lambda) x)(a) \geqslant \kappa [f_\lambda, x] g(a).$$

So, with $x = g$,

$$B(\lambda) g > \kappa [f_\lambda, g] g$$

and then

$$[F_\lambda, B(\lambda) g] > \kappa [f_\lambda, g] [F_\lambda, g].$$

Since F_λ is positive, it follows that $r(B(\lambda)) > \kappa [f_\lambda, g]$.
Therefore, $\lim_{\lambda \to -\infty} r(B(\lambda)) > \kappa \lim_{\lambda \to -\infty} [f_\lambda, g] = \infty$. Thus, $\lim_{\lambda \to -\infty} r(B(\lambda)) = \infty$.

Now, since $c \in L^\infty(0, a_{max})$, it can be shown that

$$B(\lambda) x \leqslant T(\lambda) x \leqslant [h_\lambda, x] g$$

where $[h_\lambda, x] = \bar{c} \int_0^{a_{max}} s^\star(a) P^\star(b) \int_0^b e^{-\lambda(b-\sigma)} \frac{\Gamma(b)}{\Gamma(\sigma)} x(\sigma) d\sigma db$. Thus,

$$r(B(\lambda)) [F_\lambda, g] = [F_\lambda, B(\lambda) g] \leqslant [g_\lambda, g] [F_\lambda, g].$$

Therefore, $\lim_{\lambda\to\infty} r\left(B\left(\lambda\right)\right) \leqslant \lim_{\lambda\to\infty} \left[h_\lambda, g\right] = 0$.
Furthermore, Proposition 7.5.7 implies that $r\left(B\left(\lambda\right)\right)$ is strictly decreasing for $\lambda \in \mathbb{R}$. Indeed, $B\left(\lambda\right)$ is a strictly decreasing family of operators. Hence, by the monotonicity of $B\left(\lambda\right)$, there exists a unique $\lambda_0 \in \mathbb{R} \cap \Sigma$ such that $r\left(B\left(\lambda_0\right)\right) = 1$.

□

Proposition 8.2.6
Let $\lambda_0 \in \mathbb{R} \cap \Sigma$ be the unique value such that $r(B(\lambda_0)) = 1$. Then,

$$\omega_0(A + E) = \lambda_0.$$

Proof. Recall that, from Proposition 8.2.2 and Proposition 8.2.3, $\omega_0\left(A + E\right) = sup\left\{Re\ \lambda : \lambda \in P_\sigma\left(A + E\right)\right\}$. Moreover, by Proposition 8.2.4, $\omega_0\left(A + E\right) = sup\left\{Re\ \lambda : \lambda \in \Sigma\right\}$. Hence, it remains to demonstrate the dominant property of λ_0. Let $\lambda \in \Sigma = \{\lambda \in \mathbb{C} : Id - B\left(\lambda\right)$ is not invertible$\}$ so, λ is such that 1 is an eigenvalue of $B\left(\lambda\right)$. Therefore, there exists ψ_λ such that

$$B\left(\lambda\right)\psi_\lambda = \psi_\lambda.$$

Moreover,

$$|\psi_\lambda| = |B\left(\lambda\right)\psi_\lambda| \leqslant B\left(Re\ \lambda\right)|\psi_\lambda|.$$

Indeed, $|B\left(\lambda\right)\psi_\lambda| \leqslant \int_0^{a_{max}} c\left(a\right) P^\star\left(b\right) \int_0^b \underbrace{|e^{-\lambda(b-\sigma)}|}_{=e^{-Re\ \lambda(b-\sigma)}} \frac{\Gamma\left(b\right)}{\Gamma\left(\sigma\right)} \Pi\left(b,\sigma\right)|\psi_\lambda|\left(\sigma\right) d\sigma db =$
$B\left(Re\ \lambda\right)|\psi_\lambda|$. Therefore,

$$\begin{aligned}
&\left[F_{Re\ \lambda}, B\left(Re\ \lambda\right)|\psi_\lambda|\right] \geqslant \left[F_{Re\ \lambda}, |\psi_\lambda|\right] \\
\Leftrightarrow &r\left(B\left(Re\ \lambda\right)\right)\left[F_{Re\ \lambda}, |\psi_\lambda|\right] \geqslant \left[F_{Re\ \lambda}, |\psi_\lambda|\right] \\
\Leftrightarrow &r\left(B\left(Re\ \lambda\right)\right) \geqslant 1 = r\left(B\left(\lambda_0\right)\right).
\end{aligned}$$

Since $r\left(B\left(\lambda\right)\right)$ is decreasing, that implies that $\lambda_0 \geqslant Re\ \lambda\ \forall\ \lambda \in \Sigma$. Hence, by definition of $\omega_0(A + E)$, one gets that it is equal to λ_0. □
The following theorem is the main result of the stability analysis. It states the stability of the equilibria, according to the case considered with respect to the threshold.

Theorem 8.2.1
Assume that there exists a number $\epsilon > 0$ such that $c(a) \geqslant \epsilon$ for almost all $a \in [0, a_{max}]$ and assume that $\bar{\beta}^\star$ is sufficiently small such that the following inequality holds,

$$\underbrace{1 - \exp\left(-\int_0^{a_{max}} p(\sigma)\Theta_u(\sigma) - \gamma(\sigma)\, d\sigma\right)\left(1 - \exp\left(-\int_\sigma^b \bar{\beta}^\star(\sigma)\, d\sigma\right)\right)}_{=:\kappa} > 0$$

and let $R(0)$ be defined by (8.11).
Then, if $R(0) < 1$, the disease-free equilibrium is locally stable and if $R(0) > 1$, the disease-free equilibrium is locally unstable and the endemic equilibrium is locally stable.

Proof. It can be shown that

$$(B(0)\, x)(a) \leqslant (T^\star x)(a)$$

with $(T^\star x)(a) = s^\star(a) \int_0^{a_{max}} P^\star(b)\, c(a) \int_0^b \frac{\Gamma(b)}{\Gamma(\sigma)} x(\sigma)\, d\sigma db.$
Moreover, applying $s^\star(a) P^\star(b) c(a)$ to the both sides of equation (8.9) evaluated in b and integrating from 0 to a_{max} with respect to b gives

$$\begin{aligned} s^\star(a) \int_0^{a_{max}} i^\star(b) P^\star(b) c(a)\, db &= s^\star(a) \int_0^{a_{max}} P^\star(b) c(a) \Gamma(b) \int_0^b \frac{\bar{\beta}^\star(\sigma) s^\star(\sigma)}{\Gamma(\sigma)} d\sigma db, \\ s^\star(a) \bar{\beta}^\star(a) &= s^\star(a) \int_0^{a_{max}} P^\star(b) c(a) \Gamma(b) \int_0^b \frac{\bar{\beta}^\star(\sigma) s^\star(\sigma)}{\Gamma(\sigma)} d\sigma db, \\ s^\star(a) \bar{\beta}^\star(a) &= \left(T^\star\left(s^\star \bar{\beta}^\star\right)\right)(a). \end{aligned}$$

Therefore, $s^\star(a) \bar{\beta}^\star(a)$ is a positive eigenvector (if it is not equal to 0, that is if it is not the disease-free equilibrium) of the operator $T^\star$ corresponding to the eigenvalue 1. Since $T^\star$ is a compact and non-supporting operator (it is proved by relatively similar arguments to those used for $B(\lambda)$) then Proposition 7.5.8 implies that $r(T^\star)$ is the only positive eigenvalue corresponding to a positive eigenvector. So, $r(T^\star) = 1$. By Proposition 7.5.7, since $B(0) \leqslant T^\star$ then $r(B(0)) < r(T^\star) = 1$. Furthermore, since $B(\lambda)$ is decreasing and $R(B(\lambda_0)) = 1$, it follows that $\lambda_0 < 0$. Therefore, by Proposition 8.2.6, the non-trivial endemic steady-state is stable.

The previous arguments do not apply if $i^\star$ equals zero. However, if $i^\star$ is equal to zero it can be shown that

$$\left(B(0)\left(c\tilde{\Theta}\right)\right)(a) = c(a)\, \tilde{\Theta}(a)\, R(0)$$

where $\tilde{\Theta}(a) = \exp\left(-\int_0^a p(\sigma)\theta^\star(\sigma)\,d\sigma\right)$.
So, $R(0)$ is a positive eigenvalue associated to the positive eigenvector $c(a)\,\Theta(a)$. However, since $B(0)$ is a compact and non-supporting operator, $r(B(0))$ is the only positive eigenvalue corresponding to a positive eigenvector. Thus, $r(B(0)) = R(0)$. Therefore, if $R(0) < 1$, then $r(B(0)) < 1$, using the fact that $B(\lambda)$ is decreasing and $r(B(\lambda_0)) = 1$, it follows that $\lambda_0 < 0$ and the disease-free equilibrium is locally stable. However, if $R(0) > 1$, the disease-free equilibrium is locally unstable. □

In conclusion, a state feedback for which the closed-loop system is such that $R(0) < 1$ is required in order to get disease eradication. However, this result is local. So this feedback has to be applied at the beginning of the epidemic, when the number of infected individuals is not too high.
Furthermore, notice that the method used in the analysis does not allow to conclude anything for $R(0) = 1$. That case could be studied, for instance following the methodology in (Inaba (2006).)

8.3 Numerical simulations

Previous results are confirmed using numerical simulations where no control is considered. Most of parameters are taken from (Okuwa et al. (2019)) and the NPIDE Model (8.1) is used. First, note that a_{max} is fixed to 1 in order to normalize the age interval as $[0, 1)$. The age-specific death-rate is

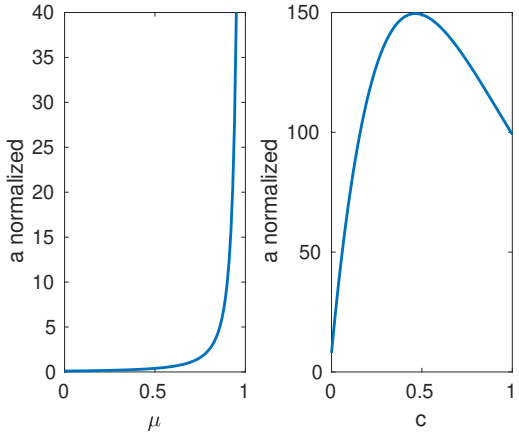

Figure 8.1 – The natural mortality rate $\mu(a)$ and the contact coefficient $c(a)$

Parameter	Symbol	Value
Maximum age	a_{max}	1
Time frame	T	20
Time step size	Δt	0.001
Age step size	Δa	0.01

Table 8.1 – Model parameters and values

given by $\mu(a) = \left(10\,(1-a)^2\right)^{-1}$ with $a \in [0,1[$. Figure 8.1 (left graph) shows that this choice corresponds to a mortality rate that increases with the individuals age. Therefore, $l(a) = \exp\left(-a/\left(10\,(1-a)\right)\right), a \in [0,1)$. If B is chosen equals to $1/\int_0^1 l(a)da$, B equals 1.2527 and the total population is normalized ($\int_0^1 N(a)da = 1$). In addition, the age-dependent recovery rate is defined by $\gamma\,(a) = 100$, and the probability of successful vaccination, $p(a)$, is set to 1 for all ages, meaning that the vaccination is perfect. Hence this is an ideal case, but more realistic functions could be used. To be consistent with the following analytical developments, the contact coefficient used is not the one in (Okuwa et al. (2019)). Indeed, in Section 9.2, $\dfrac{\gamma(a)+\mu(a)}{c(a)}$ needs to be in $C^1\,[0, a_{max}]$. Therefore $c(a)$ has to be differentiable for all $a \in [0, a_{max}]$ which is not the case in 0 for the choice in (Okuwa et al. (2019)). Thus, the contact coefficient is defined as $c(a) = c(0)\left(\sin(a)e^{-2a} + \dfrac{1}{100}\right)$, with $c(0) = 600$ or 800. This choice is depicted in Figure 8.1 (right graph) for $c(0) = 800$. One can observe that the individuals with middle age have more contacts than the younger and elder people. Moreover, the parameters that are used in the numerical simulations are listed in Table 8.1. Observe that the age is normalized. Hence there are no units for the age and no units are mentioned for the time. Finally, the initial conditions are slightly modified from (Okuwa et al. (2019)) in order to maintain consistency between initial conditions and boundary conditions (i.e when a and t are equal to 0.) Therefore, we set $s_0(a) = 1 - i_0(a), r_0(a) = 0$ and

$$i_0(a) = \begin{cases} \hat{i}_0\,(a) - \hat{i}_0\,(0) & \text{if } i_0\,(a) \geqslant 0 \\ 0 \text{ else} \end{cases}$$

where $\hat{i}_0\,(a) = \dfrac{1}{2}e^{-100\left(a-\frac{1}{2}\right)^2} \times 10^{-3}$.

The numerical method used in simulation is a forward time - backward space finite difference scheme. The stability of this scheme is ensured by the necessary and sufficient condition of Courant-Friedrichs-Lewy which requires in this

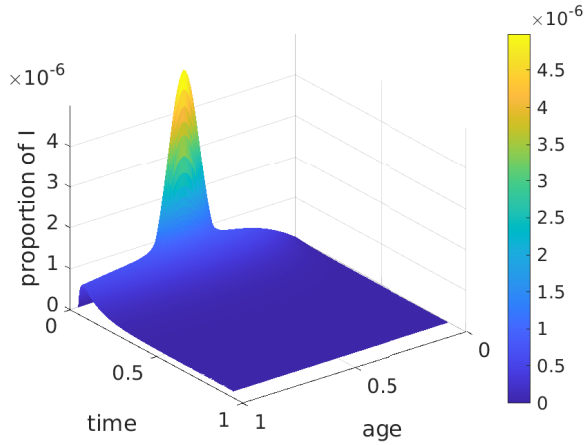

Figure 8.2 – Dynamics of the infected individuals from the NPIDE Model (8.1) with $\Theta = 0$ for $R(0) = 0.8894$

case that $\left|\frac{\Delta t}{\Delta a}\right| \leqslant 1$, as mentioned in (Alexanderian et al. (2011)). This is the case for the parameters used in the numerical simulations: see Table 8.1.
First, note that similar results as the ones shown in Figures 8.2 and 8.3, are obtained using the PIDE Model (6.11). This suggests that numerical errors between both models are negligible. Thus both systems can be used interchangeably. Second, in Figure 8.2, one can observe that the dynamics of the proportion of the infected individuals tends to 0 as time increases. This is consistent with the fact that there is only one stable equilibrium when $R(0) < 1$, which is the disease-free equilibrium. Contrariwise, in Figure 8.3, the dynamics of infected individuals tends to an endemic equilibrium where there are still infected individuals in the population when time increases.

Finally, in view of this result, it seems natural to aim at stabilizing the disease-free equilibrium when $R(0) > 1$ since this equilibrium is unstable for the NPIDE model (8.1) and the goal is to eradicate the disease.

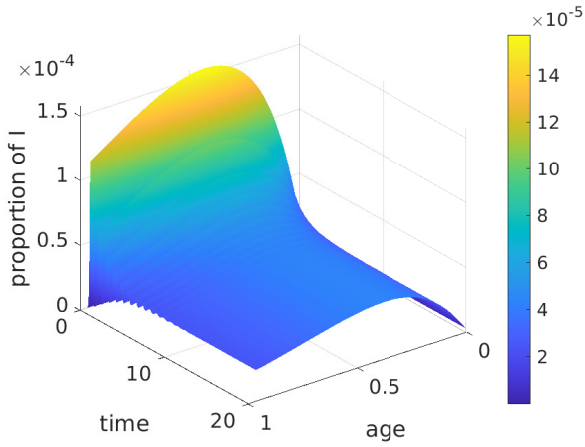

Figure 8.3 – Dynamics of the infected individuals from the NPIDE Model (8.1) with $\Theta = 0$ for $R(0) = 1.1859$

Chapter 9

State feedback

This chapter is dedicated to the design of a state feedback law representing the vaccination in the context of long-term diseases. At first, in Section 9.1, an intermediate positively stabilizing state feedback law is performed for an ODE model. This model is an approximation obtained via a discretization of the PIDE system (6.11). Results on the global stability of the intermediate control law and positivity of the solutions are obtained. The aim of this section is to guide the design of a positively stabilizing state feedback law for the PIDE model, which is described in Section 9.2. The stabilizing property of this feedback is proven. In both sections, numerical simulations corroborate the analytical results.

9.1 Finite dimensional model

As previously mentioned, the aim of this chapter is to design a feedback control law of vaccination $\theta(t, a)$, for the PIDE model (6.11) such that, when it is applied, the corresponding state trajectory converges towards the disease-free equilibrium. Since, to the best of our knowledge, there is no available theory about exact linearization by feedback for PIDE models, the idea to overcome this difficulty is to use an age-discretized intermediate model to guess a feedback law for the PIDE model (6.11). Therefore, an intermediate feedback law, detailed in this section, is obtained, using Isidori's theory (Isidori, 1995, Chapter 5), recalled in Section 2.5. Then, the vaccination law of interest, which is explained in next section, is deduced from the intermediate design but acts on the infinite dimensional system.
The current section is inspired by the methodology developed in (Alonso-

Quesada et al. (2012)) for an SEIR model without age-dependency.

9.1.1 Age-discretized normalized model

Any of the previously introduced infinite dimensional models can be approximated by using discretization by age. This yields a nonlinear finite dimensional model that allows the design of a feedback law by using well-known methods of nonlinear control design. This strategy will lead to an educated guess of the structure of the state feedback law for the PIDE model (6.11). Inspired by (Tudor (1985)), the PIDE Model (6.11) is discretized in n_a classes of age, $[0, a_1), [a_1, a_2), ..., [a_{n_a-1}, a_{max})$. The proportion of susceptible individuals in the kth class of age represents the fraction of individuals in class age k that is susceptible at time t, which gives

$$s_k(t) = \frac{\int_{a_{k-1}}^{a_k} S(t,a)\, da}{N_k} \tag{9.1}$$

where, assuming that the population has reached a time-invariant age distribution ($P(t,a) = P^\star(a)$), $N_k = \int_0^{a_{max}} P^\star(a)\, da$ corresponds to the total number of individuals in the kth class of age in the population. Similar relations hold for the proportion of infected and recovered individuals in the kth class of age at time t. Moreover, it is assumed that the continuous functions of age in (6.11) are constants for a fixed class of age. In other words, it is assumed that $\mu(a) = \mu_k, \gamma(a) = \gamma_k, c(a) = c_k$ and $p(a) = p_k$ for $a \in [a_{k-1}, a_k)$ for all $k = 1, ..., n_a$. Note that these constants are taken, in numerical simulations, as the mean values of the considered functions on this interval. Of course, other choices could be made (e.g. the values of the functions at the beginning of the interval). Remark that, since we are considering n_a quite large (even n_a that tends to infinity for the design of the feedback for the PIDE model (6.11)), this choice has no significant impact on the results. Moreover, the input is also assumed to be independent of $a \in [a_{k-1}, a_k)$ and is given by $\theta_k(t) = \theta(t, a_k)$ for all $k = 1, ..., n_a$. In addition, the number of susceptible individuals that are moving from the kth class of age to the $(k+1)$th at time t, $S(t, a_k)$, is assumed to be proportional to the size of the kth class of age, i.e there exists a transfer rate ρ_k such that $S(t, a_k) = \rho_k N_k s_k(t)$ for $k = 1, ..., n_a$. Remark that, since a_{max} is the maximum age, ρ_{n_a} equals 0. The transfer rate ρ_k is also used for $I(t, a_k)$ and $R(t, a_k)$.

As mentioned in (Tudor (1985)), integrating the equations of Model (6.11) with respect to the age variable, from a_{k-1} to a_k, for $k = 1, ..., n_a$ and using previous assumptions and initial conditions of (6.11), lead to the following system of nonlinear ODEs:

$$N_k \frac{ds_k(t)}{dt} = \rho_{k-1} N_{k-1} s_{k-1}(t) - (\rho_k + \mu_k + p_k \theta_k(t)) N_k s_k(t) - c_k N_k s_k(t) \sum_{j=1}^{n_a} N_j i_j(t) + B\delta_{1k}$$

$$N_k \frac{di_k(t)}{dt} = \rho_{k-1} N_{k-1}(t) i_{k-1}(t) - (\rho_k + \gamma_k + \mu_k) N_k i_k(t) + c_k N_k s_k(t) \sum_{j=1}^{n_a} N_j i_j(t)$$

$$N_k \frac{dr_k(t)}{dt} = \rho_{k-1} N_{k-1} r_{k-1}(t) + \gamma_k N_k i_k(t) + p_k \theta_k(t) N_k s_k(t) - (\rho_k + \mu_k) N_k r_k(t)$$

for $k = 1, ..., n_a$ where ρ_0 is chosen to be equal to 0 and δ_{ij} denotes the Kronecker symbol.
Summing those equations gives the following relations:

$$\frac{B}{N_1} = \rho_1 + \mu_1,$$
$$\rho_{k-1} \frac{N_{k-1}}{N_k} = \rho_k + \mu_k, \text{ for } k = 2, ..., n_a,$$

with B the birth rate. This leads to the identity $s_k + i_k + r_k = 1$, $k = 1, ..., n_a$. Therefore, only $2n_a$ equations are needed. Moreover, using this last assumption and the previous relations, and dividing the set of ODEs equations by N_k for $k = 1, ..., n_a$ give a set of $2n_a$ ordinary differential equations:

$$\begin{aligned} \frac{ds_k(t)}{dt} &= T_k s_{k-1}(t) - \left(T_k + p_k \theta_k(t) + c_k \sum_{j=1}^{n_a} N_j i_j(t) \right) s_k(t), \\ \frac{di_k(t)}{dt} &= T_k i_{k-1}(t) - (T_k + \gamma_k) i_k(t) + c_k s_k(t) \sum_{j=1}^{n_a} N_j i_j(t) \end{aligned} \tag{9.2}$$

for $k = 1, ..., n_a$, where $T_k = \rho_k + \mu_k$, $s_k(0) = s_{k_0}, i_k(0) = i_{k_0}$ and by setting $s_0(t) = 1$ and $i_0(t) = 0$. In the following, this model will be called the NODE Model since it is an age discretized normalized model (involving proportions as variables). The interpretations and units of the variables and parameters involved in the NODE Model are summarized in Table 9.1.

Variables	Interpretation	Range	Unit
t	Time	$\mathbb{R}^+$	day
a_{max}	Maximum age	$\mathbb{R}^+$	year
N_k	Total number of individuals at age in $[a_{k-1}, a_k)$	$\mathbb{R}^+$	Human
$s_k(t)$ $i_k(t)$ $r_k(t)$	Proportion of susceptible, infected and recovered individuals at age in $[a_{k-1}, a_k)$	$[0,1]$	no unit
$\theta_k(t)$	Rate of vaccinated individuals at age in $[a_{k-1}, a_k)$	$\mathbb{R}^+$	$\frac{1}{\text{day}}$
Parameters			
μ_k	Per capita natural death rate at age in $[a_{k-1}, a_k)$	$\mathbb{R}^+$	$\frac{1}{\text{day}}$
c_k	Mean contact between all infected and a susceptible individuals at age in $[a_{k-1}, a_k)$	$\mathbb{R}^+$	$\frac{1}{\text{Human.day}}$
γ_k	Recovery rate at age in $[a_{k-1}, a_k)$	$\mathbb{R}^+$	$\frac{1}{\text{day}}$
ρ_k	Transfer rate from the kth class of age to the $(k+1)$th	$\mathbb{R}^+$	$\frac{1}{\text{day}}$
p_k	Probability of successful vaccination for individuals at age in $[a_{k-1}, a_k)$	$(0,1]$	no unit

Table 9.1 – Parameters and variables for the NODE model

Remark that the NODE model (9.2) is similar to the one introduced in Chapter 4, except that it is an SIR model instead of an SIRD model. Moreover, contrary to Model (4.1), the NODE model (9.2) takes into account the aging effect, allowing the transfer from one class of age to another. This is an important effect that needs to be taken into account when studying long-term diseases.

9.1.2 Well-posedness

In order to have a physical meaning, it is important that the variables in the model remain between 0 and 1, since they are proportions. Inspired by (Tudor (1985)), the following result highlights that this is the case if the feedback law is nonnegative.

Proposition 9.1.1
If $\theta_k(t) \geqslant 0$ for all $t \geqslant 0$ and $k = 1, ..., n_a$, then the set

$$\mathcal{X} = \{(i_1, ..., i_{n_a}, s_1, ..., s_{n_a} : i_k \geqslant 0, s_k \geqslant 0, s_k + i_k \leqslant 1 \text{ for } k = 1, ..., n_a)\}$$

is positively invariant with respect to the NODE model (9.2).

Proof. Let t_0 be the smallest t such that $x(t_0) \in \delta\mathcal{X}$, where

$$\delta\mathcal{X} = \{(i_1, ..., i_{n_a}, s_1, ..., s_{n_a} : i_k = 0 \text{ or } s_k = 0 \text{ or } s_k + i_k = 1)\}.$$

Assume that $s_m(t_0) = 0$ ($i_m(t_0) = 0$) for some m. By definition of t_0, all the other state components are such that $s_k(t_0), i_k(t_0) \geqslant 0$ for $k = 1, ..., m-1, m+1, ..., n_a$. Therefore, using equations (9.2), $\frac{ds_m(t_0)}{dt} \geqslant 0$ and $\frac{di_m(t_0)}{dt} \geqslant 0$. On the other hand, if $i_m(t_0) + s_m(t_0) = 1$ for some m, then $s_k(t_0), i_k(t_0) \geqslant 0$ and $s_k(t_0) + i_k(t_0) \leqslant 1$ for $k = 1, ..., m-1, m+1, ...n$. By equations (9.2), it follows that

$$\begin{aligned}\frac{d(s_m + im)(t_0)}{dt} &= T_m\left(s_{m-1}(t_0) + i_{m-1}(t_0) - 1\right) - \gamma_m i_m(t_0) - p_m\theta_m(t_0)s_m(t_0) \\ &\leqslant 0\end{aligned}$$

□

Observe that the nonnegativity is no longer guaranteed for all inputs of the system when working with the discretized model, contrary to what is stated in Proposition 8.1.1 for the infinite dimensional system. It requires the nonnegativity of the input. This is consistent with the physical interpretation of the input, as the vaccination rate. Nevertheless, in the sequel, no condition on the feedback gains implying, a priori, the nonnegativity of the input are obtained. Therefore, in practice, the feedback gains need to be chosen according to the assumptions of Theorem 9.1.1 and then one has to check that the obtained input is nonnegative. In this thesis, to bypass this choice of parameters that ensures nonnegativity of the feedback (since there are 200 parameters to be chosen) a saturated law (see (9.16)) is used in the numerical simulations. Additional research is needed to ensure that this law recovers the performance of (9.15) but numerical simulations seems to corroborate this fact. Remark that when dealing with the PIDE model (6.11) in Section 9.2, conditions on the feedback gains implying nonnegativity of the input are obtained.

9.1.3 Linearizing state feedback design

The approach developed in this part is similar to the one presented in Subsection 5.2.1 for a SIRD model. In that case, the aging effect is considered but

there is no compartment for the dead individuals. The details are developed below in order to be self-contained.

The equations of the NODE Model (9.2) can be written equivalently in the state space form as a nonlinear control affine system

$$\left\{ \begin{array}{rcl} \dot{x}(t) & = & f(x(t)) + g(x(t))\, u(t) \\ y(t) & = & h(x(t)) \end{array} \right. \tag{9.3a}$$

where $x(t) = [i_1(t), ..., i_{n_a}(t), s_1(t), ..., s_{n_a}(t)]^T \in \mathbb{R}^{2n_a}$, for all $t \geqslant 0$ is the state space vector, $h(x(t)) = [i_1(t), ..., i_{n_a}(t)]^T \in \mathbb{R}^{n_a}, \forall t \geqslant 0$ is the measurable output function, assumed equal to the infectious population and $u(t) = [\theta_1(t), ..., \theta_{n_a}(t)]^T \in \mathbb{R}^{n_a}, \forall t \geqslant 0$ is the input function. Moreover,

$$g(x(t)) = \begin{pmatrix} 0_{n_a \times n_a} \\ -p_k diag(s_k)_{k=1,...,n_a} \end{pmatrix} \tag{9.3b}$$

and

$$f(x(t)) := (f_1(x(t)) \cdots f_{2n_a}(x(t)))^T \tag{9.3c}$$

where

$$f_k(x(t)) = T_k i_{k-1}(t) - (T_k + \gamma_k) i_k(t) + c_k s_k(t) \sum_{j=1}^{n_a} N_j i_j(t),$$

$$f_{n_a+k}(x(t)) = T_k s_{k-1}(t) - T_k s_k(t) - c_k s_k(t) \sum_{j=1}^{n_a} N_j i_j(t)$$

for $k = 1, ..., n_a$.
In this case the relative degree of the system is equal to the dimension of the state space for any $x \in \mathcal{D} = \left\{ x \text{ s.t } s_k \neq 0 \text{ for } k = 1, ..., n_a \text{ and } \sum_{j=1}^{n_a} N_j i_j \neq 0 \right\}$. Therefore, by Lemma 2.5.1 the "state space exact linearization problem", mentioned in Problem 2.5.1 is feasible. Hence, the nonlinear invertible (for $x \in \mathcal{D}$) coordinate change that is needed here is given by

$$\begin{aligned} \bar{i}_k(t) &= h_k(x(t)) = i_k(t), \\ \bar{s}_k(t) &= L_f h_k(x(t)) = f_k(x(t)) \end{aligned} \tag{9.4}$$

for $k = 1, ..., n_a$. Notice that in practice, $x \notin \mathcal{D}$ either if there is a class of age where there is no more susceptible individuals or if there is no more infected individual in the population. The first case is not a problem because, when

it occurs this means that one can no longer vaccinate the given class of age. Therefore this can be taken care by setting the vaccination to 0 in this case. Moreover, it is reasonable to expect that this case will not happen before the eradication of the disease. On the other hand, the second case will probably occur because it means that the end of the epidemic is reached, which is the goal of the feedback design. However, in numerical simulations, since we deal with numbers of individuals which are real and not integer, the simulation is stopped whenever there remains less than one infected individual in the population. Thanks to this coordinate change, the system is written in its normal form in the neighborhood of any $x \in \mathcal{D}$ by

$$\begin{aligned} \frac{d\bar{i}_k(t)}{dt} &= \bar{s}_k(t), \\ \frac{d\bar{s}_k(t)}{dt} &= L_f^2 h_k(x(t)) + L_{g_k} L_f h_k(x(t)) u_k(t) \end{aligned} \tag{9.5}$$

for $k = 1, ..., n_a$. That allows the design of a feedback law that linearizes the system in normal form. To do so, the following matrices are defined,

$$A(x(t)) = diag\left(-c_k p_k s_k(t) \sum_{j=1}^{n_a} N_j i_j(t)\right)_{k=1,...,n_a} \tag{9.6}$$

$$v(x(t)) = \begin{pmatrix} v_1(x(t)) & \cdots & v_{n_a}(x(t)) \end{pmatrix}^T \tag{9.7}$$

such that

$$v_k(x(t)) = -\alpha_2^k f_k(x(t)) - \alpha_1^k i_k(t), k = 1, ..., n_a$$

where α_1^k and α_2^k are some free parameters that will be adjusted to yield stability. Moreover,

$$b(x(t)) = \begin{pmatrix} b_1(x(t)) & \cdots & b_{n_a}(x(t)) \end{pmatrix}^T, \tag{9.8}$$

where

$$\begin{aligned} b_k(x(t)) &= L_f^2 h_k(x(t)) \\ &= c_k s_k(t) \sum_{j=1}^{n_a} N_j f_j(x(t)) + T_k f_{k-1}(x(t)) - (T_k + \gamma_k) f_k(x(t)) \\ &\quad + c_k f_{n_a+k}(x(t)) \sum_{j=1}^{n_a} N_j i_j(t). \end{aligned} \tag{9.9}$$

Lemma 9.1.1
The state feedback control law defined by

$$u(t) = A^{-1}(x(t))\left(v(x(t)) - b(x(t))\right), \tag{9.10}$$

where A, b and v are given by (9.6)-(9.8), applied on system (9.3), induces the linear output closed-loop dynamics given by

$$\ddot{y}(t) + \tilde{A}_2\dot{y}(t) + \tilde{A}_1 y(t) = 0. \tag{9.11}$$

where $\tilde{A}_1 = diag(\alpha_1^i)$ and $\tilde{A}_2 = diag(\alpha_2^i)$ for $i = 1, ..., n_a$.

Proof. Applying the control law (9.10) to the dynamics in normal form (9.5) linearizes the equations and gives

$$\dot{\bar{x}}(t) = \begin{pmatrix} 0_{n_a \times n_a} & Id_{n_a} \\ -\tilde{A}_1 & -\tilde{A}_2 \end{pmatrix} \bar{x}(t) := \bar{A}\bar{x}(t)$$

where $\bar{x}(t) = \left[\bar{i}_1(t) \cdots \bar{i}_{n_a}(t)\, \bar{s}_1(t) \cdots \bar{s}_{n_a}(t)\right]^T$. The solution of this ODE is given by $y(t) = C\bar{x}(t) = \left(\bar{i}_1(t) \cdots \bar{i}_{n_a}(t)\right)^T$.
Thus, a trivial computation gives $\ddot{y}(t) = \tilde{A}_1 y(t) + \tilde{A}_2\dot{y}(t)$. □

Using this feedback on system (9.3), the closed-loop model is given by

$$\dot{x}(t) = F(x(t)), \tag{9.12a}$$

for $x = \left[i_1 \cdots i_{n_a}\ s_1 \cdots s_{n_a}\right]^T$ and

$$F(x(t)) = \left[F_1(x(t)) \cdots F_{2n_a}(x(t))\right]^T, \tag{9.12b}$$

where

$$\begin{aligned} F_k(x) &= f_k(x), \\ F_{n_a+k}(x) &= \frac{1}{c_k \sum_{j=1}^{n_a} N_j i_j} \Big(f_k(x)\left(T_k + \gamma_k - \alpha_2^k\right) \\ &\quad -\alpha_1^k i_k - T_k f_{k-1}(x) - c_k s_k \sum_{j=1}^{n_a} N_j f_j(x) \Big) \end{aligned} \tag{9.13}$$

for $k = 1, ..., n_a$ with $f_0(x(t)) = 0$.

Moreover, in order to be effective, the feedback needs to ensure the eradication of the infected individuals in the population.

Theorem 9.1.1
Let the initial condition $x_0 \in R_+^{2n_a}$ be given. Assume that the control tuning parameters satisfy $\alpha_j^k > 0$ for $j = 1, 2$ and $k = 1, ..., n_a$.
Then the state feedback (9.10) implies the exponential convergence towards zero of the infected population $i_k(t)$ of NODE Model (9.2), for $k = 1, ..., n_a$, as time tends to infinity.

Proof. Since the closed-loop dynamics (9.11) is a system of decoupled ODEs it can be written as

$$\begin{cases} \dot{\bar{x}}_{new}(t) &= \hat{A}\bar{x}_{new}(t), \\ y(t) &= C\bar{x}_{new}(t) \end{cases} \tag{9.14}$$

with $\bar{x}_{new} = \begin{pmatrix} \bar{i}_1 & \bar{s}_1 & \cdots & \bar{i}_{n_a} & \bar{s}_{n_a} \end{pmatrix}^T$, $\hat{A} = blockdiag(\bar{A}_k)$, where $\bar{A}_k = \begin{pmatrix} 0 & 1 \\ -\alpha_1^k & -\alpha_2^k \end{pmatrix}$ and $C = \begin{pmatrix} 1 & 0 & \cdots & 1 & 0 \end{pmatrix}^T$.
Therefore, $\hat{A}$ is stable if all its eigenvalues are in the open left plane. However, the eigenvalues of $\hat{A}$ are those of the $\bar{A}_k$'s matrices. Moreover, those eigenvalues are the roots of the characteristic polynomial $P(s) = Det(sI - \bar{A}_k) = s^2 - s\alpha_2^i + \alpha_1^i$. Since α_1^k and α_2^k are positive, then by the corollary of Lienard-Chipart Theorem 2.5.2, the real parts of the eigenvalues of $\hat{A}$, are negative. Then the control law exponentially stabilizes the model in normal form (9.5).
Therefore, $\bar{x}(t)$ exponentially converges asymptotically to zero. It follows that $\bar{i}_k(t) = i_k(t)$ converges to zero as time goes to infinity for $k = 1, ..., n_a$. □
Theorem 9.1.1 states that, regardless of the initial condition, the number of infected individuals for each age group tends asymptotically to zero. However, it is not possible to know the behavior of the other states, unlike what was stated in Chapter 5.

Remark 9.1.1 *The control law is well-defined for $x \in \mathcal{D}$. However, since the aim is to eradicate the disease from the population, the infected population goes to zero as time tends to infinity. This implies that* $\sum_{j=1}^{n_a} N_j i_j = \int_0^{a_{max}} I(t, a)\, da$ *tends to zero. Therefore, as explained in (Alonso-Quesada et al. (2012)), a "switch-off" vaccination law is introduced, based on the fact that the disease is considered as being eradicated from the population when the infected population is greater than zero but small enough (for instance when there is numerically*

less than one individual in the population but more than zero). Therefore, a threshold is defined such that $0 < \int_0^{a_{max}} I(t,a)\,da < \delta < 1$. *Hence, in a practical situation, we use*

$$u_s(t,a) = \begin{cases} u(t,a) \text{ for } t \leqslant t^\star, \\ \\ 0 \text{ for } t > t^\star \end{cases} \tag{9.15}$$

where $t^\star = min\left\{ t \in \mathbb{R}^+ | \int_0^{a_{max}} I(t,a)\,da < \delta \text{ for } 0 < \delta < 1 \right\}$. *Consequently, Theorem 9.1.1 cannot be used directly. However, by similar arguments, we know that the linearization of Lemma 9.1.1 is valid until* $t^\star$, *when the total number of infected individuals in the population is smaller than 1. Therefore, until the time* $t^\star$, *Theorem 9.1.1 can be applied, leading to the conclusion that the infected population is exponentially globally decreasing until* $t^\star$. *In practice, this result is enough because the infected population is exponentially decaying until* $\sum_{j=1}^{n_a} N_j i_j = \int_0^{a_{max}} I(t,a)\,da < 1$ *which, in practical formulation, means that there are no more infected individuals in the population, so no more epidemic.*

9.1.4 Numerical simulations

Numerical simulations are performed to show that appropriate choices of parameters can guarantee the eradication of the infected individuals. In the simulations, parameters are taken from (Okuwa et al. (2019)) and described in Section 8.3 but are adapted to the ODE case as mentioned in Section 9.1.1. In this case 100 classes of age are considered. This number is chosen randomly, but large enough, because in the numerical context, the NODE model (9.2) can be viewed as a semi-discretization of the PIDE Model (6.11). Furthermore, a large number of classes enables a smooth representation of the graphs, as it is the case for the PIDE simulations. Moreover, the design control parameters are set to $\alpha_1^k = 16000$ and $\alpha_2^k = 280$ for $k = 1, ..., 100$. Simulations are stopped when convergence is reached with a tolerance of 10^{-8}. The code is performed using finite difference in time with a time step equal to 0.001.
Remind that the vaccination variable should be nonnegative, as stated in Subsection 9.1.2. Therefore, based on results found in numerical simulations, a new control law $u_{ps}(t)$ is designed where, for $k = 1, ..., n_a$,

$$u_{ps,k}(t) = \begin{cases} 0, & \text{if } u_{s,k}(t) < 0, \\ u_{s,k}(t) & \text{otherwise} \end{cases} \tag{9.16}$$

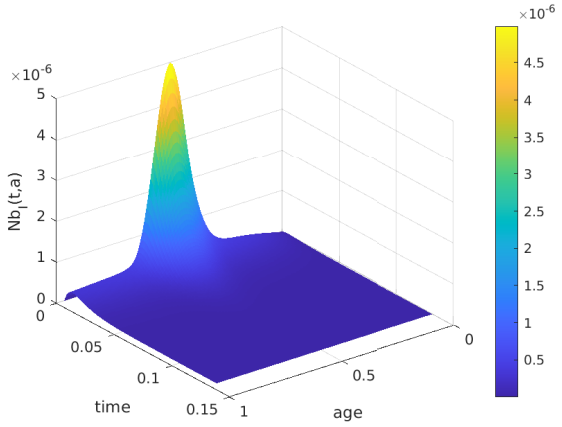

Figure 9.1 – Dynamics of infected individuals from NODE Model (9.2) with vaccination (9.16)

which is based on the control-law (9.15). Using this control law in numerical simulations shows that the stability of the system is conserved. In this case, one can observe that the infected individuals converge to zero when the control is applied. Moreover, the infected individuals remain nonnegative and are smaller than 1. This is also the case for the proportion of susceptible individuals observed in Figure 9.2. Moreover, Figure 9.3 suggests to vaccinate first individuals in the classes of age where the epidemic is absent and in a second time to vaccinate individuals from classes of age around the ages where individuals were initially infected.

9.2 Infinite dimensional model

This section is dedicated to the design of a stabilizing and linearizing feedback law for the PIDE Model (6.11). This law is obtained thanks to a formal limit using (9.10). One main advantage of this new law compared to the one of the ODE case is that conditions ensuring nonnegativity of the input are obtained.

9.2.1 Feedback design

To discover a feedback design for the PIDE model (6.11), let us define a new function

$$W(t,a) = p(a)\theta(t,a)\,S(t,a)\,. \tag{9.17}$$

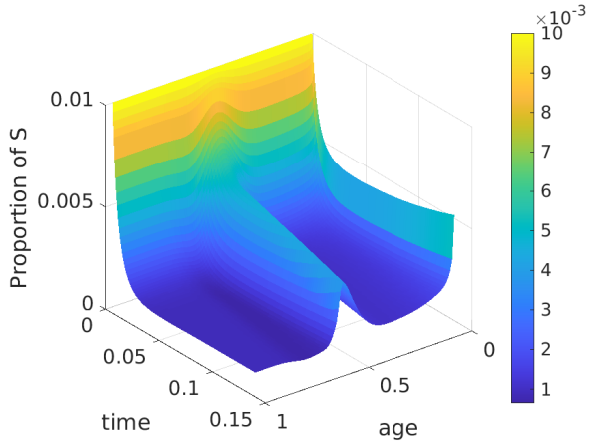

Figure 9.2 – Dynamics of susceptible individuals from NODE Model (9.2) with vaccination (9.16)

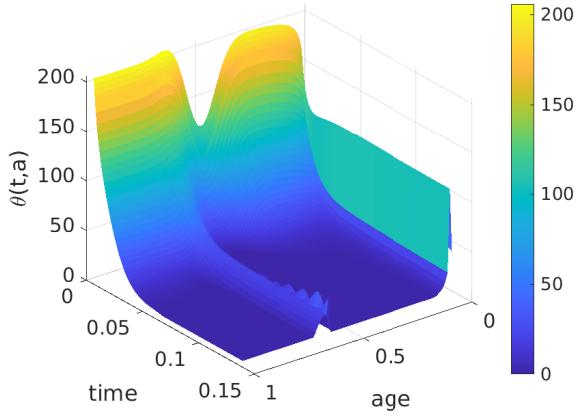

Figure 9.3 – Dynamics of vaccination (9.16)

The goal is to link the law $\theta(t,a)$ to the law $u_k(t) = \theta_k(t)$ defined in (9.10). Therefore, by introducing

$$w_k(t) = \frac{1}{N_k} \int_{a_{k-1}}^{a_k} W(t,a)\, da, \tag{9.18}$$

inspired by the change of variable (9.1) that links the PIDE variables to the NODE variables and discretizing (6.11) with respect to the age, it can be shown that $w_k(t) = p_k \theta_k(t) s_k(t)$. Using relation (9.18) and the limit of the mean value theorem for integral and assuming that $a \in [a_{k-1}, a_k)$ for all $k \in \mathbb{N}$, implies that

$$\begin{aligned} & W(t,a) = \lim_{\Delta_k \to 0} \frac{N_k w_k(t)}{\Delta_k}, \text{ with } \Delta_k = a_k - a_{k-1} \\ \Leftrightarrow & p(a)\theta(t,a) S(t,a) = \lim_{\Delta_k \to 0} \frac{N_k p_k \theta_k(t) s_k(t)}{\Delta_k}, \\ \Leftrightarrow & \theta(t,a) = \frac{1}{p(a) S(t,a)} \lim_{\Delta_k \to 0} \frac{N_k p_k \theta_k(t) s_k(t)}{\Delta_k}. \end{aligned}$$

Using relations of Section 9.1.1, the definition of the state feedback in finite dimension, (9.10), and the definition of derivative in terms of limits give the following candidate for a nonlinear state feedback control law that is continuous in age

$$\theta(t,a) = \frac{1}{p(a)} \left\{ (A + G + H_{\tilde{\alpha}})\, x(t,\cdot) \right\}(a) \tag{9.19}$$

where $x = \begin{pmatrix} S & I \end{pmatrix}^T$, $\tilde{\alpha} = \begin{pmatrix} \tilde{\alpha}_1 & \tilde{\alpha}_2 \end{pmatrix}^T$,

$$Ax(t,a) = \int_0^{a_{max}} c(a) S(t,a)\, da - c(a) \|I\|_1 - 2\mu(a) - \gamma(a),$$

$$Gx(t) = -\|I\|_1^{-1} \int_0^{a_{max}} K(a) I(t,a)\, da$$

and $H_{\tilde{\alpha}} x(t,a) = \tilde{\alpha}_2(a) + \dfrac{I(t,a) \left(\tilde{\alpha}_1(a) + K(a) (K(a) - \tilde{\alpha}_2(a)) \right)}{c(a) S(t,a) \|I\|_1}$

where $K(a)$ denotes $\mu(a) + \gamma(a)$. Note that in this feedback, there is a division by $\|I\|_1$ which is $\displaystyle\int_0^{a_{max}} I(t,b)\, db$, recalling the nonnegativity of $I(t,b)$. However, since the eradication of the epidemic is wanted, this quantity tends to zero. Therefore, in practice a switching vaccination law is used, as it was done in Remark 9.1.1. Hence, the control is defined as the one in (9.15).

9.2.2 Stabilizing law

The aim of this section is to show that the feedback law (9.19) stabilizes the PIDE model (6.11).

Inspired by the linearizing state feedback approach developed in Section 2.5, the following nonlinear coordinate changes is made,

$$\begin{aligned}\bar{I}(t,a) &= I(t,a),\\ \bar{S}(t,a) &= -K(a)I(t,a) + c(a)\,S(t,a)\int_0^{a_{max}} I(t,b)\,db.\end{aligned} \tag{9.20}$$

Observe that the second change of coordinate is not invertible. This is taken care of, in the implementation part, by using a "switch-off" vaccination law. In this formulation the the two first equations of the open-loop Model (6.11) becomes

$$\begin{aligned}&(\partial_t + \partial_a)\,\bar{I}(t,a) = \bar{S}(t,a),\\ &(\partial_t + \partial_a)\,\bar{S}(t,a) = -K(a)\bar{S}(t,a) - \partial_a(K(a))\,\bar{I}(t,a) + \left[\bar{S}(t,a) + K(a)\bar{I}(t,a)\right]\\ &\quad\times\left[-p(a)\theta(t,a) - \mu(a) - c(a)\int_0^{a_{max}}\bar{I}(t,b)\,db + \frac{\int_0^{a_{max}}\bar{S}(t,b)\,db}{\int_0^{a_{max}}\bar{I}(t,b)\,db} + \frac{\partial_a c(a)}{c(a)}\right]\end{aligned} \tag{9.21}$$

under non-homogeneous boundary conditions

$$\bar{I}(t,0) = 0, \bar{S}(t,0) = c(0)\,B\int_0^{a_{max}}\bar{I}(t,b)\,db \tag{9.22}$$

and initial conditions

$$\bar{I}(0,a) = I_0(a), \bar{S}(0,a) = \bar{S}_0(a). \tag{9.23}$$

Moreover, the vaccination law (9.19) rewrites

$$\begin{aligned}\theta(t,a) = \frac{1}{p(a)}\Bigg\{&\tilde{\alpha}_2(a) + \frac{\int_0^{a_{max}}\bar{S}(t,b)\,db}{\int_0^{a_{max}}\bar{I}(t,b)\,db} - 2\mu(a) - \gamma(a)\\ &- c(a)\int_0^{a_{max}}\bar{I}(t,b)\,db + \frac{\bar{I}(t,a)}{\bar{S}(t,a) + K(a)\bar{I}(t,a)}\left(\tilde{\alpha}_1(a) + K(a)\left(K(a) - \tilde{\alpha}_2(a)\right)\right)\Bigg\}\end{aligned}$$

Therefore, the closed-loop system is given by the linear PDEs

$$\begin{aligned}&(\partial_t + \partial_a)\,\bar{I}(t,a) = \bar{S}(t,a),\\ &(\partial_t + \partial_a)\,\bar{S}(t,a) = \bar{I}(t,a)\left[-\tilde{\alpha}_1(a) + g(a)\right] + \bar{S}(t,a)\left[-\tilde{\alpha}_2(a) + h(a)\right]\end{aligned} \tag{9.24}$$

where

$$g(a) = -c(a)\,\frac{d}{da}\left(\frac{K(a)}{c(a)}\right), \tag{9.25}$$

$$h(a) = \frac{1}{c(a)} \frac{d}{da} c(a) \tag{9.26}$$

with boundary conditions (9.22) and initial conditions (9.23). The design parameters are denoted by $\tilde{\alpha}_1(a)$ and $\tilde{\alpha}_2(a)$. We are going to show that they can be properly chosen so as to have the stability and positivity of the system. The other parameters (c, μ, γ) are given for a chosen model.
Therefore, similarly to the results of Section 2.5, a feedback that linearizes the open-loop system (9.21) is found thanks to the appropriate coordinates change (9.20).

It remains to show that the feedback (9.19) also stabilizes system (6.11). In the following it is shown that the closed-loop system (9.24) is stable which implies the asymptotic convergence to zero of the infected population. Hereafter we denote

$$G(a) = -\tilde{\alpha}_1(a) + g(a) \text{ and } H(a) = -\tilde{\alpha}_2(a) + h(a).$$

With those notations, the state-space formulation of system (9.24) is given by

$$\begin{aligned} \dot{\bar{x}} &= \bar{\mathcal{A}}\bar{x} \\ \bar{x}(0) &= \bar{x}_{B0} \end{aligned} \tag{9.27}$$

where $\bar{x} = \left(\bar{I}, \bar{S}\right)^T$, $\bar{\mathcal{A}} = \begin{pmatrix} -\frac{d\cdot}{da} & Id \\ G(a)\, Id & -\frac{d\cdot}{da} + H(a)\, Id \end{pmatrix}$,

$\mathcal{D}\left(\bar{\mathcal{A}}\right) = \left\{ \bar{x} \in L^1(0, a_{max}) \times L^1(0, a_{max}), \bar{x}, \frac{d\bar{x}}{da} \in L^1(0, a_{max}), \bar{x}(0) = \bar{x}_{B0} \right\}$

and $\bar{x}_{B0} = \begin{pmatrix} 0 \\ c(0)\, B \int_0^{a_{max}} \bar{I}(b)\, db \end{pmatrix}$.

Using the approach developed in (Fattorini (1968)) on boundary control systems and generalizing the results in (Tucsnak and Weiss, 2009, Chapter 10) to Banach spaces, system (9.27) can be rewritten as follows:

$$\begin{aligned} \dot{\bar{x}} &= \bar{\mathcal{A}}_0\bar{x} + \tilde{B}u \\ \bar{x}(0) &= (0,0)^T \end{aligned} \tag{9.28}$$

where $\bar{\mathcal{A}}_0 = \bar{\mathcal{A}}$ with $\mathcal{D}\left(\bar{\mathcal{A}}_0\right) = \left\{ \bar{x} \in L^1(0, a_{max}) \times L^1(0, a_{max}) : \bar{x}, \right.$
$\left. \frac{d\bar{x}}{da} \in L^1(0, a_{max}), \bar{x}_0 = (0,0)^T \right\}$.
Moreover $\tilde{B} = \delta_0 Id_2$ and $u = \bar{x}_{B0}$.

Indeed, one can notice that none of the arguments developed in (Tucsnak and

Weiss (2009)) requires a scalar product which is only defined on Hilbert space, except for the computation of the adjoint operator. However, in L^1 spaces, this operator can be computed using duality bracket, which is the approach used here. Therefore, according to the theory in (Tucsnak and Weiss (2009)), we need to find the operator $\tilde{B}$ such that the system $\dot{z}(t) = Lz(t)$ with $\tilde{G}z(t) = z(0) = u(t)$, with $z \in \mathcal{D}(L)$ is equivalent to the system $\dot{z}(t) = \mathcal{A}z(t) + \tilde{B}u(t)$. This operator satisfies, for $z \in Z := W^{1,1}(0, a_{max}) \times W^{1,1}(0, a_{max}) \to X := L^1(0, a_{max}) \times L^1(0, a_{max})$ and $\psi \in \mathcal{D}(\mathcal{A}^\star)$,

$$[Lz, \psi] - [z, \mathcal{A}^\star \psi] = \left[\tilde{G}z, \tilde{B}^\star \psi\right]. \tag{9.29}$$

In order to apply this theory, System (9.27) can be rewritten as $\dot{z}(t) = Lz(t)$ with $\tilde{G}z(t) = z(0)$ where $z = \left(\bar{I}, \bar{S}\right)^T$, $L = \bar{\mathcal{A}}$ and $\tilde{G} : Z \to U := \mathbb{R}^2$, where $W^{1,1}(0, a_{max})$ denotes the Sobolev space of functions defined on $[0, a_{max}]$, which are in $L^1(0, a_{max})$ and whose generalized derivatives up to order 1 are in $L^1(0, a_{max})$. Hence, $\mathcal{A}$ is defined as L restricted to[1] $X_1 := \text{Ker}\, \tilde{G}$. Thus, $\mathcal{A} = \bar{\mathcal{A}}_0 : \mathcal{D}\left(\bar{\mathcal{A}}_0\right) \to X$. It remains to find the operator $\tilde{B} : U \to X_{-1}$ by using relation (9.29).

First one can show that the adjoint of $\bar{\mathcal{A}}_0$ with $\mathcal{D}\left(\bar{\mathcal{A}}_0\right)$ is given by

$$\bar{\mathcal{A}}_0^\star = \begin{pmatrix} \dfrac{d\cdot}{da} & G(a)Id \\ Id & \dfrac{d\cdot}{da} + H(a)Id \end{pmatrix}$$

with $\mathcal{D}\left(\bar{\mathcal{A}}_0^\star\right) = \{y \in L^\infty(0, a_{max}) \times L^\infty(0, a_{max}) : y_1(a_{max}) = y_2(a_{max}) = 0$ and $[\mathcal{A}\cdot, y] : L^1(0, a_{max}) \times L^1(0, a_{max}) \to \mathbb{K}$ is bounded and linear$\}$. The proof is based on the Riesz representation theorem for L^1 space (see (Rudin, 1974, Theorem 6.16)) which implies that $[\mathcal{A}z, y] = \int_0^{a_{\max}} \langle \mathcal{A}z, y \rangle d\lambda$ for $z \in \mathcal{D}(\mathcal{A})$ and $y \in \mathcal{D}(\mathcal{A}^\star)$, where λ denotes the Lebesgue measure. Then, using relation (9.29) and the Riesz representation theorem it follows that

$$\langle z(0), \tilde{B}^\star \psi \rangle = \langle z(0), \psi(0) \rangle.$$

Hence,

$$\tilde{B}^\star \psi = \psi(0)$$
$$\left[\phi, \tilde{B}^\star \psi\right] = [\phi, \psi(0)]$$

1. The space X_1 and X_{-1} are defined in (Tucsnak and Weiss, 2009, Section 2.1). Let $A : \mathcal{D}(A) \to X$ be a densely defined operator with $\rho(A) \neq \varnothing$. Then for every $\lambda \in \rho(A)$, the space $\mathcal{D}(A)$ with the norm $\|x\|_{X_1} = \|(\lambda Id - A)x\| \ \forall x \in \mathcal{D}(A)$ is denoted X_1. Moreover, X_{-1} is the completion of X with respect to the norm $\|x\|_{X_{-1}} = \|(\lambda Id - A)^{-1} x\| \ \forall x \in X$.

$$[B\phi, \psi] = [\phi, \psi(0)]$$

Therefore, $\tilde{B}$ is given by $\delta_0 Id_2$. Finally, the assumptions needed in (Tucsnak and Weiss (2009)) are satisfied since $\bar{\mathcal{A}}_0$ is the infinitesimal generator of a C_0-semigroup.

Equivalently to (9.28) one can write

$$\begin{aligned} \dot{\bar{x}} &= \left(\bar{\mathcal{A}}_0 + \bar{D}\right)\bar{x} \\ \bar{x}(0) &= (0,0)^T \end{aligned} \tag{9.30}$$

where $\bar{D} = \begin{pmatrix} 0 & 0 \\ \delta_0 c(0) B \int_0^{a_{max}} \cdot \, db & 0 \end{pmatrix}$.

An approximation of the Dirac delta δ_0 is used so that $\bar{D}$ is bounded. Remark that this approximation allows to deal with a more realistic model since there is no sense to vaccinate instantaneously at birth. Let define $d_k(a)$ a term of a Dirac sequence which satisfies the properties developed in (Hinrichsen and Pritchard, 2010, Chapter 2, Section 3, Lemma 2.3.4) with ∞ replaced with a_{max}. Therefore, (9.28) becomes

$$\begin{aligned} \dot{\bar{x}}_k &= \left(\bar{\mathcal{A}}_0 + \bar{D}_k\right)\bar{x}_k \\ \bar{x}_k(0) &= (0,0)^T \end{aligned} \tag{9.31}$$

with $\bar{D}_k = \begin{pmatrix} 0 & 0 \\ d_k(a)\, c(0) B \int_0^{a_{max}} \cdot \, db & 0 \end{pmatrix}$.

In what follows, an approximation of model (9.30), where the unbounded operator D is replaced by the bounded operator $\bar{D}_k$, is used in order to perform the stability analysis.

Lemma 9.2.1
$\bar{\mathcal{A}}_0$ is the infinitesimal generator of a C_0-semigroup $\bar{U}(t)$.

Proof. As in (Aksikas et al. (2007)) a similarity transformation is performed to have an equivalent state space description as (9.31) with triangular infinitesimal generator. Therefore,

$$J = \begin{pmatrix} Id & 0 \\ \kappa(a)\, Id & Id \end{pmatrix} \tag{9.32}$$

is chosen where $\kappa(a)$ is a bounded C_1 solution (i.e $\exists\ K > 0$ such that $\kappa(a)) \leqslant K$ $\forall\ a \in [0, a_{max}]$) of the equation

$$\frac{d\kappa}{da} + \kappa^2(a) - H(a)\kappa(a) + G(a) = 0.$$

The existence of such solution is established in (Aksikas et al. (2007)). Applying this transformation to the operator $\bar{\mathcal{A}}_0$, i.e $J^{-1}\bar{\mathcal{A}}_0 J$, gives

$$\mathring{\mathcal{A}} = \begin{pmatrix} -\frac{d\cdot}{da} + G(a)\kappa(a)\,Id & Id \\ 0 & -\frac{d\cdot}{da} + (H(a) - \kappa(a))\,Id \end{pmatrix}$$

where $\mathcal{D}\left(\mathring{\mathcal{A}}\right) = \mathcal{D}\left(\bar{\mathcal{A}}_0\right)$. Thanks to Proposition 7.1.2, $\mathring{\mathcal{A}}$ is the infinitesimal generator of a C_0-semigroup

$$\left(\mathring{U}(t)\right)_{t\geqslant 0} = \begin{pmatrix} \mathring{U}_1(t) & \mathring{U}_{12}(t) \\ 0 & \mathring{U}_2(t) \end{pmatrix}$$

where

$$\left(\mathring{U}_{12}(t)\,x\right)(a) = \int_0^t \mathring{U}_1(t-s)\,\mathring{\mathcal{A}}_{12}\mathring{U}_2(s)\,x(a)\,ds. \tag{9.33}$$

Using Proposition 7.1.3, it holds that $\bar{\mathcal{A}}_0$ is the infinitesimal generator of a C_0-semigroup

$$\left(\bar{U}(t)\right)_{t\geqslant 0} = \left(J\mathring{U}(t)\,J^{-1}\right)_{t\geqslant 0}.$$

□

Theorem 9.2.1: Stability of $\bar{\mathcal{A}}_0 + \bar{D}_k$

The operator $\bar{\mathcal{A}}_0 + \bar{D}_k$ is the infinitesimal generator of an exponentially stable C_0-semigroup $\left(\bar{T}_k(t)\right)_{t\geqslant 0}$ with growth bound

$$\omega_0(\bar{T}_k) < -(c_2 + K) + (1 + K(c_1 - 1) - c_2)\,c(0)B < 0$$

provided that the gain functions $\tilde{\alpha}_1(a)$ and $\tilde{\alpha}_2(a)$ and the constants c_1 and c_2 are chosen such that

$$c_1 > max\left\{1,\ \sup_{a\in[0,L]}\left(\tilde{\alpha}_1(a) - g(a)\right),\ \frac{c(0)B}{K}\right\}, \tag{9.34}$$

$$c_2 > max\left\{0,\ \frac{c(0)B(1 + Kc_1)}{1 + c(0)B} - K,\ \sup_{a\in[0,L]}\left(\tilde{\alpha}_2(a) - h(a)\right)\right\}, \tag{9.35}$$

$$c_2 \leqslant K(c_1 - 1). \tag{9.36}$$

Proof. The semigroup generation is obtained thanks to the bounded perturbation Theorem 7.1.1. Indeed, the linear operator $\bar{D}_k$ is bounded on $L^1(0, a_{max}) \times L^1(0, a_{max})$ with norm $\|\bar{D}_k\|_{\mathcal{L}(L^1 \times L^1)} = c(0) B$. Moreover, by Lemma 9.2.1, $\bar{\mathcal{A}}_0$ is the infinitesimal generator of a C_0-semigroup. Now, the exponential stability can be established in few steps.

Step 1: Applying the transformation (9.32) to the operator $\bar{\mathcal{A}}_0 + \bar{D}_k$, gives the operator $\mathring{\mathcal{A}} + \bar{D}_k$. The invariance of stability under system equivalence can be used. Indeed, by Proposition 7.1.3, $\omega_0(\mathring{T}_k) = \omega_0(\bar{T}_k)$, where $(\mathring{T}_k(t))_{t \geqslant 0}$ is the C_0-semigroup generated by $\mathring{A} + \bar{D}_k$.

Step 2: *Computation of a bound to the growth constant of the C_0-semigroup $(\mathring{U}(t))_{t \geqslant 0}$ generated by $\mathring{A}$.*
By the method of characteristics, introduced in Section 7.3, one gets that

$$\left(\mathring{U}_1(t) x_{01}\right)(a) = \begin{cases} x_{01}(a-t) E_{G\kappa}(a-t, a), & \text{if } t \leqslant a, \\ 0 & \text{if } t > a, \end{cases}$$

$$\left(\mathring{U}_2(t) x_{02}\right)(a) = \begin{cases} x_{02}(a-t) E_{H-\kappa}(a-t, a), & \text{if } t \leqslant a, \\ 0 & \text{if } t > a \end{cases}$$

where $E_f(x, y) = \exp\left(\int_x^y f(\eta)\, d\eta\right)$. Moreover, using identity (9.33), we find that

$$\left(\mathring{U}_{12}(t) x_0\right)(a) = \begin{cases} x_0(a-t) \int_0^t E_{H-\kappa}(a-t, a-t+s) \\ \qquad E_{G\kappa}(a-t, a-s)\, ds & \text{if } t \leqslant a, \\ 0 & \text{if } t > a. \end{cases}$$

Therefore, $\mathring{\mathcal{A}}$ is the generator of a nilpotent semigroup, thus its growth bound ω_0 is equal to $-\infty$. Hence, by Proposition 7.4.1 it is the infinitesimal generator of an exponentially stable C_0-semigroup. Let $x_0 = (x_{01}, x_{02})^T$. Since $\mathring{\mathcal{A}}$ is stable, then by Definition 7.4.3, there exist constants $M_\alpha \geqslant 1$ and $\alpha > 0$ such that $\|\mathring{U}(t) x_0\| \leqslant M_\alpha e^{-\alpha t} \|x_0\|$.

Step 3: *Identify α and M_α.*

$$\begin{aligned} \|\mathring{U}(t) x_0\| &= \int_0^{a_{max}} \left| \left(\mathring{U}_1(t) x_{01}\right)(a) + \left(\mathring{U}_{12}(t) x_{02}\right)(a) \right| da \\ &\quad + \int_0^{a_{max}} \left| \left(\mathring{U}_2(t) x_{02}\right)(a) \right| da \\ &\leqslant \int_0^{a_{max}} |x_{01}(\eta)|\, E_{G\kappa}(\eta, \eta + t)\, d\eta + \int_0^{a_{max}} |x_{02}(\eta)| \Big(E_{H+\kappa}(\eta, \eta + t) \end{aligned}$$

$$+\int_0^t E_{H+\kappa}(\eta,\eta+s)\,E_{G\kappa}(\eta,\eta+t-s)\,ds\Big)\,d\eta$$

Using the fact that $\tilde{\alpha}_1 < g(a)+c_1$ and $\tilde{\alpha}_2 < h(a)+c_2$, for all a, by conditions (9.34) and (9.35), it can be shown that

$$E_{G\kappa}(\eta,\eta+t) \leqslant e^{-Kc_1 t} \text{ and } E_{H+\kappa}(\eta,\eta+t) \leqslant e^{-(K+c_2)t}.$$

Thus,

$$\begin{aligned}\|\mathring{U}(t)\,x_0\| \leqslant & e^{-Kc_1 t}\|x_{01}\|_1 \\ & + \left(\frac{e^{-(K+c_2)t}-e^{-Kc_1 t}}{Kc_1-(K+c_2)} + e^{-(K+c_2)t}\right)\|x_{02}\|_1 \\ \leqslant & (1+K(c_1-1)-c_2)\,e^{-(c_2+K)t}\|x_0\|.\end{aligned}$$

It follows that $\omega_0(\mathring{U}) < -(c_2+K) < 0$, thanks to condition (9.35).

Step 4: *Find $\omega_0(\mathring{T}_k)$ which is equal to $\omega_0(\bar{T}_k)$.*
By the bounded perturbation Theorem 7.1.1 it follows that $\mathring{\mathcal{A}}+\bar{D}_k$ is the infinitesimal generator of a C_0-semigroup $\left(\mathring{T}(t)\right)_{t\geqslant 0}$ satisfying

$$\begin{aligned}&\|\mathring{T}(t)\| \leqslant M_\alpha e^{\left(-\alpha+M_\alpha\|\bar{D}_k\|\right)t} \\ \Leftrightarrow\ &\|\mathring{T}(t)\| \leqslant (1+K(c_1-1)-c_2) \\ &\qquad e^{(-(c_2+K)+(1+K(c_1-1)-c_2)c(0)B)t}.\end{aligned} \tag{9.37}$$

Using (9.35) and (9.36) implies that $\omega_0(\mathring{T}) = \omega_0(\bar{T}_k) < -\alpha + M_\alpha\|\bar{D}_k\| < 0$. Therefore, by Proposition 7.4.1 the C_0-semigroup $\left(\bar{T}_k(t)\right)_{t\geqslant 0}$ is exponentially stable.
Note that the inequality (9.34) implies the feasibility of inequalities (9.35) and (9.36). □

One can notice, in the first part of the proof, that the choice of the L_1 norm, combined with the dirac delta sequence whose integral is equal to one, is really advantageous in this case because it implies that the norm of the operator $\bar{D}_k$ is independent of k. Hence, the exponential bound in (9.37) is also independent of k.

Theorem 9.2.2
Let $x_0 = [I_0, S_0]^T \in L^1(0, a_{max}) \times L^1(0, a_{max})$ be the vector of (age-dependent) initial profiles of infected and susceptible individuals, respectively. Assume that c_1, c_2, $\tilde{\alpha}_1(a)$ and $\tilde{\alpha}_2(a)$ are chosen such that conditions (9.34) - (9.36) are satisfied. Consider the description (9.31) of the PIDE model (6.11) with state feedback (9.19). Then, the first component of the state x_k of (9.31), that is the infected population $I_k(t,a)$, converges to zero exponentially fast as time tends to infinity.
More specifically, there exist constants $M \geqslant 1$ and $\alpha > 0$ such that, for all $t \geqslant 0$,

$$\|I_k(t)\|_1 \leqslant M\|I_0\|_1 e^{-\alpha t} \tag{9.38}$$

where the constants $M = 1 + K(c_1 - 1) - c_2$ and $\alpha = -(c_2 + K) + (1 + K(c_1 - 1) - c_2)\, c(0)B$ are independent of the sequence of operators $(\bar{D}_k)$.

Proof. Since Theorem 9.2.1 shows the exponential stability of the C_0-semigroup, it follows that $\bar{x}_k(t)$ exponentially converges to zero. Therefore, by relation (9.20), $\bar{I}_k(t,a) = I_k(t,a)$ exponentially tends to zero. □

Remark 9.2.1 *In view of this analysis, we conjecture that $I(t,a)$ asymptotically exponentially converges to zero.*
Intuitively, we have that $\bar{I}_k(t,a)$ and $\bar{S}_k(t,a)$ tend to $\bar{I}(t,a)$ and $\bar{S}(t,a)$ as k tends to infinity. This idea can be shown by studying the limits of the error's dynamics $E(t,a) = \left(\bar{I}_k(t,a) - \bar{I}(t,a), \bar{S}_k(t,a) - \bar{S}(t,a)\right)^T$ which is given, using (9.30) *and* (9.31) *by*

$$\dot{E} = \bar{D}\bar{x} + \bar{D}_k\bar{x}_k$$
$$E(0) = (0,0)^T.$$

This tends to $\dot{E} = \bar{D}E$ with $E(0) = (0,0)^T$ as k tends to infinity. The solution of this differential equation is $E = 0$. Therefore we can hypothesize that $I_k(t,a) = \bar{I}_k(t,a)$ and $\bar{S}_k(t,a)$ tend to $I(t,a) = \bar{I}(t,a)$ and $\bar{S}(t,a)$ as k tends to infinity.
This intuition is reinforced by the fact that, as established in Theorem 9.2.2, the exponential bound for the norm of I_k is independent of the Dirac sequence (d_k) introduced in (9.31). *Therefore, if $\|I_k(t) - I(t)\|_1$ tends to zero as k tends to infinity, it will follow from* (9.38) *that $\|I(t)\|_1 \leqslant Me^{-\alpha t}\|I_0\|_1$ for all $t \geqslant 0$. Note that this intuition is corroborated by numerical simulations.*

9.2.3 Nonnegativity of the feedback

In the following, some conditions on the design parameters are highlighted in order to ensure nonnegativity of the vaccination law.

Theorem 9.2.3
Define $\nu = \sup_{a\in[0,a_{max}]} \mu(a); \Gamma = \sup_{a\in[0,a_{max}]} \gamma(a)$ and $\bar{P}$ the total population. Taking

$$\tilde{\alpha}_2(a) = 3\nu + 2\Gamma + c(a)\bar{P} \tag{9.39}$$

$$\tilde{\alpha}_1(a) = -K(a)\left(K(a) - \tilde{\alpha}_2\right) \tag{9.40}$$

yields the exponentially stable closed-loop system (9.24)-(9.26), (9.20) with the nonnegative vaccination law (9.19).

Proof. The vaccination law (9.19) with definition (9.40) rewrites $\theta(t,a) = \frac{1}{p(a)}\left\{\tilde{\alpha}_2 + Ax(t,a) + Gx(t))\right\}$. Moreover, since $\nu \geqslant \mu(a)$ for all $a \in [0, a_{max}]$, $\Gamma \geqslant \gamma(a)$ for all $a \in [0, a_{max}]$ and $\int_0^{a_{max}} I(t,b)db \leqslant \bar{P}$, the following estimate for the vaccination law is obtained,

$$\begin{aligned}\theta(t,a) &\geqslant \frac{1}{p(a)}\left\{\tilde{\alpha}_2(a) + \int_0^{a_{max}} c(a)\,S(t,a)\,da - 2\nu - \Gamma - c(a)\bar{P} - (\nu+\Gamma)\right\} \\ &\geqslant \frac{1}{p(a)}\int_0^{a_{max}} c(a)\,S(t,a)\,da\end{aligned}$$

using definition (9.39). It follows that the vaccination law with those choices of parameters is nonnegative. □

Therefore, in the PIDE case, there is no need to use a switching vaccination law to ensure nonnegativity of the feedback.

9.2.4 Numerical simulations

Simulations are performed by using the same parameters and tolerance defined in Sections 8.3 and 9.1.4. Furthermore, a forward time - backward space finite difference scheme is used, as in Section 8.3. Moreover, notice that disease eradication can be achieve regardless of the choice of the parameters. Indeed as it can be viewed in Theorem 9.2.1, the choice of the design parameters only impacts the convergence speed of the system. Therefore they can be tuned to achieved a desired stability margin. However, in order to ensure that the vaccination rate is nonnegative, the feedback gains are chosen according to Theorem

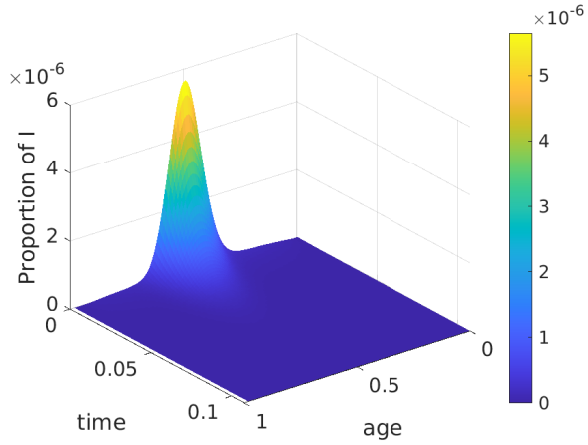

Figure 9.4 – Dynamics of infected individuals from NPIDE Model (8.1) with vaccination (9.19)

9.2.3.

Figures 9.4 to 9.6 confirm the theoretical results. Indeed, Figure 9.4 shows that the infected individuals tends to zero as time increases. In Figure 9.5, the susceptible individuals trajectory remains nonnegative, so as the vaccination that can be viewed in Figure 9.6. This vaccination law differs from the one obtained for the ODE model. This can be explained by the large choice of design parameters for both models. Since those parameters are not chosen in the same way (randomly for the ODE case and to ensure nonnegativity of the vaccination law in the PIDE case) differences occur. Moreover, there is no indication that the NODE model (9.2) is a good approximation of the PIDE model (6.11), since the first one was just a tool to obtain the vaccination law for the second one. The shape of Figure 9.6 suggests to vaccinate strongly individuals at the beginning of the epidemic with less focus on young and old individuals.

Some questions remain open. First it can be noticed that no condition is imposed a priori on the nonnegativity of the vaccination law for the NODE model, which is essential to have physical meaning and nonnegativity of the input. In numerical simulations a saturated law was used and seems to perform well. This could be theoretically validated. Moreover, in the numerical simulations, the feedback gains are chosen randomly in order to satisfy the positivity and stability conditions. Another question could be the choice of those feedback gains in an optimal way, such as the minimization of the total number

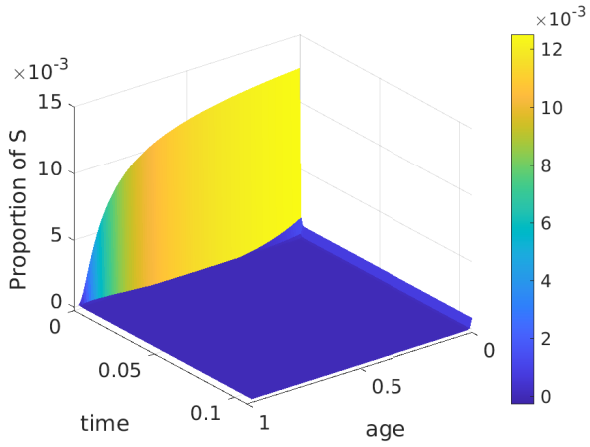

Figure 9.5 – Dynamics of susceptible individuals from NPIDE Model (8.1) with vaccination (9.19)

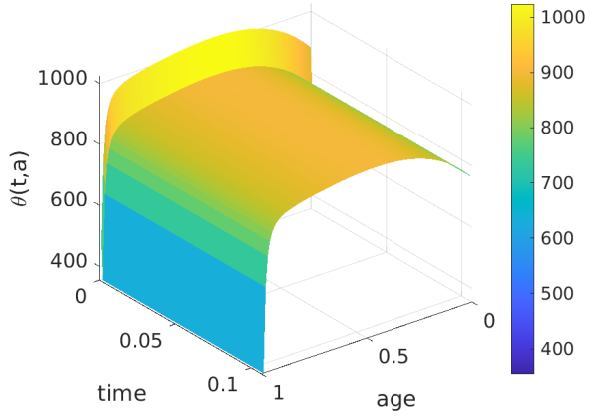

Figure 9.6 – Dynamics of vaccination for the NPIDE Model (8.1) with vaccination law (9.19)

of infected individuals, for instance. Furthermore, the control law that was designed is not applicable in practice since it requires the knowledge of all the state variables as it is a state feedback law. This is rarely the case in real situations. A way to overcome this issue is to use a state observer to estimate the whole state. The design of such an observer and the analysis of its performance in connection with the state feedback laws is an important question for further research. Finally it could be interesting to study a more complex model, for instance an SIRS model, which will allow loss of immunity or a SIRD model to fit best the fatal illness.

Conclusion and perspectives

Conclusion

To conclude this thesis, let's quote Shakuntala Devi, an indian woman, prodigious mental calculator: *"What is mathematics? It is only a systematic effort of solving puzzles posed by nature"*. In this thesis, dedicated to the study of a particular case of epidemic models, the age-structured compartmentalized epidemic models, the aim is to understand the nature behavior in the field of epidemic in order to be able to act on a disease to obtain the desired result of disease eradication.

In order to understand the nature, one needs to express it in the mathematical language. This can be done thanks to mathematical models. However, those models need to be correctly developed to reflect reality. Chapter 1 is dedicated to a brief overview of the models in epidemiology and details the ones of interest in this thesis. Then, one objective of this thesis is to study those considered models through their dynamical analysis. This is done in Chapter 4 for a nonlinear finite-dimensional SIRD model described by a set of ordinary differential equations, but also in Chapter 8 for a nonlinear infinite-dimensional SIR model described thanks to a set of partial integro-differential equations. In those chapters, the question of existence of a unique solution for the models is answered. If a model does not admit a solution, then it is not capable to describe nature. A model with multiple solutions also fails to describe nature since it is known that there is only one possible future. Therefore, ensuring the existence and uniqueness of the solution allows to trust the models. Furthermore, since the models deal with "physical" quantities, the question of nonnegativity of the state variables is also studied. Moreover, the question of stability is also addressed in order to make predictions about the future.

Models by themselves are not enough to explain a natural phenomenon. Real data are needed to allow the use of the models in real situation. This has been done in Chapter 3 for the finite-dimensional model, using data on covid-19 in Wallonia. Thanks to those data, the parameters of the model were calibrated. Therefore, predictions of future behavior of the epidemic were obtained.

Finally, control theory allows to answer the challenging question of disease eradication thanks to vaccination. For the finite-dimensional case, Chapter 5 proposed an observer-based output feedback that ensures disease eradication while ensuring that the maximum number of infected individuals is lower than without vaccination. The vaccination is chosen to be implementable in practice in terms of nonnegativity and upper bound, since the number of vaccines per day is limited. In Chapter 6, an optimal age-dependent vaccination law was designed using model predictive control, in order to achieve disease eradication. This law also satisfies some additional desirable constraints: the minimization of the number of dead individuals in the population, ensuring that the peak of the total number of infected individuals is not too high. As previously, this vaccination law is ensured to be implementable in practice. Finally, the control of the infinite-dimensional case was discussed in Chapter 9. A nonnegative vaccination law was designed thanks to a state feedback. The method proposed in this Chapter is innovative and extends the known theory of linearizing state feedback to the infinite-dimensional case.

To summarize, this thesis aims at answering some questions concerning the dynamical analysis and control of nonlinear systems, in the field of epidemiology. Throughout this thesis, theorems and proofs ensure that the results obtained are valid for a wide range of applications. The proposed methods can be used for other diseases than covid-19. However, the work is far from being completed and lots of interesting questions still need to be tackled to improve the field of control of epidemic models. Some of those improvements are discussed in the following section.

Perspectives

Throughout this thesis, some open questions have been stated. Some of those suggestions for future research are listed below.

- Concerning Chapter 3 and the model calibration, the choice of another cost function, such as a negative binomial likelihood statistic could be

investigated. Indeed, this statistic is best suited to deal with data that are over-dispersed. Because, as mentioned in (Towers (2014)), "if in fact the data are over-dispersed and the Poisson negative likelihood statistic is used in parameter optimization, the assessment of the uncertainties on the parameter estimates will be too low".

- The choice of the optimization algorithm in Chapter 3 can be discussed. Indeed, instead of using a genetic algorithm, one could think of using the Levenberg-Marquadt algorithm for instance. This is a gradient-based optimization method often used to solve parameters optimization problem but with the disadvantage to sometimes get stuck in local minima. Hence, a comparative study between both algorithms in the context of parameters calibration in epidemiology could be very interesting.
- In Chapter 3, it could also be interesting to investigate the influence of the choice of the starting time of the epidemic t_0 in the parameter calibration.
- Throughout the thesis, in order to capture the behavior of a disease at best, it could be interesting to investigate models with more compartments. The choice of the compartments can also be motivated by the available data. Indeed, since only data about the hospitalized people seem relevant, one could think to add an hospitalized compartment H to the model for instance.

  Furthermore, the models studied in this thesis rely on the strong assumption that, once recovered, an individual cannot catch the disease again. This assumption can be removed by considering systems such as SIRS, SIRDS,... where the recovered individuals can lose some immunity and become susceptible again. However, this additional term brings an additional complexity to the model and has not been studied. Now that some foundations have been developed for simple SIR and SIRD models, the next step is to extend the results of this thesis to SIRS and SIRDS models.
- Moreover the concept of age refers usually to the age of the individuals. However, the attention can be focused on the last infection period for instance, which can be viewed as the age of the disease. Several kinds of age can be defined in this context: the most known is the infection-age ($\bar{\alpha}$) which is the elapsed time since infection. In such context, other age-structured models should be studied.
- In Chapter 5 it can be interesting to find how to select the feedback gains of the observer-based output feedback in the best way possible. For instance, by finding the parameters that minimize the number of dead individuals. Then, the obtained results could be compared to the ones of Chapter 6 where an age-dependent vaccination law is obtained

thanks to model predictive control.

- Moreover, the approach proposed in Chapter 6 has been performed on a discrete-time model. It could be interesting to apply the same methodology to a continuous-time model, e.g. by extending the analysis developed in the article (Sauerteig et al. (2022)) to the case of age-dependent epidemic models.
- Concerning Chapter 9, it can be noticed that no condition is imposed a priori on the nonnegativity of the vaccination law for the NODE model, which is essential to have physical meaning and nonnegativity of the input. In numerical simulations a saturated law was used and seems to perform well. This could be theoretically validated.
- It could also be interesting, in Chapter 9, to study the possible convergence of the NODE model to the PIDE model, in open-loop and in closed-loop.
- Moreover, as for Chapter 5, the feedback gains of Chapter 9 could be selected in an optimal way, for instance, by minimizing the maximum number of infected individuals, in order to take into account the hospitals bed capacity.
- In Chapter 8, the stability analysis is performed on the linearized system. An approach using Lyapunov functions could be an interesting alternative, as it was done in Chapter 6 for instance. The reference (Haddad et al., 2010b, Chapter 2) could serve as a source of inspiration for this task, where Lyapunov stability theory for nonnegative dynamical systems is developed in the finite dimensional case.
- A key open question in Chapter 9 concerns the design of a control law that is applicable in practice. Indeed, this is currently not the case since the control law requires the knowledge of all the state variables, which is rarely feasible in real situations. A way to overcome this issue is to use a state observer to estimate the whole state. The design of such an observer and the analysis of its performances in connection with the state feedback laws is an important question for further research. Results in Chapter 5 and work developed in (Kitsos et al. (2022)), but without control, can serve as inspiration to tackle this question.
- In Chapter 9, a methodology to obtain a linearizing state feedback for an infinite dimensional system is developed. This idea and the related tools and results could possibly be extended to larger classes of systems, under appropriate conditions.

Appendix A

Lipschitz property of the saturated feedback

This chapter is dedicated to the proof of intermediate tools useful for the proof of the Lipschitz property of the constrained feedback (5.13). The regions (B_1, B_2 and B_3) mentioned in the proof refer to Figure 5.1.

Lemma A.0.1
The function $q_k : Dom(q_k) = \left[\tilde{S}_k, N_k\right] \times [0, N_k] \times \cdots \times [0, N_k] \times \left[\tilde{I}_k, N_k\right] \times [0, N_k] \times \cdots \times [0, N_k] \to \mathbb{R}$, defined by (5.15) is Lipschitz.

Proof. Let $z_k = (x_k, y_1, \cdots, y_k, \cdots, y_{n_a})^T$ and $z'_k = (x'_k, y'_1, \cdots, y'_k, \cdots, y'_{n_a})^T \in Dom(q_k)$. Several situations can be identified.

— Assume that z_k and z'_k are such that $x_k, x'_k \geqslant \tilde{\tilde{S}}_k$ and $y_k, y'_k \geqslant \tilde{\tilde{I}}_k$ (z_k and $z'_k \in B_1$). Therefore,

$$|q_k(z_k) - q_k(z'_k)| = |1 - 1| = 0 \leqslant C_1 \|z_k - z'_k\|_{l^1}$$

for all $C_1 > 0$.

— Assume that z_k and z'_k are such that $y_k, y'_k < \tilde{\tilde{I}}_k$, $y_k \leqslant \dfrac{\tilde{\tilde{I}}_k - \tilde{I}_k}{\tilde{\tilde{S}}_k - \tilde{S}_k}\left(x_k - \tilde{S}_k\right) + \tilde{I}_k$ and $y'_k \leqslant \dfrac{\tilde{\tilde{I}}_k - \tilde{I}_k}{\tilde{\tilde{S}}_k - \tilde{S}_k}\left(x'_k - \tilde{S}_k\right) + \tilde{I}_k$ (z_k and $z'_k \in B_2$). Therefore,

$$\left|q_k(z_k) - q_k(z'_k)\right| = \frac{4}{\pi}\left|\arctan\left(\frac{y_k - \tilde{I}_k}{\tilde{\tilde{I}}_k - \tilde{I}_k}\right) - \arctan\left(\frac{y'_k - \tilde{I}_k}{\tilde{\tilde{I}}_k - \tilde{I}_k}\right)\right|$$

$$
\begin{aligned}
&\leqslant \frac{4}{\pi}\left|\left(\frac{y_k-\tilde{I}_k}{\tilde{\tilde{I}}_k-\tilde{I}_k}\right)-\left(\frac{y'_k-\tilde{I}_k}{\tilde{\tilde{I}}_k-\tilde{I}_k}\right)\right| \\
&= \frac{4}{\pi\left(\tilde{\tilde{I}}_k-\tilde{I}_k\right)}|y_k-y'_k| \\
&\leqslant C_2\|z_k-z'_k\|_{l^1},
\end{aligned}
$$

using the fact that arctan is a Lipschitz function with Lipschitz constant 1, and taking C_2 equals $\dfrac{4}{\pi\left(\tilde{\tilde{I}}_k-\tilde{I}_k\right)}$.

— Assume that z_k and z'_k are such that $x_k, x'_k < \tilde{\tilde{S}}_k$, $y_k > \dfrac{\tilde{\tilde{I}}_k-\tilde{I}_k}{\tilde{\tilde{S}}_k-\tilde{S}_k}\left(x_k-\tilde{S}_k\right)+\tilde{I}_k$ and $y'_k > \dfrac{\tilde{\tilde{I}}_k-\tilde{I}_k}{\tilde{\tilde{S}}_k-\tilde{S}_k}\left(x'_k-\tilde{S}_k\right)+\tilde{I}_k$ (z_k and $z'_k \in B_3$). By a similar reasoning as the previous case, it follows that

$$
\left|q_k(z_k)-q_k(z'_k)\right| \leqslant C_3\|z_k-z'_k\|_{l^1},
$$

with $C_3 = \dfrac{4}{\pi\left(\tilde{\tilde{S}}_k-\tilde{S}_k\right)}$.

— Assume that z_k and z'_k are such that $x_k \geqslant \tilde{\tilde{S}}_k$, $y_k \geqslant \tilde{\tilde{I}}_k$, $y'_k < \tilde{\tilde{I}}_k$ and $y'_k \leqslant \dfrac{\tilde{\tilde{I}}_k-\tilde{I}_k}{\tilde{\tilde{S}}_k-\tilde{S}_k}\left(x'_k-\tilde{S}_k\right)+\tilde{I}_k$ ($z_k \in B_1$ and $z'_k \in B_2$). Therefore,

$$
\begin{aligned}
\left|q_k(z_k)-q_k(z'_k)\right| &= \left|1-\frac{4}{\pi}\arctan\left(\frac{y'_k-\tilde{I}_k}{\tilde{\tilde{I}}_k-\tilde{I}_k}\right)\right| \\
&= \left|\frac{4}{\pi}\arctan(1)-\frac{4}{\pi}\arctan\left(\frac{y'_k-\tilde{I}_k}{\tilde{\tilde{I}}_k-\tilde{I}_k}\right)\right| \\
&\leqslant \frac{4}{\pi}\left|1-\left(\frac{y'_k-\tilde{I}_k}{\tilde{\tilde{I}}_k-\tilde{I}_k}\right)\right| \\
&= \frac{4}{\pi\left(\tilde{\tilde{I}}_k-\tilde{I}_k\right)}\left(\tilde{\tilde{I}}_k-y'_k\right) \text{ since } y'_k < \tilde{\tilde{I}}_k, \\
&= C_2\left(y_k-y'_k+\tilde{\tilde{I}}_k-y_k\right) \\
&\leqslant C_2\left(y_k-y'_k\right) \text{ since } y_k \geqslant \tilde{\tilde{I}}_k, \\
&\leqslant C_2\|z_k-z'_k\|_{l^1},
\end{aligned}
$$

— Assume that z_k and z'_k are such that $x_k \geqslant \tilde{\tilde{S}}_k$, $y_k \geqslant \tilde{\tilde{I}}_k$, $x'_k < \tilde{\tilde{S}}_k$ and $y'_k > \dfrac{\tilde{\tilde{I}}_k-\tilde{I}_k}{\tilde{\tilde{S}}_k-\tilde{S}_k}\left(x'_k-\tilde{S}_k\right)+\tilde{I}_k$ ($z_k \in B_1$ and $z'_k \in B_3$). A similar reasoning

as the previous one gives

$$\left|q_k(z_k) - q_k(z'_k)\right| \leqslant C_3 \|z_k - z'_k\|_{l^1}.$$

— Assume that z_k and z'_k are such that $y_k < \tilde{\bar{I}}_k$ and $y_k \leqslant \dfrac{\tilde{\bar{I}}_k - \tilde{I}_k}{\tilde{\bar{S}}_k - \tilde{S}_k}\left(x_k - \tilde{S}_k\right) + \tilde{I}_k$, $x'_k < \tilde{\bar{S}}_k$ and $y'_k > \dfrac{\tilde{\bar{I}}_k - \tilde{I}_k}{\tilde{\bar{S}}_k - \tilde{S}_k}\left(x'_k - \tilde{S}_k\right) + \tilde{I}_k$ ($z_k \in B_2$ and $z'_k \in B_3$).

$$\begin{aligned}\left|q_k(z_k) - q_k(z'_k)\right| &= \frac{4}{\pi}\left|\arctan\left(\frac{y_k - \tilde{I}_k}{\tilde{\bar{I}}_k - \tilde{I}_k}\right) - \arctan\left(\frac{x'_k - \tilde{S}_k}{\tilde{\bar{S}}_k - \tilde{S}_k}\right)\right| \\ &\leqslant \frac{4}{\pi}\left|\left(\frac{y_k - \tilde{I}_k}{\tilde{\bar{I}}_k - \tilde{I}_k}\right) - \left(\frac{x'_k - \tilde{S}_k}{\tilde{\bar{S}}_k - \tilde{S}_k}\right)\right|\end{aligned}$$

Introduce the new variables $\bar{I}_k = \tilde{\bar{I}}_k - \tilde{I}_k$ and $\bar{S}_k = \tilde{\bar{S}}_k - \tilde{S}_k$ and consider two cases. If $\dfrac{y_k - \tilde{\bar{I}}_k}{\bar{I}_k} \leqslant \dfrac{x'_k - \tilde{\bar{S}}_k}{\bar{S}_k}$, it follows that,

$$\begin{aligned}\left|q_k(z_k) - q_k(z'_k)\right| &\leqslant \frac{4}{\pi}\left(\frac{x'_k - \tilde{\bar{S}}_k}{\bar{S}_k} - \frac{y_k - \tilde{\bar{I}}_k}{\bar{I}_k}\right) \\ &\leqslant \frac{4}{\pi}\left(\frac{y'_k - \tilde{\bar{I}}_k}{\bar{I}_k} - \frac{y_k - \tilde{\bar{I}}_k}{\bar{I}_k}\right) \\ &= C_2\left(y'_k - y_k\right) \\ &\leqslant C_2\|z_k - z'_k\|_{l^1},\end{aligned}$$

where the fact that $y'_k > \dfrac{\bar{I}_k}{\bar{S}_k}\left(x'_k - \tilde{\bar{S}}_k - \bar{S}_k\right) + \tilde{\bar{I}}_k - \bar{I}_k \Leftrightarrow \dfrac{y'_k - \tilde{\bar{I}}_k}{\bar{I}_k} > \dfrac{x'_k - \tilde{\bar{S}}_k}{\bar{S}_k}$ was used.

Moreover, if $\dfrac{y_k - \tilde{\bar{I}}_k}{\bar{I}_k} > \dfrac{x'_k - \tilde{\bar{S}}_k}{\bar{S}_k}$, it follows that,

$$\begin{aligned}\left|q_k(z_k) - q_k(z'_k)\right| &\leqslant \frac{4}{\pi}\left(\frac{y_k - \tilde{\bar{I}}_k}{\bar{I}_k} - \frac{x'_k - \tilde{\bar{S}}_k}{\bar{S}_k}\right) \\ &\leqslant \frac{4}{\pi}\left(\frac{x_k - \tilde{\bar{S}}_k}{\bar{S}_k} - \frac{x'_k - \tilde{\bar{S}}_k}{\bar{S}_k}\right) \\ &= C_3\left(x_k - x'_k\right) \\ &\leqslant C_3\|z_k - z'_k\|_{l^1},\end{aligned}$$

where the fact that $y_k \leqslant \frac{\bar{I}_k}{\bar{S}_k}\left(x_k - \tilde{\bar{S}}_k - \bar{S}_k\right) + \tilde{\bar{I}}_k - \bar{I}_k \Leftrightarrow \frac{y_k - \tilde{\bar{I}}_k}{\bar{I}_k} \leqslant \frac{x_k - \tilde{\bar{S}}_k}{\bar{S}_k}$ was used.

Finally,

$$\left|q_k(z_k) - q_k(z'_k)\right| \leqslant C\|z_k - z'_k\|_{l^1},$$

with $C = \max\{C_1, C_2, C_3\} > 0$. □

Lemma A.0.2
The function $\bar{\theta}_k : Dom(\bar{\theta}_k) = \left[\tilde{S}_k, N_k\right] \times [0, N_k] \times \cdots \times [0, N_k] \times \left[\tilde{I}_k, N_k\right] \times [0, N_k] \times \cdots \times [0, N_k] \to \mathbb{R}$, defined by (5.14) is Lipschitz.

Proof. Let z_k and $z'_k \in Dom(\bar{\theta}_k)$. As for the previous proof, several situations can be identified.

— Assume that z_k and z'_k are such that $\theta_k(z_k), \theta_k(z'_k) \leqslant \theta_{sup}$, it follows that

$$\left|\bar{\theta}_k(z_k) - \bar{\theta}_k(z'_k)\right| = \left|\theta_k(z_k) - \theta_k(z'_k)\right| \leqslant K_1\|z_k - z'_k\|$$

since θ_k, defined by (5.6), is Lipschitz on $Dom(\bar{\theta}_k)$.

— Assume that z_k and z'_k are such that $\theta_k(z_k), \theta_k(z'_k) < \theta_{sup}$, then

$$\left|\bar{\theta}_k(z_k) - \bar{\theta}_k(z'_k)\right| = |\theta_{sup} - \theta_{sup}| = 0 \leqslant K_2\|z_k - z'_k\|,$$

for all $K_2 > 0$.

— Assume that z_k and z'_k are such that $\theta_k(z_k) \leqslant \theta_{sup}$ and $\theta_k(z'_k) > \theta_{sup}$. Hence,

$$\begin{aligned}\left|\bar{\theta}_k(z_k) - \bar{\theta}_k(z'_k)\right| &= \left|\theta_k\left(z_k\right) - \theta_{sup}\right| \\ &= \theta_{sup} - \theta_k\left(z_k\right) \text{ since } \theta_k\left(z_k\right) \leqslant \theta_{sup}, \\ &\leqslant \theta_k\left(z'_k\right) - \theta_k\left(z_k\right) \text{ since } \theta_k\left(z'_k\right) < \theta_{sup} \\ &\leqslant K_1\|z_k - z'_k\|\end{aligned}$$

where K_1 is the Lipschitz constant of θ_k.

Thus, for all z_k and $z'_k \in Dom(\bar{\theta}_k)$,

$$\left|\bar{\theta}_k(z_k) - \bar{\theta}_k(z'_k)\right| \leqslant K\|z_k - z'_k\|,$$

with $K = \max\{K_1, K_2\}$. □

Proposition A.0.1

The function $q_k\bar{\theta}_k : Dom(q_k\bar{\theta}_k) = \left[\tilde{S}_k, N_k\right] \times [0, N_k] \times \cdots \times [0, N_k] \times \left[\tilde{I}_k, N_k\right] \times [0, N_k] \times \cdots \times [0, N_k] \to \mathbb{R}$ is Lipschitz, with Lipschitz constant $L > 0$.

Proof. Let z_k and $z'_k \in Dom(q_k\bar{\theta}_k)$,

$$\begin{aligned}
\left|\left(q_k\bar{\theta}_k\right)(z_k) - \left(q_k\bar{\theta}_k\right)\left(z'_k\right)\right| &\leqslant \left|q_k(z_k)\left(\bar{\theta}_k(z_k) - \bar{\theta}_k\left(z'_k\right)\right)\right| \\
&\quad + \left|\bar{\theta}_k\left(z'_k\right)\left(q_k(z_k) - q_k\left(z'_k\right)\right)\right| \\
&\leqslant \left|\bar{\theta}_k(z_k) - \bar{\theta}_k\left(z'_k\right)\right| + \theta_{sup}\left|q_k(z_k) - q_k\left(z'_k\right)\right| \\
&\leqslant K\|z_k - z'_k\| + \theta_{sup}C\|z_k - z'_k\| \\
&\leqslant L\|z_k - z'_k\|
\end{aligned}$$

using the two previous lemma, the fact that $0 \leqslant q_k \leqslant 1$, $0 \leqslant \bar{\theta}_k \leqslant \theta_{sup}$ and defining $L = \max\{K, \theta_{sup}C\}$. ▫

Bibliography

SIMID group and Funk, S. (2020). *Social contact rates (socrates) data tool: as part of the socialcontactdata.org initiative.* TransMID. Http://www.socialcontactdata.org/socrates.

Aksikas, I., Winkin, J. j., and Dochain, D. (2007). *Optimal lq-feedback regulation of a nonisothermal plug flow reactor model by spectral factorization.* IEEE Transactions on Automatic Control, 52(7):1179–1193.

Alexanderian, A., et al. (2011). *An age-structured model for the spread of epidemic cholera: Analysis and simulation.* Nonlinear Analysis: Real World Applications, 12(6):3483–3498.

Alonso-Quesada, S., et al. (2012). *An observer-based vaccination control law for an seir epidemic model based on feedback linearization techniques for nonlinear systems.* Advances in Difference Equations, 2012(1).

Arendt, W., et al. (1983). One-parameter semigroups of positive operators. Springer, Berlin, Heidelberg.

Atassi, A. and Khalil, H. (1999). *A separation principle for the stabilization of a class of nonlinear systems.* IEEE Transactions on Automatic Control, 44(9):1672–1687.

Bastin, G. and Coron, J.-M. (2016). Stability and boundary stabilization of 1-D hyperbolic systems, pages 40–43. coll. PNLDE Subseries in Control. Birkhauser, Switzerland.

Bernoulli, D. (1760). *Réflexions sur les avantages de l'inoculation.* Mercure de Paris, page 173.

Bernoulli, D. (1766). *Essai d'une nouvelle analyse de la mortalité causée par la petite vérole.* Mem. Math. Phys. Acad. Roy. Sci. Paris.

Braeye, T., et al. (2022). *Covid-19 vaccine effectiveness against symptomatic infection and hospitalization in belgium, july 2021-april 2022.* Euro Surveill.

Brezis, H. (2011). Functional analysis, Sobolev spaces and partial differential equations. Springer.

Brunner, H. (2017). Volterra integral equations. Cambridge Monographs on Applied and Computational Mathematics. Cambridge University Press.

Calafiore, G. C. and Fracastoro, G. (2022). *Age structure in sird models for the covid-19 pandemic—a case study on italy data and effects on mortality.* PLOS ONE, 17(2).

Cartocci, A., Cevenini, G., and Barbini, P. (2021). *A compartment modeling approach to reconstruct and analyze gender and age-grouped covid-19 italian data for decision-making strategies.* Journal of Biomedical Informatics, 118:103793.

Colizza, V. and Vespignani, A. (2008). *Epidemic modeling in metapopulation systems with heterogeneous coupling pattern: Theory and simulations.* Journal of Theoretical Biology, 251(3):450–467.

Curtain, R. and Zwart, H. (2020). Introduction to Infinite-Dimensional Systems Theory A State-Space Approach. Springer New York.

Daley, D. J. and Gani, J. M. (2007). Epidemic modelling: An introduction. Cambridge University Press.

Davies, N. G., et al. (2020). *Age-dependent effects in the transmission and control of covid-19 epidemics.* Nature Medecine, 26:1205–1211.

Diekmann, O., Heesterbeek, J., and Metz, J. (1990). *On the definition and the computation of the basic reproduction ratio r 0 in models for infectious diseases in heterogeneous populations.* Journal of Mathematical Biology, 28(4).

Dowd, J. B., et al. (2020). *Demographic science aids in understanding the spread and fatality rates of covid-19.* Proc Natl Acad Sci U S A.

Engel, K.-J. and Nagel, R. (2000). One-parameter semigroups for linear evolution equations. Springer.

Fattorini, H. O. (1968). *Boundary control systems.* SIAM Journal on Control, 6(3):349–385.

Fortmann, T. E. and Hitz, K. L. (1977). An introduction to linear control systems. Marcel Dekker.

Franco, N. (2021). *Covid-19 belgium: Extended seir-qd model with nursing homes and long-term scenarios-based forecasts.* Epidemics, 37:100490.

Graunt, J. (1662). Natural and Political Observations Made Upon the Bills of Mortality. John Martin.

Haddad, W. M. and Chellaboina, V. (2008). Nonlinear Dynamical Systems and control: A Lyapunov-based approach. Princeton University.

Haddad, W. M., Chellaboina, V., and Hui, Q. (2010a). Nonnegative and Compartmental Dynamical Systems. Princeton University Press.

Haddad, W. M., Chellaboina, V., and Hui, Q. (2010b). Nonnegative and compartmental dynamical systems. Princeton University Press.

Hamer, W. H. (1906). *Epidemic diseases in england: The evidence of variability and of persistency of type.* The Lancet, pages 733–738.

Hastir, A., Winkin, J., and D., D. (2020). *Exponential stability of nonlinear infinite-dimensional systems: Application to nonisothermal axial dispersion tubular reactors.* Automatica, 121:109201. ISSN 0005-1098.

Heijmans, H. (1986). *The dynamical behaviour of the age-size-distribution of a cell population.* In M. J. A. J. and D. O., editors, The dynamics of physiologically structured populations, volume 86, chapter V, pages 185–202. Springer-Verlag Berlin Heidelberg.

Hethcote, H. W. (2008). *Age-structured epidemiology models and expressions for* r_0. In M. S. and X. Y., editors, Mathematical Understanding of Infectious Disease Dynamics, volume 16 of *Lecture Notes Series, Institute for Mathematical Sciences, National University of Singapore*, chapter 3, pages 91–128. World Scientific Publishing Company.

Hinrichsen, D. and Pritchard, A. J. (2010). Mathematical systems theory I modelling, state space analysis, stability and robustness. Springer.

How, J. P. and Frazzoli, E. (2010). *Feeback control systems: Introduction to state-space models.* MITopencourseware. Https://ocw.mit.edu/courses/16-30-feedback-control-systems-fall-2010/1bfc976fcead1982d90c5057511e5ef7_MIT16_30F10_lec05.pdf.

Hui, Q., Haddad, W. M., and Bhat, S. P. (2008). *Finite-time semistability and consensus for nonlinear dynamical networks.* IEEE Transactions on Automatic Control, 53(8):1887–1900.

Inaba, H. (1990). *Treshold and stability results for an age-structured epidemic model.* Journal of mathematical biology, pages 411–434.

Inaba, H. (2006). *Mathematical analysis of an age-structured sir epidemic model with vertical transmission.* Discrete and Continuous Dynamical Systems, Series B, 6:69–96.

Inaba, H. (2017). Age-Structured population dynamics in demography and epidemiology. Springer.

Institut Pasteur (2019). *Mieux lutter contre les épidémies.* Institut Pasteur : le journal de la recherche. Https://www.pasteur.fr/fr/journal-recherche/dossiers/mieux-lutter-contre-epidemies.

Isidori, A. (1995). Nonlinear Control Systems. Springer, 3rd edition.

Jamal, R. A. and Morris, K. (2018). *Linearized stability of partial differential equations with application to stabilization of the kuramoto–sivashinsky equation.* SIAM Journal on Control and Optimization, 56(1):120–147.

Kalman, R. E. (1960). *Contributions to the theory of optimal control.* Boletín de la Sociedad Matemática Mexicana, 5.

Keeling, M. J. and Rohani, P. (2008). Modeling infectious diseases in humans and animals. Princeton University Press.

Kermack, W. and McKendrick, A. (1927). *A contribution to the mathematical theory of epidemics. the problem of endemicity.* Proceedings of the Royal Society of London A: Mathematical, Physical and Engineering Sciences, 115:700–721.

Khalil, H. K. (2002). Nonlinear systems. Prentice Hall, 3 edition.

Kitsos, C., Besancon, G., and Prieur, C. (2022). *High-gain observer design for a class of quasi-linear integro-differential hyperbolic systems—application to an epidemic model.* IEEE Transactions on Automatic Control, 67(1):292–303.

Klaus-Jochen, E. and Rainer, N. (2006). A Short Course on Operator Semigroups. Springer, New York, USA.

Kundur, P., et al. (2004). *Definition and classification of power system stability ieee/cigre joint task force on stability terms and definitions.* Power Systems, IEEE Transactions on, 19:1387 – 1401.

Marek, I. (1970). *Frobenius theory of positive operators : comparison theorems and applications.* SIAM Journal on Applied Mathematics, 19:607–628.

Nane, G. F., et al. (2023). *Covid-19 and the scientific publishing system: Growth, open access and scientific fields.* Scientometrics, 128(1):345–362.

Obitko, M. (1998). *Gentic algorithm.* Https://courses.cs.washington.edu/courses/cse473/06sp/GeneticAlgDemo/gaintro.html.

Okuwa, K., Inaba, H., and Kuniya, T. (2019). *Mathematical analysis for an age-structured sirs epidemic model.* Mathematical Biosciences and Engineering, 16:6071–6102.

Pazy, A. (1983). Semigroups of linear operators and application to partial differential equations, volume 44. Springer-Verlag New-York, USA.

Rawlings, J. B., Mayne, D. Q., and Diehl, M. (2020). Model predictive control: Theory, computation, and design. Nob Hill Publishing, 2 edition.

Roser, M., et al. (2014). *Eradication of diseases.* Our World in Data. Https://ourworldindata.org/eradication-of-diseases.

Ross, R. A. (1911). The prevention of malaria (with Addendum). London: John Murray.

Rudin, W. (1974). Real and complex analysis. McGraw-Hill.

Salih, A. (2016). *Method of characteristics.*

Sauerteig, P., et al. (2022). *Model predictive control tailored to epidemic models.* 2022 European Control Conference (ECC).

Schumacher (1981). Dynamic feedback in finite-and infinite-dimensional linear systems. Ph.D. thesis.

Sciensano (2023). *Covid-19.* Epistat. Https://epistat.sciensano.be/covid.

Sciensano, et al. (2023). *Mortalité covid-19.* Vers une Belgique en Bonne santé. Https://www.belgiqueenbonnesante.be/fr/etat-de-sante/crise-covid-19/mortalite-covid-19.

Seborg, D. E., Edgar, T. F., and Mellichamp, D. A. (2004). Process Dynamics and control. Wiley, 2 edition.

Snow, J. (1855). *The mode of communication of cholera.* London: Churchill.

Statbel (2023). *Statbel, la belgique en chiffres.* be.STAT. Https://bestat.statbel.fgov.be/bestat.

Steinberg, S. (1968). *Meromorphic families of compact operators.* Archive for Rational Mechanics and Analysis, 31:372–379.

Stoustrup, J. (2023). *Controlling a pandemic: An account of successfully applying control theory to the covid-19 pandemic in denmark [applications of control]*. IEEE Control Systems, 43(4):23–32.

The Carter Center (2023). *Guinea worm case total*. The Carter Center. Https://www.cartercenter.org/health/guinea_worm/case-totals.html.

Tolles, J. and Luong, T. (2020). *Modeling Epidemics With Compartmental Models*. JAMA, 323(24):2515–2516. ISSN 0098-7484.

Towers, S. (2014). *Poisson likelihood*. Https://sherrytowers.com/2014/07/10/poisson-likelihood.

Tucsnak, M. and Weiss, G. (2009). Observation and Control for Operator Semigroups. Birkhauser Basel.

Tudor, D. W. (1985). *An age-dependent epidemic model with application to measles*. Mathematical Biosciences, 73(1):131–147.

Webb, G. F. (1985). Theory of nonlinear age-dependent dynamics. Pure and applied mathematics. Marcel Dekker Inc., USA.

Willem, L., et al. (2020). *Socrates: An online tool leveraging a social contact data sharing initiative to assess mitigation strategies for covid-19*. BMC Research Notes, 13(1).

Yosida, K. (1980). Functional Analysis. Springer-Verlag, sixth edition.